APPLICATION OF ARTIFICIAL NEURAL NETWORK IN PAPER INDUSTRY

A THESIS

Submitted in partial fulfilment of the
requirements for the award of the degree
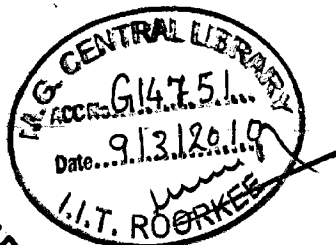*of*

DOCTOR OF PHILOSOPHY

in

Instrumentation and Control Engg.

by

RAJESH KUMAR

DEPARTMENT OF PAPER TECHNOLOGY
INDIAN INSTITUTE OF TECHNOLOGY ROORKEE
SAHARANPUR CAMPUS, P.B. 83
SAHARANPUR-247001, INDIA
OCTOBER, 2008

INDIAN INSTITUTE OF TECHNOLOGY ROORKEE
ROORKEE

CANDIDATE'S DECLARATION

I hereby certify that the work which is being presented in the thesis entitled

"APPLICATION OF ARTIFICIAL NEURAL NETWORK IN PAPER INDUSTRY" in partial

fulfilment of the requirements for the award of the Degree of Doctor of Philosophy and

submitted in the Department of Paper Technology of the **Indian Institute of Technology**

Roorkee, Roorkee is an authentic record of my own work carried out during a period

from July 2004 to October 2008 under the supervision of Dr. A. K. Ray, Professor,

Department of Paper Technology and Dr. S. Mukherjee, Professor, Department of

Electrical Engineering, Indian Institute of Technology Roorkee,Roorkee.

The matter presented in this thesis has not been submitted by me for the award of

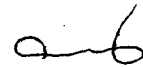any other degree of this or any other University/Institute.

(RAJESH KUMAR)

This is to certify that the above statement made by the candidate is correct to the

best of our knowledge.

(S.Mukherjee)   (A.K.Ray)
Supervisor   Supervisor

Dated: 6|10|2008

The Ph.D Viva-Voce Examination of **Mr. Rajesh Kumar**, Research Scholar, has

been held on

Signature of Supervisors   Signature of External Examiner

For consistency control one case is a SISO system for which both Lambda and Ziegler Nichols(Z-N)tuning methodologies have been used to find out the PID and PI control parameters for both analog(S-domain) and digital(Z-domain) control system. As usual for Z-N tuning, however Bode's stability criterion has been used. After developing the characteristic models, a PI/PID based control loop and the corresponding SIMULINK model have been developed. For the same case of SISO consistency control an ANN control system (BPNN) along with the necessary algorithm has also been designed. The network is trained with PI/PID simulated data. Similarly the second case of consistency control with two inputs and single output (TISO) has been dealt with assuming negligible interactions between parameters. Accordingly simulations have been carried out for both PI and ANN controllers.

For stock flow control model equations are already available. In this case mill data for training for ANN controller are employed. Data predicted from theoretical models are also used for training purposes. For the case of total head control an example of control loop with hydraulic headbox available in literature has been used for analysis. The dynamic models of all the elements of closed loop have been found out and closed loop transfer function are developed. This has been used for further analysis through MATLAB simulation and neural computation. Similar analyses have been made for stock level, pH, temperature and basis weight, first by developing appropriate dynamic models in laplace domain, converting to Z-domain, then designing classical control loops and analyzing them. These are then followed by transforming in to a neural network based control system. It is well known that if the process interactions are significant, even the best multi-loop control system may not provide satisfactory control. In these situations there are

incentives for considering multivariable control strategies such as decoupling control and model predictive control.

Hence, development of control system for MIMO systems with some examples from paper machine wet end including headbox has been attempted. The examples are: interactions of total head and stock level, air pressure and stock level (for air cushion head box), retention on forming wire and consistency control with two inputs and single output (TISO)system. For multi input multi output (MIMO) system considered in this present investigation both relative gain array (RGA) and decoupling techniques are used. For the case of MIMO system, however, the same procedures as in the case of SISO system have been followed. The only additional parameters of control included in the analysis of MIMO system for estimating the degrees of interaction and pairing of controlled and manipulated variables between different sets of control loops have been the relative gain array method (RGA) and decoupling technique for adjusting the interaction. The relative gain between 0 to 1 are only considered for analysis.

In chapter-6, an attempt has been made to compute data from various models for both SISO and MIMO system using the classical controller and neural network based control with the help of MATLAB SIMULINK toolbox. The procedures laid down in Chapter-4, the various equations presented therein, the algorithm developed for the ANN and for PID, and finally the models developed for the various wet end parameters given in Chapter-5 are used.

From the plethora of data from MATLAB Simulation of the process parameters, some dynamic characteristics have been drawn in various graphs with response as a function of time for all the above mentioned parameters when unit step input signal is applied as a forcing function and then performances are evaluated.

While for consistency control, the dynamic responses using both PI & PID are studied and compared with performances of ANN based controller, the cases of total head, stock level and pH only PI and ANN, for temperature and basis weight only PID and ANN are employed, analyzed and compared.

Conclusions based on the present study are finally drawn in the concluding Chapter-7, conclusions and recommendations. Recommendations based on the present work, limitations and scope of further study are also briefly discussed in this concluding chapter.

ACKNOWLEDGEMENT

(RAJESH KUMAR)

RESEARCH PAPERS

1. Kumar Rajesh, Ray A.K., and Mukherjee S., Using a neural network system for basis weight control, IETECH (International Engg. and Technology) Journal of advanced computations, vol-1, pp 74-78, 2007.

2. Kumar Rajesh, and Ray A.K., Artificial neural network for solving paper industry problem-A Review, Journal of scientific and industrial research, vol.65, pp.565-573, July 2006.

3. Kumar Rajesh, Ray A.K., and Mukherjee S., Application of artificial neural network (ANN) based control system in the paper industry: A Review, National conference on Frontiers in applied and computational mathematics (FACM-2005), Thaper Institute of Engg. and Technology, Patiala, pp. 199, March 4-5 2005.

4. Kumar Rajesh, Ray A.K., and Mukherjee S., ANN based soft computing technique for simulating paper industry problems, all India seminar on emerging trends in mechanical Engg., National Institute of Technology Kurukshetra, pp. 547, March 29-30,2005.

5. Kumar Rajesh, Ray A.K., and Mukherjee S., Back-propagation neural network for solving paper industry problems, International conference on computer applications in electrical engg recent advance, (CERA-2005),I.I.T.Roorkee., pp.338-342, Sept.29 to 1st Oct 2005.

6. Kumar Rajesh, Ray A.K., and Mukherjee S., Application of fuzzy logic control system in pulp and paper industry, National workshop on leveraging IT and process automation in pulp and paper industry. (IPPTA), Cochin, Kerla, pp.1 21st -22nd of Oct.2005.

7. Kumar Rajesh, Ray A.K., and Mukerjee S., Design of artificial neural network controller for fine flow head box control in paper machine, International conference on Intelligent systems and networks(IISN-2007), Computational intelligence laboratory and MAIMT, Jagadhari, Haryana, pp. 348-452. Feb. 23-25, 2007.

8. Kumar Rajesh, Ray A.K., and Mukherjee S., Evaluation of performances of artificial neural network taxonomy for paper machine head box controller design, International conference on recent advances and applications of computer in electrical engineering, Engg. College Bikaner, Rajasthan, March 24-25, 2007.

9. Kumar Rajesh, Ray A.K., and Mukherjee S., Design of artificial neural network controller for consistency control in paper machine head box, International conference on recent advances and applications of computer in electrical engineering, Engg. College Bikaner, Rajasthan, March 24-25, 2007.

10. Kumar Rajesh, Ray A.K., and Mukherjee S., Artificial neural network modeling of the paper machine, International conference on recent advances and applications of computer in electrical engineering, Engg. College Bikaner, Rajasthan, March 24-25, 2007.

11. Kumar Rajesh, Ray A.K., and Mukherjee S., Paper machine head box control using different artificial neural network taxonomy, National conference on grand challenge in electrical engg, Rayat Institute of Technology and Information Technology, Railmajra, Ropar, Punjab. April 28-29 2007.

12. Kumar Rajesh, and Ray A.K., Comparison between different artificial neural network controllers for water bath temperature control, National conference on Advances in chemical engg. & Tech, Sant Longowal Institute of Engg. and Technology, Sangrur, Punjab, March 26-27, 2007.

LIST OF CONTENTS

CHAPTER-1
INTRODUCTION

1.1 Status of Indian pulp and paper mill:

The paper Industry accounts for 3.5% of the world's industrial production and 2.0% of world trade with an employment potential of over 3.5 million people. India with 16.0 % of the world population consumes approximately only 1.0-1.25% of the world's paper production. In India the paper industry is one of the 35 high-priority industries and belongs to a core sector industry.

Paper is an essential commodity material. Per capita consumption of paper in a country is an index of civilization and directly proportional to the literacy rate of a country. In India though per capita consumption is very low, on an average 6.5-7.0% compared to developing country's average of 12.0 kg and developed country's average of 152 kg, the growth rate is very high. The present growth rates are: 5.0-6.0% for cultural paper and paper board-the largest segment (45.0%) of the market share, 4.0% for newsprint,10.0-15.0% for industrial paper, and 15.0-20.0% for corrugated packaging. This is almost three times higher than those in USA and Europe. This data amply indicates that there is an upward swing in terms of Indian economy (GDP and GNP) and growth of this industry in this country. In the year 2006, the production achieved was 54.8 lakh tonnes paper and paper board, 10.9 lakh tonnes of newsprint, totaling 6.57 million tonnes.

It has also been predicted that In the year 2010 and 2015 the demand forecasts will be in the range of 8.5-10.0 million tonnes and 10.8-14.0 million tonnes respectively. In 2010, while the growth rate of the pulp and paper industry the world over and in Asia will be 2.2% and 4.4% respectively, this rate will be much higher for India. With the expected increase in literacy rate, the growth of the economy and an increase in the per capita

consumption, a very high growth rate is expected in the near future. Massive investment in terms of capacity and technology will be required in the Indian pulp, paper and allied Industries to take up the challenges for meeting the demand of around 14 million tonnes by 2015. Therefore Indian paper industry inducts an attractive proposition to the global market for necessary investment in this sector.

This Industry is however, capital intensive in terms of consumption of raw materials, chemicals, energy (both thermal and electrical), water and labour. It also generates huge amount of pollutants (solid, particulates, liquids and gaseous emission). Approximately 2.5-3.0 t of raw materials,150-200 m^3 of water, 8-15 t of steam and 900-1500 Kwh of electrical energy are required for one tonne of paper. This leads to generation of pollution loads to an extent of 24.0-45.0 kg of BOD, 80.0-150 kg of COD, 2.0-5.0 kg of AOX in the effluents. The consumption of the above inputs are therefore disproportionately high and at the same time due to high cost of energy and other inputs compared to North American or European Industry, the Indian industry is struggling hard for its sustainability. There are around efforts in India to reduce all these inputs to the level of international standards for mere survival, for sustained production and to stand the stiff competition in international market. The main reasons for low profit-investment ratio, low capacity utilization are due to lower production capacity, adopting relatively older technology, obsolete equipment and low degree of automation. In order to keep pace with sustainable production to meet the ever increasing demand of paper in India, some of the measures to be taken by the Indian industry are: to upgrade their process and equipment technology, scaling up the process and equipment, to seek optimum design and operational parameters, introducing up-to-date process instrumentation, measurements and control. In fact, the use of automation and control is not very widespread unlike many

2

chemical process industries in Indian industry. The low degree of automation (2.0-3.0% of investment) is one of the causes for low profit to investment status of this industry. Though a few industries are slowly adopting new process and equipment, the status of sophisticated instrumentation and control has remained almost stagnant. Therefore it is felt necessary to carry out more investigation in the area of instrumentation and control.

The paper is produced through a number of unit operations and processes in a paper industry. From instrumentation view point these may be termed as subsystems like raw material preparation, pulping, washing of brown stock, bleaching, stock preparation, approach flow system, wet end operation, drying, calendaring and chemical recovery operation. Surface sizing, filling and coating are rather additional operations. Chemical recovery operation in turn consists of concentration of waste liquor, combustion, causticization and calcinations of lime sludge. Some instrumentations and control systems are in use for some subsystems of Indian mill, but the same in paper machine area is rather meagre except in drying operation. Major emphasis is thus needed in the wet end of paper machine. Even in the wet end approach flow system, headbox and former, preferential priority must be given. Use of proper measurement and control in headbox approach flow, headbox and former in Indian paper industry thus become an imperative necessity.

In Indian paper industry in paper machine wet end, manual control and offline measurements for parameters like pH, temperature(optional),flow, consistency, stock level, total head, retention have been in use in many situations. Of late if unavoidable some have started adopting on line continuous measuring instruments and classical P/PI/PID control. This is only applied when it is absolutely necessary and manual control is not providing at all the required service. One barrier to use classical control system

instead of manual control is the cost of the on-line sensor or transducer, transmitter, measurement system and the controller which Indian paper mill could not afford so far.

It is well known that most the parameters in chemical process industries usually nonlinear in nature. Paper industry wet end process parameters are not the exception. This process may be controlled usually using single input-single output (SISO) system, also referred as single loop control concept. In this case, the control problems have only one controlled variable and one manipulated variable. But in many practical control problems of chemical process industries, more than one control and more than one manipulated variable are involved. These problems are referred to as multiple-input multiple-output (MIMO) control problems. Besides, most the parameters in this subsystem of paper industry, i.e. wet end are interactive in nature, thus belonging to MIMO system which needs decoupling the loops.

Chemical process Industry in general and paper industry in particular rarely concentrate on these issues and depend largely on the consultants and suppliers of the DCS whose design philosophy for loops for control processor(CP) and application processor(AP) are not known to the customers. Linearizing a nonlinear control parameter is also an approximate one. Classical control loops can serve some purpose by suitably tuning the controller with the entire process loops by trial and error methods. It is also a fact that the assuming linear transfer functions for nonlinear parameters affect the accuracy and reproducibility of the measurands and control action will not be very satisfactory.

Hence, there is an urgent need to address these issues and enough room exists for further studies in this important area of paper machine for the benefits of Indian paper industry.

4

One important aspect for designing of a control system is the dynamics of the elements of the loop such as process, sensing device, controller or final control elements irrespective of the parameters are linear or nonlinear, non-interactive or interactive in nature. The most difficult one is to assess for the process which has dead time of significant magnitude .The time constant is also relatively unknown. In addition it is not possible to perform experiment in industry to find out the values of various parameters of control systems, such as delay time(t_d), rise time(t_r), settling time(t_s), overshoot (overdamping, critical, and underdamping), and offset. Designs of all control systems depend on the values of time constant (ζ), controller gain (k_c), and process gain (k_p). In absence of data it is practically impossible to design and analyse a robust control system and to asses its loops performance normally used in distributed control system (DCS). Researchers and designers therefore explore the possibility of using pilot plant data or computer simulated data for designing such a system. However, the data on pilot plant for control of headbox, and approach flow system are very scarce. Most of the parameters needed for designing control system or in existing industry in operation are shrouded with secrecy. There is therefore enough potential remaining to further study the parameters of dynamics of the system in order to design a classical control loop for wet end operation of paper industry. In this situation it is prudent to also re-examine the dynamics of classical control loops already reported.

On the other hand nonlinear loops can be examined by several methods like phase plane analysis, function techniques, model adaptation and knowledge based system. But the most recent one is the use of Artificial Intelligence (AI) techniques.

1.2 Artificial Intelligence and its use:

Use of artificial intelligence (AI) has of late become an indispensable tool for optimization and control of various process parameters in chemical process and allied industries including pulp and paper. The AI includes mainly artificial neural network (ANN), Fuzzy Logic (FL), Genetic Algorithm (GA) or their combinations. Typically these are: Neuro-Fuzzy, Fuzzy-GA, Neuro-FL-GA etc. Out of the so many methodologies available, in overwhelmingly majority of cases ANN is found by the designers to be the most convenient one and is currently being applied in almost all process industries for optimizing, process modeling, simulating, fault detection and diagnosis and controlling of various processes and operations. In addition, neural networks have also made significant aids in the area of continuous speech recognition and synthesis, pattern recognition, classification of noisy data, nonlinear feature detection, and market forecasting, weather forecasting and adaptive control. ANN can assimilate operating data from an industrial process and learn about the complex relationships existing within the process, even when the input-output information is noisy and imprecise. This ability makes the neural network concept well suited for modeling, especially complex industrial processes. Because industrial operating data are widely available from distributed control system (DCS), neural network modeling based on past data appears to be a generic and cost-efficient approach that can be applied across many plants including pulp and paper. It has already been indicated that all the subsystems of paper industry are intricate in nature, generally nonlinear in character and often too complicated to be accurately described with physical models. Neural networks are powerful tools that can solve a variety of nonlinear modeling problems of this industry.

ANNs represent a new technology that mimics the structure and process of biological neural systems, i.e. brain. This tool has become a remarkable one and uses a rule based systems and traditional data base manipulation techniques to form a neural network control system performing two functions: one, the creation of software sensors, which provide on-line measurements of variables that in the past could only be measured in the laboratory; other, an advisory control system to complement a regulatory control system addressing the previously described complex multi-variable applications. In fact, these abilities make the neural network technology very well suited for solving problems in the complex process industries like pulp and paper. Application of ANN in modeling and control in paper industry has been in focus in almost all areas except paper machine wet end system, especially paper machine headbox. Attempts can be made to use these important techniques in modeling and control.

However, before attempting to control system design for paper machine, some basic elements and methodology of ANN need to explained. These are discussed briefly in the following sections. For designing of ANN, a few parameters need to be defined. These are:

1.2.1 Activation function or transfer function:

This function is also sometimes referred to as squashing function.The activation function, architecture of ANN (single layer or multilayered), algorithms to be adopted and the learning process involved (supervised or unsupervised) are required for designing ANN based control system.

The transfer function takes the input (which may have any value between plus and minus infinity) and squashes the output into the range 0 to 1.Some of these transfer functions, generally used by the designers are summarized in table-1.1(Appendix-1).The log-

sigmoid transfer function is most commonly used in multilayer networks that are trained using the back-propagation algorithm, in part because this function is differentiable.

One of the major tasks in the design of a neural network is the selection of architecture which depends on the nature of the problem. Inappropriate choice of ANN results into poor performance. The commonly used network architectures for modeling and control applications, ADALINE (ADAptive LINear Element) and its extension to MADALINE (for many ADALINES), feed forward neural network (FFNN), forward-propagation and back-propagation. The architecture of feed forward is the most popular structure in practice due to its non-parametric, non-linear mapping between input and output. Networks with this architecture are known as universal approximators, including multilayer feedforward neural networks employing sigmoidal hidden unit activations. These networks can approximate not only an unknown function but also its derivative (29).

The feedforward neural networks include one or more layers of hidden units between the input and output layers. All connections point from input towards output. Multilayer of neurons with nonlinear activation functions allows this type of neural network to learn nonlinear and linear relationship between input and output vectors. Each input has an appropriate weighting vector W. The sum of the weighted inputs and the bias B or b forms the input to the transfer function. Any differentiable activation function may be used to generate outputs. Three of the most commonly used activation functions are purelin, log-sigmoid and tan-sigmoid (table-1.1, Appendix-1). The activation functions of the hidden units have to be differentiable nonlinear functions. If activation function is linear, then one can always collapse the net to a single layer and thus lose the universal approximation capabilities. Each unit of the output layer is assumed to have the same activation function.

1.2.2 Artificial neural network learning/training processes:

All artificial neural network needs learning/training which implies that the neuron somehow changes its input/output behaviour in response to the environment. Neurons in the network learn by changing the weights on the inputs. Learning methods in neural networks can be broadly classified into three basic types: supervised, unsupervised, and reinforced. These are further sub classified as: error correction gradient descent, stochastic, least mean square, backpropagation and hebbian, competitive etc. Most of the researchers and designers prefer to use supervise learning with gradient descent technique either using least square or backpropagation techniques. Augmented backpropagation networks, i.e. logarithmic neurons and exponential neurons added to the neural network's input and output layers and conjugate backpropagation neural network is used to avoid time consuming line search. In unsupervised learning method, the target output is not required to learn by itself.

These techniques have potential for training of ANN in paper machine approach flow control system design. Therefore, studies must deal with various appropriate learning techniques to design approach flow system. Perhaps there is no literature available in correction with the approach flow system design.

1.2.3 Artificial neural network control methodologies:

There are various control methodologies used for controlling the process such as supervised control, direct inverse control, model referenced adaptive control namely: direct adaptive control, indirect adaptive control, back propagation through time control and adaptive critic control etc (85). Although all are used in specific situation, former two are mostly adopted by the practicing and design engineer.

When the data to be generated, supervised control can take help of a classical control for learning whereas direct inverse control employs the input-output data from plant or process. This should be carefully examined and scrutinized.

1.3 Need for applying ANN in paper making process:

There are many problems found in pulp and paper mills that have characteristics which make this problem difficult to handle from a control standpoint. This is mainly due to the nonlinear nature of most of the subsystems of paper mill. Combination of a neural network system, a rule based system and a conventional computational system can provide a tool to handle these problems with simplicity and effectiveness. Neural networks can also be very useful for "quick and dirty" models (19). The ANNs are able to accurately represent even complex nonlinear behavior, the nature of which is not known to the user (124). It is with this intention this present problem has been undertaken to develop control system with artificial neural network application in paper machine headbox which has been dealt till now very sparingly. As already indicated, paper making process consists of a large number of subsystems (unit operations and processes). Some of the applications related to modeling and control of paper mill subsystems are depicted in chapter 2, section 2.3.

1.4 Present Objectives:

The present investigation has been planned to study the various aspects required for designing control systems using artificial neural networks for wet end paper machine parameters, approach flow and headbox in particular with the following distinct objectives:

1. To develop and analyze appropriate dynamic models in both continuous and discrete signals for consistency, total head, level, pH, stock temperature and basis weight assuming all these parameters as linear systems in approach flow system

10

and headbox of a paper machine. These models are based on unsteady state material balance or energy balance or combination of both the two.

2. To design various closed loop control systems for consistency control using classical controller (PI/PID as the case may be) and Bode stability criterion assuming servo or regulator problem and then to design the process using the estimated controller parameters. These will be followed by selecting appropriate tuning methodology and to compare the responses for both PI and PID and also with continuous and discrete signals.

3. To analyze the available data for stock flow control in industry and to compare the responses with theoretically model predicted data assuming typical flow control techniques prevalent in many Indian paper mills.

4. To study the responses of all other control parameters as mentioned in step-1 by suitably designing appropriate control loop for each parameter and to compare the responses with continuous and discrete signals.

5. To develop and analyze the models for basis weight control in approach flow in both analog and digital systems and to compare their responses.

6. To design a model for the MIMO system such as interaction of total head and stock level, air pressure and level in a pressurized headbox, stock flow and stock level, and retention process in the wet end and then to compare the results of total head and stock level assuming them as SISO system as in step-4.

7. To convert all the above models of control parameters of the wet end approach flow system including headbox as mentioned above(steps no. 1-6) in to a neural system using the various procedures for neural computation(feedforward, back

propagation, ADALINE) with changing values of ANN parameters such as momentum and learning rate, and others.

9. To compare the results of ANN based computation using MATLAB simulation with SIMULINK tools with those estimated values from classical control loops for all SISO and MIMO system.

CHAPTER-2
LITERATURE SURVEY

This Chapter attempts to review the literature pertaining to the artificial neural network, modeling, simulation and control aspects of paper mill in general, approach flow system and headbox of wet end paper machine in particular,and the application of ANN in all the aforesaid areas, especially the design of control systems in a paper mill.

2.1 Artificial neural network:

Using artificial neural networks (ANNs) paradigm has become a powerful tool and thus a potential solution strategy to solve complex problem or problems with unpredictable and imprecise information or where data are incomplete. The examples are: process engineering, process design (168,169), modeling and simulation (173), process supervision, control and estimation (92), process fault detection and diagnosis which rely on the effective processing of complex data.

The use of artificial neural networks (ANNs) and its associated factors in solving problems have been shown concisely in Chapter 4 Section 4.3. Because of its ability to represent nonlinear mappings between input and output of the problems such as modeling, simulation, optimization and control of chemical engineering systems including of paper mill sub systems, they can be most readily exploited in the synthesis of nonlinear systems.

In the following paragraphs a comprehensive review of these applications are reproduced here, just to stress on the feasibility of various methodology of ANN such as backpropagation, ADALINE, feed forward etc. in real life problems with proven technology in existing paper mills.

Viharos et al. (161) described a novel approach for learning and applying artificial neural network models based on incomplete data. The developed algorithm is compared with three data-extending-methods and resulted in a model with superior estimation capabilities. The algorithm is tested through artificial data and found that it is completely able to handle missing output data.

Hernandez et al (56) studied the stability of the model's inverse. If the neural network model of a system is trusted at least around some operating point, then the inverse dynamics of the model can provide a good indication of how the plant's inverse may behave.

Vanhala et al (160) suggested that artificial neural networks can be used to model difficult complex systems where only input-output data are available.

Irwin et al.(64) used multilayer perceptron (MLP) neural networks to offline identification of a simulation model of a 200MW boiler ,oil fired, drum type boiler with turbo generator unit at Bally lumford power station in Northern Ireland.

Ozgur et al.(98) suggested that the Levenberg-Marquardt algorithm has been found being faster and having better performance than the other algorithms in training.

Savkovic-Stevanovic (131) developed and applied neural networks for analysis and optimization of industrial production data. Artificial neural networks based on feed-forward architecture and trained by the back-propagation technique.

Andre et al (3) used neural networks successfully for steady state process modeling. He further applied dynamic neuron network (RDNN) for predicting non-linear ties such as asymmetric dynamic response including steady state modeling, steady state planning and steady state optimization.

Barry et al. (8) demonstrated model based predictive control (MBPC) through numerous on-line industrial applications to be an accurate and robust method of process control.

Wilson et al (170) presented online state estimation of process systems based on embedding a hybrid ANN mechanistic process model within an extended kalman filter. The filter algorithm calls for local linearization of the process model and general formulae for evaluation of the Jacobian matrix for a feedforward neural network are also presented.

Surya (153) suggested that neural networks have made strong advances in the areas of continuous speech recognition, pattern recognition, classification of noisy data, nonlinear feature detection, market forecasting, and process modeling. These abilities make the neural network technology very well suited for solving problems in process industries.

Bhat (15) suggested that neural networks have been shown to be successful in modeling nonlinear dynamic systems. Its use has also been proposed in model-based control algorithms and as nonlinear controllers by identifying the plant's inverse by Psaltis et al (111).

Di Massimo, et. al (32) investigated the applicability of neural networks for improving process operability. Techniques based on the use of neural network based model (NNMs) may offer significant advantages over conventional model based techniques.

Scott et al (133-137) has extensively studied on applications of knowledge based artificial neural network for various practical solutions of many intricate problems of linear model structures. The most important applications were laid in the field of CSTR modeling, design and control. He has used the known dynamics for single and multi stage CSTR battery and then converted them in to artificial neural networks based solution. He has cited comparison between conventional PID and ANN based control and demonstrated how refining of PID controller using neural networks has been possible. He further

interpreted nonlinear models by creating nonlinear NN process models. These applications can be used conveniently in CSTR system in paper industry (causticization).

2.2 Modeling, simulation, measurement and control of paper making subsystems:

Ullmann et al (159) recognized that frequent and accurate control of key pulp parameters are determining factor of end product quality.

Garceau and their co-workers (43, 44), Dion and Garceau (33-36) further developed the control strategy for on-line characterization of the fiber size of pulp by acousto-optical methods in various operations of paper industry including the wet end operations. The models developed for the purpose for both optical and acoustical techniques have been simulated through experimental results. Further models are also developed for kraft pulping delignification kinetics for making pulp and then post treatment pulps have also been characterized through on-line methods.

Ghosh (45-48) worked extensively on modeling and simulation, wet end chemistry, paper drying and optimization, refining and screening.

Ramarao and his co-workers (114,115) developed models for the gravity drainage of papermaking suspensions, pulp characterization using permeability measures, using measures obtained from drainage data based on both permeability and compressibility, establishing relationship between compressibility and permeability with lime mud and papermaking pulp, retention of filler and fine particle retention in incompressible and compressible fibrous media in the wet end of paper machine, and solved the models with numerical techniques and finally simulated the models through experimental data.

Banerjee et al (5-6) carried out extensive investigation on various aspects of many operations of a paper mill. Some of the processes include improving energy efficiency, improving centrifugal cleaner efficiency, modeling, simulation and control.

Potusek (108-110) investigated the dispersion modeling using one dimensional parameter (peclet number) and then simulated through experimental data of displacement washing of pulp in a series of experiments. These models could be used as a basis for controlling not only brown stock washers, and bleach washers but also in wet end formation for some of the parameters.

David wood(27) presented a comprehensive description of modern concept of headbox control and explained how consistent paper properties across the paper width is possible by positioning the slice as near to parallel as possible by stabilizing the headbox and slice lip mounting against temperature variations. He further emphasized that the automation and adjustable slice lip can improve headbox control. Peter Seifert investigated basis weight variations in headbox approach system and discussed the effects of pump pulsations and dampening.

Pearson J.H (105) discussed about functions of automatic headbox operations for both open and closed headboxes and design the various control loops for various concern headboxes. Further demonstrated the headbox model no.200 with the variation of speed, total head range selection, with range selector switch position, an instrumentation point and pump operation under vacuum and pressure. The discharge coefficient has been assumed as one.

Singhal (144,145) designed low cost basis weight control system for small paper mill. Basis weight control particularly when manufacturing reel orders is very important and discussed manual control and feed forward control systems. Basis weight control with feed forward control is a good choice for the small paper mills who cannot afford costly QCS system.

Johnson (66, 67) has reviewed the basic measurement and instrumentation applied to paper machine wet end operation. The principle of the measurements of flow, level, density, consistency, pressure, temperature, pH, freeness, speed and draw were presented. He further reviewed various unit processes making up wet end of paper machine from instrumentation and control stand point aspects with the design of strategy of various control, sub loops. He further shown how an integrated system with feed forward technique developed to improve the process automation through the microprocessor technology and distributed control system.

The headbox modeling in terms of process response has been done from the first principle by Mardon (83) and Smith et al(150) by including conservation of mass of the liquid and gas phases assuming ideal gas law which relates air pad mass, pressure and volume, the relationship have been linearised about operation point based on machine speed. Donald cited the advantage of mechanistic model developed by the above investigator in terms of automatic tuning facility which schedules the controller parameters based on machine speed and indicated that the response of headbox parameters can be modeled from the first principles.

Talvio(154), Smith(150), and Chao et al(22) for their investigation on theoretical and experimental studies in to the stability and control of paper machine headboxes, and control system with linear transfer functions.

Dumdie(37) has developed the system approach to the consistency control and dry stock blend. Bhartiya and his coworkers (14) developed a thermo-hydraulic model based management of kappa profile for feedstock grade transition in a continuous digester which can simulate the plug flow behaviour of the motion of blends of hardwood and

softwood wood chips. Two controller strategies, namely decentralized PI and linear Model Predictive Control were explored.

Francis and his co-workers (40,41) has reported application of model-based control strategy for to the pulp and paper industry with particular reference to kappa number profile control of continuous pulp digester by empirically derived process model using subspace identification techniques. A state space model predictive control algorithm is used to adjust five manipulated inputs in order to regulate five process outputs, in response to five randomly varying process disturbances (of three are measurable) .Profile sensitivity to closed loop response is also explored.

Paulonis and Krishnagopalan (102-104) developed adaptive inferential control system based on mathematical models with on-line liquor analysis to predict kappa number using In-Situ conductivity sensor. Ion chromatography refractive index and UV absorbency analysis measures various other parameters. Kinetics of kraft delignification based on liquor analysis, liquor concentration measurement for causticizing control and later the state space modeling of modified kraft pulping were also developed.

Balderud et al (11) presented numerical experiments for both mixing characteristics and transport delays in the piping network have a significant effect on wet-end attenuation of stock concentration disturbances. The transport delay in the pipe runs introduces resonance frequencies that can be enhanced by both operating conditions and process design.

Turnbull et al (158) derived a one-dimensional model of a paper forming process on a single wire crescent former from fundamental conservation laws. The model can describe dynamic and steady state behavior of the forming process.

Rigopoulos et al. (121) studied the paper properties such as basis weight, moisture content and caliper which are the functions of the direction along which the paper moves-machine direction, direction across the width of the paper machine, and cross direction.

Waller (163) has made an extensive survey of developments of control of paper making headboxes and their in-corporation into forming section. Detailing about the headboxes for twin-weir and fourdrinier machine with their equipment and control description has been emphasised.

Panda (99, 100) in his various publications discussed theoretical approaches for improvement of pulp yield, energy consumption aspects of pulp and paper mills, analysis of detailed cost for newsprint production from Hindustan Paper Corporation, India and indicated how to make the industry more energy efficient and cost effective & also analysed the pulp samples collected from different sections, namely stuff box, headbox and couch press of three newsprint mills in India. The pulp samples were collected from mills based on chemical bamboo pulp, imported CTMP, eucalyptus CMP and refined in both PFI mill and Sproud Waldron refiner up to the same freeness level. The parameters determined were: freeness, drainage time, ash content, fiber fractions based on Mc-Nett Bauer classifier and finally print through (Macbeth density) properties of hand sheets through IGT printability tester.

Tuladhar et al(157) studied nonlinear dynamic modeling of headbox and wet end pressure pulsation analysis derived from first principle for Sym-Flo headbox, the hydraulic headbox with certain assumptions. Results were presented of mill test on an operating paper machine and MD basis weight signal flow were analysed. The result indicated the presence of very low frequency variation, caused by consistency dynamics. Silicon clay addition has been shown to cause a blending problem. The pressure pulsation analysis

20

has also been shown to significant improvement in the wet end performance after adding a second screen. The simulation result indicated that the decoupled control action is feasible using MPC controller.

Kumar Prasanna et al(77) has described paper machine control and optimization for different sub system of paper machine loop including consistency control in approach flow, headbox, mainly single variable and total head have been controlled traditionally by controlling air pad for stream flow valve, the recirculation valve or by fan pump speed control. The jet wire ratio is cascaded with the total head and any changes in wire speed are feed forward to the total head controller in order to maintain jet wire ratio. They suggested also the control strategy for consistency and furnish control using ratio control. Method of analyzing variability that exists at a particular period is discussed and suggested an elimination method.

Whalley et al(166)addresses the problem of regulating the flow of pulp solution or stock from a fourdrinier paper making machine headbox. A multivariable, time invariant model for a fourdrinier machine headbox is considered. An optimum, minimum control effort strategy is proposed. The headbox model contains a perfect integrator which slowly changes the head box level and hence the output flow rate.

Keswani (72) has reported the status of various instrumentation and control system in pulp and paper industry including the wet end operation. Indigenous capability for design and manufacturing of electronic process control in pulp and paper industry has been emphasized.

The designing of measuring systems for flow, pressure, level, temperature, consistency, moisture, basis weight, and speed, tension and draw have been exemplified. The feasibility of on-line measurement system and the control application are extensively dealt

with from the industrial point of view. He further analyzed in details the relative gain of using microprocessor/electronic control system under the roof of DCS application as a whole in the paper mill.

The necessity of various types of process control applications in a pulp and paper mill have been dealt with by Mishra (87), Rao (116-118), and Bihani et al. (16-18). However most of the works of the above researchers are devoted to pulping and bleaching of woods, mixed hardwoods and non woods. Economic utilization of alum in sizing has been emphasized by Rao (119).

Rao, Bansal, and Ray (119) studied the application of various methods to measure the relevant parameters in a pulp and paper mill emphasizing the status of instrumentation in paper mill with particular reference of paper machine. They have further retreated the selection of instrumentation in terms of cost and added that in paper machine section the measurement and control of headbox temperature along with headbox level are essential. And also developed a model for profitability analysis of synthetic wire in wet end section of a paper mill and simulated the model with various data from the wire of a number of mills.

Sankaranarayanan and his co-workers (127-129) reviewed exhaustively the use of electronic control and the parameters of importance for monitoring /control to maintain the paper quality in mills such as basis weight, moisture content, thickness or caliper, brightness, color and opacity of paper, ash content, consistency of stock, headbox consistency and quality of pulp. Developments of indigenously microprocessor based instruments for designing real time high consistency transmitter, low consistency monitor based on radio frequency technique, real time scanning or measurement of basis weight with wide range (40 gsm-500 gsm) by neucleonic technique, moisture monitor, and profile

control of paper machine for bone weight, moisture and basis weight by both analogue and digital techniques have been made. Further, dynamic measurement of thickness, measurement of color and turbidity, nondestructive technique for measuring tensile strength and breaking length using sonic wave propagation and coat thickness measurement have been demonstrated. In all the cases of measurement of parameters field testing were performed. For control of basis weight dynamic models were developed, simulated and used for testing in the mills for single loop feedback control in paper mill. Besides the development principles of computer control of digester were reported.

Aidun et al (1) studied two kinds of secondary flows in headbox derived from geometric effects and kinematics and the other from turbulent motion of the flow field and the developed model was analysed through direct numerical simulation.

Scott. Pantaleo(138) developed a new headbox design featuring consistency profiling decoupled from fiber orientation response which provided narrower basis weight response than a slice bending system.

In the area of dry end of paper machine, modeling and control system were developed by Chen (24) through analytical modeling and process identification and implemented and tested on different types of paper machines. Heaven et al. (55) examined some of the traditional parametric identification techniques applied to data collected from a paper machine. Process data obtained from a paper machine excited with pseudo random binary sequences (PBRS) are used to determine process dynamics needed to evaluate exciting and new control strategies. Rigopoulos et al (121) developed control relevant disturbance modeling of paper machine full profile properties using adaptive PCA. Development of state variable model by Berrada et al.(13), parameter optimization by Akesson Johan (2),modeling and control for drying section of paper machines by Xia et

al.(172) , modeling and simulation of paper drying by Wilhelmemsson et al.(167), optimizing paper machine dryer control by Nelson and Gardner(93).

Orccotoma et al (97) investigated the effect of disturbances on the two output variables of paper machine with twin wire formers (gap formers), viz, basis weight and first pass retention by using the concept of controllability. Time delays and high frequency disturbances of the thick stock consistency were shown to affect the process. Importance of consistency loop in the mixing chest of pulp preparation area of paper machine has been found to be critical. Analysis of a paper machine forming zone in a newsprint mill was performed to determine the maximum allowable variability of pulp furnished to the process. First-pass retention is considered an uncontrolled variable and found to be dependent on fines content of the thick stock. They have demonstrated that the nonlinear processes (basis weight and first pass retention) can well be represented by linear models. Non-linearity did not pose any significant error.

Nissinen, et. al. (95) studied the feasibility of designing multivariable PI controller for headbox with rectifier rolls without overflow provided with air cushion in a multi-grade paper machine. The system has been considered as multiple input-multiple output (MIMO) instead of single input- single output (SISO) system. The process dynamics for such system was identified. Based on the process model and the structure of the multivariable PI controller a process simulator was built using Simulink. The simulator was used to test different tuning methods which could be applied to the system.

2.3 Modeling in paper mill subsystems with ANN:

Qian et al (113) modeled and implemented a complex wood-chip refining system using feed forward neural network. A neural network model was trained using data from a

commercial CTMP refiner. The model's predictions of pulp and paper properties were in excellent agreement with industrial refiner data.

Inferential models for kappa number are developed using the methods of partial least square regression (PLS) and feed forward neural networks.

Dayal et al (28) investigated above technique to build empirical models for kappa number using historical data from an industrial continuous kamyr digester. A static model for kappa number based on the 21 input process parameters has been developed.

The purpose of the model is to provide a real time indication of brightness so that operators can reduce chemical use. Zhu et al (173) developed the neural network models for D_0, E_{0p}, D_1 and E_2 to D_2 stages using ANNIE(artificial neural network integrated environment), in which, data preparation, network topology selection, network training, evaluation, modification, code generation and simulation are integrated. A single global neural network model for the bleach plant (D2 brightness) has also been developed and selected the back-propagation algorithm for multilayer feed forward networks.

Rooke et al.(122) presented a novel approach for modeling the retention of material(fines and fillers) on the papermaking wire using a combination of black box (neural networks) and physically derived models. ANNs model the complex evolution of the white water stock concentration very accurately, whilst the physical models of the mixing and blending chest, multistage centricleaners (hydro cyclones) and pressure screens are used to describe the headbox stock concentration.

Nenad et al. (94), studied feedforward neural networks applied to estimate the outlet water temperature of the scrubber process. The networks are trained with data obtained from experiments carried out on two pilot scrubbers. The neural networks consisted of seven inputs and one output. The inputs were mass flow rate, temperature, inlet humidity

of the supply air, mass flow rate of the water, inlet water temperature, height of the scrubber and water pressure in the nozzle. The output was the outlet water temperature from the scrubber.

Paper has different properties such as physical, mechanical strength, structural, optical and surface properties. Defect of paper is also defined in terms of some unwanting properties. Curl is one of such properties normally characterized as defect. Paper can be rejected if care is not taken during processing to eliminate curling. Paper "curl" can only be measured reliably OFF-LINE after manufacture, making it difficult to control.

Edward et al (39) predicted curl, normally an unwanting property (defect) of paper (from parameters defining the current characteristics of a reel and the plant machinery using neural network techniques and developed a model for the two tasks and used multilayer perceptron (MLP) neural networks with a sigmoidal output stage for the "in-specification" prediction and a linear output stage for the curl prediction task.

Temesgen (156) worked on the process design of black liquor multiple effect evaporator system after developing the modeling of the system and then solving by both numerical techniques-Newton Raphson or its modified methods and back propagation neural networks and compared the results. The superiority of ANN technique over the convention techniques was reported.

Kooi et al (76) proposed a backpropagation NN as a controller to replace the self-tuning regulator for providing a closed loop control of the energy in the woodchip refining processes. Both static and dynamic NN controllers perform very well in emulating the self-tuning regulator for processes having a non minimum phase properties. The dynamic NN controller provides a satisfactory control compared to the self tuning regulator.

Rudd (124) reported that there are many network paradigms in use today. For the multivariable continuous processes in pulp and paper mills, one successful network paradigm is the backpropagation network. It is one of the easiest networks to understand because it's learning and updated procedures are intuitively appealing.

Rudd (125) used the NN to determine real time values for soda loss, washer mat consistency & washer mat unit density in brown stock washer, the former is used as soft sensor. The target is to control stabilize the black liquor solids carried out by the pulp mat to the bleach plant. Results show a 25% reduction in standard deviation of the black liquor solids using an eight day trial. The controller also maintained larger disturbances in an automatic mode for the input variables. These values are used to control the washing operation. Data from a process domain is collected along with known results to develop training sets used to train a configured neural network. The structural configuration of NN controller is shown in Fig. 2.1. The NN based control strategy consists of dilution factor controller (DC), consistency (K), weight (w), speed(s) and flow controller (FC). NN controller (NNC) gets a signal for a set point or target value. The output signal from NNC goes to dilution factor controller which in turn sets out a signal to the flow controller in a cascading mode. The output signal from DC goes to control the flow of water to the filter mat. Similar configuration can be drawn for single stage bleach plant washer.
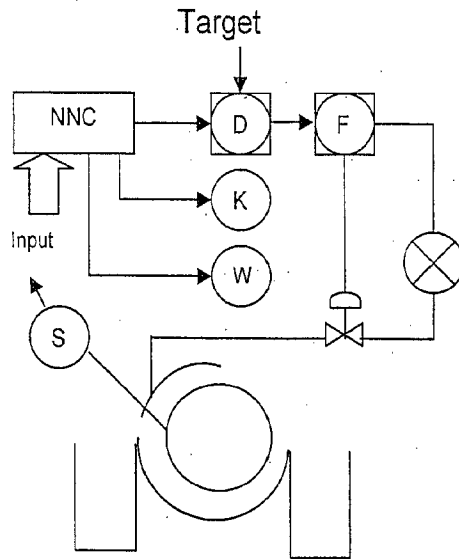
Fig-2.1 Neural network based control Strategy

Ozaki has described a system where the bed shape from the image analysis system is first classified by three layers back propagation NN in to three classes as ideal shape, wide based, and high. This is followed by a fuzzy logic controller which changes the air flows in to the recovery boiler by using the classifier information.

While the dynamic mathematical model has been developed by Smith (150) and Edwards (39), the model predictive control of an industrial kiln was developed by Charos et al. (23) without the application of ANN. The internal model control strategy (IMC) for the rotary lime kiln control has been suggested by Ribeiro. It uses multilayer feed forward back propagation network with 8 inputs, 2 outputs, and 2 hidden layers with 20 and 10 nodes. Fig.2.2 shows the principal control strategy of lime kiln. Expert systems and NN have been used in quality control system in paper mills. The primary objectives of a paper quality expert system are: to secure the quality of paper,

u(k)

Filter | Neural network kiln controller | Lime kiln plant

y (K)

Neural network kiln model

Ym(k)

'(k+1)
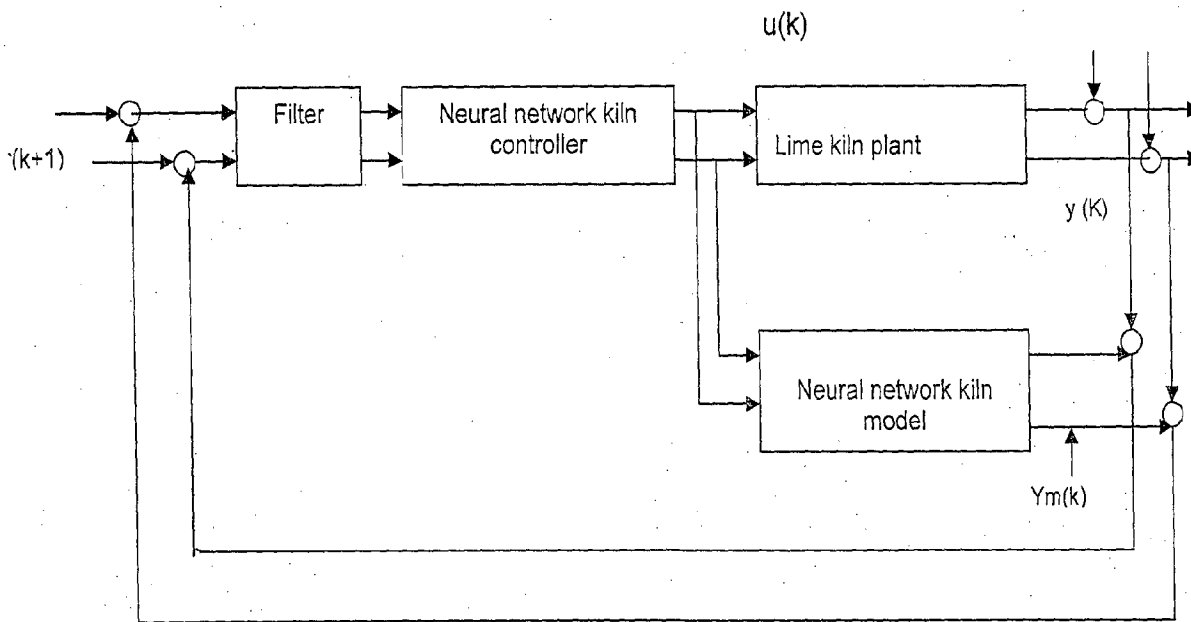
d

Fig.-2.2 Neural network based control strategy for lime kiln

minimize variations between shifts, reduce production costs, support operators, provide a flexible simulation tool, use existing knowledge, and train new staff members. The basic functions of one system are to collect real time process and quality data, evaluate the measured quality against customer specifications, recommend necessary corrective actions and simulate fulfilling of these actions.

Gornik et al (50) developed models to estimate brightness, opacity, gloss and print gloss of coated paper which are based on radial basis function neural network.

Desmond et al (31) presented a design of hybrid controller consisting of a neural network and classical control technique and tested the scheme on the bilinear model of a paper making machine (headbox) as well. Scharcanski Jacob et al. (132) presented a new approach to the controllable simulation of paper forming, using artificial neural network methods. The model incorporates dynamics of the forming process, like turbulence, drainage speed, and preferential drainage through earlier less-dense regions and fiber

properties, like propensity to clump, or "flocculate," fiber flexibility, and concentration of fibers in the suspension. Results for mono-fiber layer structures are described, showing effects of turbulence and its decay during drainage in causing clumping, or "flocculation." The commercial process has one of its main goals, the reduction to tolerable levels of the non-uniformity in mass distribution resulting from flocculation.

2.4 Conclusion:

A comprehensive review of artificial neural network strategy and its architecture have been outlined and available algorithm is cited to arrive at the result. A review of feedforward backpropagation network is highlighted with supervisory strategy. Applications of neural network for modeling, simulation, control and fault diagnosis have been exemplified with the subsystems used in a paper mill notably modeling of kappa number in kamyr digester, pulp bleaching process, and control of brown stock washer and bleach washer, incineration of black liquor, lime kiln, quality control and finally prediction of a typical paper property known as curl. Advantages of using ANN based control systems are cited to demonstrate how to achieve a robust control of the above paper mill subsystems which are difficult to control by conventional controllers. It is evident from the literature that use of NN technology is beneficial if the process model is strongly nonlinear or its structure is unknown. From the survey of literature it is also found that feedforward artificial neural networks (FANNs) have emerged in recent years as useful tools in ẹmical process engineering system applications. It is important to mention that ɔording to Rumelhart et al (126) out of so many varieties of NN, the feed forward back ɔpagation network is found to be most widely used control tools for different application real life problem in industry. Overwhelmingly majority of applications in pulp and paper nill and allied industries also favoured this network. Other networks such as ADALINE,

single layer perceptron, adaptive resonance theory, augmented back propagation are infrequently used. MADALINE, resilient back propagation, radial basis function etc. have been used only very sparingly. It is also evident that large volumes of works on ANN are devoted to the areas of modeling compared to those for control system design. The areas of control in paper mill covered are pertinent to fiber processing such as pulping, bleaching and also in recovery section. Though these works have been concentrated on ANN based modeling and control, the ANN based work in the paper machine wet end areas are extremely limited. The modeling and simulation on paper machine pressurized headbox have been dealt with by Whalley et al. and other investigators (166). Although Whalley attempted to modify the previously developed aforesaid models for air cushion headbox and optimized the linear multivariate MIMO models, these are limited to only classical control technique and did not include ANN concept. Only one work available which used the ANN in designing a nonlinear control system of head-box of wet end of paper machine is due to Desmond et al. (31) which used a hybrid controller consisting of an ANN to solve nonlinearity of the problem and a classical controller. However, there is a reticent silence about the detailed derivation or description of design. It appears that the design of control system using single or multivariable algorithm for real life problem with or without ANN or adaptation logic are secret. It may be emphasized that most of the researchers or practioners in Indian paper mills were mostly confined to production of pulp, its processing and control.

In this present investigation efforts will be made to develop various dynamic models of approach flow system parameters and headbox in both analog and digital signals and then various ANNs in the design of control system in paper machine pressurized headbox with emphasis on air cushion type will be applied for control purposes. They will be

compared with each other followed by the comparison with the application of classical controllers (P/PI/PID). Attempts will also be made to solve some problems with retention in hydraulic headbox.

CHAPTER-3
PAPER MANUFACTURE, OPERATIONAL PARAMETERS AND CONTROL PRACTICE IN A TYPICAL INTEGRATED INDIAN PAPER INDUSTRY

3.1 Brief description of paper manufacturing process:

The paper machine is the last part of the long chain of processes for making paper. In fact it is an important subsystem at the end of the entire paper making system, consisting of the raw material preparation steps to paper finishing stage as shown in fig. 3.1.

Paper making process starts with preparation of raw material (size reduction-chipping, cutting, grinding etc., size separation-screening), pulping(cooking) to convert raw material to pulp. Making of pulp consists of getting the cellulose fiber separated by chemical treatment of suitable raw material under proper pressure and temperature in a reactor under pressure called digester operated in a batch manner (batch digester) or in a continuous way in continuous digester. Kamyr digester is a typical continuous digester employed for converting mostly forest based raw materials (wood, bamboo) into pulp which necessitates sophisticated control of pulp parameters. For agri-residues like bagasse and straw, the design of continuous digester is radically different. Pandiya digester is an example. The pulping process can be of many types-Kraft, soda, sulphite etc, depending upon the type of chemicals used and level of pH employed. In kraft pulping (also called sulphate pulping), pulp quality is generally measured by kappa number which is related to the lignin content remaining in the pulp. Output product-pulp from the digester is treated in brown stock washer (BSW), one of the most important subsystems of a pulp mill to separate clean brown pulp from black liquor through a multi-stage countercurrent washing system. The main variables affecting the process are: input consistency in the vat, rpm of washer, input flow rate, temperature, vacuum and vat level

etc. The washed pulp is the treated in several stations for multiple stage cleaning (centri-cleaners) and screening operations (pressure screens).The pulp is then bleached in multistage-multi-sequence bleaching operations.

The objective of bleach plant is to obtain the brightness of pulp at a desired level while minimizing the use of bleaching chemicals like Cl_2, ClO_2 etc. There are various sequences of bleaching like CEH, CEDD, DEDED etc. mainly used by Indian paper mill. An ON-LINE measurement of D-stage brightness is desired for process control. However, because of sensor limitations, brightness is measured OFF-LINE by an hourly manual test. To ensure adequate pulp brightness, operators occasionally control to a higher than required brightness with a corresponding increased use of bleaching chemicals.

For CMP (Chemi-mechanical pulping)/CTMP (Chemi-thermo- mechanical pulping) refiner (generally chip refiner) is used to produce pulp under mild conditions of chemical treatment.

For paper making process the stock after refining need special treatment in stock preparation section of the paper machine, where stock fiber is broken into very small pieces of few microns in size by using mechanical devices (called pulp refiners or beaters) followed by chemical addition(sizing agent for internal sizing) and a host of other inorganic and organic chemicals. Internal sizing agents are added if papers are required to be made water resistant. For acid sizing, rosin is added along with alum to set the size on the individual fiber. On the other hand, for alkaline sizing process, AKD with alum to (Alkyl Ketene Dimers) or ASA (Alkenyl Succinic Anhydride) are used instead of rosin-alum system. Neutral sizing employs dispersed rosin and works slightly above acid sized pH.

The fiber/water ratio is decided on the type of paper to be manufactured. The above chemicals improve paper properties. The chemicals (clay, talc, soapstone, $CaCO_3$, TiO_2 called fillers) and fibers should be retained on the wire as maximum as possible. This can be done by combination of physical entrapment and complex physico-chemical interactions generally reflected by the addition of polymeric retention aids and also by drainage aids. This means that the retention of fiber and filler on the wire section is an extremely difficult process to describe using derived physical equation only.

After several cleaning and fiber treatment steps, the slurry normally around 4.0-6.0% consistency is delivered to the main feed, or machine chest at about 3.0% consistency. Stock from this chest is then fed to the fan pump via the basis weight valve. The main feed to the fan pump is dilution water from the white water chests that hold water that is drained from the machine. The machine chest stock is injected into this dilution water at the fan pump suction, with the fan pump acting as an in-line mixer. The stock is now <1.0% consistency. Stock then is pushed to the paper machine headbox also called flow box through machine chest and box via some final cleaning and screening equipments.

The dilute stock from the headbox is spread on the wire. The primary function of the headbox is to uniformly distribute the stock on the next element of wet end of paper machine, called wire. This is situated just below the opening of the headbox as a continuous wire mesh, moving at a constant speed such that when stock falls on it, the water is drained out to give shape of loose wet sheet of fiber which goes to the press section. The speed of the moving wire mesh should be so adjusted in relation to the falling rate of stock on it from headbox such that a uniform sheet of a particular grade is formed. For high speed machine or for better property development, twin wire or hybrid wire are used instead of open wire.

Water drains from the stock through the wire and is returned to the white water chests. Only 50-80% of the fibers are retained on the wire, so this water contains 50-20% of the fiber originally delivered to headbox. Thus, the re-circulating fibers can be equivalent in mass flow rate to the fiber delivered from the machine chest. Simple and vacuum assisted drainage can only remove a limited amount of water, typically giving a web of about 20% solids (or 80% water). This web is then fed to a set of presses which remove more water for squeezing out from the wet sheet by pressing the sheet between metal cylinders and thick woolen textile/synthetic fiber sheet known as felt with high water absorbing and retaining. The sheet leaves the press at 40-50% solids. The press water is typically filtered and used on various showers; some is re-circulated for stock dilution. The semi-dry web of approximately 40% dryness is then fed to a series of dryers (MF or MG or combination) where the final water is removed by evaporation. Other kinds of dryers like air-floatation, through dryers, infrared dryers etc. are available for special applications capacity. The MF/MG dryer consists of hollow cast iron cylinders heated internally with steam inside, provided with hoods where it becomes dry paper and is finally taken out on the pope reel through calendars. Just like felts in press section screen is used as dryer fabrics.

Paper machines require a large quantity of heated dry air for the drying process in paper machine. This air is used for the machine hood and pocket ventilation. After the drying process, the mixture of hot air and evaporated water, which has a specific enthalpy several times greater than the air delivered to the drying hood is conducted through the system of heat exchangers called recuperators. The last stage of the system of the heat exchanger usually represents a scrubber.

37

Recovery Section:

The important section of a paper mill which brings economy in one hand by supplying thermal and electrical energy for process heating and sustainability of the mill, reducing and controlling pollution on the other is its recovery and recycle section. This section mainly consists of multiple effect evaporation for concentrating black liquor obtained from brown stock washer up to 55-65% concentration, incineration of concentrated black liquor by spraying in the recovery furnace for combustion in the black liquor furnace and finally causticization and calcinations in lime kiln. In the black liquor furnace, the inorganic components(Na_2CO_3, Na_2S and very small amount of NaOH) remains in the same form or the other and sink through the char bed (principally carbon) which is formed by decomposition, and pyrolysis of organic constituents(lignin, hemicelluloses etc.) present in black liquor. The shape and size of the char bed are the important parameters for control of combustion in recovery furnace. Lime kiln is used primarily to produce lime required to convert green liquor to white liquor by causticization process in three to four stage co-current causticizing reactors (back mix flow reactor-CSTR). The white liquor is then feed to the digester to get pulp from various fibrous raw materials. The control of lime kiln is essential for getting good quality of lime in terms of size and reactivity. The control itself includes both burning zone control and combustion control.
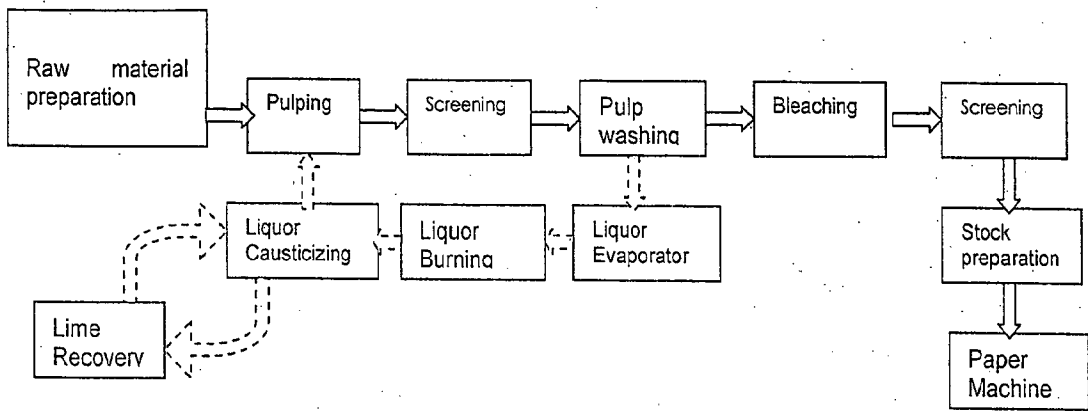
Fig.-3.1 Pulp and paper making system

3.2 Status of approach flow system and wet end of paper machine in mills:

In order to get paper of desired quality various measurement and control systems have been attempted for sensing and controlling numerous parameters in the paper mill. But these are not adequate and constant efforts are being made to upgrade the measurement and control of the operations and processes. The following section details about the existing practices of control and instrumentation of the wet end section. The subsystem selected for modeling in this present investigation starts from the machine chest to mainly headbox, and retention for wet end machine. However, the complete paper machine is extended up to the pope reel through presses, driers and calendars as shown in fig.3.2 (a).
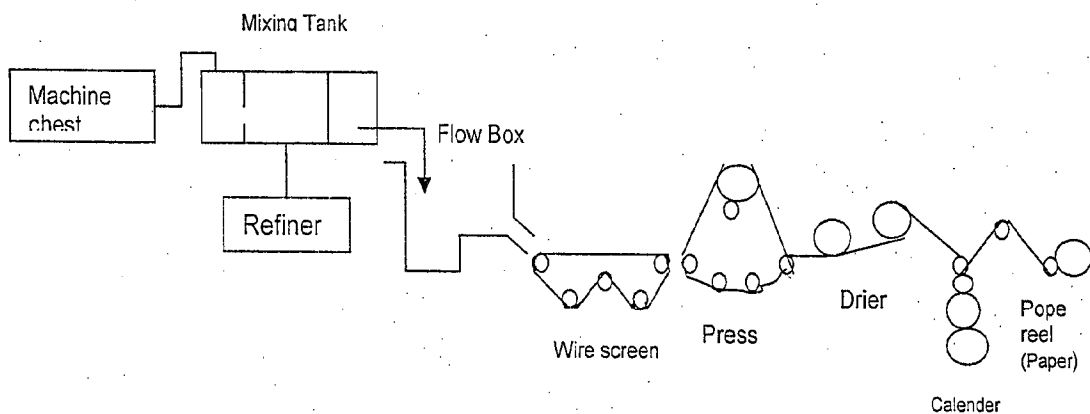
Fig.-3.2 (a) Process flow in Paper Machine

39

A typical wet end machine is drawn for Fourdrinier machine (fig.3.2 b).
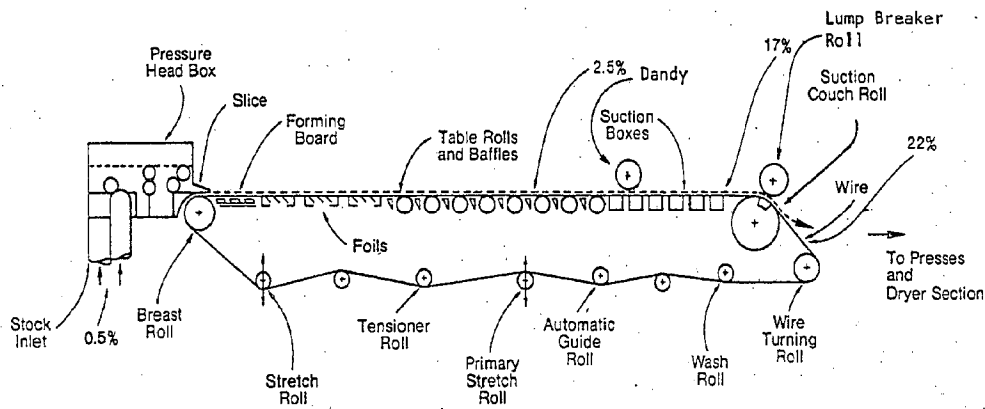
Fig.3.2 (b) A typical sketch of wet end formation equipment (Fourdrinier Machine)

The flow diagram for approach flow system is shown in fig. 3.3(21). This system includes

blending chest, consistency regulators and controllers, flow control devices and constant

head tank/stuff box, magnetic flow meter, basis weight valve(stock valve),secondary

refiner, mixing box(to mix with white water) and machine chest. The stock is pumped by

primary fan pump to a series of centri-cleaners at a consistency of 0.6-1.0% consistency

and then again to vacuum treatment and screening operation. Then comes the headbox

that stores the stock for further processing. The headbox consists of a pond section,

dispersing devices and slice open equivalent to the width of wet end paper machine at its

bottom that can be controlled if necessary. It can be either open to atmosphere or closed

with arrangement for applying air pressure at the top of the stock. The open and air

padded headbox invariably contains a number of rotating rectifier rolls (perforated rolls)

called holey rolls. Hydraulic headbox, another important improvement of open head or air

pressure headbox, used for high speed machine, does not contain moving parts or rotary

devices and is controlled by the pressure of fan pump. A hydraulic headbox also

additionally uses air pressure. Symflo headbox is an example which may be treated as a hydraulic headbox with an integral attenuator tank.
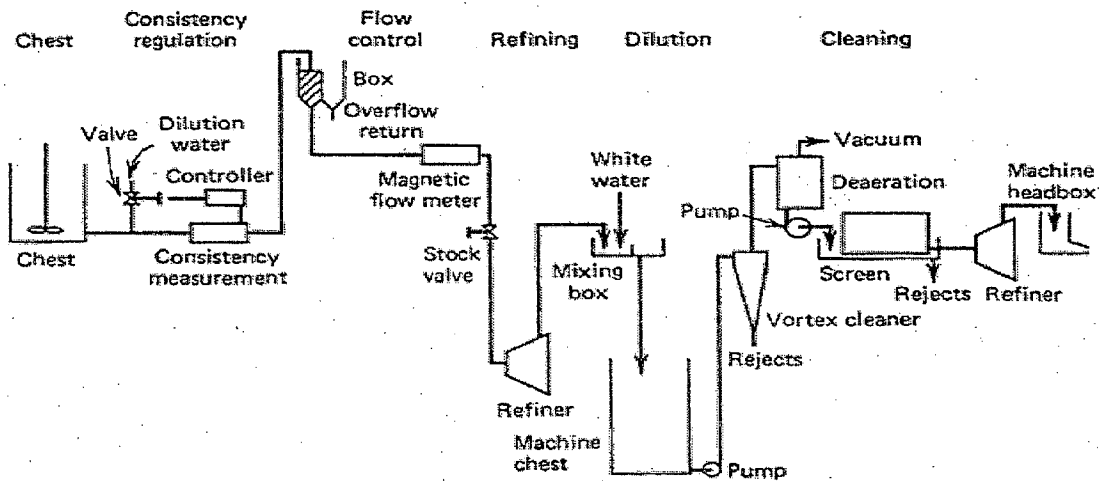
Fig. 3.3 Approach flow system schematic diagram

The headbox must not only spread out the stock evenly across the width of the machine at the correct speed and angle, but must level out cross-currents, machine direction velocity gradients, and consistency variations as shown in fig.3.4. Fiber flocking must be controlled by the creation of turbulence with a piece of precision equipment which must be easy to operate and maintain while minimizing production.

and process design aspects and the current status of instrumentation and control system used in wet end of Indian paper mill.

3.3.2 Mechanical and process design features of headbox:

There are various designs for headbox available marketed by numerous manufacturers with their trade names, even for the same kind of headbox, like open headbox, air pressure headbox, and hydraulic headbox compatible with former(Fourdinier, twin wire or hybrid wire). The original designers were Beloit/Harnischfeger, Black clawson, Sandy hill, Sulzer-Escher wyss, Valmet/ Ahlstrom, Voith, Wartsilla, and KMW. Some of the manufacturers are not presently existing. However, whatever may be the design features, the basic parameters are the same. In the following paragraphs the process and design parameters and their relationship are discussed:

3.3.2.1 Head, Jet velocity and spouting velocity (Tappi 0410-05, Tis 0410-02-04):

The total head H is referred to the datum level at the middle of the slice opening. The total head includes the height of stock above the slice, added pressure or vacuum of an enclosed headbox, and corrections for the position of the head measurement. The symbols are given in Chapter of nomenclature.

The model for flow velocity and volumetric flow can be obtained from Bernoulli equation for incompressible fluid like stock as under:

$$(P_a/\rho) + gZ_a + (\alpha_a v^2_a/2) + (\eta W_p) = (P_b/\rho) + gZ_b + (\alpha_b v^2_b/2) + h_f \qquad [3.1a]$$

For the case of stock flow from head box slice the gZ_a and gZ_b are cancelled out, and work added by pump ηWp is neglected. Therefore the equation in reduced form can be represented as

$$(\alpha_b v^2_b/2) - (\alpha_a v^2_a/2) = [(P_a - P_b)/\rho] - h_f \qquad [3.1b]$$

Using continuity equation $v_a=(D_b/D_a)^2 v_b$, and defining $\varphi=(D_b/D_a)$ the above equation can be written as

$$v_b=[1/(\alpha_b- \varphi^4\alpha_a)^{0.5}][2(P_a-P_b)/\rho]^{0.5}- F \qquad [3.1c]$$

Where F is defined as $(2h_f/\alpha_b- \varphi^4\alpha_a)^{0.5}$

The equation for v_b is reduced to $v_b=[C_v/(1- \varphi^4)^{0.5}][2(P_a-P_b)/\rho]^{0.5}$

Usually the ratio of diameter is less than 0.25, the approach velocity and the term φ can be neglected and resulting equation stands as $v_b=C_v[2(P_a-P_b)/\rho]^{0.5}$ $\qquad$ [3.1d]

Deleting the suffix b, one can write $v= C_v(2gh)^{0.5}$ $\qquad$ [3.1e]

If H is measured close to the slice, and v is measured at the vena contracta of the jet, $C_v\approx1$ for most slices. The relationship between total head (sometimes referred to as theoretical head) and jet velocity is thus given by the following simplified formula.

$$v=\sqrt{(2gH)} \qquad [3.2]$$

Friction losses, due to holey roll or to boundary drag along a very small angle nozzle will reduce C_v possibly to around 0.98.

Velocity at vena contracta:

The jet leaving the slice continues for a short while to contract in thickness to a vena contracta, at which point the spouting velocity is reached. The spouting velocity at the vena contracta can be found out as follows:

If A_v is the cross-sectional area at the vena contracta, A_s the area of slice opening, then $A_v=C_cA_s$, C_c , the coefficient of contraction whose value can be estimated accurately from the detailed model equations given in the Appendix -3.

Neglecting φ^4 as discussed earlier one can get the following equation

$$v =C_cC_v\sqrt{(2gH)}=C_q\sqrt{(2gH)} =C_q \sqrt{(2gH)} \qquad [3.3a]$$

For true nozzle slice, $C_c \approx 1$, otherwise for different geometry of slices designed by various manufacturer the values are different (Voith design, $C_c = 0.85-0.95$; Nielson slice, $C_c = 0.65-0.75$). The velocity v is at the vena contracta following contraction of the jet which can only be obtained from the detailed design of the slice flow.

The actual head/velocity relationship is not as precise as implied by these simple theoretical relationships which have ignored the effects of factors such as temperature, viscosity, and approach velocity.

3.3.2.2 Head and slice flow:

The total flow (Q) through the headbox (making allowance for any header bypass, bleed flows, etc.), slice opening (b), slice width (w) are related to the jet velocity by the following relation. Volume of stock which flows per unit time from the headbox is also equal to

$$Q = A_v v = A_v [C_v/(1- \varphi^4)^{0.5}][2(P_a-P_b)/ \rho]^{0.5}$$

Neglecting φ^4 as discussed earlier one can get the following equation

$$Q = C_c C_v A_s \sqrt{(2gH)} = C_q A_s \sqrt{(2gH)} = C_q w b \sqrt{(2gH)} \qquad [3.3b]$$

In most cases the value of C_q and C_c are almost numerically equal. Using various unit conversion factors, one can write the following equation.

$$Q = b w V_s K_1 = b w V C_c K_2 = bw C_c K_2 K \sqrt{H} \qquad [3.4]$$

As already mentioned, the contraction coefficient, C_c can be found from the slice geometry, angle and the model developed (given in Appedix-3). The values of K of eqn[3.4] depends upon the conversion unit as shown in the Appendix-3.

3.3.2.3 Relation between paper production and stock flow:

The volumetric flow of stock on the former can be calculated from paper production on the pope reel located at the end of the paper machine as under:

$$Q = m_s 10^4 / [C(100-S_s) \rho_{sus}] \qquad [3.5]$$

one can write, $m_s = w_n V_n q S_k$ [3.6]

Combining the above eqn.[3.5] through [3.6], the following equation can be written as

$Q = w_n V_n q S_k 10^4 / [C(100-S_s)\rho_{sus}]$ [3.7]

By comparing the eqn.[3.3] and eqn.[3.7], the following eqn. is obtained:

$b = w_n V_n q S_k 10^4 / [C(100-S_s)\rho_{sus} \, v \, w]$ [3.8]

Slice opening can also be obtained in other way as

$b = Q.S_k (100+S)(100-\delta_s)/(C\xi\beta \, 10^6)$ [3.9]

Width of paper web on the pope reel and width of stock stream flowing on the wire can be related as under:

$w = w_m (100-\delta_s)/100$ [3.10]

Width of slice opening w can be expressed in terms of trimmed width of paper

$w = w_o + 2z + [(w_o + 2z) \, \delta_s]/(100- \delta_s) + 2r$ [3.11]

Total head can also be calculated based on the types of headbox design (given in Appendix-3). For air cushion headbox the eqn.[3.12] is valid:

$H = h_m + P_{air}/\rho_{sus} g = \xi^2 \beta^2 V_n^2/\Phi^2 2gk_j = (V_n \xi \beta /\Phi)^2/2gk_j$ [3.12]

Along with the values of the contraction coefficient, C_c, the thickness of the jet, d the angle of outflow can be estimated accurately based on the geometric configuration of slice. There are many kinds of slices. Three primary types of slice, vertical slice, 45° slice and inclined slice. The geometry of the slice and the operational parameters derived from the geometric configurations are given in (Appendix-3). The headbox flow rate, Q_h can be calculated as under

$Q_h(gsm/inch) = 0.052(Slice \, opening)(vC_o)$ [3.13]
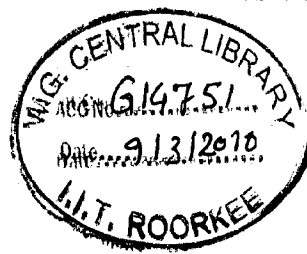
3.4 Status of existing sensors and their dynamics:

For design of control systems, apart from controllers and final control elements, the other important subsystems are sensors/detectors, transmitters(combination of transducer and signal conditioning devices) and measuring instruments. For development of total system dynamics, the static and dynamic characteristics of each subsystem are required to be evaluated. These are important for developing closed loop characteristic system equation. As measuring element is a subsystem of the total control system, the selection of most appropriate instrument from a range of commercially available instruments necessitates the knowledge of these factors. The static characteristics include parameters like range,span,turndown,sensitivity,resolution,repeatability,accuracy or precision, bias and measurement error, threshold, dead band, dead space, and dead zone, scale readability, zero shift(zero error).The dynamic characteristics generally include steady state gain, K_c or proportional band, time constant, order, and transfer function, G ,delay time depending upon the positioning of the sensors and measurement system and the characteristics of second and higher order systems(overshoot, period of oscillation, settling time, rise time, and resonance etc.) are reviewed in the following paragraphs:

As indicated earlier the sensors used in the wet end (approach flow, headbox and wire control) are: consistency, flow, total head, stock level, pH, and basis weight.

The time constant of the sensor is usually much lower than that of the system. So it should not be a factor. However, the time constant may depend upon how the sensor is used. Optical sensors (made of CdS or CdSe) have time constant of about 100ms and 10 ms respectively. Photovoltaic cells have time constants on the order of 1-100 μs.

The overwhelmingly majority of consistency sensors which most of the Indian mills are using at present are of mechanical type (rod or rotor) though many special sensors of non

50

contact type have been developed over the years. These include optical sensors based on depolarization or absorption and scattering based principle, microwave and NIR (near-infrared reflectance spectroscopy. These are reported in various publications and reviewed in tables 3.1 & 3.2, Appendix-1.

Temperature sensors generally used by mills are: RTD, Thermistor and thermocouple. Other temperature sensors include integrated circuit(IC), bimetallic strip and optical pyrometer. Electrical position sensors include potentiometer, capacitive, resistive, inductive and reluctance type sensors. Reluctance type sensors, a type of transformer are the basis of the prevalent LVDT (linear variable differential transformer) has sensitivity on the order of 0.001 mm movement.

The various values of static and dynamic characteristics of sensors are given by Johnson (66,67) and more details in various manufacturer's catalogue such as Omega. A comprehensive description of the sensors and their characteristics are presented in table 3.1 and 3.2 (Appendix-1) for the present investigation.

3.5 Headbox system of a paper mill:

Headbox, sometimes also called flow box is the most important equipment for paper machine of a paper mill in its approach flow section of paper machine. The paper machine headbox consists of three sections, inlet manifold, headbox pond section plus dispersion elements and slice. The function of head box is to take the stock delivered by the fan pump and transform the pipe flow into a uniform rectangular flow equal in width to the paper machine wet end section, spread stock at a uniform velocity in the machine direction and match approximately the slurry speed at the jet (jet velocity or spouting velocity) with forming section speed (called wire speed). The other objectives of headbox are to level out cross currents and consistency variations, machine direction velocity

gradients and to create controlled small scale turbulence (called micro turbulence) to eliminate fiber flocking and impinge on the wire at the correct location and angle. Turnbull (158) predicted that 2.0% disturbances in jet velocity may result in nearly 7.0% variation in the basis weight due to the aforementioned resonance of the fundamental mode. There are mainly two types of head box, open headbox (open to atmosphere) and enclosed or pressurized headbox. The open headbox was generally used earlier older slow speed paper machine(600-800 ft/min, requiring a variation of approximately 14.5 inches in level to change the corresponding spouting velocity(jet velocity).For higher speed(at least greater than 1000 ft/min,3000-5000ft/min)a level change hundreds of inches of water was necessary to produce the required spouting velocity. In such a situation, it is impossible to control cross-flow currents or to ensure that all fiber aggregates are broken up before the stock reaches the slice. This made practically impossible to operate the open headbox. To overcome these deficiencies, one has to use enclosed headbox. The later again is classified into two types: air cushion/air padded headbox and hydraulic headbox.

3.6 Status of control loops in head box:

Installation of a good headbox control system is considered probably one of the most fruitful investments in the area of paper machine automation if one goes for economic justification and to ensure uniform quality paper (21).

A comprehensive control system solves the complexity of headbox operation and allows papermaker to conveniently alter operating conditions (speed, drag, flow through the box etc.). With implementation of sophisticated control system, it is easier to achieve increases in production (through speed-ups).

To ensure uniform quality paper few factors should be brought under control, out of which three are most important. Flow through the headbox, liquid level and total head. The

others are consistency, pH, and temperature (although the later two influences to a slight extent). To minimize basis weight variations in the sheet, headbox total head must be tightly controlled. In addition, when machine speed changes occur, the ratio between jet velocity and wire speed must be automatically maintained to minimize production. A typical control system for a hydraulic headbox is shown in fig. 3.5:

3.6.1 Total head pressure control:

Total head pressure is controlled by positioning the fan pump recirculation control valve. The stream valve will be manually positioned to keep the fan pump recirculation control
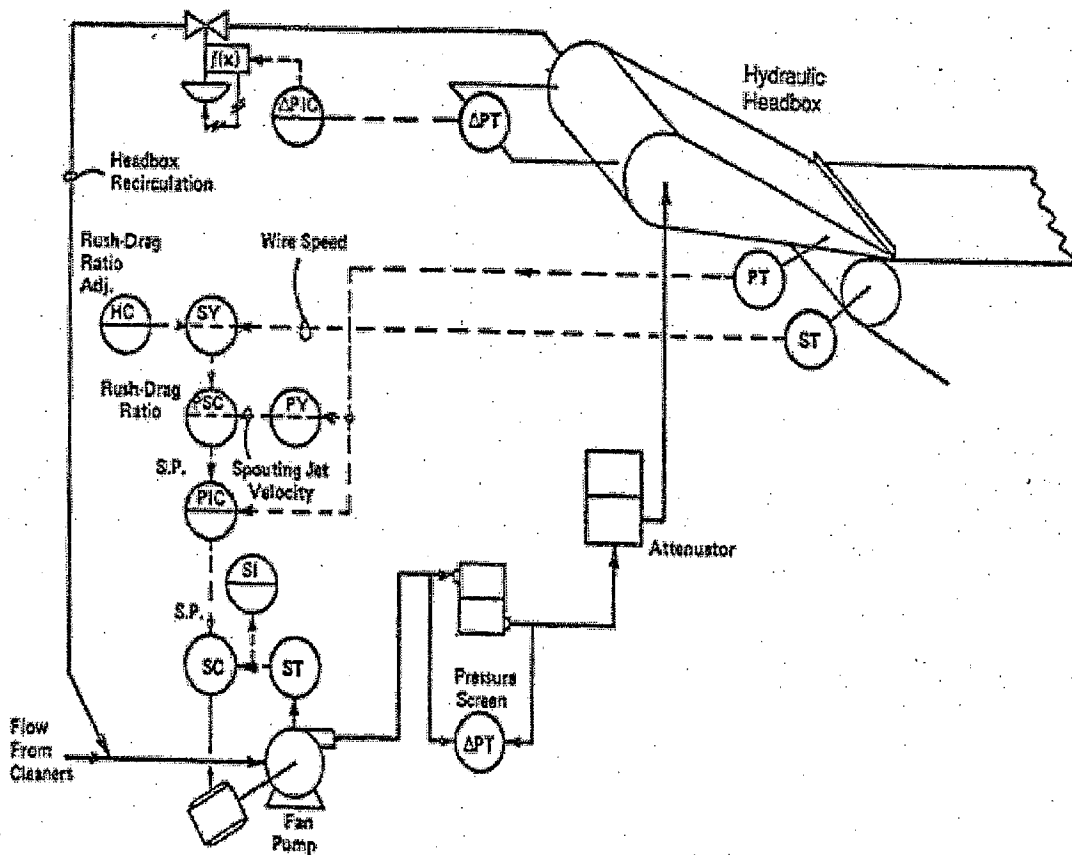
Fig. 3.5 Hydraulic headbox control system

valve within operating range. Some paper machines use a trim valve in parallel with the stream valve or by using variable speed fan pump, the speed of which can be precisely set with SCR motor control.

3.6.2 Total head control:

Total head is controlled to achieve control of the velocity of the stock jet issuing from the slice, because this factor must be adjustable if a constant drag (wire speed – jet velocity) between wire and jet is to be maintained. Total head is sensed via a D/P cell mounted to measure gauge pressure at the floor of the box. This serves as the feedback signal for a controller that usually modulates the position of the valve controlling flow into the headbox. The prime function of a total head controller is to maintain a constant drag on the wire. As a result total head set point is a function of wire speed, it is necessary to adjust it when changes in speed occur. This requires a system that sense wire speed; takes note of drag set point and calculate an appropriate total head set point. Such a task can be accomplished via analog or digital hardware. The later is favoured in most of the modern installations. Total head itself is most frequently controlled via electronic, analog hardware with PI action and a remote set point feature. With this hardware, loop tuning is normally by cut-and-try methods, unless decoupling with liquid level is being attempted, via digital algorithms, in which case, complex identification and tuning procedures must be employed.

3.6.3 Wire speed control:

Wire speed is measured and used in computation of the rush-drag ratio. Calculated jet velocity is compared with measured wire speed in a rush-drag ratio controller. The output of this controller provides a cascaded set point for the headbox total head controller. A manual adjustment is provided for setting the desired rush-drag ratio. Should there be

temporary failure of the wire speed digital transmitter; this rush-drag ratio cascaded set point control can be uncoupled from the total head controller. Stock flow to the headbox can then still be controlled on a single-loop basis from total head pressure.

3.6.4 Headbox stock level control:

Headbox stock level is controlled to maintain proper holey roll emersion and to prevent large level variation for practical reasons. This is control on a single loop basis by controlling the padding air and vent control valves. These valves are usually arranged so that the headbox pad can be controlled with a positive pressure or under vacuum. Since actual headbox level is less critical than total head, level is used to control the slower responding padding air and vent control valves.

Headbox level is usually sensed by a D/P cell with one side sensing pressure at the bottom of the box and the other the pressure in the air pad at the top. The output of the D/P cell goes to level controller. Liquid level is most commonly controlled by conventional pneumatic, analog hardware with PI action. Controller tuning is usually by manual cut-and-try methods, unless decoupling of liquid level from total head is being attempted, whereupon, digital controllers are used and sophisticated identification and tuning procedures are required.

3.6.5 Headbox stock flow control:

Stock flow through the headbox is controlled to allow compensation for changes in pulp drainage properties and easy adjustments of formation characteristics of paper. Flow through the headbox is best measured by a magnetic flow meter located just upstream of the box. The variable manipulated by most flow controllers is slice position. Changes in slice position cause upsets in total head that are compensated by adjustments in the position of the valve controlling flow to the box. Normally, only proportional action is

55

required of the flow controller, but it is usually advisable to include a dead band around the set point. This is most easily accomplished digitally. Controller tuning is normally by trial and error methods and seldom is required for the flow controller. Headbox slice position is used to control the "water rate" which determines headbox consistency. Headbox slice position can be set manually or by computer.

3.6.6 pH control of stock:

Paper machine headbox pH is usually controlled by adding acid (sulfuric acid, alum or both) to the suction of the fan pump depending upon the requirement of desired system pH value.
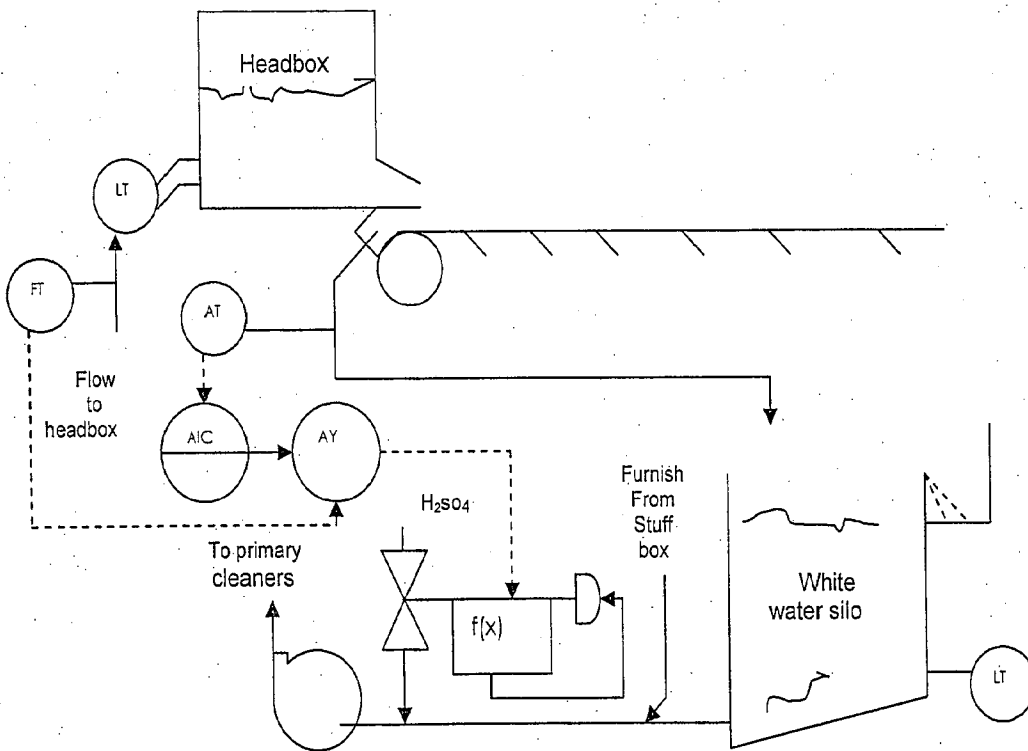
Fig.3.6a Paper machine pH control

A portion of the paper machine whitewater drainage is usually sampled for pH. The flow to the headbox is used as a feed forward index to position the sulfuric acid/alkali valve. This control valve position is then readjusted from the pH controller. An alternative pH

sample location is off the headbox recirculation line. The higher flow velocity at this point .combined with longer fibers tends to keep the electrodes cleans. On-Off control is also used in many situations. A typical control system for acid sized stock is shown in fig. 3.6a. Another important consideration is the shower water pH to the felt cleaner system. Maintaining the shower water pH at the same level as the headbox pH assists in more effective operation of the felt conditioners. Another scheme given in fig.3.6b(144,145) has also been proposed.

Alum Tank

Stock box

Electro
Mechanical
Actuator

pH sensor

PID

Transmitter

Machine chest

Dosing valve controller

Stock Pump
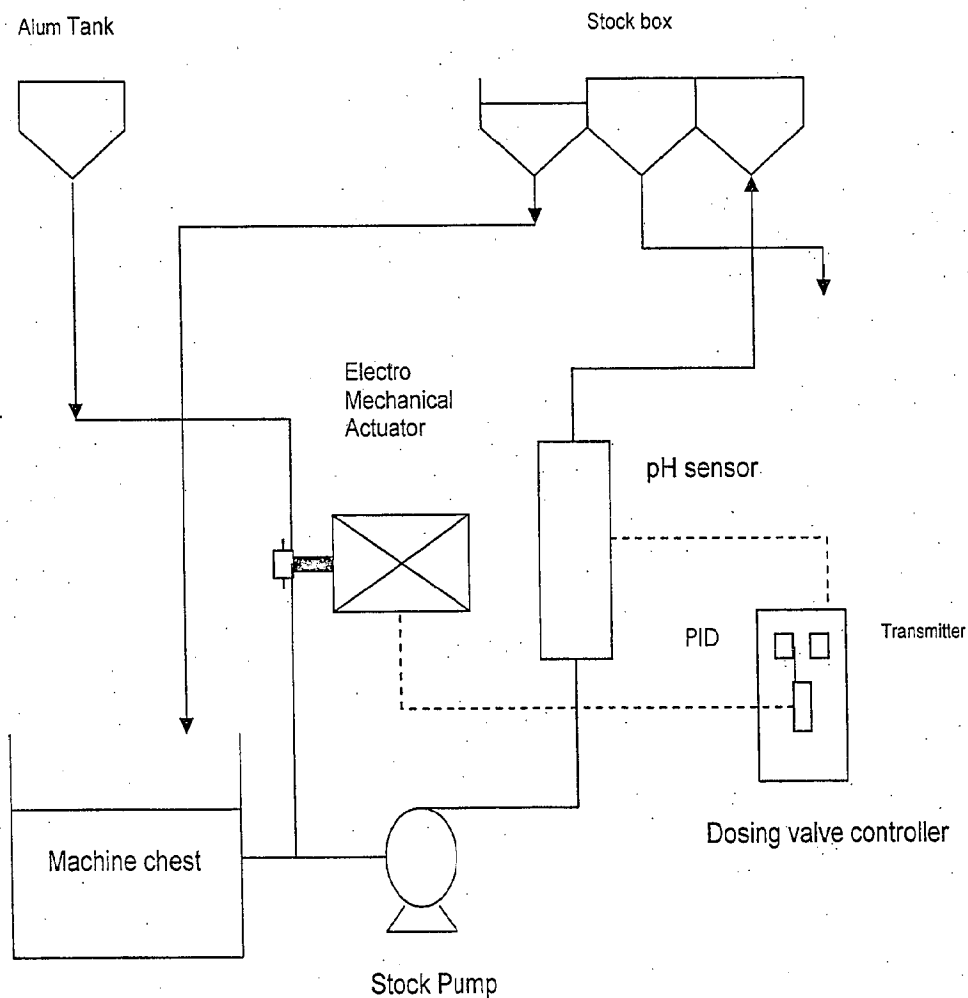
Fig. 3.6 b pH control system

the stock coming from the broke chest is the same consistency as that in the machine chest. (Machine control attempts to do this, but the dynamics of the process prevent excellent control) with consistency to the machine chest upset, the mass flow of fiber to the headbox changes. Breaks may last 5-10 minutes (and sometimes a lot longer) which is sufficient time for the basis weight control to drift rather significantly from its target. When the web is re-established on the reel, the sensor then resumes control and attempts to bring all measurements back in line. This may take several minutes and the production made in this period is off quality, hence, may need to be rejected.
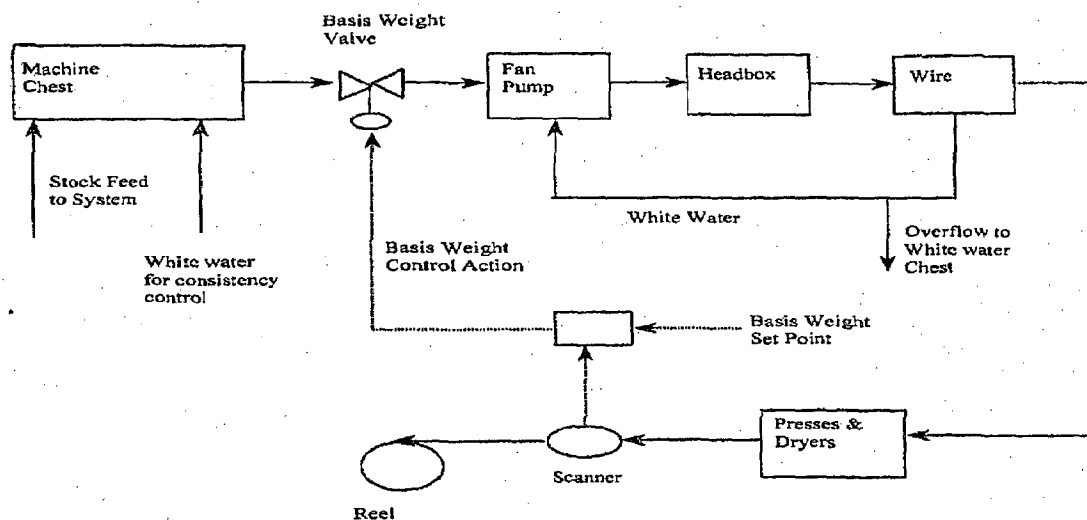
Fig.3.7 A typical control loop of basis weight control

3.7 Conclusion:

In this chapter, a comprehensive description of the manufacturing process is outlined along with present status of approach flow system in Indian paper mill, the various unit operations and processes involved and design features of headbox flow system. The up-to-date review of existing control practice and their loops, and status of various sensors are made. The details of both static and dynamic characteristics of sensors are compiled. The controlling parameters which are focused in connection with the approach flow

system and headbox are: consistency, flow, total head, level, pH, and temperature and basis weight. The design information regarding various loops for controlling the parameters in and around the headbox is stressed upon. From the study it is found that the dynamics for all sensor parameters are extremely fast with very small time constant values compared to the values for the process alone. In addition, the systems approach first order with gain nearly equal to 1.

CHAPTER- 4

METHODOLOGY OF SYSTEMATIC INVESTIGATION, PARAMETER ESTIMATION AND SELECTION OF ALGORITHMS

In this Chapter detailed methodology for systematic investigation in the present work are developed as under:

4.0 Development of strategy of systematic investigation:

The strategy adopted for systematic investigation of the present problem is as follows:

1. Development of dynamic models for consistency, flow, total head, level, pH, stock temperature, and basis weight assuming all these parameters as linear or approximately linear systems in approach flow system of a paper machine. As usual these models are based on unsteady state material balance or energy balance or combination of both the two from fundamental principles.

2. After deriving the dynamic models, if some of the models of control parameters of process are found to be nonlinear, these are linearized using usual Taylor series expansion technique or by Pade's approximation for dead time if at all it exists.

3. Designing a negative feedback loop for classical control system for consistency using Bode plot and designing the complete process using the conventional controller (PI and PID). For this purpose flow chart are to be designed (fig. 4.1a and 4.1 b).

4. Identifying the static and dynamic characteristics of measurands and the characteristics (table-3.2, Appendix-1) of each and every elements of the closed loop of the intended control system as a whole and then following the development of their dynamic models as in steps1-2 and analyzing the stability as in step 3. The

classical control system is then designed adapting various appropriate tuning methodology such as Ziegler- Nichols, and lambda tuning.

5. Studying the variation of the response of each and every parameter as a function of time using control loop assuming servo and regulator problem.

6. For comparison purposes the response models using both analog and digital methods(analog and discrete) are to be developed for all parameters such as consistency, total head, stock level, stock pH , stock temperature, and basis weight control. For stock flow, data from the industry and those predicted from model are to be compared.

7. Developing model for the MIMO system indicating interaction of input and output parameters such as total head and stock level, air pressure and level in a pressurized headbox, input stock flow and stock level, and retention process in the wet end.

8. Comparisons between analog and digital models both SISO and MIMO systems are to be accounted for.

9. Designing a model for the MIMO system as discussed in step 7 such as interaction of total head and stock level, air pressure and level in a pressurized headbox, input stock flow and stock level, and retention process in the wet end and then to compare the results with those of SISO system. Analysis should be made based on relative gain array (RGA) method and decoupling control techniques.

10. Selecting the appropriate methodology of ANN for the control parameters such as back propagation neural network, adaptive linear neural element network (ADALINE), perceptron, adaptive resonance theory (ART1), and augmented back propagation network.

11. Comparing the results obtained from the MATLAB simulation for each and every parameter (either in analog or digital form) for both SISO and MIMO system using both classical control system and neural network control system.

12. In order to achieve the objectives mentioned in step 11, convert all the models of control parameters of the wet end approach flow system including headbox as mentioned above (steps 1-2) in to a neural system using the various procedures for neural computation as described in step 10 with changing values of ANN parameters such as momentum rate, learning rate, and others. A flow chart for General ANN computation is given in fig.4.1b.Individual flow charts and algorithms for different ANN methodologies are given in figs. 4.5- 4.6.

13. Comparing the results of ANN computation using MATLAB simulation with SIMULINK tools with those estimated values from classical control loops for all SISO and MIMO systems.

4.1 Design and analysis of classical control systems:

Methodology of design and analysis of a classical control system is well known. It requires the design of the loop (single or multiple) for SISO or MIMO systems which in turn demands the knowledge of individual loop elements, their dynamic and static characteristics, defining characteristics equation of individual as well as the system as a whole, stability analysis based on continuous or discrete signals, linear time invariant in time domain(Routh Hurwitz criterion/Root Locus) or frequency domain(Bode or Nichols plot/ Nyquist plot), then finally adjusting the controller parameters by various tuning methodologies . This is then checked for response as a function of time. The procedure followed in this present investigation is depicted in flow chart (fig.4.1). MATLAB software is used to design and analyze the system.

4.2 Procedures for estimation of parameters:

The following paragraphs describe some salient features of parameters and their relative importance for computation of classical control system (P/PI/PID) and ANN for this present investigation. Though the estimation procedure for parameters for classical control system well known, it is important to mention that even for classical control loop the time constants for various elements such as process(SISO and MIMO), measuring element, controller and final control element are required to be obtained. These are either found out from published information or self generated through simulation technique by MATLAB software. The parameters for ANN are relatively less known and thus require attention. Therefore in this chapter procedure for estimating ANN parameters are described here.

For learning or training of ANN, the parameters of importance are: momentum coefficient(rate or factor),α, learning rate(or coefficient) η, number of hidden nodes n, activation function(or transfer function, or squash function), threshold function, identity function, weight vectors ,W,V, mean squared error, tolerance, accuracy, gradient descent term for back propagation network(BPN), and gain(sigmoidal gain for sigmoid function),λ or scaling factor and delta rule. Some the above parameters are defined as under:

4.2.1 Momentum coefficient: The momentum coefficient, α is implemented by adding a fraction of the last weight change to the next set of the weights eqn. [4.1]. There are various algorithms that can change the level of this momentum based on the error involved. The momentum coefficient has been used for reducing the training time of network and also overcomes the effect of local minima.

$$[\Delta W]^{n+1} = -\eta \partial E / \partial W + \alpha [\Delta W]^n \qquad [4.1]$$

The values of α being positive (<1), lie in the range of 0.0-0.9, generally between 0.5-0.9.

In the present investigation, the value of α has been selected iteratively using MATLAB programming detailed in Chapter-5.

4.2.2 Learning rate: Learning rate determines the size of the weight adjustments made at each iteration and hence influences the rate of convergence. The values of η lie between 0.01-1.0 though higher value of even 0.6 has been assumed in specific situation. However, if the learning rate coefficient is too large, the search path will oscillate and converges more slowly (58). On the other hand if the coefficient is too small, the descent will progress in small steps significantly increasing the time to convergence. During training, the training process stops when the error for all the cases falls below the learning tolerance. If the learning rate is too small, the learning process never stops. The learning rate always starts with a higher tolerance level and monitors the weight changes with decreasing tolerance levels.

In order to get quick convergence and best results in the present investigation, the optimized value of learning coefficient has been selected based on error rate as a function of learning rate as detailed in Chapter-5.

4.2.3 Number of hidden layers and hidden nodes:

The number of hidden layers and hidden nodes are very important factors in order to optimize the physical number of calculations in both the training and operational mode. If all factors in ANN computational procedure (value of momentum coefficient, value of learning rate etc.) fail, increase the number of neurons in the hidden layer to improve the model. For getting best results for feed forward network in BPN, normally equivalent single hidden layer for a multilayer system is assumed, and then the number of hidden nodes is calculated in a single layer.

Dimension of probability theory proposed the following equation to calculate the required number of hidden nodes.

Number of hidden nodes= $10*T/(I_1+I_3)$;

where I_1 and I_3 denote input and output nodes and however, one commonly used method is to train different networks with varying number of neurons in hidden layer and to test their predicted accuracy. As an approximation (91) suggested the following equations to predict the number of hidden neurons in hidden layer.

No. of hidden neurons= [(no. of inputs) + (no. of outputs)]/2

Or No. of hidden neurons= $[(no. of inputs)^2 + (no. of outputs)^2]^{0.5}/2$

4.2.4 Accuracy:

As the number of the hidden nodes increases, the accuracy increases until a point is reached where the network is over-parameterized. When the curve reaches the bottom of the knee, that number of hidden nodes is the proper number. The no. of hidden neurons has been selected based on error rate as detailed in Chapter- 5. Many times the accuracy is referred to as the training threshold or learning threshold. The learning threshold can be calculated as under

Learning threshold= $0.8*(\Sigma\varepsilon^2/2)$. [4.2]

4.2.5 Gradient descent term:

Gradient descent term is based on the minimization of error, E defined in terms of weights and the activation function of the network. Also, it is required that the activation function employed by the network is differentiable, as the weight update is dependent on the gradient of the error, E (161).

Thus, if ΔW_{ij} is the weight update of the link connecting the ith and j^{th} neuron of the two neighbouring layers, then ΔW_{ij} is defined as

68

$$\Delta W_{ij} = \eta \frac{\partial E}{\partial W_{ij}}$$

[4.3]

where, η is the learning rate parameter and $\partial E/\partial W_{ij}$ is the error gradient with reference to the weight W_{ij}.

Now using the above parameters the algorithms of mainly four types of ANN methodologies are either modeled or selected from available from published information. Though there are some other ANN methodologies are available like resilient back-propagation, radial basis function network (RBF) and ART2.

4.3: Modeling techniques through ANN: Development of flow chart and selection of algorithms:

As indicated in Section 4.2 there are many ANN methodologies available for design of control system which are process specific. A general algorithm is presented here (174). However, for detail analysis in this investigation the flow charts and algorithms of five methodologies are attempted as under.

- Adaptive linear neuron network(ADALINE)

- Perceptron neuron network(PNN)

- Back propagation neuron network(BPNN)

- Adaptive resonance theory(ART1)

- Augmented back propagation network(ABPN)

The results using MATLAB software will be compared in Chapter-6.These are described in the following paragraphs:
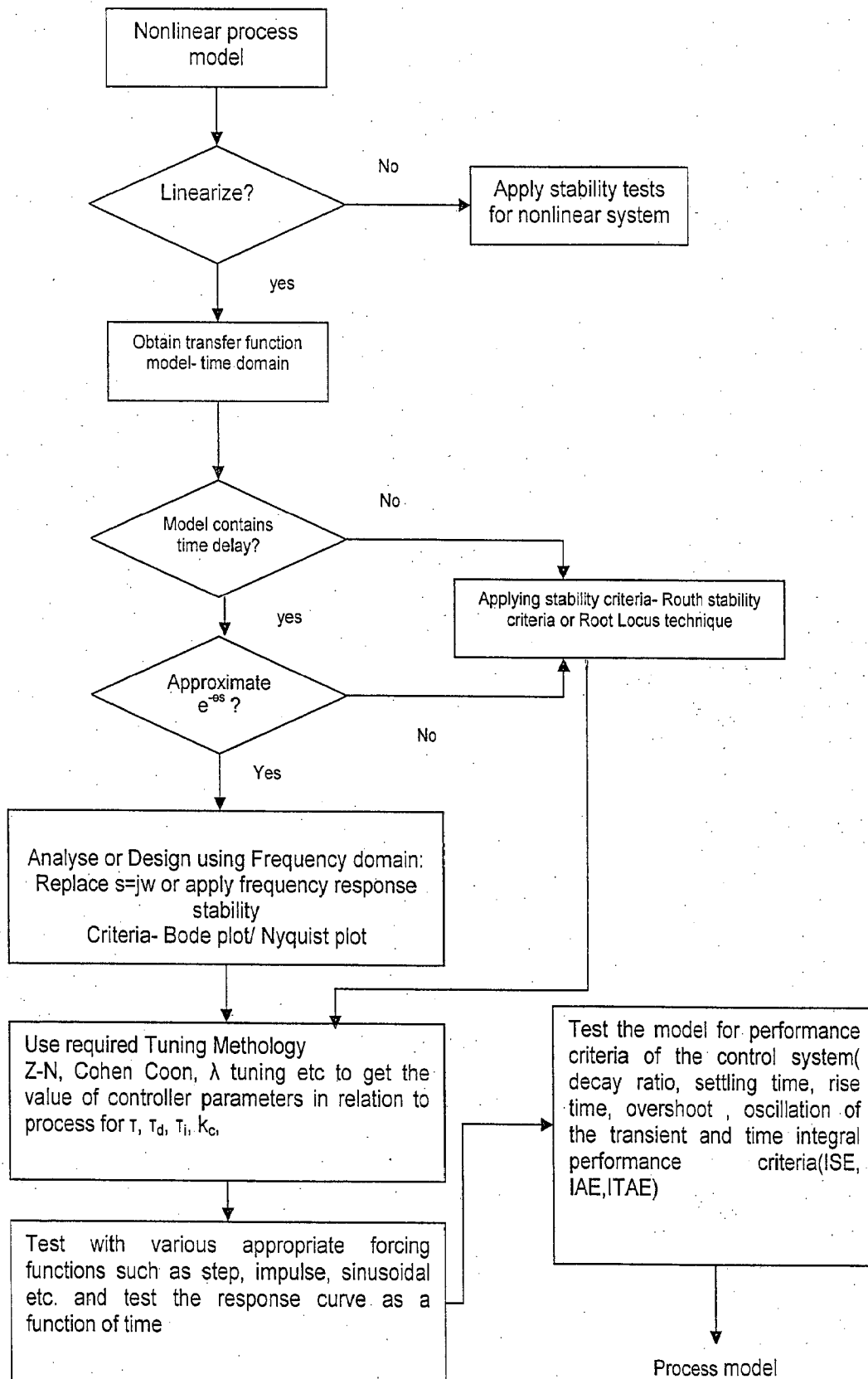
Fig. 4.1a Flow chart for the design of the classical control system including stability
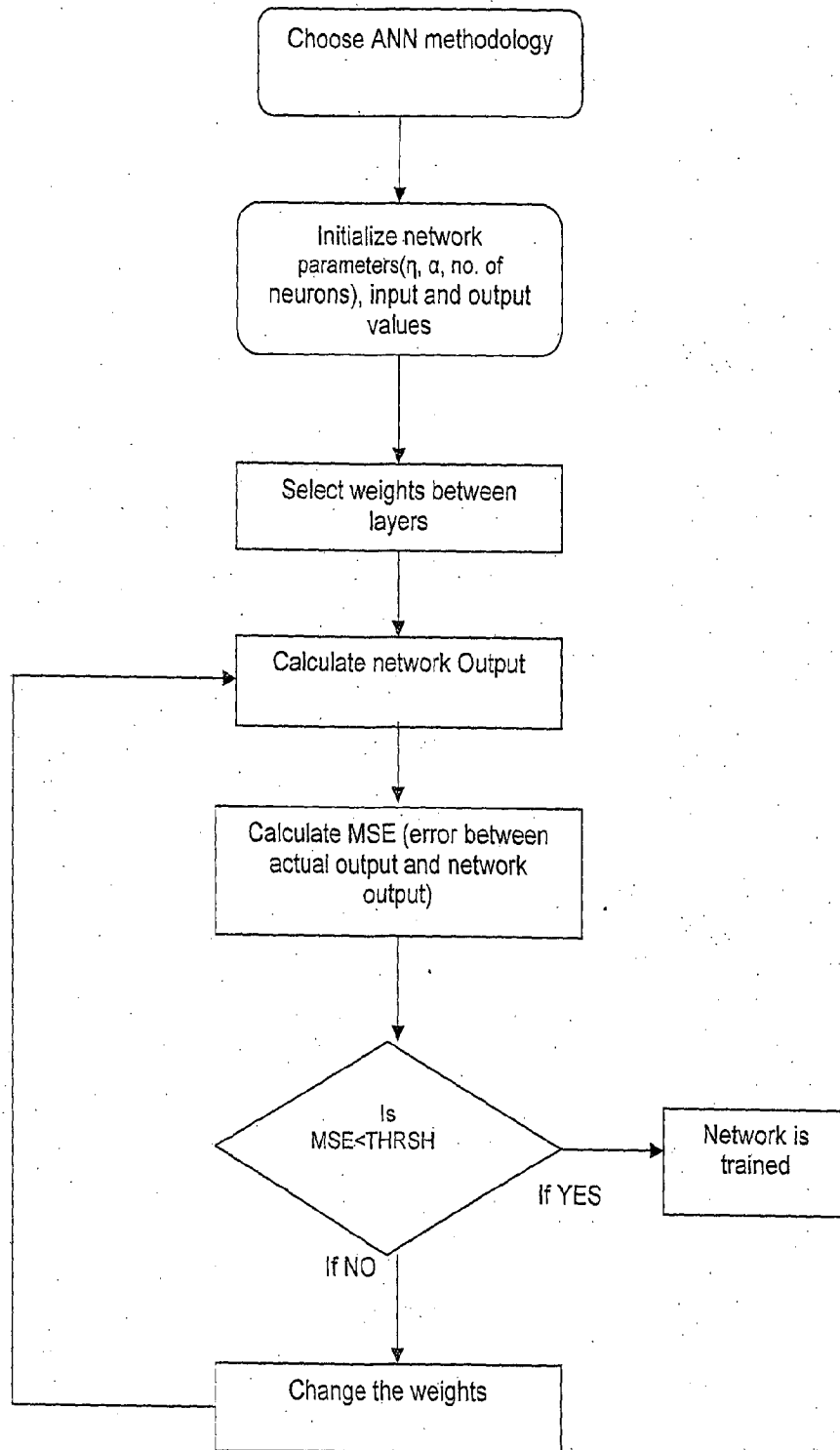
Fig. 4.1b Flow chart for general neural network algorithm

71

4.3.1 Algorithm for solving problem through ADALINE:

This Adaptive linear neural element network(ADALINE) which uses supervised learning algorithm, consists of a single output neuron and the output values are bipolar(-1 or +1). The input x_i could be binary, bipolar or n real valued. It also has a bias whose activation is always '1'. If the weighted sum of the inputs is greater than or equal to zero then the output is 1, otherwise it is -1. An ADALINE network is shown in fig.4.2 (148).
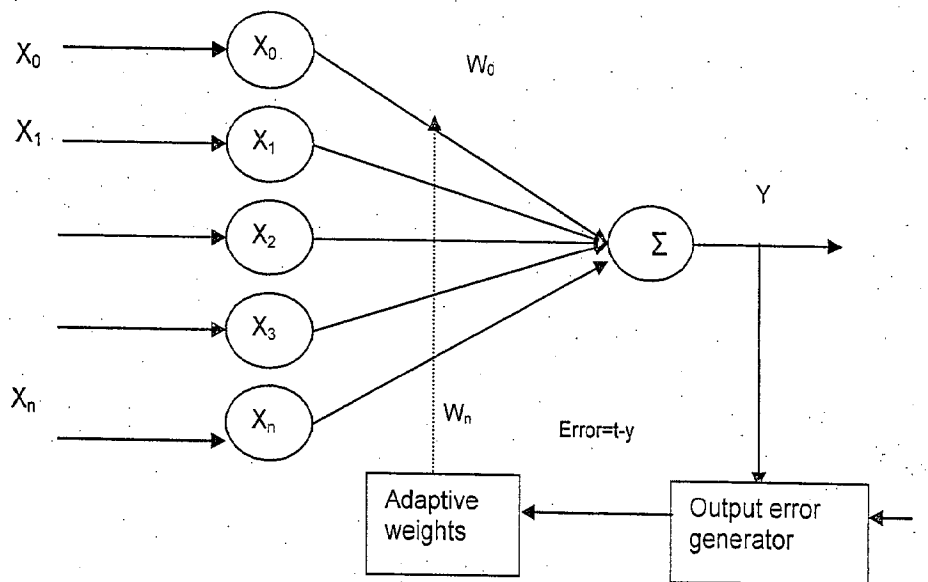
Fig.-4.2 ADALINE neuron model

The input to the neuron, x is represented as

$X=[x_0, x_1, x_2 \ldots \ldots x_n]$

X_0=bias=1;

α= Learning coefficient

t=target output

y=computed output

$W=[w_0, w_1, w_2 \ldots \ldots w_n]^T$ represents the weight factor

y_{in}=WX=output of the neuron before the non linearity

y=sgn(y_{in})= sgn (WX)= output from the neuron after the non linearity

72

The weighted sum of the inputs including a bias term is calculated and it is compared with target output and based on the delta rule, the weights are adjusted. To teach an adaline model, the following steps are used:

ADALINE algorithm:

Step:1 Randomly choose the value of weights in the range -1 to 1.

Step:2 While stopping condition is false, follow steps 3 to 7.

Step:3 For each bipolar training pair s:t, do step 4-7.

Step:4 Select activations to the input units, $X_0=1$, $X_i=s_i(i=1,2.....n)$.

Step:5 Calculate $y= \Sigma_{i=0}^{n} X_i W_i$.

Step:6 Update the bias and weights.

$$W_0(new)=W_0(old)+ \alpha(t-y)X_0, \quad (X_0=1) \qquad [4.4]$$

$$W_i (new)=W_i(old)+ \alpha(t-y)X_i \qquad [4.5]$$

Step:7 If the largest weight change that occurs in step 3 is smaller than a specified value, stop, else continue.

4.3.2 Algorithm for solving problem through perceptron network:

A typical model of the perceptron (PNN) is given in fig.4.3.
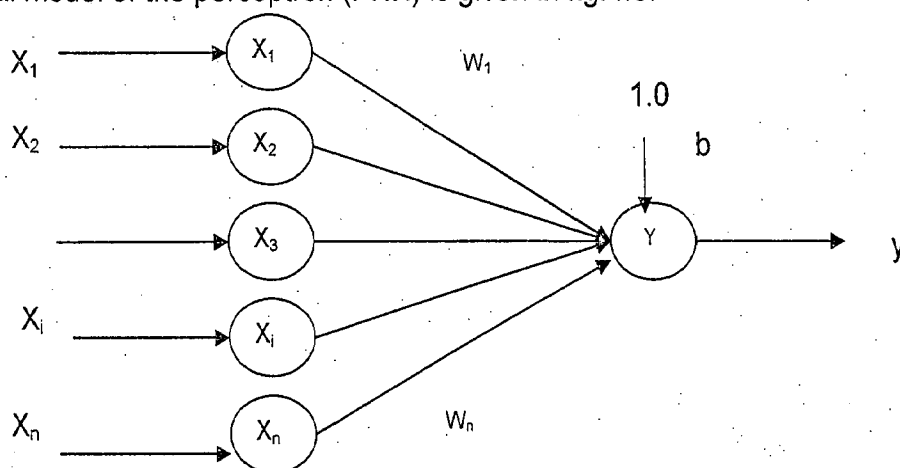
Fig. 4.3-Perceptron neural network

The learning algorithm of PNN is enumerated as under:.

Step:1 Select weights and bias. The value of learning rate has been used from 0 to 1.

Step:2 while stopping condition is false, do steps 3 to 7.

Step:3 For each training pair s:t, do step 4-6.

Step:4 Select activations to the input units, $X_i=s_i(i=1,2.....n)$.

Step:5 Compute input to the perceptron and calculate the perceptron output

$$Y_{in}=b+\Sigma^n_{i=1} X_iW_i \qquad\qquad [4.6]$$

$$y = \begin{cases} 1 & y_{in}>\theta \ ; \ \theta \text{ is the threshold} \\ 0 & \theta<=y_{in}<= \theta \\ -1 & y_{in}< \theta \end{cases} \qquad\qquad [4.7]$$

Step:6 Update the bias and weights if the target is not equal to the output value.

If $t\neq y$; If $x_i \neq 0$

$$W_i(new)=W_i(old)+ \alpha X_i t \qquad\qquad [4.8]$$

Else no change in weights

$$b(new)=b(old)+ \alpha t \qquad\qquad [4.9]$$

Step:7 Test for stopping condition, if no weight change in step 3 stop else continue.

4.3.3 Algorithm for solving problem through backpropagation neural network (BPNN):

Backpropagation networks consist of multiple layers of neurons. For a three layer NN system (Fig.4.4), there are an input layer, a middle layer (commonly referred to as a hidden layer), and an output layer. The network is constructed in such a way that nodes of each layer are connected to the nodes of the next layer. In a back propagation network, a randomized set of weights on the interconnections are used to present the first pattern to the network and the calculations are made for input and output of hidden and output layers. The process is repeated until the prescribed performance criteria are achieved.

The network must be trained by various learning processes as mentioned in the Section 1.2.2. For control application, the Algorithm based on Delta-Rule has been found to be most appropriate. For step by step computation of ANN, the following notations are followed.

Three layer network with input layer having I nodes, hidden layer having m nodes, and output layer with n nodes. The flow chart for the calculation procedure is depicted below (Fig.4.5).

Input layer
(l= 1,2......i)

Hidden layer
(m=1,2.........j)
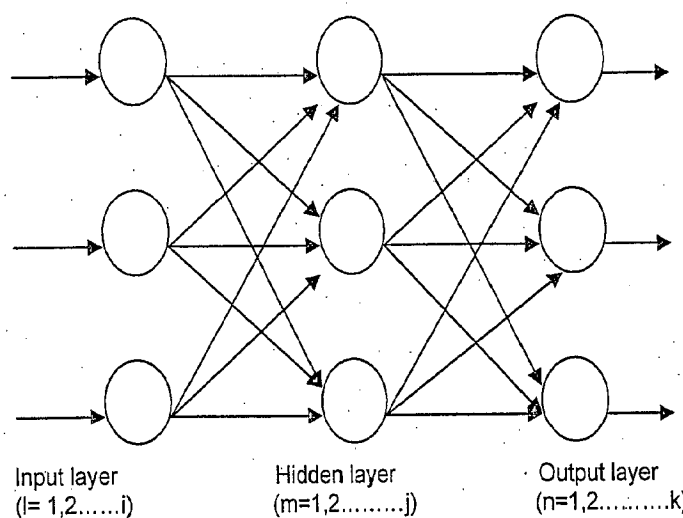
· Output layer
(n=1,2..........k)

Fig.4.4 Multi layer feedforward neural network

Output from input layer O_i

ıut from hidden layer O_H

ıut from output layer O_o

ep: 1 Normalize the inputs and outputs values to their maximum values.

Step: 2 Select the number of neurons in hidden layer which lie between $l < m < 2l$.

Step: 3 Select the weights V (between input and hidden neurons) and W (between hidden and output neurons),

Step: 4 Introduce the input into the neural network; calculate the output from first layer (input layer) using equation.

75

$O_i = I_i$,

Step: 5 Calculate the input to the hidden layer using following equation.

$I_H = V^T * O_i$

Step: 6 Knowing the output from the first layer, Calculate the output from second layer (hidden layer) using equation

$$O_H = 1/(1+e^{-I}{}_{Hi})$$ [4.10]

Step: 7 Knowing the output from second layer, Calculate result from output layer using sigmoid function.

$$I_O = [W]^T \{O_H\}$$
$$O_o = 1/(1+e^{-I}{}_{oj})$$ [4.11]

Step: 8 Calculate total mean square error, E for j^{th} training set.

$$E = sqrt(\Sigma\ (T_J - O_{oJ})^2/n.$$ [4.12]

Step: 9 Calculate gradient descent term, D.

$$D = (T_k - Oo_k)\ Oo_k\ (1-O_{ok})$$ [4.13]

Step: 10 Calculate gradient descent for j^{th} node on the hidden layer

$$y = \{O\}_H * D$$ [4.14]

Step: 11 Knowing gradient descent term for hidden, calculate weight changes between input & hidden layer nodes.

$$[\Delta W]^{t+1} = \eta[y] + \alpha[\Delta W]^t$$ [4.15]

Step: 12 Knowing gradient decent term for hidden and output layer, calculate weight changes between hidden layer & output layer nodes.

$$[\Delta V]^{t+1} = \eta[x] + \alpha[\Delta V]^t$$ [4.16]

Where $[x] = \{O_i\}\ D^*$

$$D^* = e_i\ (O_{Hi})\ (1-O_{Hi}),$$ [4.17]

$$\{e\} = [w]D$$

where η is the learning rate, and α is the momentum coefficient, momentum is simply an added weight used to speed up the training rate.

For example, if one calculates the changes in weights, $[W]^{t+1}$ and $[V]^{t+1}$. It requires arbitrarily to set the learning rate η =0.9, momentum coefficient, α=0.7.
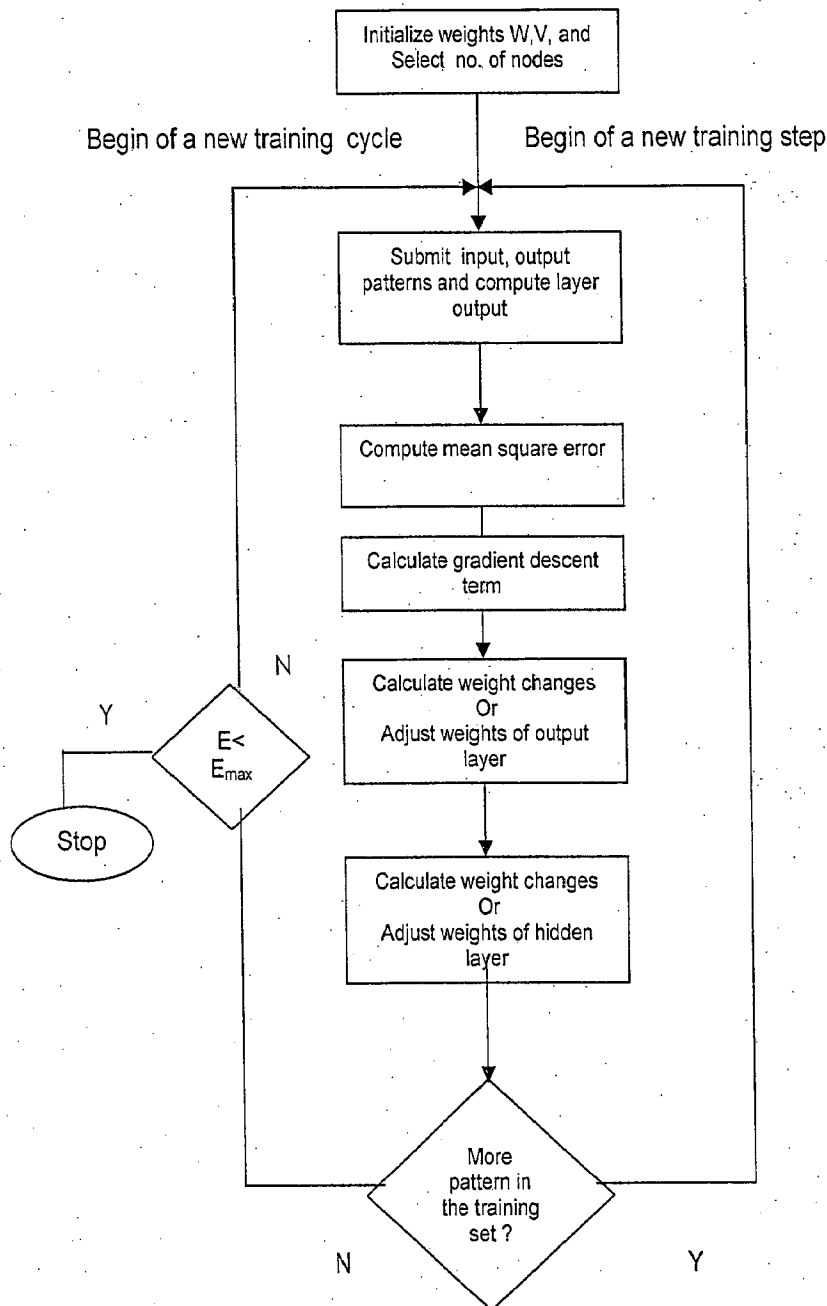
Fig. 4.5 Back-propagation training flow chart

Step: 13 After knowing weight changes, update the weights according to the equations

77

$$[W]^{t+1} = [w]^t + [\Delta w]^{t+1} \qquad\qquad [4.18]$$
$$[V]^{t+1} = [v]^t + [\Delta v]^{t+1} \qquad\qquad [4.19]$$

Step: 14 Find error rate

Error rate= $\Sigma E/n$ set $\qquad\qquad$ [4.20]

Step-15: This process is continued until the network predictions are within some defined tolerance of acceptability.

4.3.4 Algorithm for solving problem through adaptive resonance theory (ART1):

ART is capable of developing stable clustering of arbitrary sequences of input patterns by self-organisation. Pattern can be viewed as points of N-dimensional feature space. There are two distinct models based on ART, namely ART1 and ART2 networks. ART1 self organizes recognition categories for arbitrary sequence of binary input patterns and ART2 does the same for either binary or analog inputs. The novel property of the ART1 network is the controlled discovery of clusters.

The ART1 algorithm has been described step by step as follows. Flow chart of the ART1 algorithm is shown in fig.4.6.

Step:1 The vigilance threshold ρ is set, and for n input vectors and M top layer neurons the weights are initialized. The matrices W,V are calculated as(174).

$$W=[1/(1+n)] \qquad\qquad [4.21]$$

$$V=[1] \; ; 0< \rho <1$$

Step:2 Input vector x is represented at input nodes as

$$x_i=0,1, \text{ for } i=1,2 \ldots\ldots,n.$$

Step:3 All matching scores are computed as

$$y^0_m = \Sigma^n_{i=1} = W_{im}x_i, \text{ for } m=1,2,\ldots.M \qquad\qquad [4.22]$$

In this step, selection of the best matching existing cluster, j is performed as follows

$$y^0_j = \max_{m=1,2\ldots M}(y^0_m). \qquad\qquad [4.23]$$

Step:4 The similarity test for the winning neuron j is performed as follows

$[1/\|X\|]\ \Sigma^n_{i=1}=V_{ij}x_i > \rho$, where ρ is the vigilance parameters if it is passed then go to step 5,

if the test is failed, the algorithm goes to step 6 only if the top layer has more than a single

active node left. Otherwise goes to step 5.

The norm $\|X\|$ is defined for the purpose of this algorithm as follows

$$\|X\|=\Sigma^n_{i=1}|x_i| \hspace{8cm} [4.24]$$
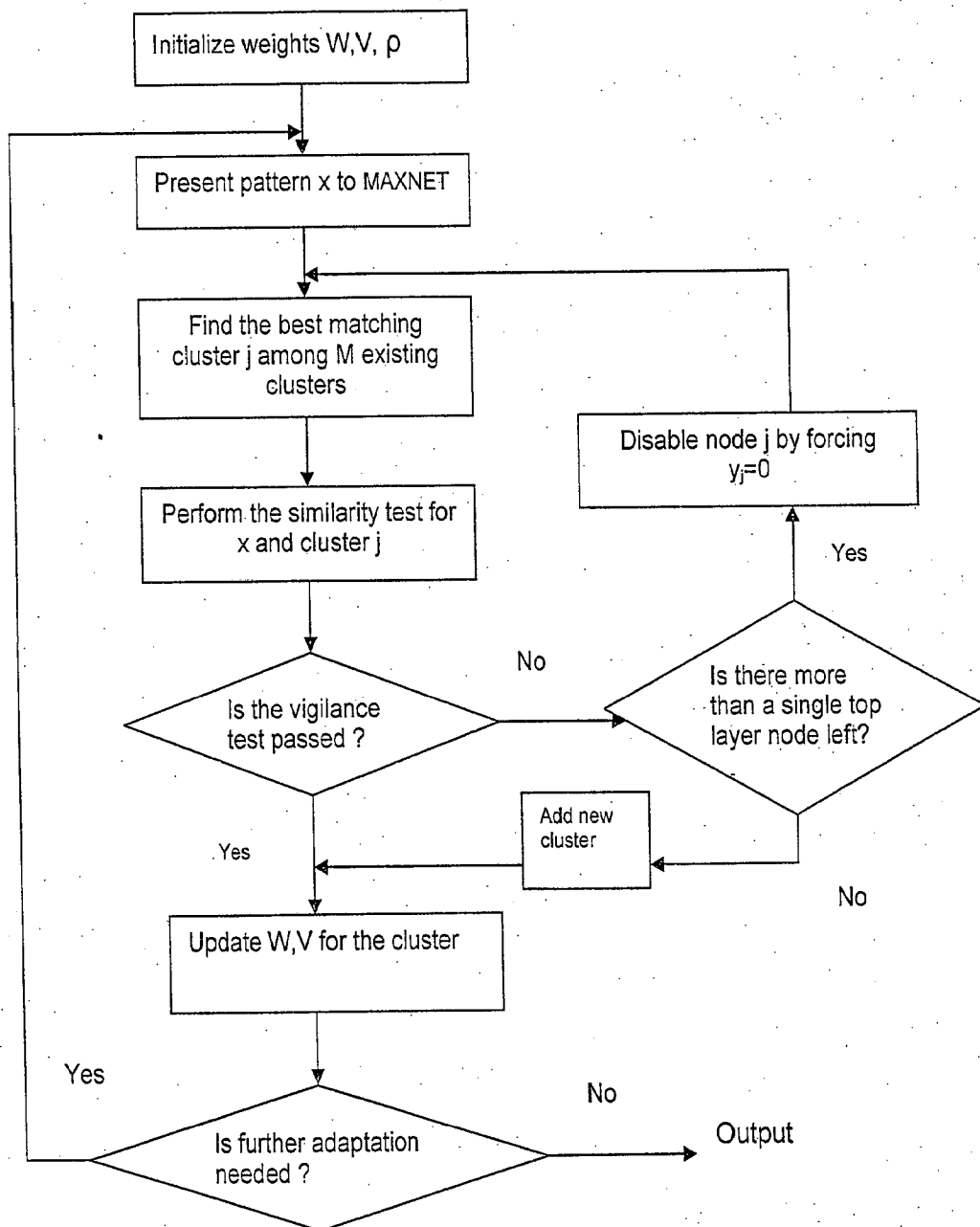
Fig. 4.6 Flow chart of the ART1 algorithm

Step: 5 Entries of the weight matrices are updated for index j passing the test of step 4, updates are only for entries (i, j), where i= 1,2,......M and are computed as follows

$$W_{ij}(t+1)=[\ V_{ij}(t)x_i/\ .5+\ \Sigma^n_{i=1}V_{ij}\ (t)x_i]$$ [4.25]

$$V_{ij}(t+1)=\ x_i\ V_{ij}\ (t)$$ [4.26]

This updates the weights of the jth cluster. The algorithm returns to step2.

Step: 6 The node j is deactivated by setting y_j to 0. The algorithm goes back to step 3 and it will attempt to establish a new cluster different than j for the pattern under test.

4.3.5 Augmented back propagation network:

The architecture is of a standard back propagation network, mathematically expressed in eqn.[4.27]. The augmented neurons are highly sensitive in the boundary domain, thereby facilitating the construction of accurate mapping in the model's boundary domain. The network denotes each input variable with multiple input neurons, thus allowing highly interactive functions on hidden neurons to be easily formed. The architecture of the augmented neural network is shown in fig.4.7.
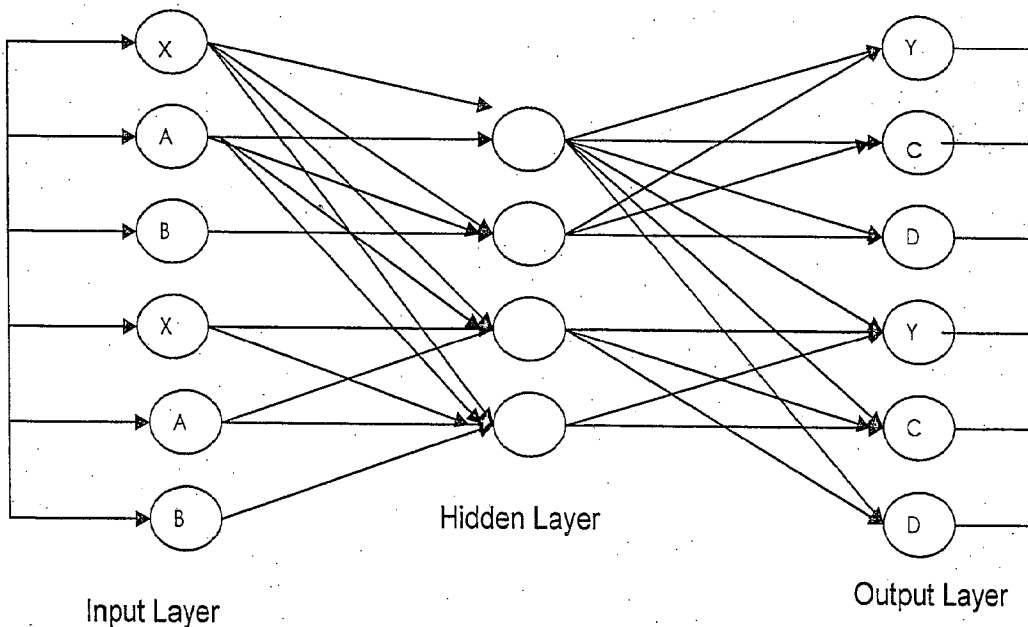
Fig. 4.7 Architecture of augmented neural network

$$A_i=\ln(1.175X_i+1.543) \hspace{4cm} [4.27]$$

where X_i is the ith input value of training data and A_i, the output of ith logarithmic neuron in the input layer. The input layer's exponent neurons receive natural exponent transformation of the corresponding input value by the training data using the following eqn.[4.28].

$$B_i=0.851\exp(X_i)-1.313 \hspace{4cm} [4.28]$$

Where B_i is the output of ith exponent neuron in the input layer. The logarithm neuron and exponent neuron of the output layers are given as under

$$C_j=\exp(1.718y_j+1) \hspace{4cm} [4.29]$$

$$D_j=\exp(0.6931y_j-1) \hspace{4cm} [4.30]$$

Where C_j is the output of jth exponent neuron in the output layer and y_j is the output or the network output which can be represented as under

$$y_j=y\{f(X,A,B)\} \hspace{4cm} [4.31]$$

Although multilayer feedforward networks using backpropagation have been widely employed for classification and function approximation, existing theoretical results provide only very loose guidelines for selecting these parameters in practice(162).

4.4 ANN control methodologies:

Once the ANN methodology has been identified it is prudent to write the control architecture for learning as well as actual process for parameter control. The ANN methodology as described in Section 4.3 is now used for control application with the following architectures.

In this investigation experimental data on stock flow and basis weight for digital system are used for comparison purposes. Reported experimental data are also used for retention and ash simulation for neural computation.

The control loops for all the parameters are simulated through MATLAB Simulink tool. If dynamic characteristics of a process parameter is not known, that can be found out by iterative procedure using again Simulink tool within a broad range of parameter available in literature. The simulation is, however, based on the analysis of closed loop control system including adjustment of selected controller parameters.

A step by step procedure as described in section 5.1.3 for SISO consistency control is used to train the artificial neural network (ANN) for all the cases of SISO and MIMO system using MATLAB software. The MATLAB programming for all above mentioned parameters have been shown in Appendix-2. The performance of classical controller (PI/PID) and ANN controller are compared in terms of simulated results in Chapter-6.These are discussed as a case to case basis as follows:

[A] DEVELOPMENT OF MODELS OF SISO SYSTEM OF PAPER INDUSTRY

CASE-5.1 Modeling of consistency of stock in the approach flow to the headbox:

The diagram of consistency control for a headbox is shown in fig.-5.1. In order to achieve the above objective, it is an imperative necessity to develop system model of consistency control of headbox. The sensors largely used in measuring consistency are reported in Chapter-3, Section 3.4.The models developed as already indicated are based on mass balances in steady and unsteady state forms as follows:

One of the most important aspects in the design of consistency controller is to make sure that the dilution water added is well mixed with the stock before reaching the consistency sensor. It is possible to control consistency on the basis of either a sample taken from the

main stream or by making the appropriate measurement directly in the main channel of flow. Consistency is usually measured at three different points in the system as shown in fig.5.1. The various possibilities of sensing consistency are shown through dotted lines. However sensors or transmitters have not been shown. These are: thick stock before dilution in the approach flow system, usually 2.0 to 4.0 percent consistency, paper machine headbox, usually 0.1 to 1.0 percent consistency, and white water usually below 0.5 percent consistency. At present, it appears that direct in-line sensing is not used in Indian mill but it should be preferred (21). These can be measured with more sophisticated on–line non-contact consistency sensor or transmitter (like optical based, microwave based or NIR based) with very fast dynamics. These are described in Chapter 3, Section 3.4 and table-3.2(Appendix-1). Consistency can be controlled by controlled dilution of the stock with the computer doing the necessary calculations. This produces more satisfactory results even when using white water for dilution which has an appreciable consistency.

5.1.1 Headbox dynamics for consistency in analog and digital forms:
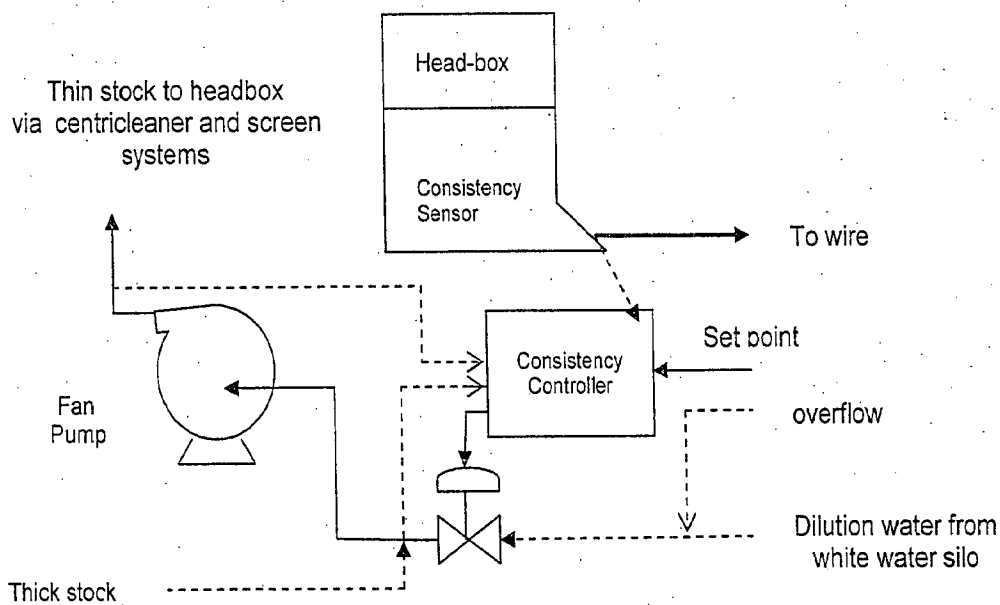
Fig.-5.1 Consistency control for a headbox

The mass balance for a steady state system with respect to consistency in headbox consists of two inlet flows with two inlet consistencies. The symbols are given in Chapter of nomenclature.

$$m_i\, c_{yi} + m_d\, c_{yd} = m_o\, c_{yo} \qquad [5.1]$$

Overall mass balance on the same system

At steady state, $t=0$, $m_o = m_{os}$; $m_i = m_{is}$; $m_d = m_{ds}$

$$m_o = m_i + m_d \qquad [5.2]$$

At unsteady state, Input=output +accumulation

For fiber balance using consistency of each flow

$$m_i\, c_{yi} + m_d\, c_{yd} = m_o\, c_{yo} + d(V\rho\, c_{yo})/dt \qquad [5.3]$$

Also, overall mass balance is written as,

$$m_i + m_d = m_o + d(V\rho)/dt \qquad [5.4]$$

For constant density and constant volume thin stock system at steady state,

$d(V\rho)/dt=0$ and therefore $m_i + m_d = m_o$

Eqn.[5.3] can be written as

$V\rho\, d(c_{yo})/dt= m_i\, c_{yi} + m_d\, c_{yd} - m_o\, c_{yo}$ or $d(c_{yo})/dt= (1/V)\{(m_i / \rho)\, c_{yi} + (m_d/ \rho)\, c_{yd} - (m_o/ \rho)\, c_{yo}\}$

Or $d(c_{yo})/dt= (1/V)\{q_i\, c_{yi} + q_d\, c_{yd} - q_o\, c_{yo}\}$ \qquad [5.5]

Expressing in terms of deviation variables, eqn.[5.5] can be written as given below

At $t=0$,

$c_{yi} \longrightarrow c_{yis}$

$c_{yd} \longrightarrow c_{yds}$

$c_{yo} \longrightarrow c_{yos}$

$d(c_{yo} - c_{yos})/dt=(1/V)\{ q_i(c_{yi} - c_{yis}) + q_d\,(c_{yd} - c_{yds}) + q_o(c_{yo} - c_{yos})\}$

$$d(C_{yo})/dt=(1/V)\{Q_i C_{yi} + Q_d\, C_{yd} - Q_o\, C_{yo}\} \qquad [5.6]$$

where $C_{yo} = c_{yo} - c_{yos}$; $C_{yi} = c_{yi} - c_{yis}$; $C_{yd} = c_{yd} - c_{yds} = 0$

Eqn.[5.5] can be dealt with for two cases:

Case -a: Constant dilution water density, volume, flow and consistency at a variable inlet stock flow consistency which is clearly a SISO system.

Case –b: Variable inlet stock flow at constant consistency and constant dilution water flow consistency and variable input consistency which indicates an interactive process containing two variables which is a MIMO system.

Case-a: The balance eqn. [5.6] reduces to

$$d(C_{yo})/dt = (1/V)\{ Q_i C_{yi} - Q_o C_{yo}\} \qquad [5.7]$$

If $Q_i = Q_o$, flow remains constant

$$d(C_{yo})/dt = (Q/V)\{C_{yi} - C_{yo}\} \text{ or } C_{yi} = C_{yo} + (V/Q) dC_{yo}/dt = C_{yo} + \zeta dC_{yo}/dt$$

$$C_{yi}(s) = C_{yo}(s) + \zeta s C_{yo}(s) = C_{yo}(s)[1 + \zeta s]$$

$$C_{yo}(s)/ C_{yi}(s) = [1/(1 + \zeta s)] \qquad [5.8]$$

Effective process transfer function for the consistency control

$$G_p = K_p/(\zeta s + 1) \qquad [5.9]$$

Case-b:

The balance equation can be written as

$$\dot{}_{yi} + m_d c_{yd} = m_o c_{yo} + d(V \rho c_{yo})/dt \qquad [5.10]$$

$$\mathbf{1}(c_{yo})/dt = m_i c_{yi} + m_d c_{yd} - m_o c_{yo}$$

$$(c_{yo})/dt = (1/V)\{q_i c_{yi} + q_d c_{yd}\} \qquad [5.11]$$

In terms of deviation variables,

$$d(c_{yo})/dt = (1/V)\{Q_i Cy_i + Q_d C_{yd} - Q_o C_{yo}\} \qquad [5.12]$$

Where,

$$d(c_{yo}V)/dt = V d(c_{yo})/dt + c_{yo} dV/dt$$

Substituting the value of $d(c_{yo}V)/dt$ in eqn.[5.10], eqn.[5.10] can be written as

or $m_i c_{yi} + m_d c_{yd} = m_o c_{yo} + \rho V\, dc_{yo}/dt + \rho c_{yo}\, dV/dt$ [5.13]

or $c_{yi}\, q_i + c_{yd}\, q_d - c_{yo}\, q_o = V\, dc_{yo}/dt + c_{yo}\, dV/dt$

Substituting dV/dt from the overall mass balance and canceling terms, one can get:

$dc_{yo}/dt = Q_i/V\, (c_{yi} - c_{yo}) + Q_d/V\, (c_{yd} - c_{yo})$ [5.14]

or $c_{yo}(s + Q_i/v + Q_d/v) = Q_i/v(c_{yi}) + Q_d/v(c_{yd})$

if $c_{yd}=0$; then eqn.[5.14] can be written as

$c_{yo}(s + Q_i/v + Q_d/v) = Q_i/v(c_{yi})$

or $c_{yo}/c_{yi} = [Q_i/(sv + Q_i + Q_d)]$

or $c_{yo}/c_{yi} = [Q_i/(\zeta_1 s + 1)]$ [5.15]

if $c_{yi}=0$, then eqn.[5.14] can be written as

$c_{yo}(s + Q_i/v + Q_d/v) = Q_d/v(c_{yd})$

$c_{yo}/c_{yd} = [Q_d/(sv + Q_i + Q_d)]$

$c_{yo}/c_{yd} = [Q_d/(\zeta_2 s + 1)]$ [5.16]

Analysis of consistency control loop with known process dynamics:

The consistency control loop can be designed by various configurations (91) such as negative feedback, cascade, feedforward and feedback combination, feedforward and cascaded feedback, and ratio control. For simplicity negative feedback control configuration has been considered in this present study. It is usual that the dilution water from various sources(white water from papermaking wire and/or overflow re-circulated from headbox /spreader) is always added to the thick stock immediately before fan pump and then led to flow to a consistency sensor, and then to the other equipments of approach flow system including headbox. A feedback signal is obtained from the consistency sensor which is transmitted to the consistency controller through a

90

transmitter. A comparator is used in the loop to compare the set point and measured variable to produce an error which goes to the controller to determine an appropriate position of the valve controlling the flow of dilution water to the stock immediately ahead of the pump. The most important point in the design of consistency controller is to make sure that the dilution water added is well mixed with the stock before reaching the consistency sensor by incorporating a pump after the point of dilution water addition. The other important point to consider is the minimum length of the line between the point of water addition and location of consistency sensor to minimize the dead time or distance velocity lag. The value of the dead time for consistency control depends upon type of the process, loop design and location of sensor as given in the table 3.2, Appendix-1.

The transfer function of consistency control process can be adequately represented (91) by first order plus dead time as under

$$G_p(s) = K_p \left[e^{-\theta ds} / (1 + \zeta s) \right] \qquad [5.17a]$$

Carrying out bump test on the approach flow system flow loop, Nancy (91) developed dynamic equations (given in Appendix) in form of first order with dead time. In one of such equation, the dead time was reported of the order of 6.84s which is due to transmitter location relative to the dilution point. The time constant of 3.84s is due to the sensor measurement dynamics.

$$G_p(s) = -0.0407 \, e^{-6.84s} / (1 + 3.84s) \qquad [5.17b]$$

The eqn.[5.17b] must be expressed in terms of effective process gain, $K_{P(effective)}$. The effective process gain is defined as the ratio of % consistency and % controller output (2% to 4%). Using these values, one can get the following effective process transfer function with effective process gain of the order of -2.035.

$$G_p(s) = -2.035 \, e^{-6.84} / (1 + 3.84s) \qquad [5.17c]$$

(a) Lambda tuning:

According to Lambda tuning, one can write the following equation for open loop control system

$G_c(s) * G_p(s) = 1/\lambda s$,

So, $G_C(s) = 1/\lambda s * 1/G_p(s)$,

And the corresponding closed loop transfer function can be written as

$H(s) = G(s)/1+G(s) = 1/(1+\lambda s)$

After first order Pade's approximation of $e^{-6.84s}$, the process transfer function for open loop can be written as

$G_p(s) = -2.035 * (-3.42s + 1) / (1+ 3.84s) (3.42s + 1)$,

$G_p(s) = -2.035 * (-3.42s + 1) / (13.13 s^2 + 7.26s +1)$,

$G_c(s) = 1/\lambda s * (13.13 s^2 + 7.26s +1)/ -2.035 (1-3.42s)$,

Or $G_c(s) = [(13.13 s^2 + 7.26s +1)/ \lambda s (1-3.42s)*(-2.035)]$ [5.19]

Eqn.[5.18] can be written as

$G_c(s) = K_c[\zeta_I \zeta_d s^2 + \zeta_I s+1] /\zeta_I s$ [5.20]

Eqn.[5.20] multiplying by (1-3.42s) to both numerator and denominator,

$G_c(s) = K_c/\zeta_I * (\zeta_I \zeta_d s^2 + \zeta_I s+1) (1-3.42s) / s (1-3.42s)$

Or $G_c(s) = K_c/\zeta_I * [-3.42s \zeta_I \zeta_d s^3 +(\zeta_I \zeta_d -3.42 \zeta_I) s^2 +(\zeta_I -3.42) s+1] / s (1-3.42s)$ [5.21]

Comparing eqn.[5.21] and eqn.[5.19], one can find

$\zeta_I -3.42 = 7.26$, or $\zeta_I = 10.68$ s

$\zeta_I \zeta_d - 3.42 \zeta_I = 13.13$,

$\zeta_d = 4.65$ s

$K_c/\zeta_I = 1/-2.035\lambda$

$K_c = -5.248/ \lambda$

By using various values of lambda, the minimum of which equals to sum of process time constant and dead time(10.68s in this case),one can find out the values of the controller gain, K_c from the above equation. As λ is user defined value that determines the closed loop time constant, one can choose the value of lambda suitably which can give less overshoot. Higher value of lambda provides a slower response (91). A value of lambda sets the closed loop speed of response equal to open loop response. Typically the closed loop speed of response is set at half speed of the open loop response (lambda=2ζ). This prevents excessive control action. In this present investigation the value of lambda is selected on the basis of trial and error method above 2 to 3ζ or $\zeta + \zeta_d$ equal to 10.68s. Nancy also recommended a value of lambda of 15s. It has also been found in this present investigation the values of lambda between 15s-16s the system gives less overshoot.

(1) For λ=15 s.

K_c=-5.248/15 =-0.3498

G_c (s)= $K_c[1+1/\zeta_i s + \zeta_d s]$ or

G_c (s)=-0.0328[49.662 s^2 +10.68s +1]/s   [5.22]

$G_p(s)$ = -2.035 * (-3.42s + 1) / (13.13 s^2 + 7.26s +1),   [5.23]

Gc_L= [G_c (s)*G_p (s)/1+ G_c (s)*G_p (s)],

Gc_L = [(-11.34s^3+ 0.8766s^2+0.4845s+0.0667) /(1.79s^3+ 8.1366s^2+1.8445s+0.0667) [5.24]

(2) For λ =16 s.

K_c=-5.248/16 = -0.328

$G_c(s)$ = $K_c[1+1/\zeta_i s + \zeta_d s]$

$G_c(s)$ =-0.0307[49.662 s^2 +10.68s +1]/s

G_p (s)= $K_p [e^{-\theta_{ds}}$ (1+ ζs)]s

     =-2.035 $e^{-6.84}$/ (1+3.84s)

After Pade's approximation of $e^{-6.84}$, the process transfer function can be written as

$G_p(s) = -2.035 * (-3.42s + 1) / (13.13 s^2 + 7.26s + 1)$,

$Gc_L = [G_c (s)*G_p (s)/1 + G_c (s)*G_p (s)]$,

$Gc_L = [(-10.614 s^3 + 0.823 s^2 + 0.4453s + 0.06625)/ (2.516 s^3 + 8.0835 s^2 + 1.4453s + 0.06625)]$

[5.25]

Digital form of the closed loop transfer function:

Closed loop transfer function in eqn.[5.24] can be written for discrete system as under

$$\frac{-6.335 \ z^3 + 19.01 \ z^2 - 19.01 \ z + 6.34}{z^3 - 2.955 \ z^2 + 2.911 \ z - 0.9556}$$

[5.26]

Sampling time: 0.01

Closed loop transfer function in eqn. [5.25] can be written for discrete system

$$\frac{-4.219 \ z^3 + 12.66 \ z^2 - 12.66 \ z + 4.222}{z^3 - 2.968 \ z^2 + 2.937 \ z - 0.9684}$$

[5.27]

Sampling time: 0.01s

(b)Z-N tuning:

For the sake of comparison Z-N tuning of the controller has been attempted as it is the most commonly used method for controller parameters setting for other processes. However Z-N tuning requires the analysis of frequency response characteristics of the control system which will estimate the values of controller parameters for specified gain and phase margin. In order to get the controller parameters (K_c, ζ_I, ζ_d) by Z-N method for various control actions (P/PI/PID) stability analysis should be followed by using ultimate gain and ultimate period. The estimation of gain and period can be estimated by Nyquist and Bode stability criterion. Though the Nyquist criterion can be applied to the all systems but involved polar plot of the system frequency response in the complex plane.

In this present problem the Bode plot is used, because the Bode plot of a transfer function is simpler than Nyquist analysis, though it applies only to system for which amplitude ratio and phase shift vary monotonically with frequency. It is however very easy to see the effect of performance of changing system parameters on the Bode plot. It is to be noted that by adding derivative term, the cross over frequency increases which is desirable, whereas the amplitude ratio also gets increased which is not at all desirable. The following step by step procedure of Bode's plot is to be followed.

Step-1:

For estimation the cross over frequency, one should use phase margin or phase angle as under:

Total phase angle=Controller phase angle+ Process phase angle+ Transportation phase angle

$\phi=\phi_1+\phi_2+\phi_3$

$-\pi=0-\tan^{-1}(3.84\omega_{co})-\omega_{co}*\theta_d$

$-\pi=0-\tan^{-1}(3.84\omega_{co})-6.84*\omega_{co}$

$\tan^{-1}(3.84\omega_{co})=\pi-6.84\omega_{co}$

$3.84\omega_{co}=\tan(\pi-6.84\omega_{co})$ or $3.84\omega_{co}=-\tan(6.84\omega_{co})$

By iterative method, one can find $\omega_{co}=0.3278$ rad/sec.

Step-2:

For estimation of Gain margin or amplitude ratio (AR) is as follows.

Total amplitude ratio = (Amplitude ratio for controller) x (Amplitude ratio for process) x (Amplitude ratio for transportation lag)

$1= K_c* [-K_p/\sqrt{(1+\zeta^2\omega^2)}]* 1$ [5.28]

$1= K_c*[-2.035/\sqrt{[1+(3.84)^2(0.3278)^2]}]*1$

$K_c = -0.789 = K_{cu}$

$P_u = 2\pi/\omega_{co} = 19.158$ min/cycle

For PI controller (according to Zeigler-Nichol (Z-N) controller setting table)

$K_c = 0.45*K_{cu}$, $= -0.355$, $\zeta_i = P_u/1.2 = 15.965$,

After substituting these values, the controller transfer function can be written as

$G_c = [-0.355(15.965s+1)/15.965s]$ [5.29]

After Pade's approximation, the process transfer function can be written as

$G_p = -2.035/(3.84s+1)*[-3.42s+1)/(3.42s+1)]$ [5.30]

In paper mill, the most important paper property i.e. basis weight of paper depends on consistency of pulp. According to GSM requirement, consistency has to be changed. Thus changing consistency in a consistency control system can be termed as servo problem.

For closed loop servo problem of consistency control, transfer function for PI controller can be written as

$Y(s) = G_c G_p/ (1+ G_c G_p)$

$G_c G_p = [(-5.6675s-0.355)/15.965s][(-2.035+6.9597s)/(13.1328s^2+7.26s+1)]$

$\qquad = (-39.444s^2 +9.06s+0.722)/(209.665s^3+115.9059s^2+15.965s)$

$Y(s) = \dfrac{(-39.444s^2 +9.06s+0.722)/(209.665s^3+115.9059s^2+15.965s)}{[(209.665s^3+115.9059s^2+15.965s-39.444s^2+9.06s+0.722)/(209.665s^3+115.9059s^2+15.965s)]}$

$Y(s) = [(-39.44s^2+9.06s+0.722)/(209.67s^3+76.46s^2+25.02s+0.722)]$ [5.31]

Taking inverse Laplace transform one can get eqn. [5.31] for analog system

$Y(t) = [1-\exp(-0.1654t)(.4438\cos(0.2946t)+0.9518\sin(0.2946t)]$ [5.32]

For PID controller (according to Z-N tuning method)

$K_c = 0.6 \times K_{cu} = 0.6 \times (-0.789) = -0.474$

$\zeta_i = P_u/2 = 19.158/2 = 9.579$

$\zeta_d = P_u/8 = 2.39$

$G_c = K_c[1 + 1/\zeta_i s + \zeta_d s]$

$G_c = -0.474[1 + 9.58s + 23s^2]/9.58s$ [5.33]

After Pade's approximation the eqn.[5.33] can be written as

$G_p = -2.035 \, e^{-6.84s}/(3.84s+1) \times (-3.42s+1)/(3.42s+1)$ [5.34]

The closed loop transfer function for PID controller as under

$Y(s)/X(s) = [G_c G_p/(1 + G_c G_p)]$

      $= [(-7.86s^3 - 0.97s^2 + 0.616s + 0.1)/(5.27s^3 + 6.28s^2 + 1.616s + 0.1)]$

$Y(s) = [(-7.86s^3 - 0.97s^2 + 0.616s + 0.1)/(5.27s^3 + 6.28s^2 + 1.616s + 0.1)] \times 1/s$ [5.35]

Taking inverse Laplace transform of eqn. [5.35], eqn.[5.36] is obtained as.

     $Y(t) = [5.27 - 9.38e^{-.8612t} + 0.202 \, e^{-.2379t} - 3.95 \, e^{-.0926t}]$ [5.36]

Response Equation in digitized(z-domain) form:

Transforming in discrete form, eqn.[5.35] can be written as

$Y(z) = [(-1.491z^3 + 4.473z^2 - 4.471z + 1.49)/(z^3 - 2.988z^2 + 2.976z - .9882)]$ [5.37]

Expressing in discrete form(z-domain) for digital control system, eqn[5.31] can be written

as
$$\frac{-0.001876 \, z^2 + 0.003756 \, z - 0.001881}{z^3 - 2.996 \, z^2 + 2.993 \, z - 0.9964}$$ [5.38]

The control loop configuration for analog system is shown in fig. 5.2a. The Simulink MIMO

model for consistency control is shown in fig. 5.2b.(Case-b).The simulation results of PI &

PID controllers are shown in figs. 6.1&6.2,chapter-6.

gain and time constant, and tuned the controller using hit and trial method using Simulink tool. The control loop for the case b is shown as under.
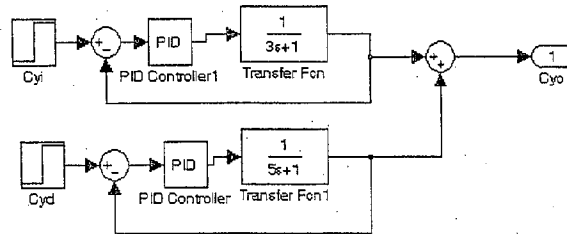
Fig. 5.2b Simulink model for consistency control (case-b)

CASE: 5.2 Modeling of stock flow control of the headbox:

5.2.1 Model for stock flow:

The static models for stock flow are described in Chapter 3,Section 3.4, eqns.[3.1-3.13] and table-3.2 (Appendix-1) wherein the equations for stock flow velocity at the outlet of slice and at the vena contracta have been shown. The simplified formula derived from Bernoulli's equation relating continuum mechanics for mechanical energy balance is reproduced below:
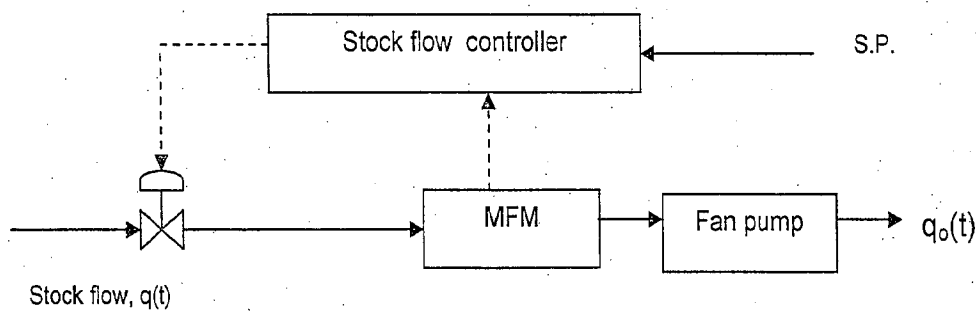
Fig. 5.3a   Flow control loop

Velocity of slice discharge $V = C\sqrt{(2gh)}$ [5.39a]

Using q for flow, Q for deviations from steady state value, h for stock level, H deviation from steady state value, h_s, the equations can be rewritten as

$q=C_CC_vA_S\sqrt{(2gh)}=C_qA_S\sqrt{(2gh)}=C_q\,w\,b\sqrt{(2gH)}=C_cwb\sqrt{(2gh)}$ [5.39b]

$Q=q-q_s=4.429C_cwb(h-h_s)=4.43wb(H)^{0.5}$

Thus it is clear that the model for stock flow is connected with level control problem. The equation is thus a nonlinear control problem.

The derivation for dynamics for both stock flow and stock level from first principles will be discussed in details in Section 5.2.2. The simple flow diagram for a stock flow control is shown in fig 5.3a. Flow can be measured with different types of flow-meters but electromagnetic flow-meter is widely used for corrosive acids, slurries etc, especially for paper pulp. The measuring element, the magnetic flow meter (MFM) supplies the feedback signal for the flow controller which in turn, compares the measured flow with set point and adjusts a flow control valve accordingly.

As far as dynamic model of stock flow is concerned the following linear stock flow model of first order has been the representative one. As already indicated,using q as a volumetric flow rate (fig.5.3a) and Q , the deviation from steady state value one can write,

$\zeta dQ_0/dt +Q_0(t) =Q(t)$

$\zeta sQ_0(s) +Q_0(s)=Q(s)$

$Q_0(s)/Q(s) =[1/(1+\zeta_p s)]$

In reality, for flow control there are three elements joined in series, hydraulic flow in pipe, valve and flow measuring devices. Nancy (91) has reported the overall transfer function is a third order process with time constants of the order of 0.5s, 0.8s and 2.0s respectively and process gain 1.5. This when coupled with a PI controller and considering interactions with the other parameters of the system, the control problem become more complicated

to analyse. To avoid this complexity majority of Indian pulp and paper industry use the coarse flow and fine flow control techniques for stock flow to the head box and its approach flow. These are analyzed below:

The fine flow controller receives the total head and wire speed as inputs. It then calculates the jet/wire ratio and uses this as process variable. The controller compensates for all minor disturbances with the help a bypass valve to reach set value as shown in fig.-5.3b.
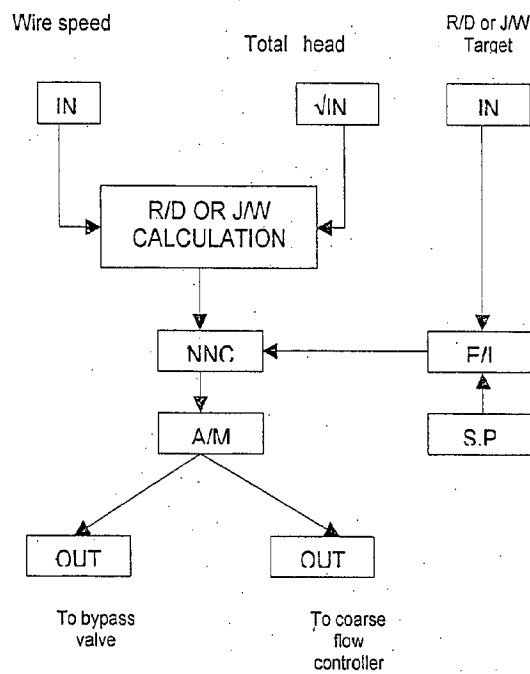
Fig.-5.3b Fine flow control

5.2.2 Development of ANN controller for the case of stock flow control in approach flow system:

Fig.-5.4 shows a simplified control block diagram for neural control of head box system. As already indicated, J/W is the system output representing the ratio of speed of the jet and speed of the wire and e is the error. Several important parameters must be properly determined in neural network design such as the learning rate and the neuron numbers in each layer. The program runs n iterative training cycles for the neural network with a fixed

hidden neuron numbers which progressively increase as shown in fig.5.5. Relationships

between wire speed and pressure or vacuum applied to head box at various values of

coefficient of discharge, C_v and coefficient of contraction, C_c obtained from theoretical

model for industry as well as detailed models are shown in table 6.3(Appendix-1). Using

the above artificial neural controller for stock flow control has been designed and

simulated. For ANN controller, the back propagation algorithm is used and neural network

is trained using MATLAB program shown in Appendix-2. In order to get the desired

results the algorithm developed in chapter 4, section 4.3.3 is employed. The comparisons

of data for industry and those obtained from models with simulated data from ANN

controller are discussed in Chapter-6.
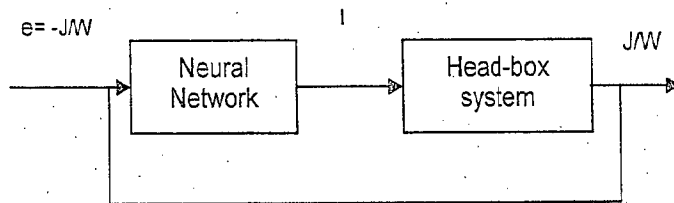
Fig.-5.4 A neural network control for
fine flow control
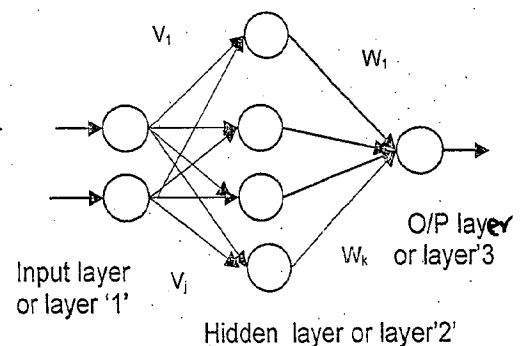
Fig.-5.5 Multi-layer neural
network structure

CASE:5.3 Modeling of total head of the headbox:

5.3.1 Model for total head:

Paper machine head box total head control is one of the most important control

applications on a paper machine. It achieves the transformation from stock to sheet. It is

also extremely fastest loop in the papermaking process(91).The total head measurement

on the side of the headbox and the PI controller which adjusts the fan pump reference

Sampling time: 0.01

The model for both open loop and closed loop transfer functions for analog and digital control system are subjected to MATLAB simulation. The stability test and tuning for PI controllers have been done. The results of Simulation are shown in Chapter-6 for both analog and digital system. MATLAB Simulink model of headbox total head control is shown in fig. 5.7.
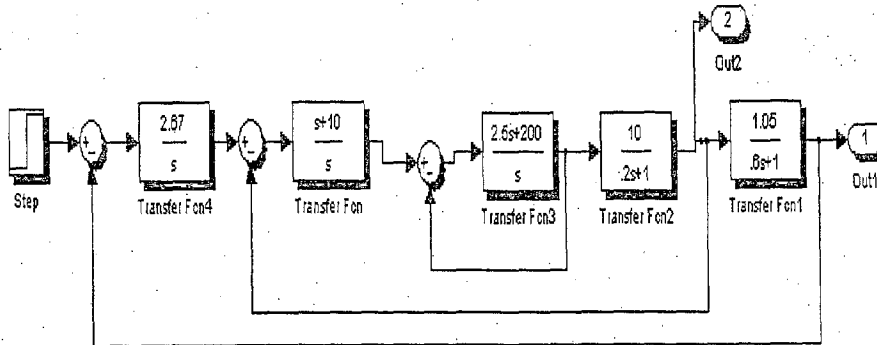
Fig. 5.7 Simulink model of headbox total head control system

5.3.2 Development of ANN controller for the case of total head control in approach flow system:

The reference total head and actual total head are used as input for ANN and these inputs are represented by one vector. The input of process uses an output for ANN controller which is the appropriate signal for the head box total head at desired level. The training pattern required for training the ANN are obtained from PI controller using the back propagation algorithm.

The number of layers and number of neurons in different layers are decided by trial and error procedure as already discussed in earlier section. The ANN controller is designed with 2 neurons in the first layer, 8 neurons in hidden layer and 1 neuron in output layer. In this network log-sigmoid activation functions are used.

CASE : 5.4 Modeling for stock level control of headbox:

The modeling of level control is well documented in all control literature both for linear and nonlinear systems. Here we apply this model for dynamics of stock level in open headbox, or in closed air pressure headbox where interactions with other parameters are considered negligible. For open headbox the head due to stock level is the only driving force for the stock flow as the external force implied on the stock is atmospheric pressure. For closed headbox (air padded) the additional air pressure are added to the stock head and in hydraulic headbox the entire driving force is from fan pump. The force balance equations for controlling stock level in various types of headbox are given in Appendix-3.

In the case of air cushion headbox, two interactive parameters are involved namely, stock level and stock flow conforming to MIMO system. The interaction between two parameters for MIMO system is described in section B. This can be measured with different types of transmitter (like differential pressure, potentiometric and intelligent) with very fast dynamics. These are described in Chapter 3, Section 3.4 and table-3.2, Appendix-1.

5.4.1 Model for stock level:

As usual it starts with material balance across equipments at steady and unsteady state conditions as shown in the following paragraph. In this case only the density of pulp suspension within the range of consistency 0.1 to 1.0% is included, resulting slight variation of density from that of water. For practical calculation however the density can be assumed the density of water.

For development of model of stock level control in open headbox the fig.5.8 is depicted as a simplified sketch of the headbox slice system actually drawn in Appendix-3. Using the

symbols for various input and output parameters given in the Chapter -Nomenclature the following Mass balance equation can be written for all types of level control systems (25).
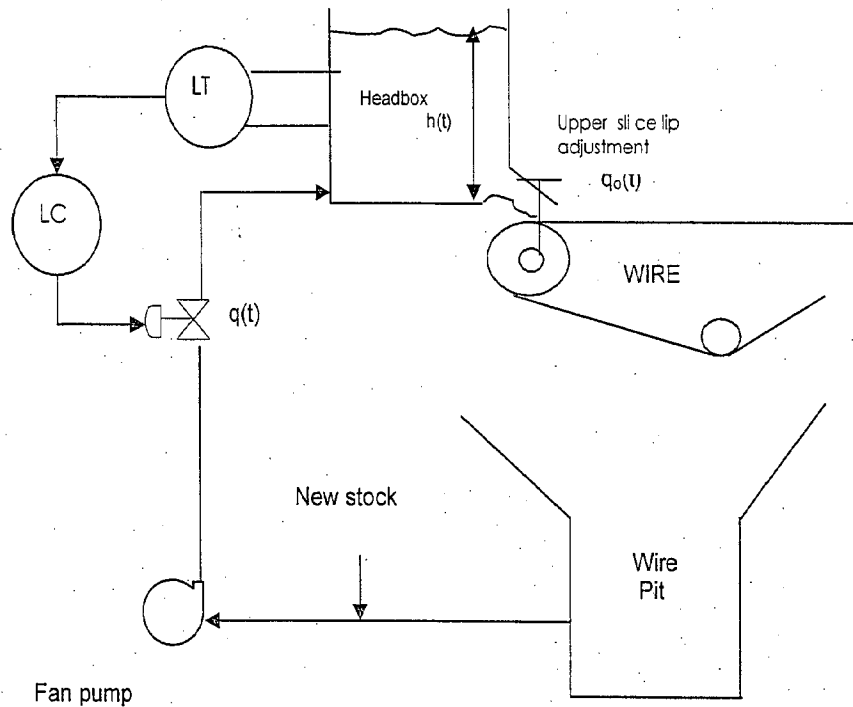
Fig.5.8 Model for stock level

For Linear or Non-Linear System

$$q(t)\rho - q_0(t)\rho_0 = d(v\rho)/dt = d(Ah\rho)/dt \tag{5.44}$$

Stock being incompressible fluid all density terms in eqn.[5.44] are cancelled out.

$$q(t) - q_0(t) = Adh/dt$$

The output flow $q_0(t)$ depends on level of stock and resistance of valve, R, the above equation can be written as for both linear and nonlinear system as under:

$$q(t) - h(t)/R = Adh/dt$$

or, $Adh/dt + h/R(t) = q(t)$

The systems can be defined linear, or nonlinear or with constant flow output (with a pump or a flow controller). Depend upon the nature of q_0 as under:

Linear: $q_0 = h/R$

Integrator: q_0 = constant

Nonlinear: $q_0 = Ch^n$ where n may have values such as 0.5, 1.5 etc.

if t=0, then h=hs, q=q_s, q_0=q_{0s}

$$[Ad(h-hs)/dt + (h-hs/R)] = q - q_s \qquad [5.45]$$

or $\qquad AdH/dt + H/R = Q$

Taking Laplace transform for linear first order system, one can get

$AsH(s) + H(s)/R = Q(s)$

$RAsH(s) + H(s) = Q(s).R$

$\zeta sH(s) + H(s) = Q(s).R$

$\zeta sH(s) + H(s) = Q(s)R$

$H(s)[\zeta s+1] = QsR$

$$H(s)/Q(s) = [R/(1+\zeta s)] \qquad [5.46]$$

If R tends to infinite, the eqn.[5.46] reduces to 1/As, the transfer function for a liquid level system with constant flow outlet i.e. an integration.

The eqn.[5.45] is of first order

When, $H/R = q_0$ or $H = q_0R$

$q_0(t) - q(t) = A(q_0R)/dt = ARdq_0/dt$

$\zeta dQ_0/dt + Q_0(t) = Q(t)$

$\zeta sQ_0(s) + Q_0(s) = Q(s)$

$$Q_0(s)/Q(s) = [1/(1+\zeta s)] \qquad [5.47]$$

Non Linear System Dynamics:

If valve is nonlinear

$q(t) - q_0(t) = Adh/dt$

$q_0 = ch^{1/2}$

111

$q_0 = q_{0(s)} + q_0'(h_s) + qo''(h_s)(h-h_s)^2/2! + qo'''(h_s)(h-h_s)^3/3! + \text{----------}$

$q_0'(h_s) = 1/2ch_s^{-1/2} = (R_1)^{-1}$

$q_0 = q_{os} + 1/2ch_s^{-1/2}(h-h_s) = q_{os} + 1/R_1(h-h_s)$

if $q-q_0 = Adh/dt$,then

$q_{(s)} - [q_0(s) + 1/R_1(h-h_s)] = Adh/dt$

$(q_0 - q_{os}) - 1/R_1(h-h_s) = Ad(h-h_s)/dt$

$Q - (1/R_1H) = AdH\backslash dt$

$Q(s) - (1/R_1H(s)) = AsH(s)$

$H(s)/Q(s) = [R_1/(1+\zeta s)]$ [5.48]

Analysis of SISO level control closed loops

The parameters for process gain, K_P and time constant (product of resistance and capacitance) depend upon the type of headbox, and the designs of both approach flow design and headbox itself. In absence of any dynamic characteristics of headbox system, the process gain is arbitrarily assumed to be 1.0 and the time constant is varied to any realistic value which will give the required response, corresponding to 63.2% of the ultimate value. Eqn.[5.48] has been tuned and simulated with the help of MATLAB Simulink toolbox using trial and error method as indicated above, one can get the transfer function for stock level.

$G_P(s) = 1/(0.2s+1)$ [5.49]

Digital form of process dynamics

Transforming the eqn.[5.49] for digital form(z-domain), one can get the following equation.

$G_P(z) = 5Z/(Z-0.9512)$.

However the above equation can not be applied for digital control system as does not content hold dynamics. In order to simulate through the MATLAB software hold dynamics

must be taken into account in all cases. Conversion of analog to digital form in MATLAB software the procedure is as follows:

The MATLAB command sysd=c2d (sysc, Ts, Method) converts the continuous time model sysc to a discrete time model sysd with sample time Ts. The String Method selects the discretization method such as zoh (zero order hold),foh (first order hold),imp(impulse), etc. Using MATLAB program, eqn.[5.49]can be transformed in discrete(z-domain) form as under

$$G(z) = [(0.04877)/(z-0.9512)] \hspace{4cm} [5.50]$$

The model of level control in headbox system in both analog and digital forms are simulated with the help of Simulink tool in MATLAB software and results are displayed in figs.6.28, 6.29(Chapter-6).
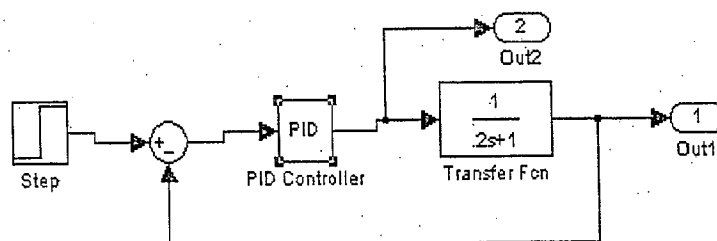
Fig. 5.9 Closed loop control strategy

5.4.2 Development of ANN controller for the case of stock level control in approach flow system:

Based on the procedure detailed in Chapter-4, the ANN controller is designed with 2 neurons in the first layer, 3 neurons in hidden layer and 1 neuron in output layer. In this network log-sigmoid activation functions are used. The number of layers and number of neurons in different layers are decided by trial and error procedure.

CASE-5.5: Modeling for pH control of stock:

The pH of the stock being handled by a wet end of paper machine has a pronounced effect on drainage and retention. The pH is a difficult variable to control, particularly so in the region of pH 7.0, because the major difficulties with pH sensors are inherent nonlinear characteristics, noise and sensitivity. However, this range of pH is very important for manufacturing various kinds of paper.

In Chapter 3 it is indicated that based on sizing principles at the stock preparation section of the paper mill, various sizing chemicals are added to maintain the pH of the stock. For acid sizing paper, rosin and alum are usually used to maintain head box pH in the range

Fig. 5.10a pH control strategy

between pH range 4.4-4.6(av.4.5) while for alkaline sizing, AKD or ASA or both are used to maintain pH generally above 7.0 (for AKD, pH range 6.0-9.0 but most effective at level of 8.0-9.0, for ASA, pH range, 5.0-9.0).The neutral sizing with dispersed rosin works in the pH range between 4.6-5.3 in the stock at the point of sheet formation. Whatever the desired value of the pH is required, that can be achieved by proper adjustment of the local conditions to secure optimum overall results. Some control system uses feed forward control to compensate for certain disturbances, variable gain feed back control to offset the nonlinearity of pH and large process capacities to damp out variations in pH. The above objective can also be fulfilled by controlling the flow rate of the acidic or basic reagent with the help of control valve operated by PI or PID controller in a negative feedback loop. This is obtained using the feedback signal and the stem position of the alum/acid, or alkali or dispersed rosin valve as manipulated variable. The chemicals can be added preferably at the suction side of the fan pump (shown in fig.5.10a) or at the thick stock in the blending chest or at the machine chest or at the machine chest pump. The pH measurement can be made at various locations: measurement from the stock entry to the headbox in the recirculation line before distribution header, in the discharge from the fan pump, in the white water from the trays or from the white water from the wire pit entering to the fan pump. Out of these alternatives, the first one is most recommended location.

5.5.1 Model for pH of stock:

Analysis of various available pH control strategies

pH though widely defined as $pH=-log_{10}[H^+]$ is not however amenable to measurement and controlling. Hence a pH meter is expected to show a nonlinear response to a step or sinusoidal changes in solution concentration, since the pH depends on the logarithm of the concentration.

Therefore it needs operational definition of pH by specifying the e.m.fs of two standard cells (electrodes) provided with a high impedance voltage measuring device. The pH of the paper machine stock is measured by the potential difference between a glass electrode and a reference electrode (usually Ag electrode, or calomel electrode or others).The measured potential across the system, can be written as $E = E_{ir} + E_m + E_j - E_{er}$, where E_{ir}, E_m, E_j, E_{er}, are the e.m.fs generated at the internal reference electrode, membrane, liquid junction and the external reference electrode. Under normal conditions the e.m.f at liquid junction is negligible and the same at the internal reference electrode and at the external reference electrode are constant. Therefore the above equation can be written as $E = E_o + E_m$, where E_o is a constant. For any ion selective electrode (H^+ ion in this present case), one can rewrite the Nernst equation, $E = E_o + (RT/nF)$ where a is the activity of H^+. Hence equation for sensing and measuring pH can be expressed as

$$pH = F(E_o - E)/2.303\ RT = (E_{ref} - E_{observed})/kT, \qquad [5.51]$$

where k=R/F

The electrode assemblies can be either immersed directly in stock lines or installed in a sample box or flow through electrode chamber through which a sample of stock is continuously run. All electrodes demand periodic servicing and cleaning preferably through ultrasonic cleaning devices. There are usually three models available, equilibrium constant models, the process identification with simulation or experiment and the titration curve method as under:

(a)Equilibrium Constant model

The approach for modeling pH dynamics requires that the various chemical species pertinent to the process must be known and also their equilibrium constants. In many actual plant situations, this data are not available. Schnelle et.al.,Wright and Kravaris(59)

116

have developed various techniques for linear and nonlinear control of pH of many chemical processes including waste water treatment. Mahuli et al.(59) and Sung et. al.(59) also investigated the pH control for nonlinear system using statistical technique for continuous on-line model adaptation or through identification reactor. But they have limitations for controlling effective pH control of headbox stock in papermaking wet end due to complicated nature of thin stock, and their time varying nature. Modeling of pH control using equilibrium constant model needs thorough understanding about the chemical environment and charged species inside the mixing box in the commercial stock which can be correlated to the $[H^+]$ ion concentration.

(b) Process identification techniques:
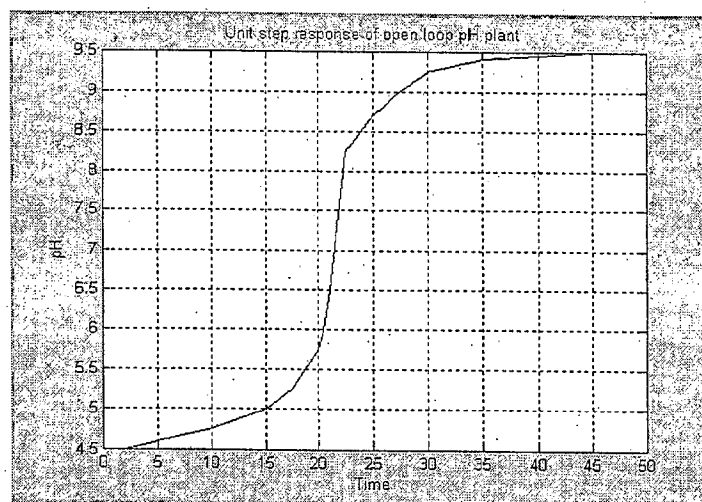
Fig. 5.10b pH dynamics

When the dynamic model of the process is not known for which either PID constants are to be found, its open loop response for a step input is determined experimentally or by simulation (90). The dynamic response is S-shaped (sigmoid function). Similar curve is also found for pH as a function of concentration in the titration curve but it passes through origin instead of intercept in the pH axis. The response curve is characterized by two constants, dead time and time constant, ζ which are determined by drawing a tangent at

117

the inflection point (control point) and finding its intersection with the time axis and the line corresponding to the steady state value of output. The response in this case can be again modeled as first order with dead time as shown above.

The gain K_p corresponds to the steady state value of the output response, after finding the values of K_p, ζ_p, ζ_d. The values of PI and PID control parameters can be found out by Z-N (Zeigler-Nichols)open loop tuning method using the following(given in Appendix-1).

$K_c = 1.2\, \zeta / \zeta_d$, $K_i = 2\, \zeta_d$, $K_d = 0.5\, \zeta_d$

Nagrath and Gopal (90) derived the titration curve of pH is a function of time from the actual set up of pH control plant (Approximate data is shown in the Appendix-1). If the pH of stock is to be obtained at a set point in the pH range 4.0 to 7.0, the gain of the valve is found of the order of 5.6ml/s of basic reagent/rad. opening of the valve.

On the analysis of open loop step response of the plant by drawing the tangent of inflection point one can get the value of dead time, time constant , controller gain, integral time and derivative time of the order of 19.9s,1.8s,0.108, 39.8s, and 9.95s respectively. The PID controller is tuned to this values and the closed loop step response is shown in fig 5.10b. The performance indices are found as % overshoot, rise time and settling time, 26%, 0.3s, 9.2s respectively. The dynamic equation of the pH control system can be written as under:

$G(s) = 5.67e^{-19.9s}/(1.8s+1)$

(c) Titration curve method:

The third model- the equivalent titration method requires the titration curves for systems with or without buffering the solution. The dynamic model keeps track of the amount of each stream that is in the vessel at any point in time.

For the paper machine stock depending on the range of pH at the headbox at least three types of neutralization curve are required for dynamic modeling of the system. In this present investigation only one type of neutralization curve for desired pH either at 5.5(neutral sizing) or at 8.0 (alkaline sizing)are taken as a base case. Unfortunately no data were available to draw the titration curve for papermaking approach flow system. Hence the titration curve (shown in fig.5.10c) obtained by from Harriott (53) is taken for analysis. This curve is the same as drawn by Hong Wang et. al. pH as a function of dimensionless concentration for papermaking.
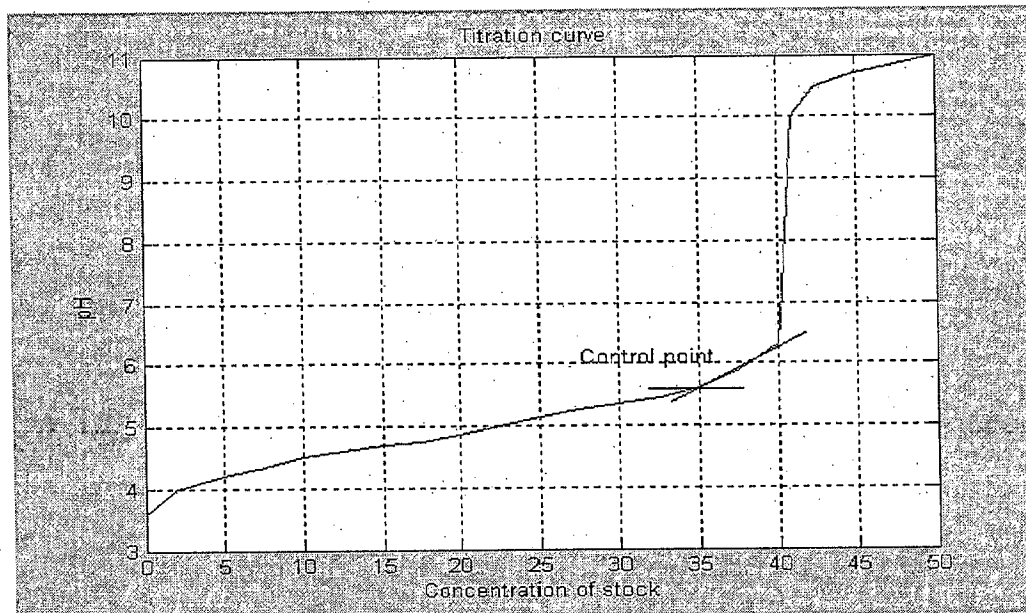

Fig. 5.10c Titration curve for pH

Analysis of the titration curves which are strongly nonlinear, indicate that there are two inflexion points which are considered as control points. This can be assumed as a combination of two first order systems joined at the first inflexion point. It can also be modeled as first order system with time lag as shown below:

$$G(s) = K_p e^{-\zeta_d s} / (\zeta_p s + 1)$$

Actually the two time constants are associated with the standard flow cell for industrial pH control-one hold up time, v/q, if the cell is well mixed and a diffusion time constant with a

119

special low hold up cell response (which is usually of very low order of magnitude, hence negligible) is more nearly first order but too fast to show clearly the effect of flow rate.

These are affected by the changes in load resulting from change in concentrations and changes in flow. The load changes affect the process gain and may alter the time constants of the system. From the curve, the slope at the control point is determined first and then value of process gain, K_P is evaluated as a ratio of % change in pH and % change in flow. For all practical design the value of K_P is kept normally above 1. Harriott recommended this value at about 6 for nearly neutral pH(pH=7.0)and 64 for pH of the order of 8.0, both based on pH range of 5.This data is a prerequisite in order to calculate the controller gain, K_C.

To estimate K_{max}, in eqn.[5.52],one has to estimate the time constants of all the elements in the open loop and A.R. is then determined after assuming a suitable value of critical frequency to get the target 180° phase lag in an iterative way. The gains for the other elements are to be determined or assumed.

$K_{max}=1/A.R.$ at 180°lag [5.52]

$K_{Cmax}=K_{max}/(K_1 K_2K_3...K_n)$ [5.53]

For stable operation the product of maximum gain and the critical frequency as an index of controllability has been used.

A control system designed for regulator operation must minimize the effect of load changes on the process output. At the optimum controller settings, the response to a load change is similar to that of underdamped second order system, and the frequency is 10-30 per cent less than the critical frequency and the decay ratio is usually ¼. For a gain that gives a decay ratio of ¼ , the damping coefficient, ξ is 0.22 and the peak error is 1.5

120

times the steady state error(offset).Therefore load changes at the start of the system the peak error can be represented as under which is applicable for proportional control only.

Peak error$\approx$1.5 $K_L/(1+K)$ where $K=K_C(K_1\,K_2K_3...K_n)$ [5.54]

To apply the above in actual pH control system provided with proportional or proportional reset controller, the elements comprising of dynamic modeling of the process, the acid or alkali mixing tank(K_P, ζ_P) ,dynamics of control valve(K_v, ζ_v),electrodes((K_E, ζ_E),cell(K_{cl}, ζ_{cl}), the transportation lag in mixing tank(ζ_{P1}) and due to sampling ζ_{P2}) must be known. For all the elements instead of theoretical time constants, effective time constants are used.

To estimate the time constant for process one has to know the capacity and resistance of the process (size of the mixing tank and volumetric flow rate), but for pH electrodes the following equation is used.

$\zeta_E=0.5z^2/D_v$ [5.55]

Where z is the effective film thickness and D_v , the volumetric diffusivity. The value of ζ_E generally varies between a minimum 0.4 s to 2.0 s for buffered solution and 10s to 20 s for unbuffered solution depending upon the velocity and the ion concentration. The value could be reduced significantly to 30 μs if necessary by using a high velocity flow cell and cleaning by sudden jet of solution. The detailed data used for dynamic study for pH control process are shown in the Appendix-3.

Development of Model of pH control system

On analysis of the three types of pH control procedure and in absence of experimental data the titration curve method is the most suitable for industrial practice. Hence it is adopted in this work.In the preset investigation based on the data reported, the dynamics of the pH control system is assumed to be of first order for a control pH. The values of

(K_P, ζ_P) are varied between 5.0- 8.0 and 1.0 s-2.0 s. The parameters for other loop elements except the controller are assumed as follows:

ζ_d= ζ_E= ζ_{cel}= ζ_v= 0.0 and the corresponding gain values are: K_E= K_{Cel}= K_v=1.0.

The values of time constant and process gain are found through MATLAB simulation and found to be of the order of 1.5 s and 7.0(% change of pH)/(% change in flow) respectively.Therefore the process transfer function can be represented as

G(s) = 7.0/(1.5s+1) [5.56]

From the plant experience the value as mentioned earlier K_p=6.0 and time constant 1.5 to 1.8s closely tally with the simulated values (7.0 and 1.5s). The block diagram for closed loop system for pH control is shown in fig.5.10d.
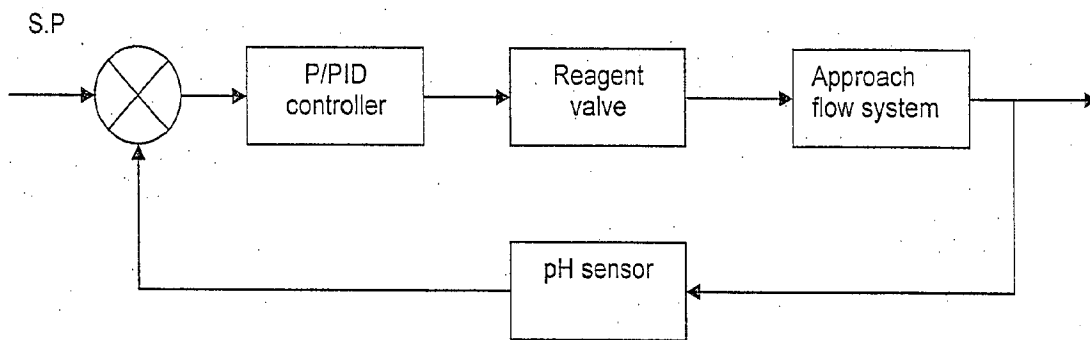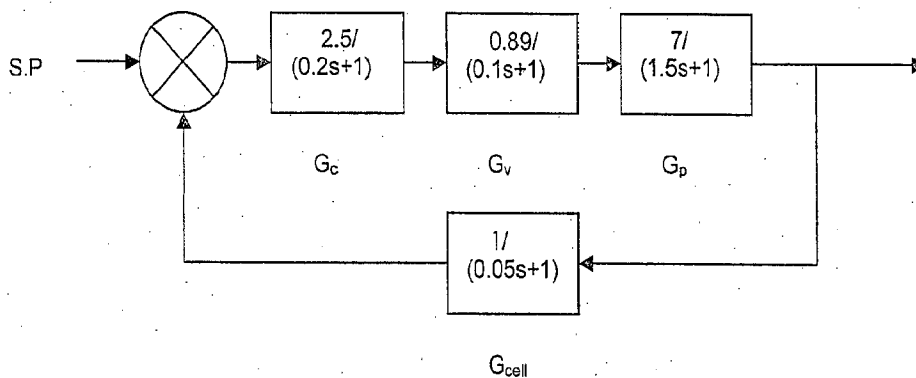

Fig.5.10d pH control strategy

Fig. 5.10e Block diagram for stock pH control process

Digital form of process transfer function:

The eqn.[5.56] should be discretized for digital computer simulation. The discrete time model of pH can be developed in two ways in terms of z-transform or modified z-transform and with the use of difference equation. Both discrete models are inter convertible and are demonstrated by Seborg et al. (139). The model based on difference equation has been developed by Hong et al.(59)which is shown in the Appendix-3.

However more simple approach is to get the analog model by simulation and transforming the same to discrete form applicable for digital system.

The eqn.[5.56] can be written in z-domain(z-transform) as

$4.6z /(z-0.5132)$

The procedure of conversion for continuous to discrete form using MATLAB software is detailed in section 5.4.1. The continuous model in discrete form (z-domain) with zero hold order can be written as

$$\frac{3.406}{z - 0.5134} \qquad\qquad [5.57]$$

with sampling time of 1.0s

The closed loop system with a fixed PID controller for the pH is shown in fig.5.10f.The pH process transfer function has been described by eqn.[5.56].The PID controller parameters are based on a trial and error approach owing to difficulties in establishing an analytical solution for the nonlinear process. The controller parameters on MATLAB simulation are found are: $K_C=2.5$, $\zeta_c=0.8$.
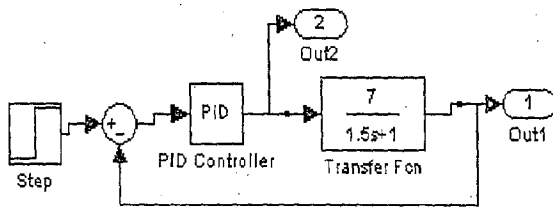
123

Fig. 5.10f Closed loop system

5.5.2 Development of ANN controller for the case of pH control of stock in approach flow system:

The ANN controller is designed with 2 neurons in the first layer, 12 neurons in hidden layer and 1 neuron in output layer. In this network, logsig activation functions are used. The number of layers and number of neurons in different layers are decided by trial and error procedure.

CASE: 5.6 Modeling for stock temperature control:

5.6.1 Model for stock temperature:

It is well known fact that higher temperature of stock will increase the drainage rate on the wire by reducing surface tension and viscosity of water. Stock temperature can be measured by different types of sensors-transmitters with reasonable dynamic characteristics. The sensors which provide measurement in terms of electrical signal such as thermocouples, resistance bulb thermometers, and thermistors are most common types. The dynamic response of most sensors is usually much faster than the dynamics of the process itself. The time constants for various temperature measuring devices vary widely depending upon the construction type. These are described in Chapter 3, Section 3.4 and Appendix-1, table-3.2. Luyben (81) has reported for thermocouples of the order of

124

30 s with a heavy thermo well but Nancy(91) reported this to be of the order of 2 s .The value of time constants of thermistors, semiconductors and optical sensors(photoconductors, and photovoltaic cell) are of the order of 0.3s,0.01s,10ms,1-100μs respectively whereas the same for resistance temperature detector(RTD) though possess very fast dynamics, may have the values intermediate between thermocouples and thermistors. Their basic dynamic behaviour can also be examined in terms of temperature profiles. For temperature control of approach flow system including the headbox there are two kinds of dynamics available. One for the measurement system itself with appropriate sensor and the other when temperature of the stock is controlled in the system. However, the temperature control system can preferably be used before entering to the headbox. In most cases, the temperature of stock in headbox or silo with temperature as a feedback signal is controlled by modulating the amount of live steam as manipulated variable entered to the silo or the flow of gas to a special gas fired white water heater. The controller used is usually a conventional PI controller.

Eqns.[5.63-5.69] represent the dynamic models of temperature measurement as well as approach flow system to the headbox. In this present investigation, the models considered are as under.
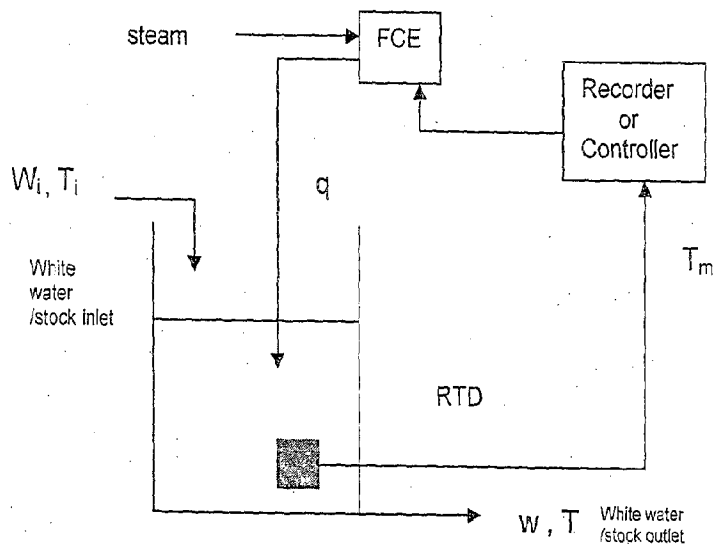
Fig.5.11 Temperature control strategy

Dynamics of temperature measurement system (thermo well or thermocouple):

The energy balance equation on the thermo well can be expressed as

$$mC_P \, dT_m/dt = UA(T-T_m) \qquad [5.58]$$

The above equation can be rearranged as

$$[(mC_P/UA)dT_m/dt] + T_m = T$$

Converting to deviation variables and taking the laplace transform, one can write

$$(\zeta s+1) \, T'_m(s) = T'(s) \quad \text{or} \quad T'_m(s)/T'(s) = 1/(\zeta s+1) \qquad [5.59]$$

Where m=mass, C_P=specific heat, T_m= measured temperature, T=surrounding temperature, U= heat transfer coefficient, A= heat transfer area

The dynamics of thermocouple-thermowell combined system when the resistance of thermowell is not neglected one can derive a second order system with two first order interacting system joined in series.

In general temperature measurement system can be modeled as under:

One capacity process

$$G(s)=T'(s)/T_i'(s) = K_P/(\zeta s+1) \tag{5.60}$$

For two capacity processes

$$\zeta^2 \, d^2T/dt^2 + 2\xi \, \zeta dT/dt + T = T_i \tag{5.61a}$$

$$G(s)=K_P/[\zeta^2 \, s^2 + 2\xi \, \zeta s + 1] \tag{5.61b}$$

Two capacity processes joined in series (non-interacting type)

$$G_P(s)=K_P/(1+\zeta_1 s)(1+\zeta_2 s) \tag{5.62}$$

Dynamics of temperature control process:

Fig.5.11 is a typical temperature control system (shown as a purpose of model building) for heating a stock storage tank where steam is used as manipulated variable.

An unsteady state energy balance equation can be written as

$$\rho C_P \, VdT/dt = q + wC_P \, (T_i-T_o) - wC_P \, (T-T_o) \tag{5.63}$$

At steady state condition $dT/dt=0$; then eqn.[5.63]becomes

$$q_s + wC_P \, (T_{is}-T_o) - wC_P \, (T_s-T_o)=0 \tag{5.64}$$

subtracting eqn.[5.63] from eqn.[5.64] one can write

$$q-q_s = wC_P \, [(T_i-T_{is})-(T-T_s)] = \rho C_P \, Vd(T-T_s)/dt \tag{5.65}$$

if deviation variables $Q= q-q_s$; $T_i' = T_i-T_{is}$; $T' = T-T_s$

Eqn.[5.65] can be written as

$$Q = wC_P \, (T_i'-T') = \rho C_P \, VdT'/dt \tag{5.66}$$

Taking laplace transform of eqn.[5.66]

$Q(s)= wC_P \, [T_i'(s)-T'(s)] = \rho C_P \, V \, sT'(s)$ or $T'(s)[(\rho C_P /w)s+1]=Q(s)/wC_P + T_i'(s)$

Or $T'(s)= [(1/wC_P)Q(s)]/(\zeta s+1) + T_i'(s)/(\zeta s+1)$

If there is a change in $Q(t)$ only, then $T_i'(t)=0$, the transfer function relating T' to Q

127

$T'(s)/Q(s) = (1/wC_P)/(\zeta s+1)$ [5.67]

If there is a change in $T_i(t)$ only, then $Q'(t)=0$, the transfer function relating T' to T_i

$T'(s)/T_i'(s) = 1/(\zeta s+1)$ [5.68]

There are many dynamic models available in literature for temperature control system which belongs to either first order or second order, or first order with dead time or two first orders joined in series. However in real situation, dynamics of temperature measurement is found to be an over damped system. The dynamic parameters used by various process control engineers are summarized in table 5.5, Appendix-1.

In the present investigation the time constant has been taken on the order of 0.2 and the value of K_P has been varied between 1 to 100 during MATLAB simulation. The best value of K_p was found on the order of 60. This indicates that small changes in Δ input give very high Δ output. In other word the system appears very sensitive as it displays very high K_P value for small change in input.

The equation is representing temperature control process as under

$G_p(s)=[60/(0.2s+1)]$ [5.69]

Digital form of process transfer function:

Transforming the equ.[5.69] for digital form(z-domain), one can get the following equation.

$$G_p(z) =30z/(z-e^{-5t})$$

The procedure of conversion of analog to digital form in MATLAB software is already detailed in section 5.4.1. Eqn.[5.69]can be written in discrete form(z-domain) using zero hold order as under:

$G_p(z) =[(2.926)/(z-0.9512)]$ [5.70]

As already indicated, the model for stock temperature control is simulated with the help of Simulink tool in MATLAB software and results are shown in Chapter-6.
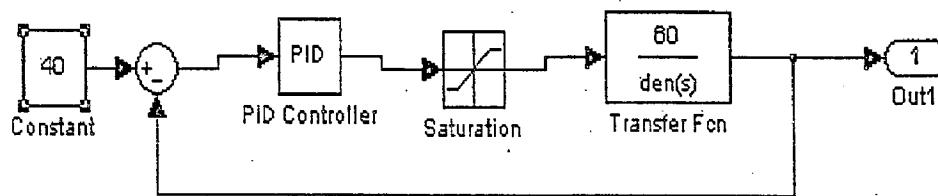
Fig.-5.12 Closed control loop (Simulink model)

5.6.2 Development of ANN controller for the case of stock temperature control in approach flow system:

The artificial neural network controllers have been developed using three multilayer perceptron methodologies such as MLP, DLFANN(direct linear feed through ANN), MFLANN(modified functional link ANN). A single hidden layer MLP is employed to develop the direct inverse controller which is used for implementation of neuro-control. The DLF ANN used in this investigation to model the process makes use of additional weights, which directly connects the input layer to the output layer. Rest of the architecture is akin to that of MLP. The DLFANN is able to model the linearity in stock temperature control system. But M-FLANN adds only self and lateral feedback connections to the output layer.

In the present study, two neurons account for two inputs, stock flow rate F, stock inlet temperature T_j .One neuron in the output layer is used to determine control signal. The network is 2:10:1. The training of MLP as direct inverse of a headbox stock temperature is shown in fig. 5.13.
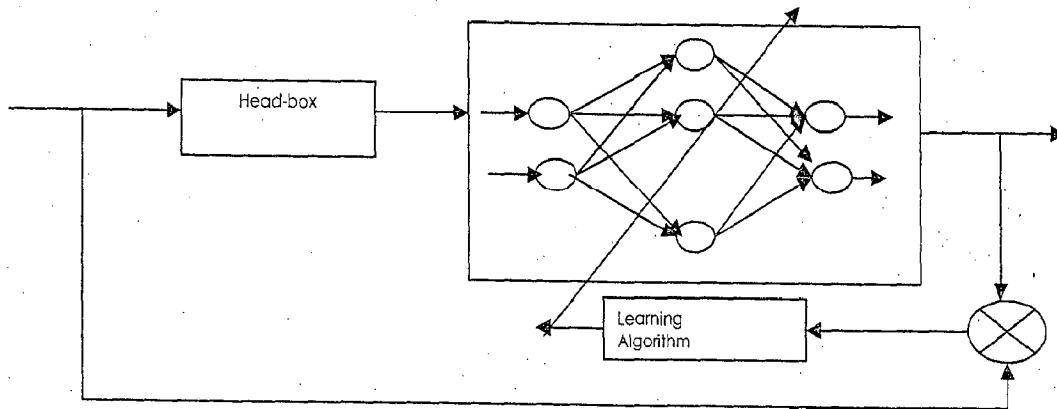
129

Fig-5.13 Training of MLP as direct inverse of a head box system

CASE: 5.7 Modeling of basis weight of the paper (Analog system):

For high quality rolls and reels of paper, basis weight as well as its moisture content is necessary to control. Basis weight of paper depends on the headbox slice opening as the adjustment of slice has a decided effect on the flow of stock through several of the adjoining sections of the slice. This must be taken into account in any controller (analog or digital) that is to be successful in leveling basis weight. Analog system is characterized by the fact that this is continuous. Both error detection and control actions are carried out continuously. The control action required of an analog controller is developed by applying the error detected to an accurate electronic or pneumatic analog of the control action wanted. This is inexpensive for small control jobs and usually quite simple but it is very difficult to implement complex control algorithms. It is also virtually impossible to adjust the amount of proportional, integral or derivative action derivable from an analog controller on a continuous basis. One of the most common controllers available commercially is the proportional integral controller. Incidentally many mills are currently using a PI controller for the basis weight control (144).
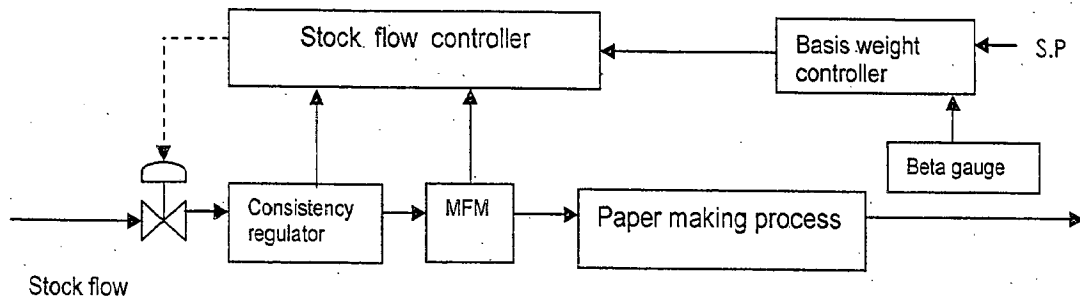
130

5.7.1 Model for basis weight:

Fig. 5.14a Basis weight control loop

Fig.5.14a shows a simplified loop for basis weight control. The relation in between, stock flow to the paper machine and the basis weight of the paper have been approximated by the following transfer function models by Ogunnaike and Ray (120) for the SISO system.

$$Y(s)=[0.55e^{-8s}/(7.5s+1)]u(s) \qquad [5.71a]$$

$$Y(s)=[0.40e^{-10s}/(8.0s+1)]u(s) \qquad [5.72a]$$

where u= Stock flow rate and Y=Basis weight of paper

Digital form of the response

Transforming eqns.[5.71a & 5.72a] in discrete form(z-domain)

Transfer function:
$$z^{\wedge}(-3) * \frac{0.1287\ z + 0.02717}{z^{\wedge}2 - 0.7165\ z} \qquad [5.71b]$$

Sampling time: 2.5

Transfer function:
$$z^{\wedge}(-6) * \frac{0.02423\ z + 0.04415}{z^{\wedge}2 - 0.829\ z} \qquad [5.72b]$$

Sampling time: 1.5

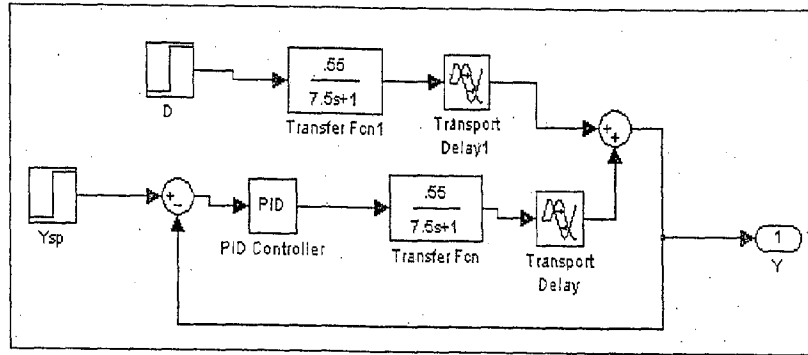The Simulink model for basis weight control is shown in fig.5.14b.

Fig.-5.14b Closed control loop

5.7.2 Development of ANN controller for the case of basis weight control:

The reference basis weight and actual basis weight are used as input for ANN and these inputs are represented by one vector. The input of process uses an output for ANN controller, which is the appropriate signal for the paper basis weight at desired level. The training pattern required for training the ANN is obtained from PI controller. The ANN is trained using the back propagation algorithm. During training, weights and biases of neural network are adjusted to minimize the network performance- the negative of gradient and the training is stopped when desired goal is reached.

The ANN controller is designed with 1neuron in the first layer, 5 neurons in hidden layer and 1 neuron in output layer. In this network log-sigmoid activation functions are used. The number of layers and number of neurons in different layers are decided by trial and error procedure.

CASE:5.8 Modeling of basis weight of the paper(Digital system):

In the above case, analog controller has been used for controlling the basis weight. With the advent of microprocessor based computer control, it would be advantageous to employ digital control technique for controlling basis weight. The well known two mode analog PI is replaced by software based control algorithm which resides in the computer.

132

The merit of digital controller is not only in its efficiency to control but the simplicity with which it can be tuned i.e. by proper adjustment of controller parameter for obtaining the best result.

5.8.1 Model development for basis weight:

The dynamics of basis weight in digital form has already been reported (127,128) though detailed derivation was not available and probably is not in line. The approaches were also quite different. Some used the basis of first principles whereas the other employed order reduction process. As a result analysis of the available closed loop in direct digital control system became difficult.

Model development from first principles:

To re-examine the dynamics, the control scheme used by Shankarnarayan(127) shown in the diagram(fig.-5.15) is again subjected to analysis. To compare the role of position of hold element another control scheme (fig.5.16a) has also been proposed. The development of both the loops and the transfer function of the process in terms of z-transform equation are shown below:
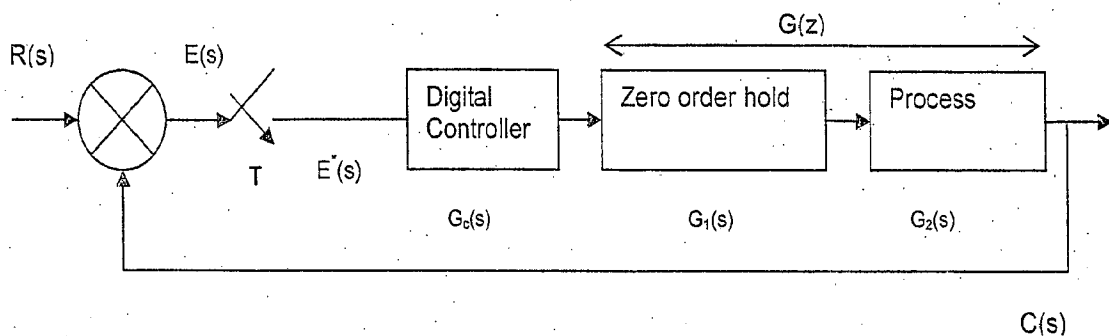

Fig. 5.15 Digital closed control loop

If the output is specified, the transfer function of a digital controller is determined to give desired output for the process. The output can be expressed as

$$C(z)=[G(z)G_c(z)R(z)/1+G(z)G_c(z)] \text{ or } G_c(z)=[C(z)/G(z)[R(z)-C(z)]]$$

Or $G_c(z) = 1/G(z)[\{C(z)/R(z)\}/\{1- C(z)/R(z)\}]$ [5.73a]

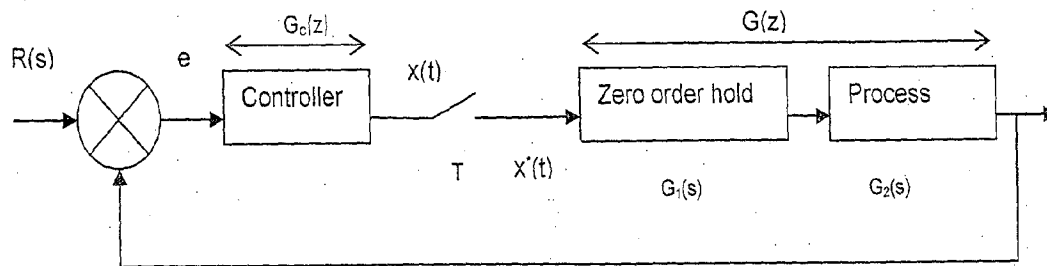The following digital control scheme is proposed by Sankranaranan (128).

Fig. 5.16a   Digital closed control loop

The transfer function of a zero hold device is an important element in designing a digital control loop, which is described as under.

The device retains the value of x(t) at each sampling instant, $x_{hold}(t)$ in a series of steps.

$x_{hold}(t)=x(0)[u(t)-u(t-T)]+x(T)[u(t-T)-u(t-2T)]+x(2T)[u(t-2T)-u(t-3T)]+......$ [5.73b]

where u(t) is unit step function starting at t=0, u(t-T) is unit step function starting at t=T.

Taking laplace transform of eqn.[5.73b], one can write

$x_{hold}(s)=x(0)[(1-e^{-Ts})/s]+x(T)[(e^{-Ts}- e^{-2Ts})/s]+x(2T)[(e^{-2Ts}- e^{-3Ts})/s]+.......$

or $= (1- e^{-Ts})/s[x(0)+x(T)e^{-Ts}+x(2T)e^{-Ts}+........]$ or $(1- e^{-Ts})/s[x^*(s)]$

The laplace transform of a zero hold device in s-domain can be written as

$G_1(s)= (1- e^{-Ts})/s$ [5.73c]

Process transfer function can be assumed as first order

$G_2(s)=K_c/(t_cs+1)$ [5.73d]

Or $G(s)=G_1G_2(s)$

$G(s)= [(1- e^{-Ts})/s][K_c/(t_cs+1)]$

Or $=(1- e^{-Ts})[K_c/s(t_cs+1)]$

$= (1-z^{-1})K_c * \text{Z-transform of}[(1/s)-(t_c/\ t_cs+1)]$

Or $G(z)=(1-z^{-1})K_c[z/(z-1)-z/(z-e^{-t/tc})]$

Or $\quad =K_c(z-1)[(z-e^{-t/tc})-(z-1)]/\ (z-e^{-t/tc})(z-1)\quad$ or $\quad K_c[(z-e^{-t/tc})-(z-1)]/\ (z-e^{-t/tc})$

$=K_c[z^{-1}(1-e^{-t/tc})]/(1-e^{-t/tc}z^{-1})\quad$ or $\quad =(\ K_cPz^{-1})/(1-(1-P)z^{-1})$; Where P= $(1-e^{-t/tc})$ [5.73e]

Because of N+1 sampling period, eqn.[5.73e] becomes

$G(z)=[K_c\ PZ^{-(N+1)}/\ 1-(1-P)Z^{-1}]$ [5.73f]

T, the sampling time, K_c, the process gain, t_c, time constant, Z^{-1}, delay due to one sampling time, $Z^{-(N+1)}=$ delay due to (N+1) sampling periods

If the required response $G_{cl}(z)$ is exponential having a closed loop time constant t_o, then

$G_{cl}(s)=[(1-e^{-st})/s][1/1+st_o)]$

Or $G_{cl}(z) = QZ^{-(N+1)}/\ 1-(1-Q)Z^{-1}$ [5.74]

Where Q= $(1-e^{-t/to})$

The desired closed loop response is $G_{cl}(z)$ (output/input) can be written as

$G_{cl}(z)=[G(z)G_c(z)/1+G(z)G_c(z)]\quad$ or $\quad G_{cl}(z)+G(z)G_c(z)G_{cl}(z)=G(z)G_c(z)$

Or $G_c(z)G(z)[1-G_{cl}(z)]= G_{cl}(z)\quad$ or $\quad G_c(z)= [G_{cl}(z)/1-G_{cl}(z)]*\ 1/G(z)$ [5.75]

Putting the value of $G_{cl}(z)$ in eqn.[5.75] , one can get

$G_c(z)=(1/G)[Qz^{-(N+1)}/1-(1-Q)z^{-1}-Qz^{-(N+1)}]$ [5.76a]

$G_c(z)= [[Qz^{-(N+1)}/\ 1-(1-Q)z^{-1}]/\ [1-(1-Q)z^{-1}-Qz^{-(N+1)}/\ 1-(1-Q)z^{-1}]] *[1-(1-P)z^{-1}]/\ KPz^{-(N+1)}]$

Or $G_c(z) = Q[1-(1-P)z^{-1}]\ /\ KP[1-(1-Q)z^{-1}-Qz^{-(N+1)}]$ [5.76b]

Converting the above positional eqn.[5.76b] into an incremental one

$\Delta G_c(z)$ = change in controller output/ controller input

$\Delta G_c(z) = Q[1-(1-P)z^{-1}]\ (1-z^{-1})/\ KP[1-(1-Q)z^{-1}-Qz^{-(N+1)}]$ [5.77]

The eqn.[5.77] enables writing an appropriate algorithm for providing digital control.

Modeling by Order reduction process:

If each section of the paper making process is considered separately then the process is quite complex. But under certain ideal conditions, it can be considered a single input/single output system with the gate opening of the mixing tank as input and basis weight of paper (weight of unit area of paper i.e., of $1\ m^2$) in gram per square meter (gsm) as output. The input/output data collected by Tee et al(155) have been used for the purpose of obtaining model of the system. Experiments were conducted on a Fourdrinier machine manufacturing 50 g/m^2 wood free book paper where input variable was the scale reading on the stock gate opening located in the mixing box and the output was recorded in terms of gsm of paper measured by weighing three samples taken out every 1 minutes. The equation [5.77] can be written in form below (eqn.5.78) which has been the starting model reported by Mukherjee(89) in his attempt for order reduction process .The same has been reproduced for further development of neural model and analysis with experimental data and MATLAB simulation as under:

$$\text{If } G(z) = \frac{X(z)}{U(z)} = \frac{a_0 + a_1 z^{-1} + \ldots\ldots + a_m z^{-m}}{1 + b_1 z^{-1} + \ldots\ldots\ldots + b_n z^{-n}} \qquad [5.78]$$

Eqn.[5.78] can be put in the form of difference equation as.

$$X_k = \sum_{i=0}^{m} a_i\, u_k - \sum_{i=1}^{n} b_i\, X_{k-l} \qquad [5.79]$$

Where

$u_j\ (i = 1,2\ldots\ldots\ \ N)$

$x_i\ (i = 1,2\ldots\ldots\ \ N)$

u_j , x_i are input and output of the system recorded N-times each after constant interval of time known as sampling time. In order to determine the parameters a_0, a_1........a_m and $b_1, b_2..b_n$, following eqn. can be formed out of [5.79]

$$\begin{pmatrix} u_k & u_{k-4}...u_{k-m} & -x_{k-1} & -x_{k-2}........-x_{k-n} \\ u_{k+1} & u_k & ...u_{k-m+1} & -x_k & -x_{k-1}........-x_{k-n+1} \\ \cdot & & & & \\ \cdot & & & & \\ u_{k+p-1} & u_{k+p-2} & ...u_{k+p-m-1} & -x_{k+p-2} & -x_{k+p-3}........-x_{k+p-n-1} \end{pmatrix} \begin{pmatrix} a_0 \\ a_1 \\ \cdot \\ a_m \\ b_1 \\ b_2 \\ b_n \end{pmatrix} \cdot = \begin{pmatrix} x_k \\ x_{k-1} \\ \cdot \\ \cdot \\ \cdot \\ x_{k+p-1} \end{pmatrix}$$ [5.80]

Where k = n+ 1, p= m+n+ 1

Here the data is assumed to be noise free. After having obtained the parameters a_0, a_1,......, a_n, and b_1, b_2 ....b_n for a particular value of m, n, it has to be ascertained whether the orders selected i.e., values of m and n are proper. For this, the method of Graupe et al (51) is used. As per this method, if a system is modeled as

$$G(z)= \frac{1+a_1 z^1 +a_2 z^2+.......................+ a_m z^m}{1+ b_1 z^1 +b_2 z^2 + ... +b_n z^n}$$ [5.81]

$$G(z) = \frac{g}{1+ c_1 z^1 +c_2 z^2 + ...}$$

By cross multiplication and equating the coefficients of powers of z yields, then the coefficient are

$b_1 = a_1 + c_i$

$b_2 = a_2 + a_1 c_i + c_2$,

....

$.b_n = a_n + a_{n-1} C_1+.............Cn$

$0 = a_n c_i + a_{n-1} C_{i+1} ....C_{n+i}$ for i=1,2

where $a_j = 0$ for j = m+1, m+2,........   n. Then the following relationship is obtained as

137

$$\begin{bmatrix} C_n & C_{n-1} & C_{n-m+l} \\ C_{n+1} & C_n & C_{n-m+2} \\ C_{n+m-1} & & C_n \end{bmatrix} \begin{pmatrix} a_1 \\ a_2 \\ a_m \end{pmatrix} = \begin{pmatrix} C_{n+1} \\ C_{n+2} \\ C_{n+m} \end{pmatrix} \qquad [5.82]$$

The square matrix involving c_j in [5.82] gives an idea of the minimal order of m and n.

Denoting the matrix as $\bar{A}_{n,m}$, its determinant is calculated, n and m are minimal if

$|\bar{A}_{n,m}|=0$ for n > n, m > m $\qquad\qquad$ [5.83]

As suggested by Graupe et al , the condition eqn. [5.83] can be replaced by a test

$|\bar{A}_{n,m}|^2 \leq \sigma$ for some n > n, m > m and some small $\sigma > 0$.

The system modeled is stable and hence after identifying the parameters for a minimal n

and m, its stability is also to be tested by finding out the poles and ensuring them to be

within the unit circle. Ultimately making a reasonable compromise, a system is

synthesized which is both stable and satisfies the order test as given in eqn. [5.83]. In this

case, with the input / output data available of a paper machine, the constants a_0, a_1, a_m

and b_1, b_2,........b_n, are computed for different values of m and n like(m=2, n=2), (m=2,

n=3)........(m=2,n=7), (m=3, n=3) ......(m=3, n=7) ... (m=4, n=4) ... and so on and each

time the value of the determinant $|\bar{A}_{n,m}|$ is calculated as shown in above eqn.[5.82]. It is

found to give satisfactory result at m=2; n=7 i.e., determinant $|\bar{A}_{n,m}|$ is zero for these

values of m and, at the same time do not increase enormously for subsequent higher

values of m and n. Hence the order of the identified model is seven. The final results are

given as under. If G(z) is the z-transfer function of the system considered, one can write,

$$G(z) = \frac{a_0 + a_1 z^{-1} + a_2 z^{-2}}{1 + b_1 z^{-1} + b_2 z^{-2} + b_3 z^{-3} + b_4 z^{-4} + b_5 z^{-5} + b_6 z^{-6} + b_7 z^{-7}} \qquad [5.84]$$

Substituting the values of all constants in eqn.[5.84], one can obtain the overall transfer function of the system as under

$$G(z) = \frac{-2.1606+2.4865z^{-1}-0.0299z^{-2}}{1-0.2570z^{-1}-0.1309z^{-2}-0.1629z^{-3}-0.0739z^{-4}-0.0375z^{-5}-0.0599z^{-6}-0.0848z^{-7}}$$

$$G(z)= \frac{[-2.161z^{7}+2.4865z^{6}-0.0299z^{5}]}{[z^{7}- 0.257z^{6}-0.1309z^{5}-0.1629z^{4}-0.0739z^{3}-0.0375z^{2}-0.0599z-0.0848]} \qquad [5.85a]$$

Transfer function:

$$\frac{-2.161\ s^{\wedge}7 - 40.19\ s^{\wedge}6 - 2217\ s^{\wedge}5 - 2.524e004\ s^{\wedge}4 - 4.707e005\ s^{\wedge}3 - 1.886e006\ s^{\wedge}2 - 6.472e006\ s + 2.778e007}{s^{\wedge}7 + 24.67\ s^{\wedge}6 + 1454\ s^{\wedge}5 + 2.104e004\ s^{\wedge}4 + 4.735e005\ s^{\wedge}3 + 3.21e006\ s^{\wedge}2 + 2.954e007.s + 4.87e007} \qquad [5.85b]$$

This system is controlled using the digital control algorithm as shown in eqn.[5.76], which includes the ZOH element with the time delay dynamics. There are several different digital controller design techniques that fit into general direct synthesis schemes such as deadbeat controller, Dehlin's controller, and Vogel-Edgar controller. In this present investigation only Dehlin's controller has been used. If $t=t_r=t_0=1$, $K=1/t_0$, so that eqn.[5.76] becomes

$$G_{dc}(z)=1/G(z)\ [0.632z^{-1}/(1-z^{-1})] \qquad [5.85c]$$

$$G_{dc}(z)=\frac{[1-0.257z^{-1}-0.1309z^{-2}-0.1629z^{-3}-0.0739z^{-4}-0.0375z^{-5}-0.0599z^{-6}-0.0848z^{-7}]*0.632z^{-1}}{[-2.1606+2.486z^{-1}-0.0299z^{-2}]*[1-z^{-1}]}$$

$$G_{dc}(z)=\frac{0.632[z^{7}-0.257z^{6}-0.1309z^{5}-0.1629z^{4}-0.0739z^{3}-0.0375z^{2}-0.0599z-0.0848]}{[-2.161z^{8}+2.4865z^{7}-0.0299z^{6}][1-z^{-1}]}$$

Or $G_{dc}(z)= \dfrac{0.632z^{7}-0.162z^{6}-0.827z^{5}-0.1029z^{4}-0.0467z^{3}-0.023z^{2}-0.0378z-0.0346]}{-2.161z^{8}+4.647z^{7}-2.516z^{6}+0.0299z^{5}} \qquad [5.85d]$

The simulink model for digital time controller is shown in fig. 5.16b. The simulation results have been depicted in Chapter 6.
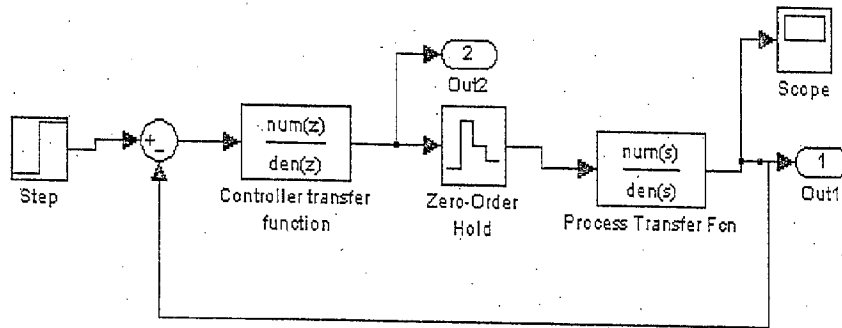
Fig.5.16b Simulink model for a discrete time controller

5.8.2 Development of ANN controller for the case of basis weight control:

The first step is that the process data are re-examined for their suitability for model development. More specifically, it is important that the data used to develop the process models are sufficiently exciting to extract accurate input and output relationships. Once these data are suitably exciting for identification purposes, it is important to consider the effects of feedback controllers when collecting data. If the model is to be used for control purposes, then using the data collected under closed loop operation may introduce problem. If however the model is to be used for monitoring purposes, then the process data should be collected with the system in its standard configuration. As per conventional linear modeling, the performance of the developed neural network is very much dependent upon the amount of the process data collected and used during training. Once the data is collected, these can be divided into three sets: one set for the training which comprise of half the available data and the remaining data is split evenly between testing and validating data sets. The artificial neural network models for basis weight of paper are shown in fig.-5.17.
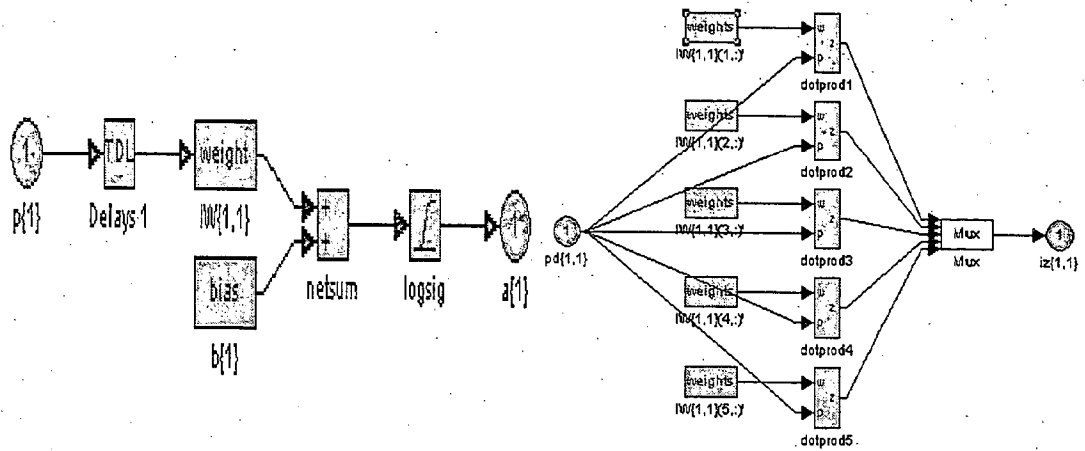
Fig.-5.17 Artificial neural network models

The network is consisting one neuron in input layer (gate opening as input), five neurons in hidden layer and one output layer.

[B] DEVELOPMENT OF MODELS OF MIMO SYSTEM OF PAPER INDUSTRY

For analysis and control of MIMO system the following cases related to approach flow system and headbox are developed and analyzed:

CASE: 5.9 Modeling of total head and stock level of rectifier roll headbox:

The total head and stock level are two variables which interact with each other. The interaction between the total head and stock level can be compensated using MIMO controller. The comparators compare feedback signal with reference point and create error signals which affect the control input of the air valve and fan pump as shown in fig. 5.19a. Changes in total head are taken into account in the control input of the stock level using a cross controller C_{21}, before the error signal exists. The normal feedback control of the stock level corrects possible errors which are not compensated with C_{21}.

141

process dynamics. The steady-state process transfer function(s=0) is called the process gain matrix, K.

$y_1 = K_{11}u_1 + K_{12}u_2$; $y_2 = K_{21}u_1 + K_{22}u_2$

K_{ij} denotes the steady state gain between y_i and u_j

For stable processes, the steady gain model related to the dynamic model is expressed as $K = G_p(0) = \lim_{s \to 0} G_p(s)$

$K_{11} = (\partial y_1/\partial u_1)_{u2}$; $K_{12} = (\partial y_1/\partial u_2)_{u1}$; $K_{21} = (\partial y_2/\partial u_1)_{u2}$; $K_{22} = (\partial y_2/\partial u_2)_{u1}$

Pairing of controlled and manipulated variables:

In a multi loop control scheme, the controlled variables and the manipulated variables have been paired for stable operation. An incorrect pairing can result in poor control system performance and reduced stability margin. The relative gain array(RGA) is a systematic approach for determining the best pairing of controlled and manipulated variables.

After estimating the steady -state gains, one can get relative gain arrays

$\lambda_{11} = 1/[1 - (K_{12}K_{21}/K_{11}K_{22})] = \lambda_{22}$; $\lambda_{12} = \lambda_{21} = (1 - \lambda_{11})$

Thus the relative gain array can be expressed as

$$\lambda = \begin{bmatrix} \lambda & 1-\lambda \\ 1-\lambda & \lambda \end{bmatrix}$$

There are mainly five cases arising as under:

(i) $\lambda = 1$. In this situation, opening or closing loop2 has no effect on loop 1. It means that y_1 should be paired with u_1.

(ii) $\lambda = 0$. In this case, the open loop gain between y_1 and u_1 is zero, and thus u_1 has no direct effect on y_1. Consequently, u_1 should be paired with y_2 rather than y_1.

144

(iii) $0<\lambda<1$. The open loop gain between input,u_1 and output,y_1 is smaller than the closed loop gain. Within this range, the interaction between the two loops is largest when $\lambda=0.5$.

(iv) $\lambda>1$. For this situation, closing the second loop reduces the gain between y_1 and u_1. Thus, the control loops interact. When λ is very large, it is impossible to control both outputs independently.

(v) $\lambda<0$. In this case, the open loop and closed loop gains between y_1 and u_1 have different signs. It follows that y_1 should not be paired with u_1. The closed loop system may become unstable.

For steady state gain matrix, s=0 (120), the above eqns. will not work since their (2,1) & (2,2) elements contain the integrator term(represented by 1/s→I). The eqns.[5.86, 5.87 expressed in matrix form are as under:

K_{11}=0.528, K_{12}= 0.0630, K_{21}= 0.0001, K_{22}=0.0007

$$K = \lim G(s)_{s \to 0} = \lim_{l \to \infty} \begin{bmatrix} 0.528 & 0.0630 \\ 0.00011 & -0.00071 \end{bmatrix}$$

$\zeta = (K_{12}*K_{21})/ (K_{11}*K_{22})=0.017045$

From a matrix, the values of arrays are found out as follows:

$\lambda_{11} = \lambda_{22} = 1/1- \zeta = 0.98$,

$\lambda_{12} = \lambda_{21} = -\zeta /1- \zeta , =0.02$,

After solving the relations, the relative gain array λ can be expressed in matrix form as follows

$$\begin{bmatrix} \lambda_{11}=0.98 & \lambda_{12}= 0.02 \\ \lambda_{21}=0.02 & \lambda_{22}= 0.98 \end{bmatrix}$$

Pairing recommendation:

In the present investigation, In headbox control system as shown in fig.-5.20, th interaction exists between the total head and the stock level. Changing the stock leve

145

with the pressure of the air cushion also affects the total head by the same amount. On the other hand, total head control using the fan pump also affects the stock level. Therefore y_1 and y_2 to be paired with u_1 and u_2 respectively.

Decoupling control:

The above MIMO control problem for total head and stock level can also be solved by partial or full decoupling of loops. In this investigation perfect decoupling has been made as the accurate process transfer functions are available. The transfer functions can be used to determine the effect of a change in either u_1 or u_2 on Y_1 and Y_2 as under (fig.5.19a).

$$Y_1(s) = G_{11}(s)u_1(s) + G_{12}(s)u_2(s) \qquad [a_1]$$

$$Y_2(s) = G_{21}(s)u_1(s) + G_{p22}(s)u_2(s) \qquad [a_2]$$

The decoupling control system for MIMO process is shown in fig. 5.19b. By adding additional controllers called decouplers to a conventional multiloop configuration, the design objective of reducing control loop interactions can be realized. The decoupler expressions have been described as under.
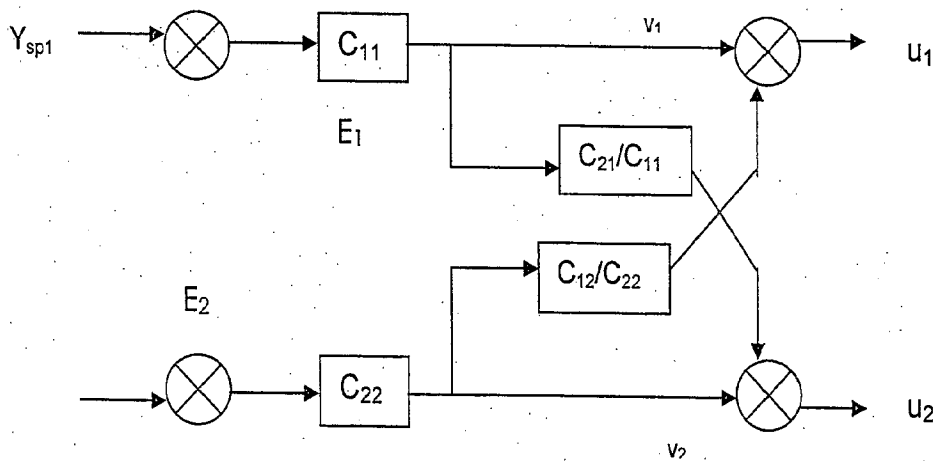

Fig. 5.19b A decoupling control system

$$u_1 = v_1 + (C_{12}/C_{22})v_2 \qquad [b_1]$$

$$u_2 = v_2 + (C_{21}/C_{11})v_1 \qquad [b_2]$$

Substituting eqns.$[b_1,b_2]$ into eqns.$[a_1,a_2]$, one can get

$$Y_1(s)= (G_{11}+G_{12} C_{21}/C_{11})v_1 + (G_{11}C_{12}/C_{22}+G_{12})v_2$$

$$Y_2(s)= (G_{21}+G_{22} C_{21}/C_{11})v_1 + (G_{21}C_{12}/C_{22}+G_{22})v_2$$

When v_1 affect Y_1 & eliminate the effect of v_2 on Y_1, then

$$G_{11}C_{12}/C_{22}+G_{12} =0 \quad \text{or} \quad C_{12}/C_{22}= -G_{12}/G_{11} \hspace{3cm} [c_1]$$

When v_2 affect Y_2 & eliminate the effect of v_1 on Y_2, then

$$G_{21}+G_{22} C_{21}/C_{11}=0 \quad \text{or} \quad C_{21}/C_{11}=-G_{21}/G_{22} \hspace{3cm} [c_2]$$

The expressions c_1 and c_2 are for ideal decoupler. One can interpret a decoupler as a type of feed forward controller with an input signal that is manipulated variable rather than a disturbance variable. The corresponding two SISO systems can be obtained by decoupling the loops as shown in fig.5.20. The overall transfer functions can be written as under.

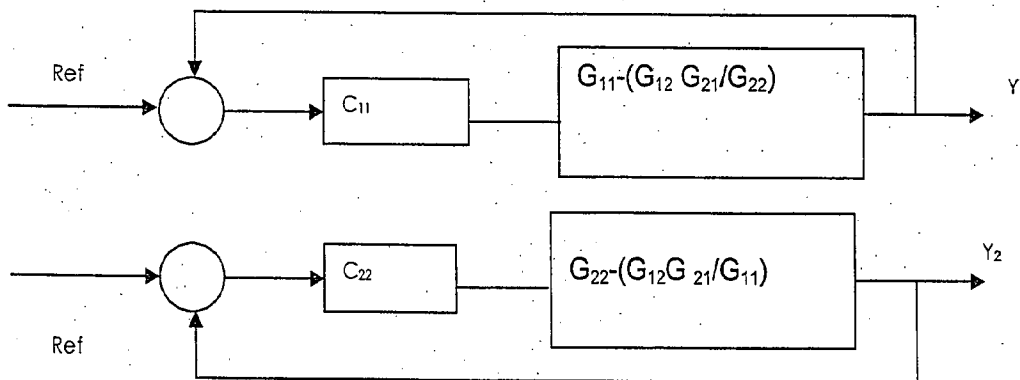$$Y_1=(G_{11}-(G_{12} G_{21}/G_{22})v_1; \quad Y_2= G_{22}-(G_{12}G_{21}/G_{11})v_2$$

Fig.-5.20 Two SISO systems for total head and stock level

As the present decoupling appears to be good the independent tuning of each decoupled loops can be easily carried out without detrimental to the stability of the whole system. As the process is approximated as linear, there is no need of using adaptive decouple

Again these models have been simulated with the help of Simulink tool (MATLAB software). The simulated data have also been used for designing PID and ANN controllers. The comparison between PID and ANN controllers are also interpreted.

Assuming all constants, dynamic equations of pressurized headbox have been modeled and simulate with the help of Simulink tool. The simulated results have been used for artificial neural network modeling. In this present investigation, the dynamic responses of both mathematical and ANN models are compared.

(a) Headbox filled with stock:

Using the fig.5.21, the following mass balance equations are developed.

For equilibrium condition, the equation can be written as

$$dm_{fb}/dt = m_{in} - m_{out} - m_{ol} \tag{5.92}$$

Eqn.[5.92] may be represented by the following relationship

$$d\Delta m_{fb}/dt = \Delta m_{in} - \Delta m_{out} - \Delta m_{ol} \tag{5.93}$$

where $\Delta m_{fb} = m_{fb} - m_{fb\infty}$; $\Delta m_{in} = m_{in} - m_{in\infty}$; $\Delta m_{out} = m_{out} - m_{out\infty}$; $\Delta m_{ol} = m_{ol} - m_{ol\infty}$

$m_{fb} = V_1 \rho_s$ or $A_{fb} h_1 \rho_s$

Rise in Δm_{fb} amounts to $A_{fb} \Delta h_1 \rho_s$ or $\Delta m_{fb} = A_{fb} h_{1\infty} u_1 \rho_s$ or $\Delta m_f = m_{fb\infty} u_1$

Amount of inlet stock m_{in} depends on opening of inlet valve C_1, the term m_{in} can be written as $m_{in} = m_{in}(C_1, P_{11}, P_{12})$

$$\Delta m_{in} = (\partial m_{in}/\partial C_1)_\infty \Delta C_1 + (\partial m_{in}/\partial H)_\infty \Delta P_{11} + (\partial m_{in}/\partial P_1)_\infty \Delta P_{12} \tag{5.94}$$

Assume that the characteristic of inlet valve of stock is linear, then

$(\partial m_{in}/\partial C_1)_\infty = m_{inmax}/C_{1max}$ or $(\partial m_{in}/\partial C_1)_\infty \Delta C_1 = (m_{inmax}/C_{1max}) \Delta C_1$

$$(\partial m_{in}/\partial C_1)_\infty \Delta C_1 = m_{inmax} \mu_1 \tag{5.95}$$

Flow of stock through the regulating valve C_1 as under

$m_{in} = A_c . C_{c1} \sqrt{2\rho_s(P_{11} - P_{12})}$

$(\partial m_{in}/\partial H)_\infty \Delta P_{11} = -1/2\ m_{in\infty}\ \rho_s g(h_{1\infty}/\ P_{11}-P_{12})\ u_1$ $\qquad$ [5.96]

$(\partial m_{in}/\partial P)_\infty \Delta P_{12} = -1/2\ m_{in\infty}\ (P_\infty/\ P_{11}-P_{12})\ P'$ $\qquad$ [5.97]

Flow of stock from slice lip

$m_{out} = m_{out}(C_2,\ h_1, P),$

$\Delta m_{out} = (\partial m_{out}/\partial C_2)_\infty \Delta C_2 + (\partial m_{out}/\partial h_1)_\infty \Delta h_1 + (\partial m_{out}/\partial P)_\infty \Delta P$ $\qquad$ [5.98]

$(\partial m_{out}/\partial C_2)_\infty = m_{outmax}/C_{2max}$ or $(\partial m_{out}/\partial C_2)_\infty \Delta C_2 = (m_{outmax}/C_{2max})\ \Delta C_2$

$(\partial m_{out}/\partial C_2)_\infty \Delta C_2 = m_{outmax}\mu_2$ $\qquad$ [5.99

Flow of stock through the slice

$m_{out} = A_{lip}.C_{d2}\sqrt{2}\rho_s(h_1 g\ \rho_s + P)$

$(\partial m_{out}/\partial h_1)_\infty \Delta h_1 = 1/2\ m_{out\infty}\ \rho g(h_{1\infty}/\ h_1 g\ \rho_s + P)\ u_1$ $\qquad$ [5.100

$(\partial m_{out}/\partial P)_\infty \Delta P = 1/2\ m_{out\infty}\ (P_\infty/\ h_1 g\ \rho_s + P)\ P'$ $\qquad$ [5.101]

Flow of stock through overflow

$m_{ol} = C_{d3}b\ \rho_s\sqrt{2}g(h_3)^{1.5}$ or $\Delta m_{ol} = 3/2\ C_{d3}b\ \rho_s h_{3\infty}\sqrt{2}gh_3\Delta h_3/\ h_{3\infty}$

$\Delta m_{ol} = 3/2 m_{ol\infty}\ u_3$ $\qquad$ [5.102

Substituting above all eqns. in eqn. [5.93], one can write

$d(V_1\ \rho_s\ u_1)/dt = [\ m_{inmax}\mu_1 - 1/2\ m_{in\infty}\ \rho_s g(h_{1\infty}/\ P_{11}-P_{12})\ u_1 - 1/2\ m_{in\infty}\ (P_\infty/\ P_{11}-P_{12})\ P' - m_{outmax}\mu_2$

$1/2\ m_{out\infty}\ \rho g(h_{1\infty}/\ h_1 g\ \rho_s + P)\ u_1 - 1/2\ m_{out\infty}\ (P_\infty/\ h_1 g\ \rho_s + P)\ P' - 3/2m_{ol\infty}\ u_3]$ $\qquad$ [5.10

If C_2 is constant value therefore $\mu_2 = 0$, equ.[5.103] can be written as

$V_1\ \rho_s\ du_1/dt = [\ m_{inmax}\mu_1 - 1/2\ m_{in\infty}\ \rho_s g(h_{1\infty}/\ P_{11}-P_{12})\ u_1 - 1/2\ m_{in\infty}\ (P_\infty/\ P_{11}-P_{12})\ P'$

$-1/2\ m_{out\infty}\ \rho g(h_{1\infty}/\ h_1 g\ \rho_s + P)\ u_1 - 1/2\ m_{out\infty}\ (P_\infty/\ h_1 g\ \rho_s + P)\ P' - 3/2m_{ol\infty}\ u_3]$

Or $(V_1\ \rho_s\ /m_{inmax})\ ^*(du_1/dt) = [\mu_1 - [(m_{in\infty}/m_{inmax})\ 1/2\ \rho_s g(h_{1\infty}/\ P_{11}-P_{12})]\ u_1 - [(m_{in\infty}/m_{inmax})$

$1/2(P_\infty/\ P_{11}-P_{12})]\ P' - [1/2\ \rho g(h_{1\infty}/\ h_1 g\ \rho_s + P\ )(\ m_{out\infty}/m_{inmax})]u_1$

$-[(\ m_{out\infty}/m_{inmax}\ )1/2(P_\infty/\ h_1 g\ \rho_s + P)\ ]P' - 3/2m_{ol\infty}/m_{inmax}\ u_3]$

Or $T_{fbl}du_1/dt = [\ \mu_1 - (w_1 K_{1v1} + w_2\ K_{2v1})\ u_1 - (w_1 K_1\rho + w_2 K_2\rho)P' - 3/2w_{31}\ u_3]$ $\qquad$ [5.10

Considering that $h_1=h_0+h_3$ or $\Delta h_1=\Delta h_3=1$, so $u_3=(h_{1\infty}/h_{3\infty})\,u_1$ or $a_{13}\,u_1$,

Eqn. [5.104] can be rewritten as

$$T_{fbl}du_1/dt=[\,\mu_1-(w_1K_{1v1}+w_2\,K_{2v1})\,u_1-(w_1K_1\rho+w_2K_2\rho)P'-3/2w_{31}\,a_{13}\,u_1]$$

Or $T_{fbl}du_1/dt+A\,u_1=\mu_1-BP'$ \hfill [5.105]

Where $A=w_1K_{1v1}+w_2K_{2v1}+3/2w_{31}\,u_3$; $B=w_1K_1\rho+w_2K_2\rho$, $a_{13}=u_3/\,u_1$

(b) Material balance for overflow system:

Equation for material balance for overflow can be written as

$$dm_{ch}/dt=m_{ol1}-m_{ol2}$$ \hfill [5.106]

or $m_{ch}=A_{ch}h_{ch}\rho_s=V_{ch}\rho_s$

Rise in m_{ch}

$$d\Delta m_{ch}/dt=\Delta m_{ol1}-\Delta m_{ol2}$$ \hfill [5.107]

$$\Delta m_{ch}=A_{ch}h_{ch\infty}\rho_s\,u_2$$ \hfill [5.108]

Flow of stock can be written as

$$m_{ol2}=A_{op}C_{d4}\sqrt{2}\rho s(h_{ch}\,\rho_s g+P).$$

$$\Delta m_{ol2}=1/2\,m_{ol2\infty}\,\rho_s g(h_{ch\infty}/\,h_{ch}\,g\,\rho_s+P\,)\,u_2+1/2\,m_{ol2\infty}\,(P_\infty/\,h_{ch}g\,\rho_s+P)\,P'$$ \hfill [5.109]

Substituting the values of Δm_{ol1}, Δm_{ol2} & Δm_{ch} into eqn.[5.107], one can get

$$d(V_2\,\rho_s\,u_2)/dt=3/2m_{ol\infty}\,u_3-1/2\,m_{ol2\infty}\,(P_\infty/\,h_{ch}g\,\rho_s+P)\,P'-1/2\,m_{ol2\infty}\,\rho_s g(h_{ch\infty}/\,h_{ch}\,g\,\rho_s+P\,)\,u_2$$

or $V_2\,\rho s(du_2/dt)=3/2m_{ol\infty}\,a_{13}u_1-1/2\,m_{ol2\infty}\,(P_\infty/\,h_{ch}g\,\rho_s+P)\,P'-1/2\,m_{ol2\infty}\,\rho_s g(h_{ch\infty}/\,h_{ch}\,g\,\rho_s+P\,)\,u_2$

or $(V_2\,\rho s/\,m_{ol2\infty})\rho_s\,(du_2/dt)=[3/2m_{ol\infty}/\,a_{13}u_1-1/2\,m_{ol2\infty}\,(P_\infty/\,h_{ch}g\,\rho_s+P)\,P'-1/2\,m_{ol2\infty}\,\rho_s g(h_{ch\infty}/$

$h_{ch}\,g\,\rho_s+P\,)\,u_2]/\,m_{ol2\infty}$ or $T_{fblo}\,du_2/dt=w_{21}\,u_1-K_3\rho P'-K_{1v2}\,u_2$

or $T_{fblo}\,du_2/dt+K_{1v2}\,u_2=w_{21}\,u_1-K_3\rho P'$ \hfill [5.110]

(c) Material balance for air cushion:

Equation for material balance for air cushion can be written in the form as under

$$m_{air}=m_{sup}-m_{rem}$$ or $dm_{air}/dt=\Delta m_{sup}-\Delta m_{rem}$ \hfill [5.111]

$\Delta m_{air} = m_{air} - m_{air\infty}$; $\Delta m_{sup} = m_{sup} - m_{sup\infty}$; $\Delta m_{rem} = m_{rem} - m_{rem\infty}$

$$m_{air} = V_3 \rho_a \qquad [5.112]$$

$$V_3 = V_o - V_1 - V_2 \qquad [5.113]$$

$$\Delta m_{air} = \rho_{a\infty} \Delta V_3 + V_{3\infty} \Delta \rho_a \qquad [5.114]$$

Putting the value of V_3 in eqn.[5.114], then

$$\Delta m_{air} = \rho_{a\infty}(\Delta V_1 - \Delta V_2) + V_{3\infty}\rho_a \Delta P/P_\infty \text{ or } \Delta m_{air} = -\rho_{a\infty}\Delta V_1 - \Delta V_2 \, \rho_{a\infty} + V_{3\infty}\rho_a P' \qquad [5.115]$$

Loss of air through valve C_5 & C_6

$$m_{sup} = A_{c5}K_5\sqrt{2\rho_a(P_{51} - P_{52})} \qquad [5.116]$$

$$m_{rem} = A_{c6}K_6\sqrt{2\rho_a(P_{61} - P_{62})} \qquad [5.117]$$

$$\Delta m_{sup} = m_{supmax.} (\Delta C_5/C_{5max}) - 1/2 \, m_{sup\infty.} (P_{52\infty}/P_{51} - P_{52})P'$$

if valve C_5 is linear, the term Δm_{sup} can be written as

Or $\quad \Delta m_{sup} = m_{supmax.} \, \mu_5 - 1/2 \, m_{sup\infty.} (P_{52\infty}/P_{51} - P_{52})P'$

$$\Delta m_{rem} = m_{remmax.} (\Delta C_6/C_{6max}) - 1/2 \, m_{rem\infty.} (P_{61\infty}/P_{61} - P_{62})P'$$

Or $\quad \Delta m_{rem} = m_{remmax.} \, \mu_6 - 1/2 \, m_{rem\infty.} (P_{61\infty}/P_{61} - P_{62})P' \qquad [5.118]$

C_6 is constant, so $\mu_6 = 0$;

$$\Delta m_{rem} = -1/2 \, m_{rem\infty.} (P_{61\infty}/P_{61} - P_{62})P' \qquad [5.119]$$

Putting the values of Δm_{air}, Δm_{sup}, Δm_{rem} into eqn.[5.111], one can get

$$d/dt(\rho_{a\infty}\Delta v_3 + v_{3\infty}\Delta\rho_a) = m_{supmax.} \, \mu_5 - [(1/2 \, m_{sup\infty.} \, P_{52\infty}/(P_{51} - P_{52}) - 1/2 \, m_{rem\infty.} (P_{61\infty}/P_{61} - P_{62})]P'$$

or $\quad d/dt(-\Delta v_1 \, \rho_{a\infty} - \Delta v_2 \, \rho_{a\infty} + v_3 \, \rho_a P') = m_{supmax.} \, \mu_5 - (1/2 \, m_{sup\infty.} (P_{52\infty}/P_{51} - P_{52}) - 1/2 \, m_{rem\infty.}$

$(P_{61\infty}/P_{61} - P_{62})P' \qquad\qquad$ or

$(v_3\rho_a/m_{supmax})(dP'/dt) + P'[(1/2m_{sup\infty}(P_{52\infty}/P_{51} - P_{52}) + 1/2 \, m_{rem\infty.} (P_{61\infty}/P_{61} - P_{62})] = \mu_5 + v_1\rho_a du_1/dt$

$v_2\rho_a du_2/dt \quad$ or $\quad T_{air}dP'/dt = w_4(k_4 + k_5)P' = \mu_5 + T_{tv1} \, du_1/dt + T_{tv2} \, du_2/dt \qquad [5.12($

Where

$T_{air} = (v_3\rho_a / m_{supmax})$; $\quad w_4 = m_{sup\infty}/ m_{supmax}$; $\quad k_4 = 1/2(P_{52\infty}/P_{51} - P_{52})$, $k_5 = 1/2(P_{61\infty}/P_{61} - P_{62})$;

or in discrete form(z-domain)

$$\frac{1.382e\text{-}005\ z^2 + 7.971e\text{-}005\ z - 9.298e\text{-}005}{z^3 - 2.989\ z^2 + 2.977\ z - 0.9886}$$ [5.131]

when $\mu_1 = 0$;

$L_{head2} = [(-.0004s^3 - .000947s^2 - .001035s - .0062)/(s^4 + .584s^3 + .034569s^2 + .0001358s)]$ [5.132]

or in discrete form (z-domain)

$$\frac{-4.036e\text{-}006\ z^3 + 1.201e\text{-}005\ z^2 - 1.192e\text{-}005\ z + 3.941e\text{-}006}{z^4 - 3.994\ z^3 + 5.983\ z^2 - 3.983\ z + 0.9942}$$ [5.133]

$P_{head2} = [(-.001s^3 + .0040868s^2 + .0034719s + .0122)/(s^4 + .5284s^3 + .005429s^2 + .0092)]$ [5.134]

or in discrete form(z-domain) can be expressed as

$$or\ \frac{-0.001\ z^3 + 0.003041\ z^2 - 0.003081\ z + 0.001041}{z^3 - 2.995\ z^2 + 2.989\ z - 0.9947}$$ [5.135]

The Simulink models for air pressure and level of stock have been developed using Simulink tool in MATLAB software. These are shown in figs. 5.22-5.25.
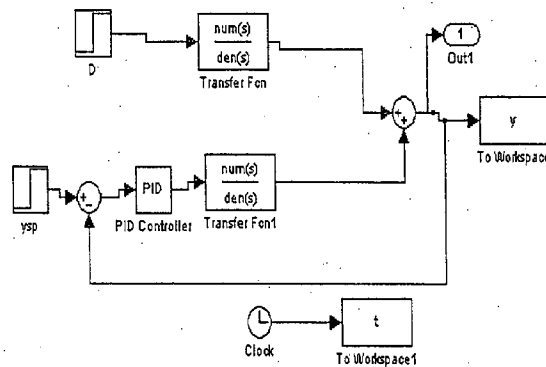

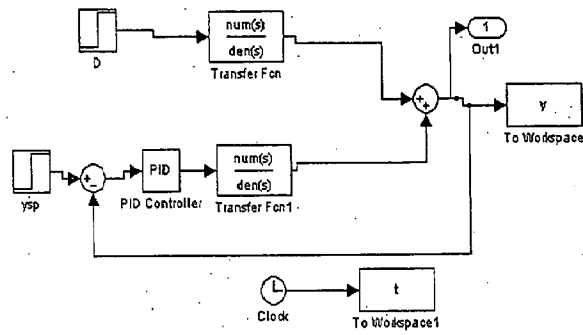Fig. 5.22 Closed loop system for L_{head1}, when $\mu_5 = 0$

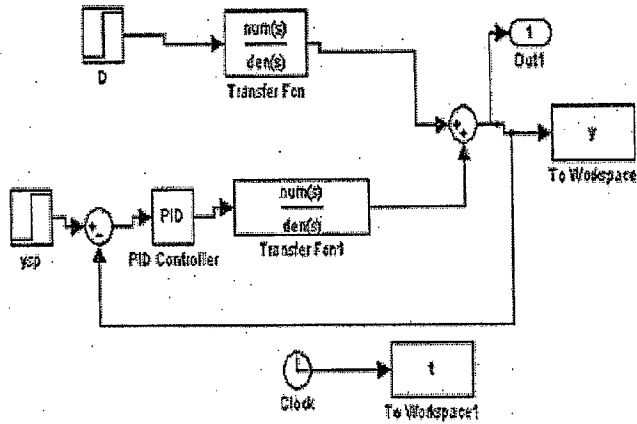Fig.-5.23 Closed loop system for P_{head1}, when $\mu_5=0$

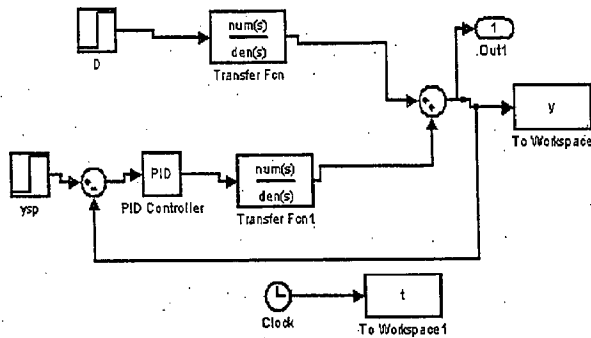Fig.-5.24 Closed loop system for L_{head2}, when $\mu_1=0$

Fig.- 5.25 Closed loop system for P_{head2}, when $\mu_1=0$

5.10.2 Development of ANN controller for the case of air pressure and level control of stock in air cushion headbox:

For the case of air pressure (P_{head}) and level of stock (L_{head}), the ANN controllers have been designed with back-propagation algorithm. The MATLAB programs for the same are shown in Appendix-2.

CASE: 5.11 Modeling of stock flow and stock level of the pressurized headbox:

5.11.1 Model for stock flow and stock level:

The pressurized headbox is used to project a stream of pulp in a 99% aqueous solution on to a wire. Drainage occurs as the pulp is transported towards the presses, where further water is removed from the remaining fibre by pressure, whilst forcing the pulp in to greater contact. Thereafter, drying using steam heated cylinders, before calendaring and reeling the sheet, forms the dry-end operation. Fourdrinier machine is widely used for the manufacture of paper.

The head box arrangement will produce output interaction in that changes in the stock flow will produce stock level and output stock flow rate changes. The physical configuration of the paper making machine, and the sheet forming system depicted by Whalley (166) is shown in figure.5.26.
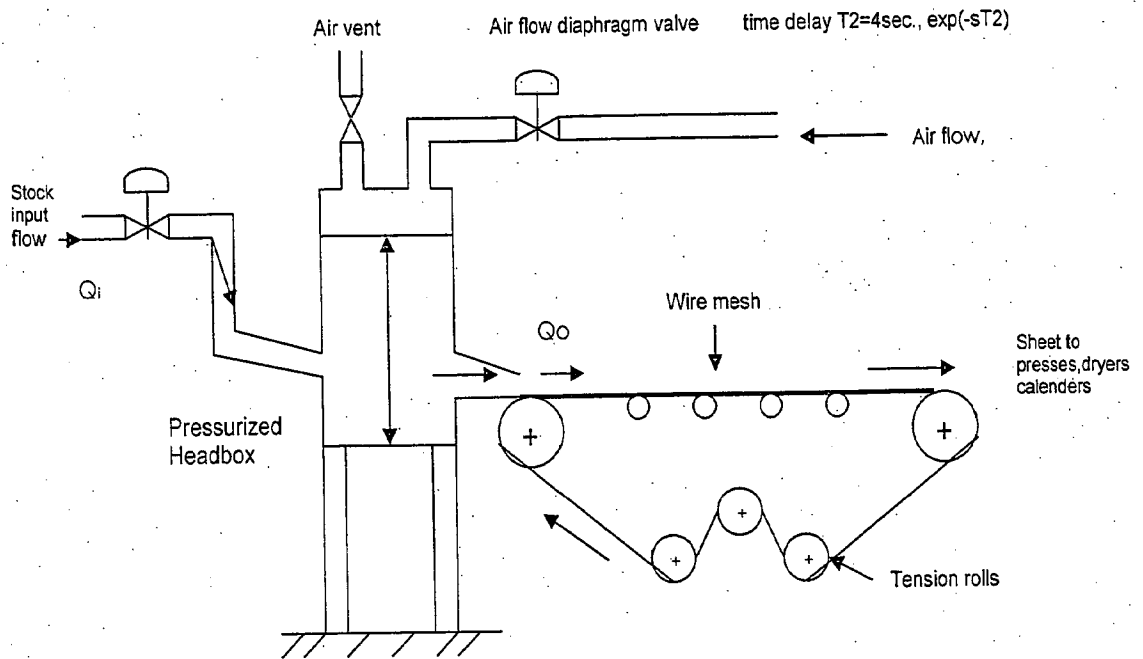
Fig.5.26 Headbox arrangement

Model of this type of pressurized headbox is derived by Rosenbrock et al(123).

Headbox model:

Pressurised headbox model with general multivariable system models may be represented by an input-output relationship. Herein, transformed, pre-compensated models are assumed to be linear, finite dimensional, in Laplace variable s, and denoted by G(s).

System transfer for matrix

$$G(s) = G_p(s)P(s)T(s)$$ [5.136]

Models with "m" i/p & "m" o/p admit a rational factorization

$$G(s) = L(s) \{A(s)/d(s)\} R(s) T(s)$$ [5.137]

Where L(s), A(s), R(s), T(s) & d(s) € RH∞, s≥0,

The transformed input-output disturbance relationship can be written as

$$y(s) = G(s)u(s) + \delta(s)$$ [5.138]

if the control law is $u(s) = [k(s)r(s) - h(s)y(s)]$ [5.139]

CASE: 5.12 Modeling of retention process in the wet end:

Retention is an important variable which describes the efficiency in the wet end of paper machines. It is defined in many ways such as first pass retention (FPR), first pass ash retention, first pass fines retention, overall retention, first pass fiber retention, first pass solids retention etc. First pass retention is defined as the ratio of the amount of material that leaves the headbox slice compared to the amount of material that is contained in the paper web leaving the couch roll (typically 20-90%) and mathematically expressed as

FPR (%)=100x(C_{HB} –C_{ww})/C_{HB}

The corresponding first pass ash retention, % can also be written as

First pass ash retention (FPAR)=100x(C_{HB} A_{HB}–C_{ww} A_{ww})/$C_{HB}A_{HB}$

First pass fines retention (FPFR)=100 x[(C_{HB} F_{HB}–C_{ww} F_{ww})/$C_{HB}F_{HB}$

Where C_{HB}, C_{ww} refer to the headbox and white water consistencies respectively and A refers to the ash level in the respective equipment.

First pass total solids retention can also be defined as 100x total solids flow in paper/total solids flow from headbox. Overall retention can be defined in the same way as the ratio of the amount of material that is sent to the wet end of a paper machine compared to the F or control of amount that goes in to the reel at the dry end of the machine(typically 90-95%).

In a recently developed feedback closed loop retention control system, total first pass retention, first pass ash retention, and total recycled white water consistency are evaluated to determine which parameter would give the most rapid response to a significant process disturbance. The control scheme utilizes two consistency sensors (headbox and white water tray) and a computational module. The sensors are capable of determining both the total consistency and ash consistency of the sampled streams.

Based on the analysis it has been concluded that the total recycled white water consistency measurement provided the quickest response to a process disturbance and would therefore be the best control variable. For control purposes, the following equation is useful. $\quad y(k)=K_{ret}(1-C_{ww}/C_{HB})$ $\qquad\qquad$ [5.143]

K_{ret} is a machine dependent constant, y(k) reflects the percentage of fiber and other additives remaining in the final produced paper at sample number, k and thus indicates both the efficiency of the use of raw material and the run ability of paper machines. New demands for better retention control have arisen from increased production speed, improved use of various chemicals, enhanced formation, and environmental requirement and so on. Owing to the complicated nature of the wet end of paper machines, retention is affected by many variables. Typical examples are retention aids(polymers), stock pH values, stock flow rate, sheer forces, pulp quality (CSF), head box slice geometry, raw material contaminants, drainage, machine speed and structure of white water system etc.
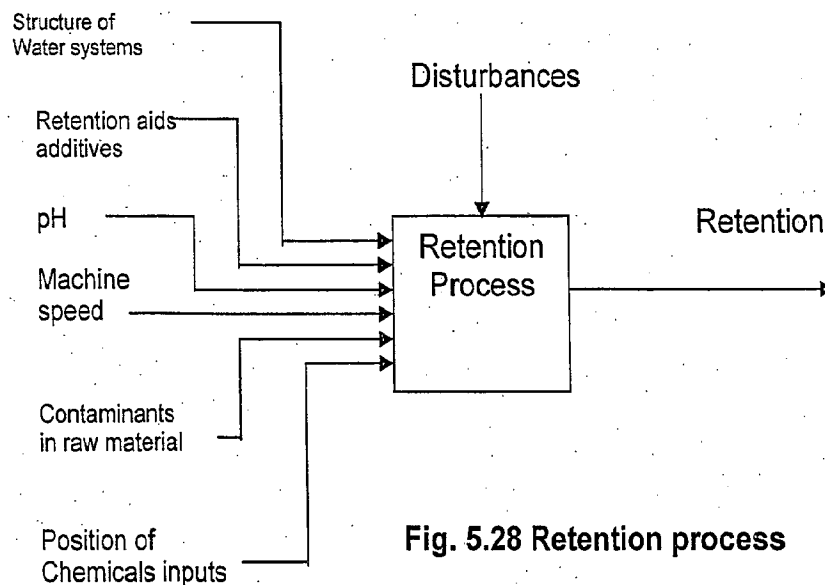

Fig. 5.28 Retention process

It is a multiple input and single output system, as shown in the fig.5.28. Moreover, owing to constant variation of all of the input variables during paper production and the

163

involvement of fluid dynamics during the formation phase on the wire section, the system is dynamic, non linear and stochastic. An added complexity is that the retention is coupled strongly with other chemical systems in the wet end, such as sizing and wet strength control systems. This means that an accurate physical model of the retention process is very difficult to obtain. As a result, model-based feed back control retention has remained a unsolved problem (94).

5.12.1 Model of retention process:

The paper machine retention process model is divided in to two zones. The parameters (total fibrous material retention, long fiber retention, fines retention, water retention) for both zones represent the fraction of each pulp component that is retained on the web during paper forming. The first pass retention considers the effect of the fines content in the pulp stream from the headbox. This can be calculated as follows:

$$\gamma = (\gamma_f + \gamma_F) \, \gamma_f + \gamma_F \qquad [1.144]$$

In eqn.[1.144] , γ is the retention and subscripts f and F represent the fines and fibers respectively. The model of retention process developed by Orccotoma et al.(97) contains the first pass retention,γ as output variable. There is one input variable, thick stock flow, F_1, and two disturbances, the consistency, and the fines content of the thick-stock stream, denoted by C_1 and Y_1, respectively. The modeling equation of retention is as follows:

$$\gamma(s) = [(G_c G_v G_{21})/(1 + G_c G_v G_{11} G_m)]BW_{sp}(s) + [G_{d21} - \{(G_{d11} G_m G_c G_v G_{21})/(1 + G_m G_c G_v G_{11})\}]C_1(s)$$

$$+ [G_{d22} - \{(G_{d12} G_m G_c G_v G_{21})/(1 + G_m G_c G_v G_{11})\}]Y_1(s) \qquad [1.145]$$

$$F_1(s) = G_c(s)(BW_{sp} - BW)$$

Where G_c, G_m, G_v are the controller, the measure delay and the thick-stock control valve, respectively. G_{ij} and G_{dij} are the ijth elements of the process and the disturbance transfer functions on eqn.[5.146]. It is noteworthy to mention that in a commercial paper machine,

the flow of a retention aid polymer is used as input variable for control of retention. Therefore, the model represents the short recirculation loop when no chemical is used for control of retention. The scaled transfer function of the paper forming section is as follow.

$$\gamma = \left(\frac{1.28(s+1.44)(s+0.28)}{(s+1.40)(s+0.44)} \right) F_1 + \left(\frac{.26(s+1.44)(s-0.01)}{(s+1.40)(s+0.44)} \right) C_1 + \left(\frac{-0.63(s+1.44)(s+0.80)}{(s+1.40)(s+0.44)} \right) Y_1$$

[5.146]

Transforming the eqn.[5.146] in discrete form(z-domain) as under

$$\gamma(z) = \frac{1.28z^2 - 2.538z + 1.258}{Z^2 - 1.982z + 0.9818} F_1 + \frac{0.26z^2 - .5163z + 0.2563}{Z^2 - 1.982z + 0.9818} C_1 + \frac{-.63z^2 + 1.2446z - 0.616}{Z^2 - 1.982z + 0.9818} Y_1$$

[5.147]

Retention control strategy:

Retention aids have limited power to control retention. The control range of retention aids can be improved by also controlling the head box consistency (especially filler consistency). The proposed control system manipulates both headbox ash content and retention simultaneously. Ash content is the ratio of the ash consistency to the total consistency expressed as a percentage as already mentioned. This is shown in fig. 5.29, in which the filler is controlled by a PID controller.
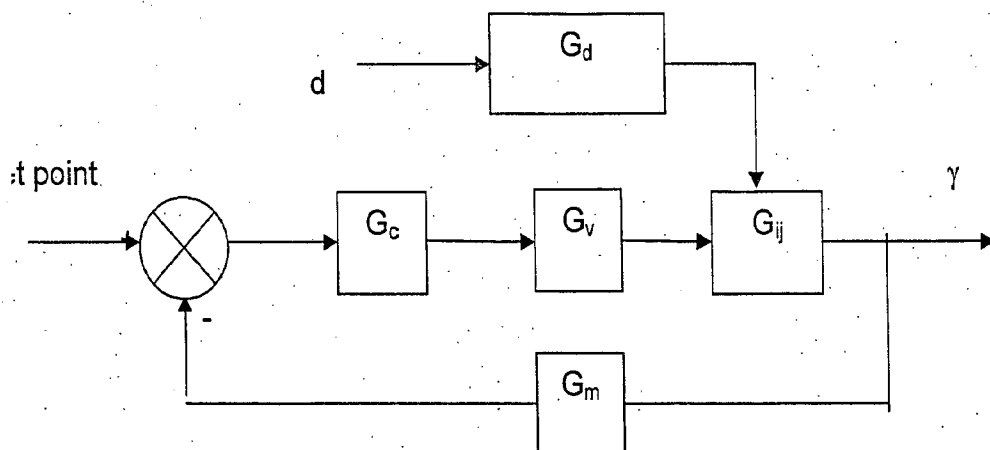

Fig. 5.29 Retention control system

The results are shown in Chapter-6.

5.12.2 Development of ANN controller for the case of retention control of stock in wet end:

The design procedure of a multi-layer neural network controller is described in chapter 4. The network is designed with 2:4:1 network. It indicates two neurons in input layer, four neurons in hidden layer and one in output layer with purelin activation functions. The training program is shown in appendix 2. The supervised control methodology for retention process has been used as shown in section 4.4, Chapter-4.

5.13 Conclusion:

In this Chapter, modeling and control of various parameters pertinent to approach flow system and head box operation of a paper machine are described using both single input-single output (SISO) system (also with one control variable and one manipulated variable) and multiple input multiple output(MIMO)have been attempted. The modeling begins with a brief survey of the status of the existing models , selecting the appropriate procedure for modeling and then finally their development. Firstly the development of dynamic equations of various SISO parameters modeled from both steady state and unsteady state material and/or energy balance equations along with rate equations (if applicable) are attempted. This is then followed by developing a traditional PID SISO system and single loop control architecture and then converting to neural network based control system. The parameters to be measured and to be controlled in this section are: stock consistency, stock flow, total head, stock level, pH of stock, stock temperature and basis weight. For SISO system as an example, the total head and stock level are controlled independently which means that the calculated control output is based only on the error signal between the set point and the measured value of the variable. Interaction between

variables is assumed negligible. But in many practical control problems, multiple input multiple outputs, MIMO control problems (also number of control variables and a number of manipulated variables) do exist if the process interactions are significant. In these cases, even the best multi-loop control system may not provide satisfactory control and one has to consider multivariable control strategies such as decoupling control and model predictive control.

In this present problem MIMO system in headbox considered are: total head and stock level, air pressure and level, stock flow and stock level, and retention of fibre fines.

As experimental data on dynamics for most of the processes are not available on industrial scale, either known dynamics were considered or simulations run were taken. However, in this investigation experimental data from industry on stock flow, and basis weight for digital system are used for comparison purposes.

All dynamic models of the process in both analog and digital form (either known or derived) are analysed through MATLAB simulation in order to get the unknown parameters of process (gain or sensitivity) or controllers.

The open or closed control loops for all the parameters are simulated through MATLAB Simulink tool.

As already indicated, if dynamic characteristics of a process parameter is not known, that has been found out by iterative procedure using again Simulink tool within a broad range of parameter available in literature. The simulation is, however, based on the analysis of closed loop control system including adjustment of selected controllers. Models are converted from analog to digital or vice versa and then a neural controller for the closed loop system is designed.

A step by step training procedure developed in this investigation is used to train the artificial neural network (ANN) for all the cases of SISO and MIMO system using MATLAB software. The performance of classical controller (PI/PID), (both analog and digital) and ANN controller are compared in terms of simulated results.

CHAPTER-6
ANALYSIS OF DATA AND DISCUSSIONS

An attempt is made in the section to compute data from various models for both SISO and MIMO systems using the classical controller and neural network based control with the help of MATLAB Simulink toolbox. The procedures laid down in Chapter-4, the various equations presented therein, the algorithm developed for the ANN and for PID, and finally the models developed for the various wet end parameters given in Chapter-5 are used. From the plethora of data from MATLAB simulation dynamic characteristics of process control parameters for both MIMO and SISO system have been drawn in terms of response as a function of time. The details of dynamics of process parameters are given in Chapter-5. These are interpreted as follows:

[A] ANALYSIS OF SISO SYSTEM OF PAPER INDUSTRY:

The SISO control system consists of consistency, stock flow, total head, stock level, stock pH, stock temperature, and basis weight. These are explained as under:

Case-6.1: Consistency control:

For consistency control, the effects of tuning parameter, types of signals (continuous and discrete), and types of controllers (PI and PID) for SISO and MIMO system on response are shown. The training responses for the design of ANN controller are given. Comparison of performances of both conventional and ANN are made. These are discussed in the following sections.

6.1.1: Effect of tuning on consistency control:

Both lambda tuning and Ziegler-Nichols tuning are attempted to examine their effects on responses for comparison purposes. These are shown in figs. 6.1-6.2.

In Chapter 5, Section 5.1 it has been found that as we increase the λ value of the PI/PID controller, the settling time decreases and offset value becomes zero. It also reduces overshoot but more oscillation occurs. It has been proved that the values of lambda time must lie between 15s-16s. Using the eqns.[5.24,5.25], the figs.6.1a and 6.1b have been drawn for both values of λ. The simulated data are given in tables-6.1a & 6.1b (Appendix-1) for 15s, and 16s respectively. It can be concluded that higher values of λ of the order of 15s or 16s would be the best tuning parameter for consistency controller.
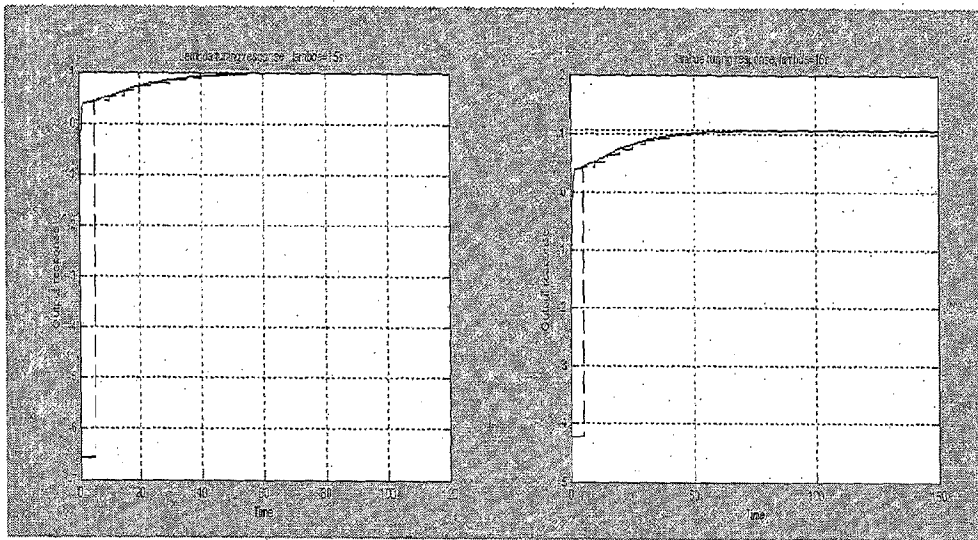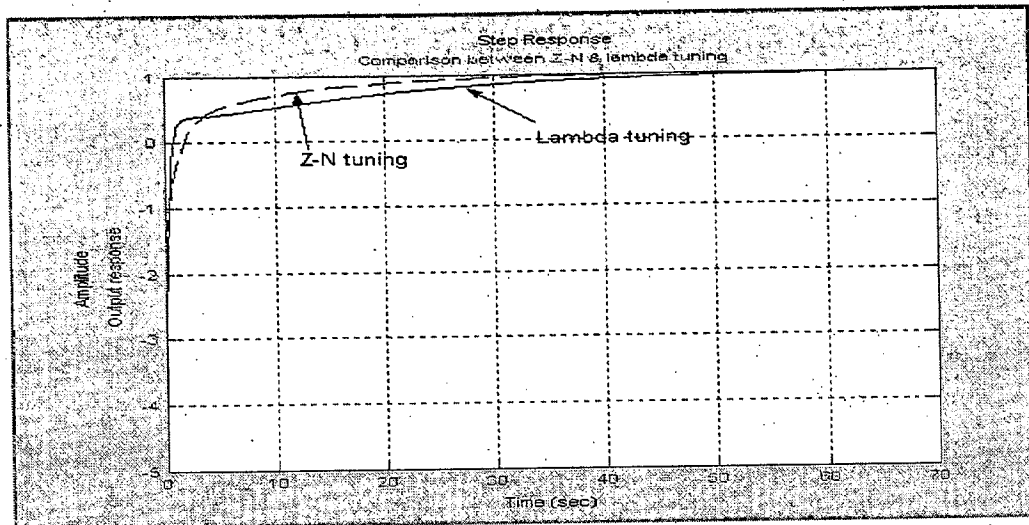

Fig.6.1a (when λ =15 seconds)   Fig.6.1b(when λ =16 seconds)

Figs. Lambda tuning responses

Higher values of λ of the order of 15s or 16s would be the best tuning parameter for consistency controller.

Figs. 6.2 Comparison between Lambda & Z-N tuning method

Fig. 6.2 has been drawn for comparing Z-N and Lambda tuning method for consistency

control; it indicates that the Z-N tuning method is found to be more suitable in this case

compared to lambda tuning though no oscillations were found. This is most unlikely. The

performances are more clearly shown in table 6.1c.

Table: 6.1c Comparison of performances between Lambda and Z-N tuning

Performance criteria	Lambda tuning	Z-N tuning
Delay time	6s	4s
Rise time	50s	40s
Settling time	45s	35s

The negative values in all the responses in both analog and digital system are common ii

MATLAB simulation of step response models (Seborg(139), Nagrath(90) etc).Therefore

is not a very surprising phenomena.This is usual for model based control.

6.1.2: Effect of discrete and continuous signals for consistency:

The results of simulation for continuous and discrete system using the eqns.[5.31an

5.35], are shown in figs. 6.3,and 6.4. While fig.6.3 for PI controller indicates an ov(

damped system (ξ>1) displaying non oscillatory but sluggish characteristics, the fig. 6

for PID controller represents an under damped system ($\xi<1$) with overshoot and oscillatory behaviour. The nature of the curves for both continuous and digital signals in each case (PI or PID) are found to be the same. The time average value of consistency over the time range of 0 to 100 s is estimated statistically. The data for both analog signal and digital signal for PI as well as PID are compared in table 6.1d. The minimum value of consistency exhibit negative values for all the cases. It might be due to the consistency dynamics reported by Nancy with negative steady state gain values. It is interesting to note that both digital and analog systems display overdamped systems. The negative values in the lower range obtained in the response curves with both PI and PID controller are not unusual for model based control.

Table:6.1d Comparison of statistical data for consistency control

Performance criteria	PI controller		PID controller	
	Continuous	Discrete	Continuous	Discrete
Minimum	-0.163	-0.151	-1.491	-1.491
Maximum	0.999	0.999	0.999	1.000
Mean	0.925	0.994	0.860	0.869
Median	0.994	0.994	0.977	0.994
Std. deviation	0.182	0.185	0.314	0.399
Range	1.163	1.151	2.491	2.491

From the statistical analysis given in table 6.1 d, It can be concluded that the results for continuous signal as compared to digital signal are more appropriate which is expected for chemical process industry.

6.1.3: Comparison between conventional and ANN controller data:

The consistency responses of head box controllers using unit step input for both PI, and PID are shown in figs.6.5 to 6.8. Fig. 6.5 for PI control with normalized values, figs. 6.7
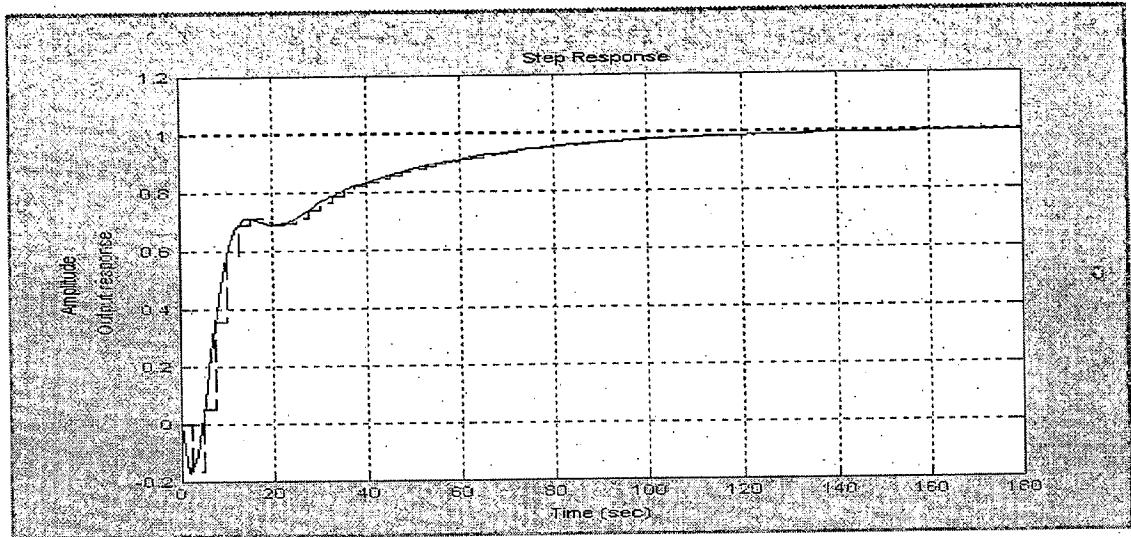

Fig.6.3 Step responses of PI controller for continuous and discrete system
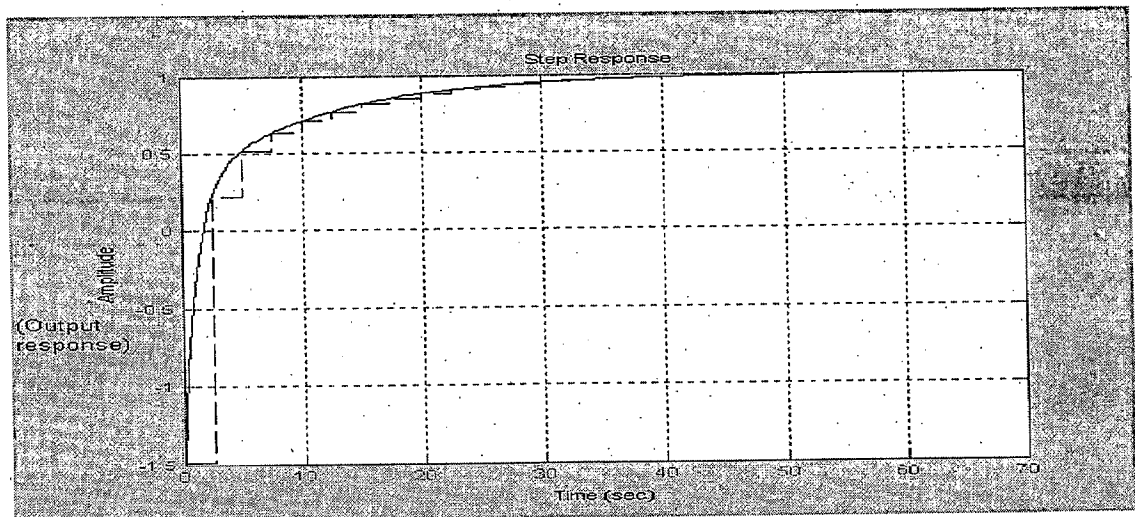

Fig. 6.4 Step responses of PID controller for continuous and discrete system

without normalization for PID control whereas figs. 6.6 and 6.8 with normalized, withou normalized value for ANN controller are drawn. The analyses of the responses for all th above cases are made and compared in tables 6.1e and 6.1f .The comparisons betwee conventional controller(PI and PID) and ANN controller are made for predictin

performances in terms of the parameters ,delay time, settling time and overshoot parameters.

Table:6.1e Comparison between PI and ANN controller for consistency(case-a)

Performances criteria	PI Controller	ANN Controller
Delay time (s)	7.0	0.1
Settling time(s)	40	0.5
Overshoot (%)	8.7	0.0

Table: 6.1f Comparison between PID and ANN controller for consistency (case-a)

Performances criteria	PID Controller	ANN Controller
Delay time (s)	5.0	0.0
Settling time(s)	30	0.1
Overshoot (%)	2.0	0.0

These tables show that the ANN controller is best suited for consistency control because it gives immediate control action(means less delay time),removes overshoot, and settling time is very less as compared to conventional controllers.

Firstly the training patterns are obtained from conventional PI and PID controllers. During training, the values of gradient descent term for PI controller in network performance calculations of the order of 9.99995e-005 and error goal 0.0001 are met at 6062 epochs. Similar calculation for PID controller, shows the value of the order of 9.99997e-006, and error goal e-005 at 12308 epochs. The training responses for both PI and PID are shown in figs.-6.9 & 6.10. The training responses are found to be quite satisfactory.
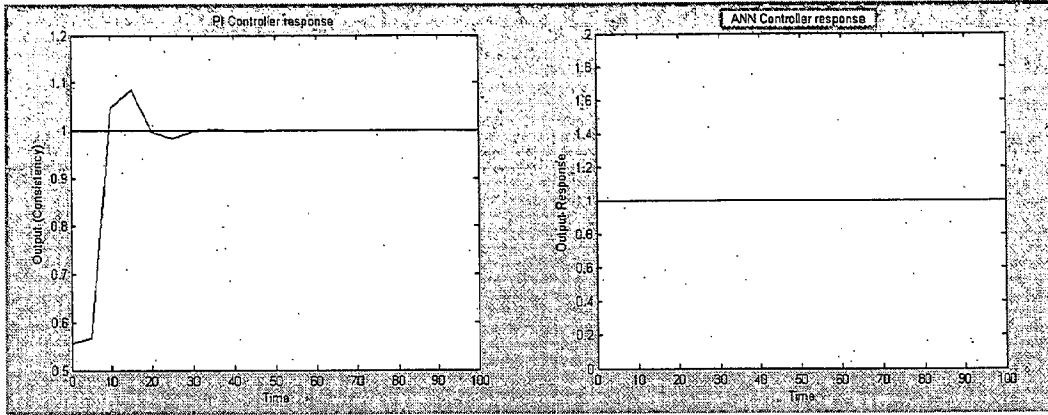
Fig.-6.5 Response for closed loop system
(normalised data)

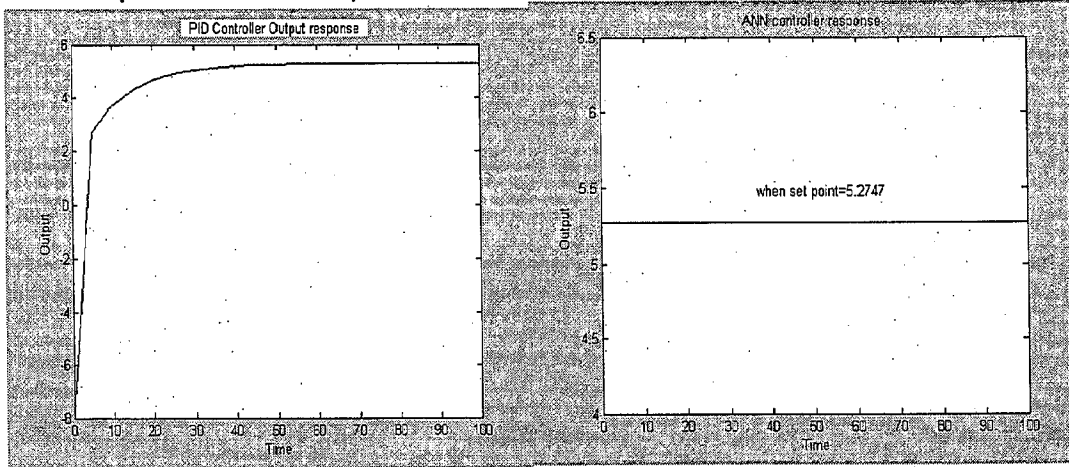**Fig.-6.6 ANN controller response**
(normalised data)

Fig.-6.7 Response for closed loop system   **Fig.-6.8 ANN controller response**
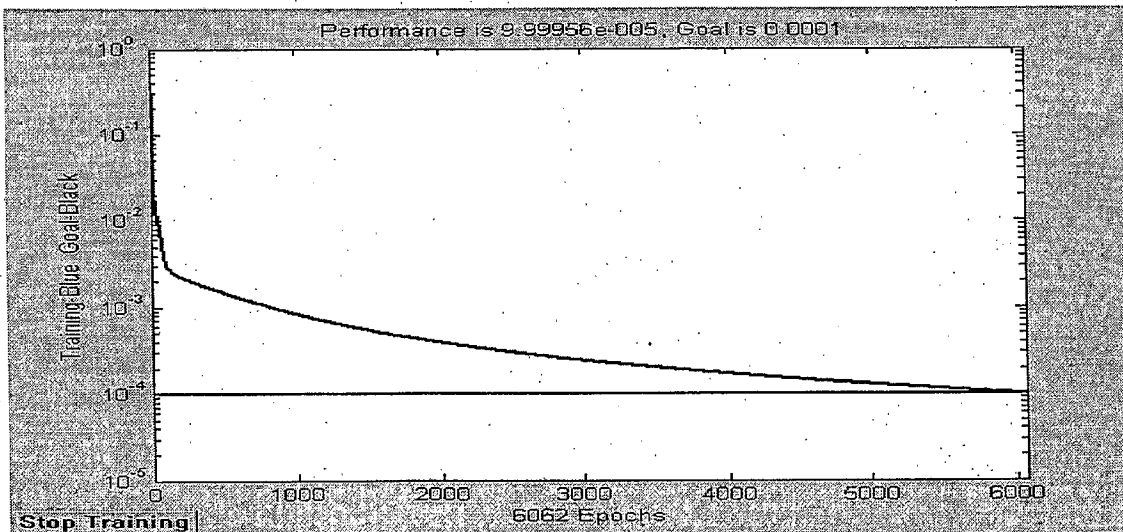**Fig.-6.3 to 6.8 Consistency responses(PI/PID/ANN)controllers**

Fig.- 6.9 Error goal with respect to epochs during training.(PI controller data)
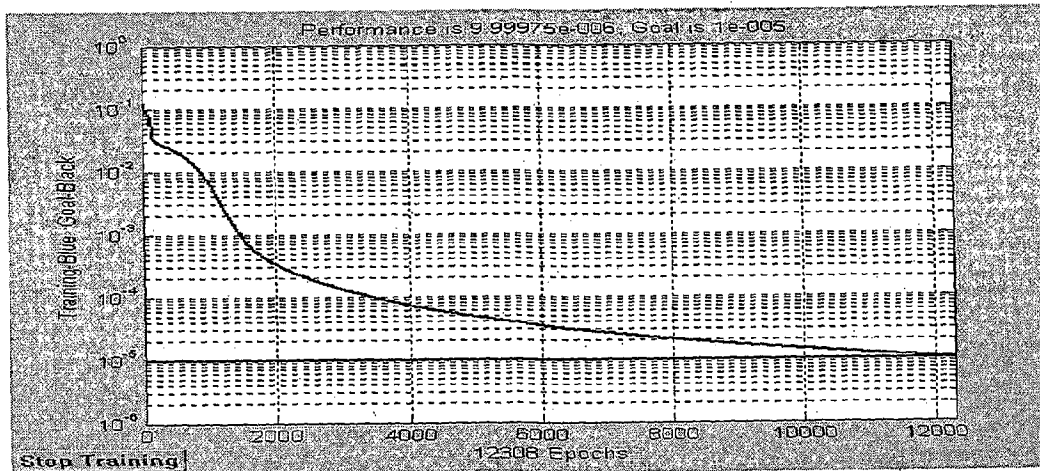
175

Fig.-6.10 Error goal with respect to epochs during training.(PID controller data)

For case-b given in Chapter-5, the closed loop control system is simulated with two consistency parameters namely: dilution water consistency, C_{yd} and thick stock consistency, C_{yi}. When consistency model is treated as MIMO system (two input but one output), the simulation results are plotted in figs.6.11& 6.12 and also used for training the neural network. During training, the fig.6.13 indicates the gradient descent term of the order of 9.9983e-006, and error goal of 0.00001 at 5791 epochs. After training the network, the ANN controller is tested at the rated normalized consistency 0.97 as shown in fig.-6.14. The comparison between controller parameters for case-b is given in table 6.2(Appendix-1).

Table:6.2 Comparison between ANN and PI controllerfor consistency(case-b)

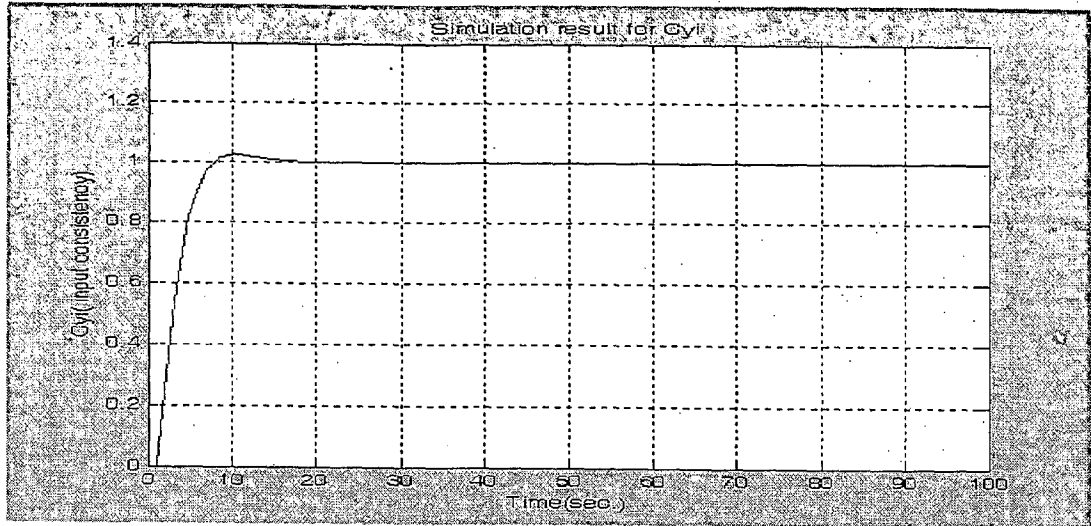| Performances criteria	PI Controller(C_{yi})	PI Controller(C_{yd})	ANN Controller
Delay time(s)	3.75	4.0	2.5
Settling time(s)	15.0	25.0	3.0
Overshoot (%)	2.6	10.9	0.99
Rise time(s)	7.5	8.0	5.0

Fig. -6.11 Input consistency of stock simulation response(case-b)
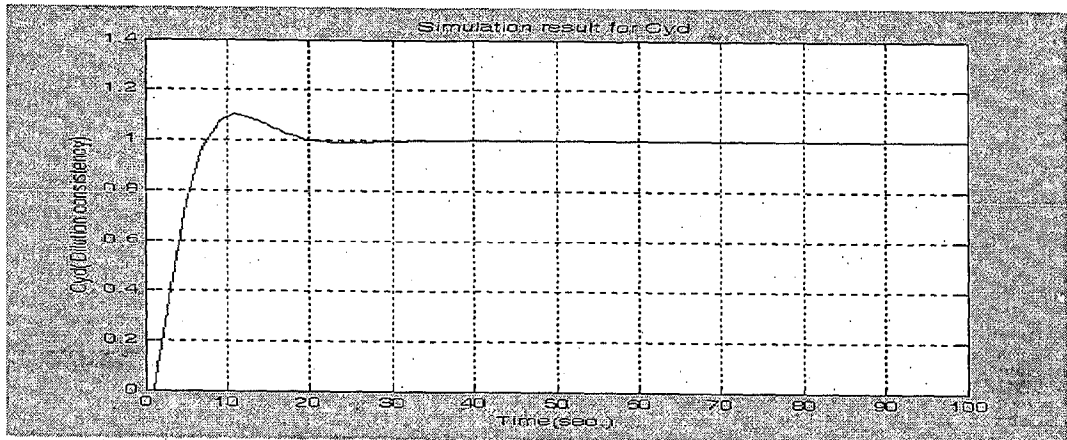
Fig. 6.12 Dilution water consistency simulation response(case-b)
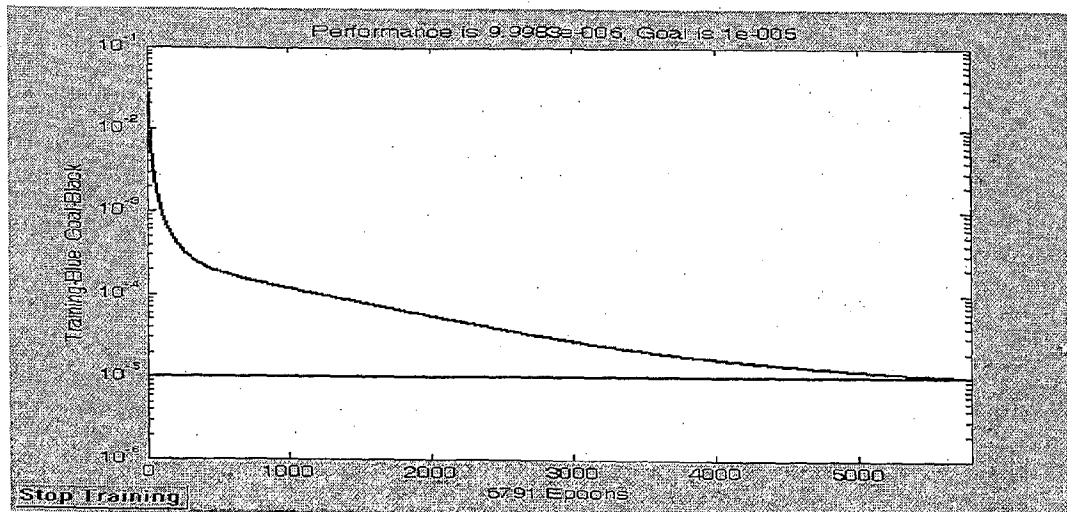
Fig. 6.13 Artificial neural network training response (case-b)

It reveals that for higher velocity the error almost becomes equal to zero for higher value of iterations (>600).

Plot between Error Vs No. of hidden neurons
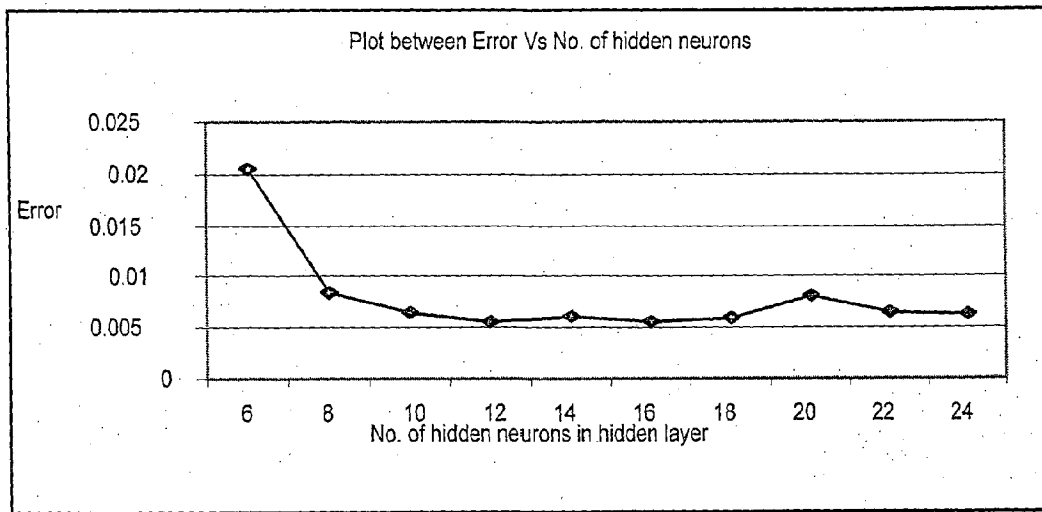
Fig-6.15 Plot of error vs hidden neurons

Plot between Errors Vs no. of iteration
When no. of hidden neurons 18, samples 15
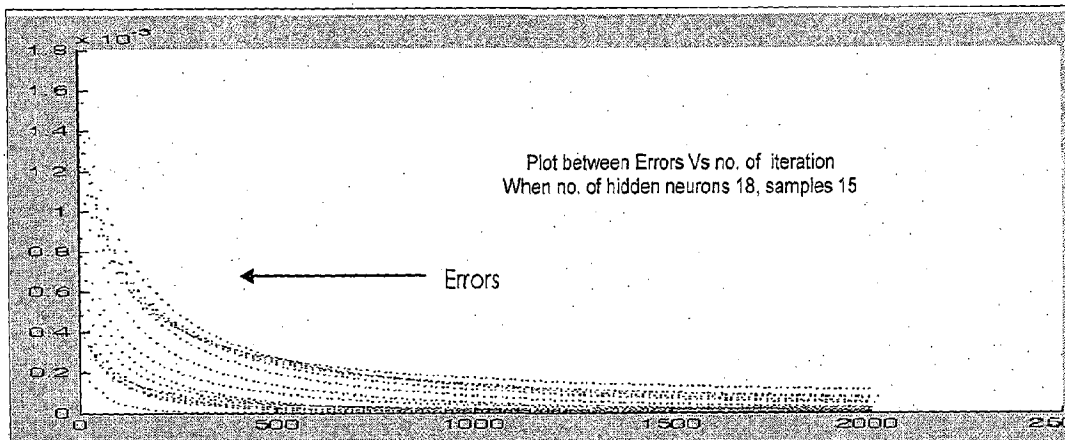
Errors

Fig.- 6.16 Effect of iterations on error

Learning rate versus Error in Total head

Fig.-6.17 Effect of learning rate on the error of total head

180

Fig.-6.18 Effect of changing momentum

Fig.-6.19 Effect of changing learning rate

Fig.-6.20 Effect of changing of momentum

Fig.-6.21 Effect of changing of hidden neurons
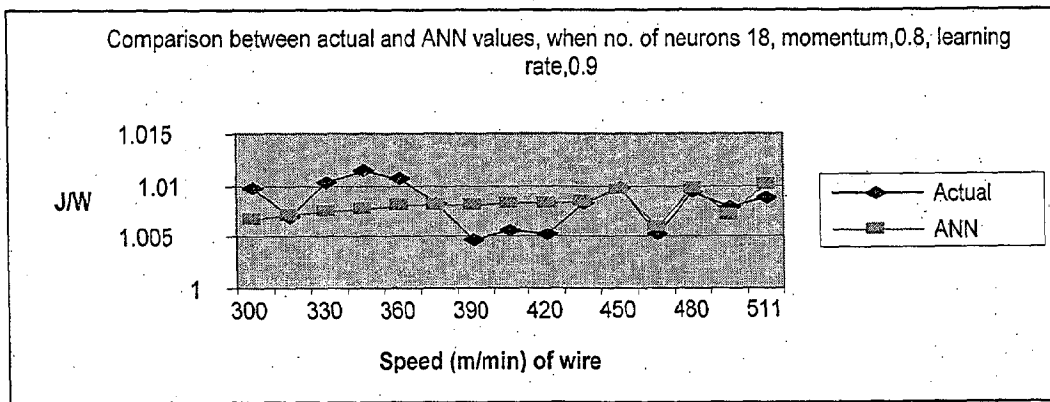
Fig.- 6.22 Comparison between actual and ANN data
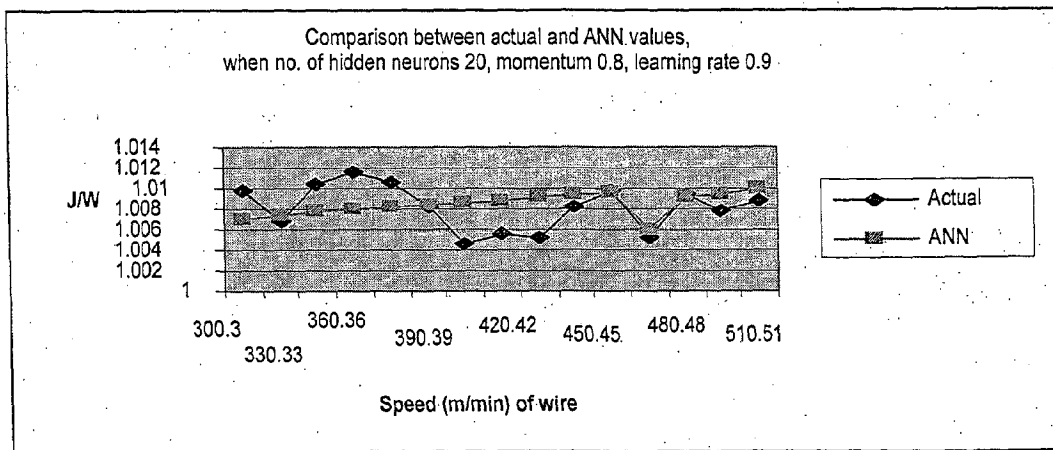
Fig.6.23 Comparison between actual and ANN data

From the analysis of plots of ANN parameters as a function of error, it can be found that the neural network parameters indicate satisfactory results of J/W values or total head at the values shown in table 6.4.

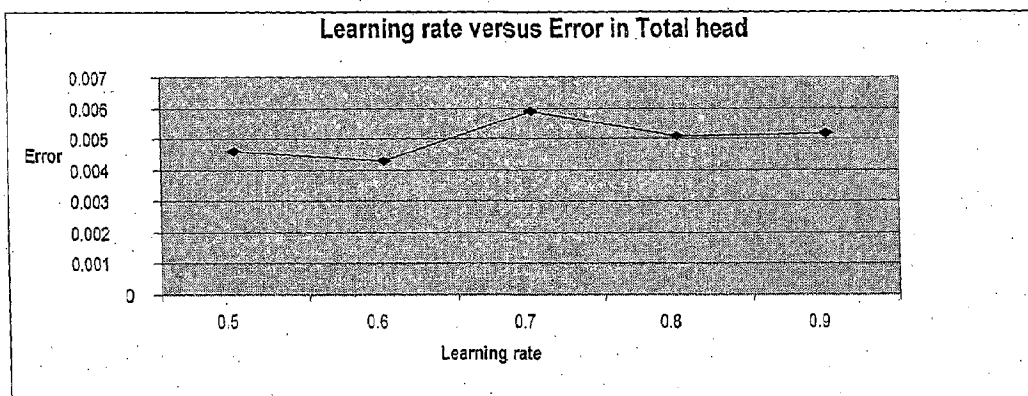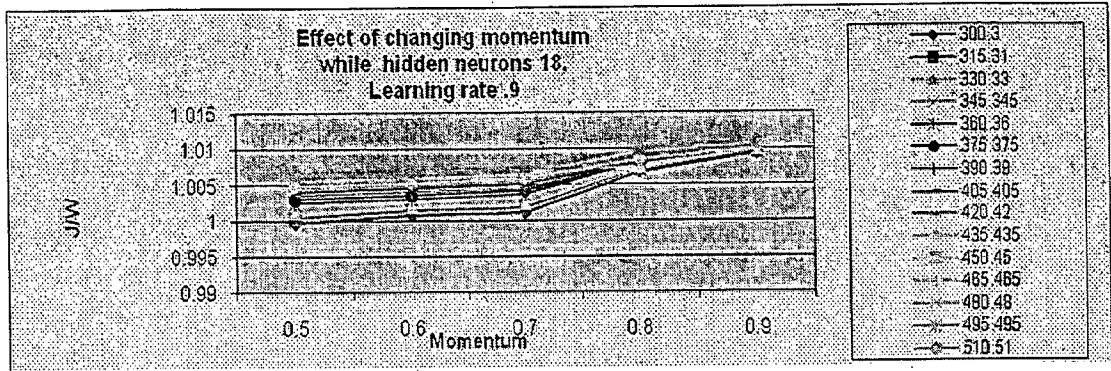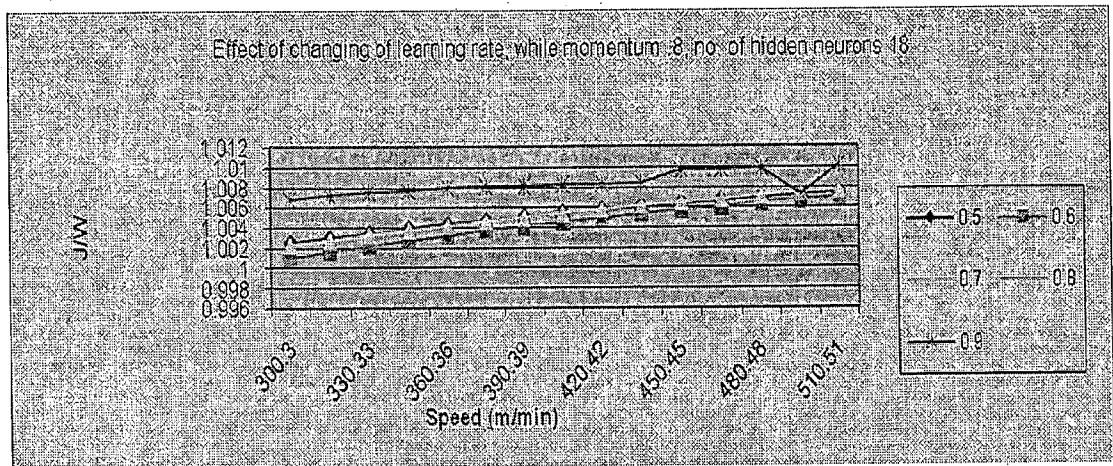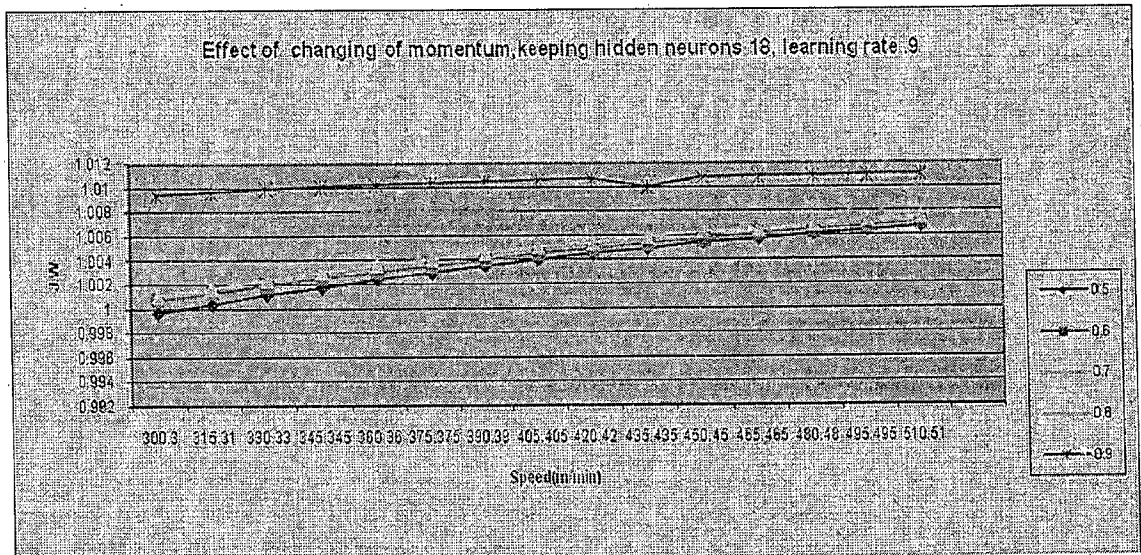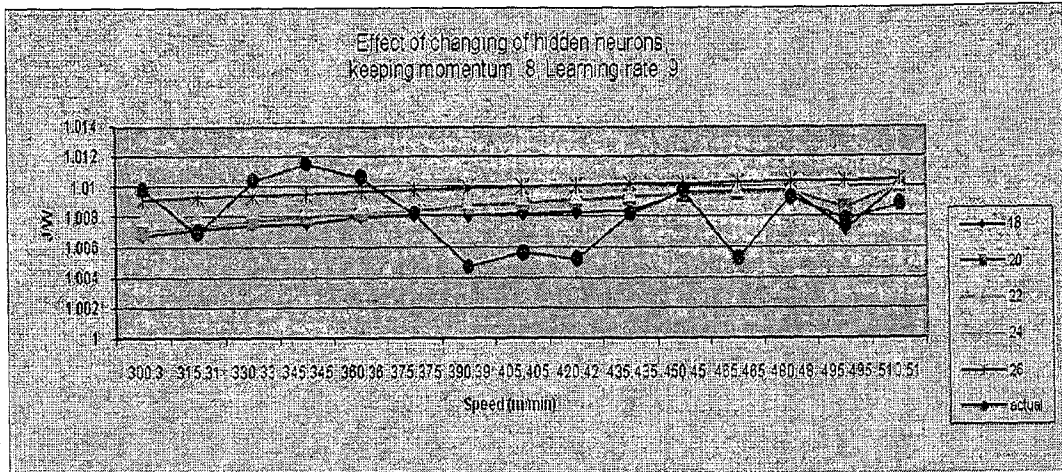J/W ratio profiles as a function of speed indicate that ANN controller give better prediction than the same from the data obtained from industry. The plots also reveal that above the speed of 450 m/min the values obtained from ANN simulated results and the data obtained from industry closely tally with each other. However there are noticeable deviations in the range of values between 300.3 m/min to 450 m/min.

Table:6.4 The range of parameters for neural network controller design

Number of hidden layers	Number of hidden neurons	Learning rate	Momentum
1.0	18-20	0.6	0.9

Case-6.3: Total Head control:

6.3.1: Effect of discrete and continuous signals for total head:

Using the eqn.[5.42] in chapter-5, the simulation result for continuous and discrete models of total head dynamics with PI controller is shown in fig. 6.24. The data from fig.6.24 have been analysed statistically in terms of maximum, mean, median, standard deviation and range. These are shown in table 6.5. From the analysis of data it can be concluded that continuous signal as compared to digital signal which gives delayed response due to sampling.

Table:6.5 Comparison of statistical data for total head control

Performance criteria	Continuous model	Discrete model
Minimum	0.000	0.000
Maximum	1.282	1.018

Mean	0.992	0.955
Median	1.000	1.000
Std. deviation	0.101	0.214
Range	1.282	1.018

6.3.2: Comparison between conventional and ANN controller data:

The model for total head is simulated with the help of MATLAB Simulink toolbox (fig.5.7, chapter-5). The simulation result is shown in fig.6.25 and used for training the neural network. The neural network error goal 0.0001 is met at 100200 epochs during training. The responses of total head of head box using PI and ANN controllers at rated total head are shown in figs.-6.26,and 6.27. The responses of PI controller and ANN are more clearly reflected in figs.6.25 and 6.26 respectively. The plots reveal the following characteristics:

Overshoot, decay ration, rise time and response time for both analog and digital signals. The performances of both the controllers are compared in fig.6.27.
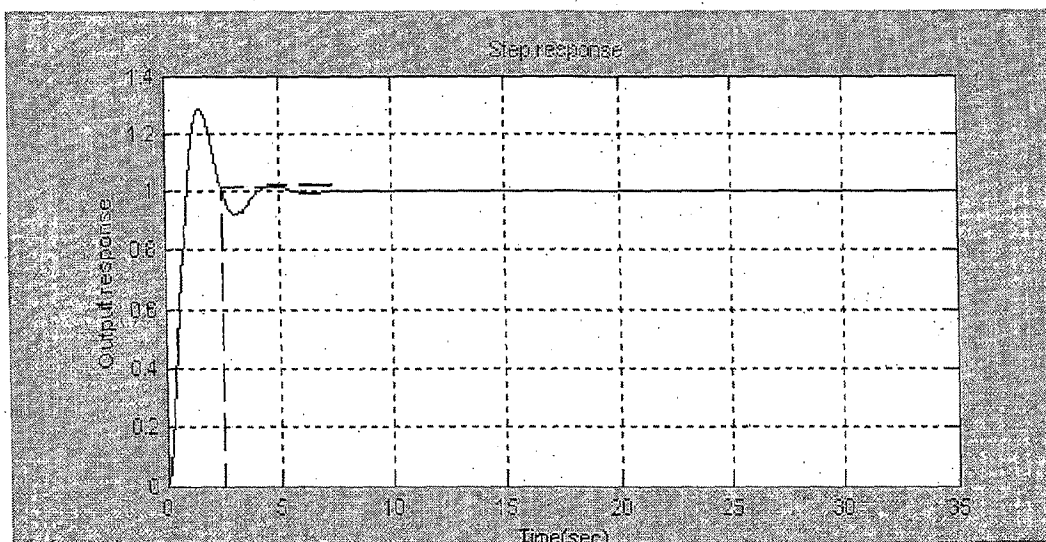
Fig.6.24 Plot between continuous and discrete data
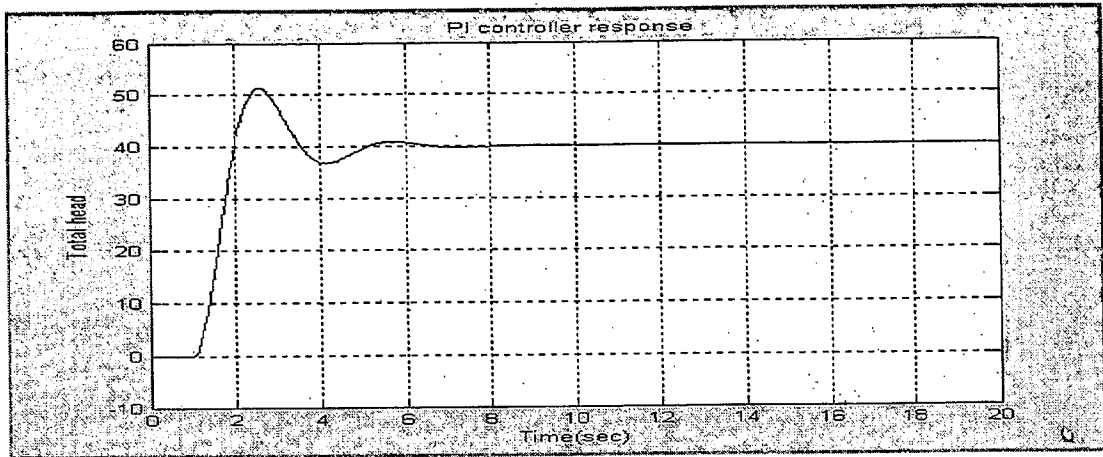
Fig. 6.25 Simulation of head-box total head control system(PI controller)
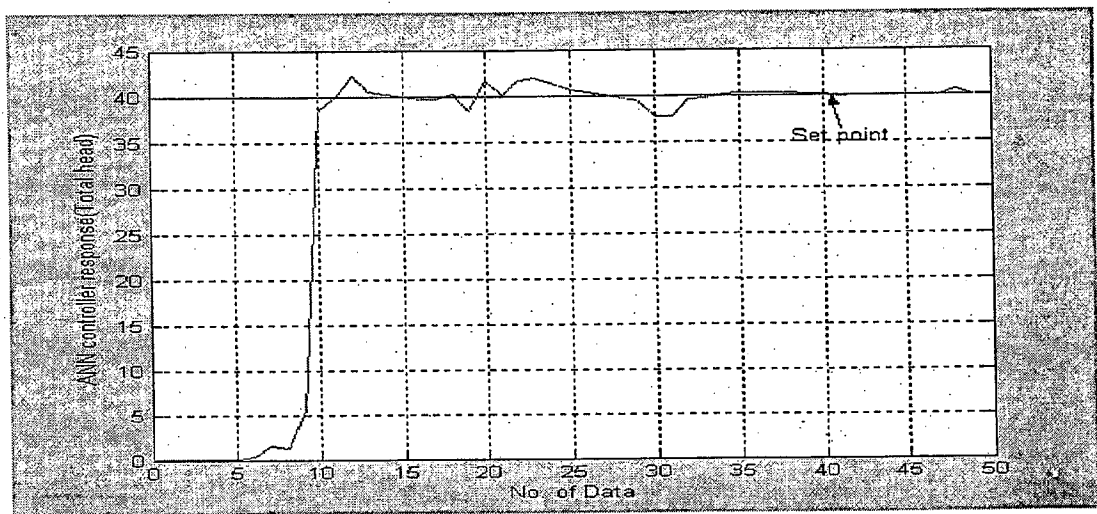
Fig.6.26 ANN controller response
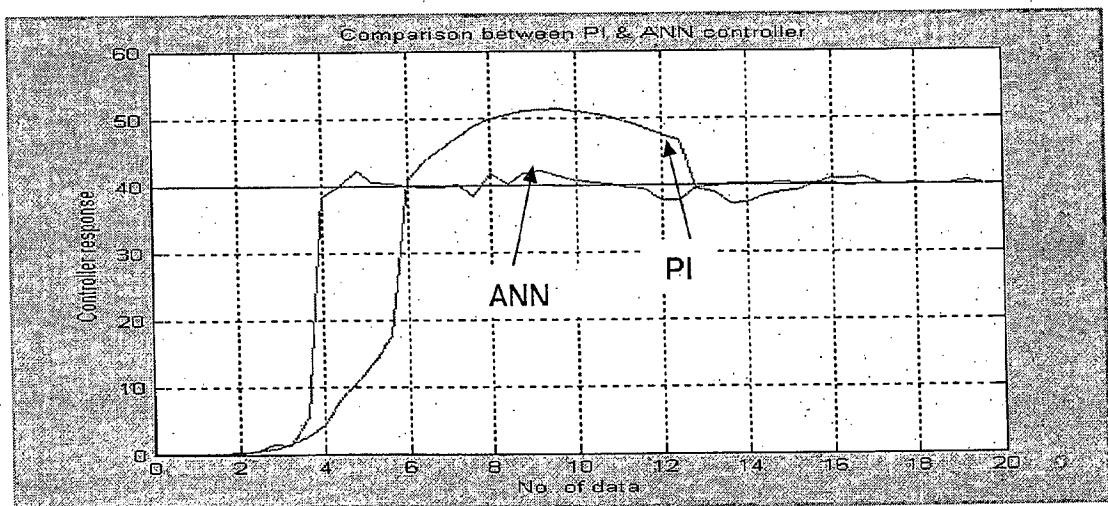
Fig.6.27 PI and ANN Controller response

From the analysis of rise time, overshoot and settling time of both the controller, it is revealed that the ANN controller gives better results. The performance indicators between ANN and PI controller is more clearly shown in table 6.6, which indicates that the ANN controller is more reliable than conventional controller because ANN controller reduces the delay time, and minimizes the overshoot.

Table:6.6 Comaprison between ANN and PI controller for total head

Performances criteria	ANN controller	PI controller
Minimum value	0.00003	0.0
Maximum value	42.25	51.25
Mean	32.24	31.88
Median	39.89	39.99
Standard deviation	15.88	19.14
Range	42.25	51.26
Maximum overshoot,%	≈ 5.6	≈ 28.1
Delay time, s	0.8	1.8

Case-6.4: Stock level control:

6.4.1 Effect of discrete and continuous signals for stock level:

The first order dynamics proposed in eqn.[5.49] given in chapter-5 has been simulated with the help of MATLAB software. The simulation results with unit step input for continuous and discrete system with PI controller are shown in fig. 6.28. It indicates approximately the same values for both continuous and discrete systems. The profiles coincide with each other.

6.4.2: Comparison between Conventional and ANN controller data:

Stock level response of headbox using PI controller is shown in fig. 6.29. The performance of PI and ANN are compared in fig.6.30. The plot shows that the PI controller indicates the settling time of 12s and delay time of 3s whereas ANN controller shows the same of the order of 10s, and 2.1 s respectively. The performance of ANN and

PI controller in terms of statistical data is also shown in table.6.7. It concludes that the ANN controller is best suited for the stock level control.

Table:6.7 Comparison between PI and ANN controller for stock level

Performances criteria	PI data	ANN data
Delay time,s	3.0	2.1
Settling time,s	12.0	10.0
Mean value	14.91	15.8
Maximum value	19.93	19.93
Std.	6.79	5.91
Median	18.47	19.09
Range	19.93	19.93
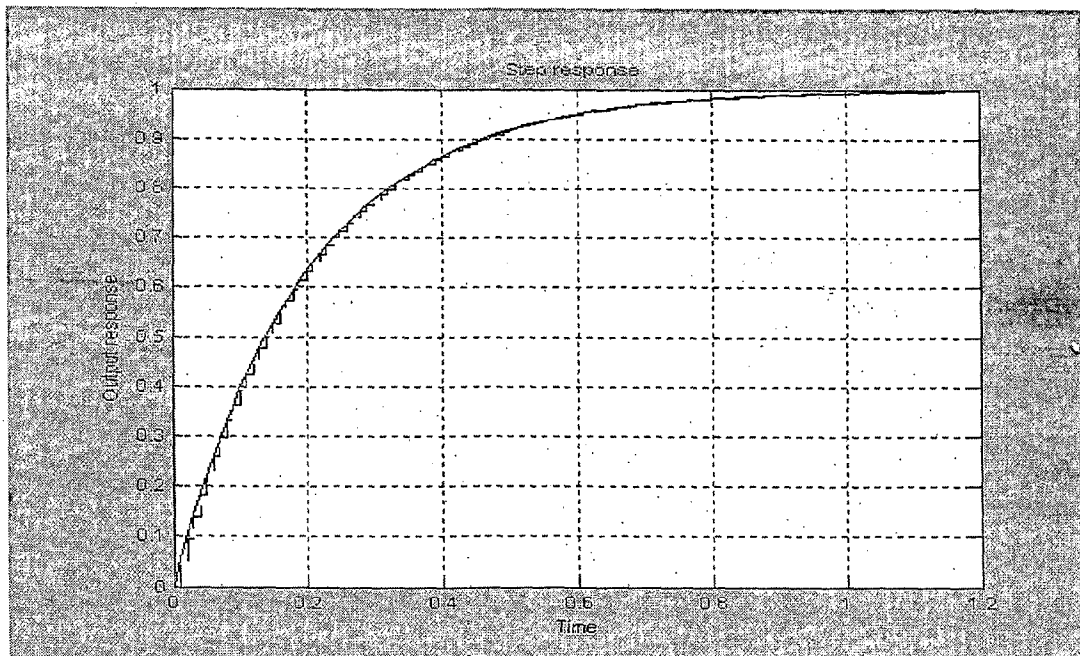
Fig.6.28 Plot between continuous and discrete data (without controller)
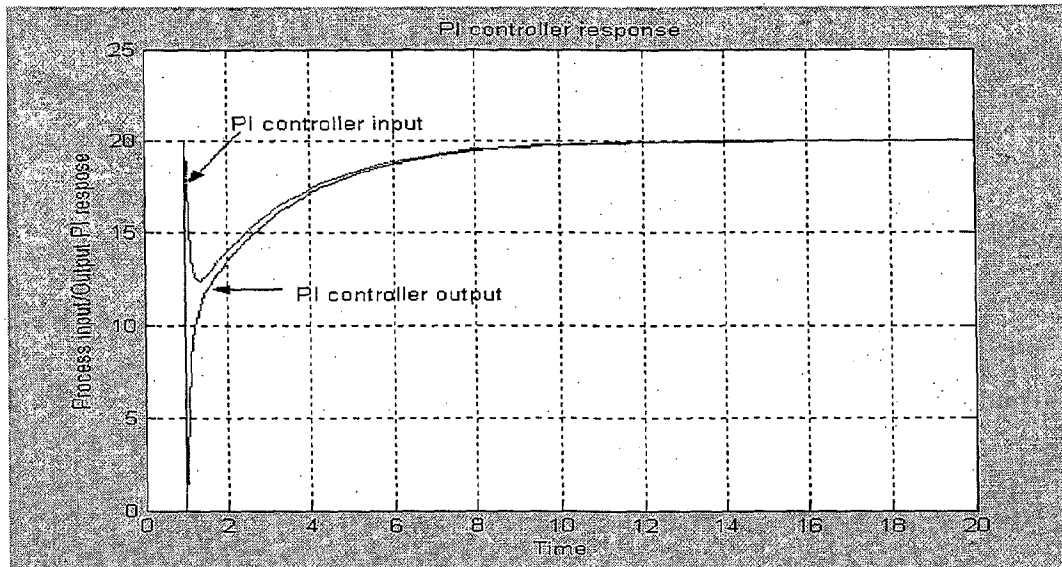
Fig. 6.29 PI controller response (simulation of model)
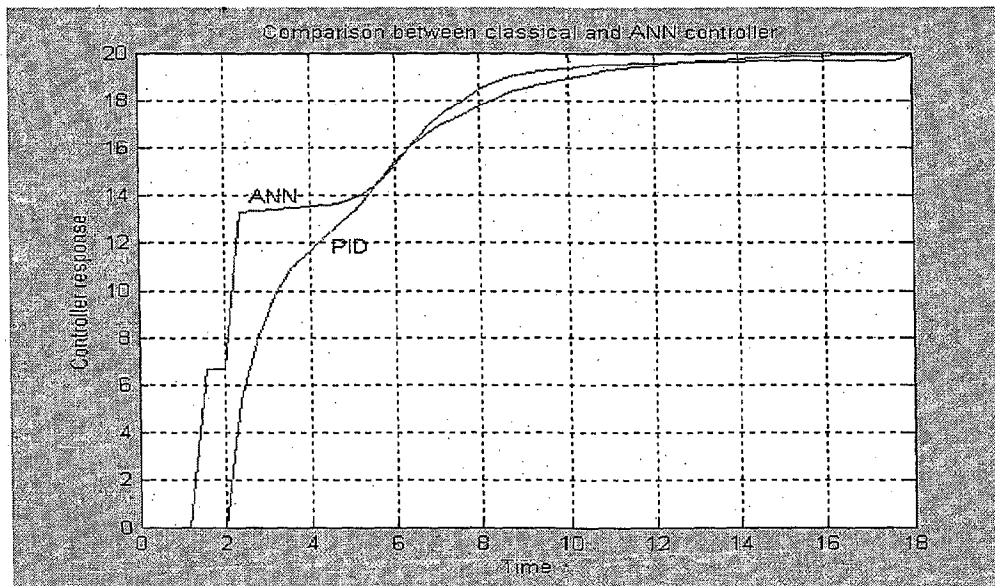
Fig. 6.30 Controller response

Case-6.5: pH control of stock:

6.5.1: Effect of discrete and continuous signals for stock pH:

In case of pH, the dynamic equation of first order eqn.[5.56] developed in Chapter 5, simulated with the help of MATLAB software. The simulation results for continuous and discrete system with conventional controller (PI) are shown in fig. 6.31. Subsequently the simulated data are used for training the neural network. The data from fig.6.31 are

analysed statistically. Std. deviation of the order of 1.493, mean of the order of 6.21 for continuous signal while std. deviation of the order of 1.505, mean of the order of 6.19 for discrete signal are obtained. It reveals that there is no appreciable variation in continuous and discrete signal.

6.5.2: Comparison between conventional and ANN controller data:

The artificial neural network training response is shown in fig.6.32. It shows the network performance of the order of 0.000301793, error goal of the order of 0.0003 at 80000 epochs. After training, the conventional controller has been replaced by ANN controller.
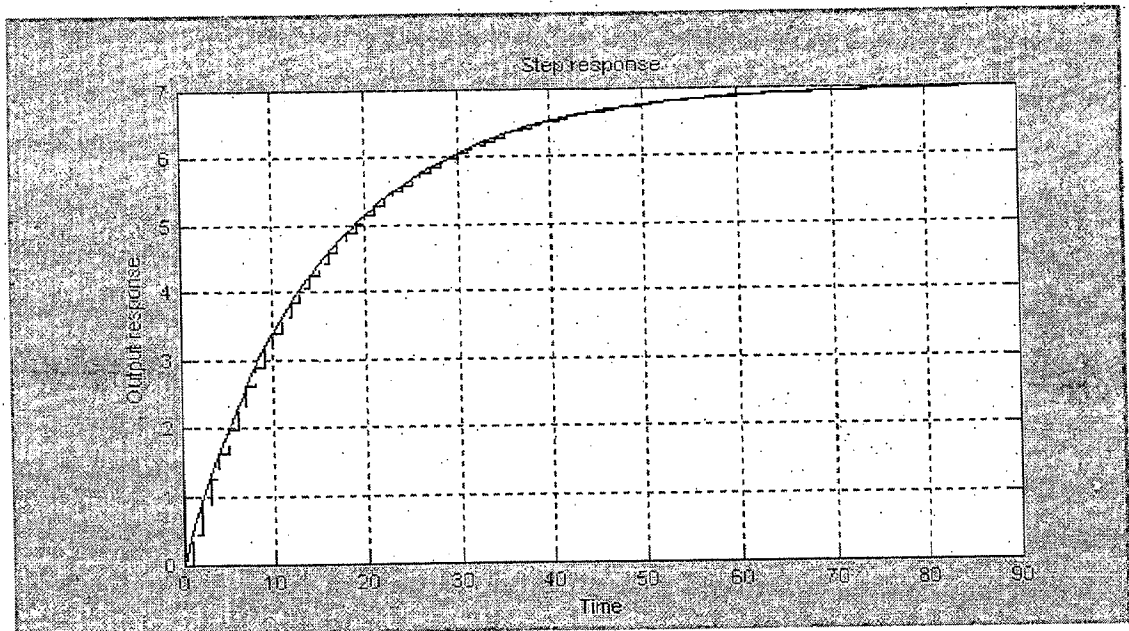
Fig. 6.31 Plot between continuous and discrete data(without controller)

6.6.2: Comparison between conventional and ANN controller of different designs data:

The performances of the PID controller, MLP, MFLANN (modified functional link ANN) and DLFANN (direct linear feed through ANN) controllers for temperature are compared in table-6.9 and responses shown in figs.6.35 to 6.38. Table-6.8 shows that the MLP response gets the steady state value of the order of 38.88s in a very short period (settling time) with rise time when the set point is 40^0c. The performances of all the ANN methodologies along with PI are compared in table 6.9.
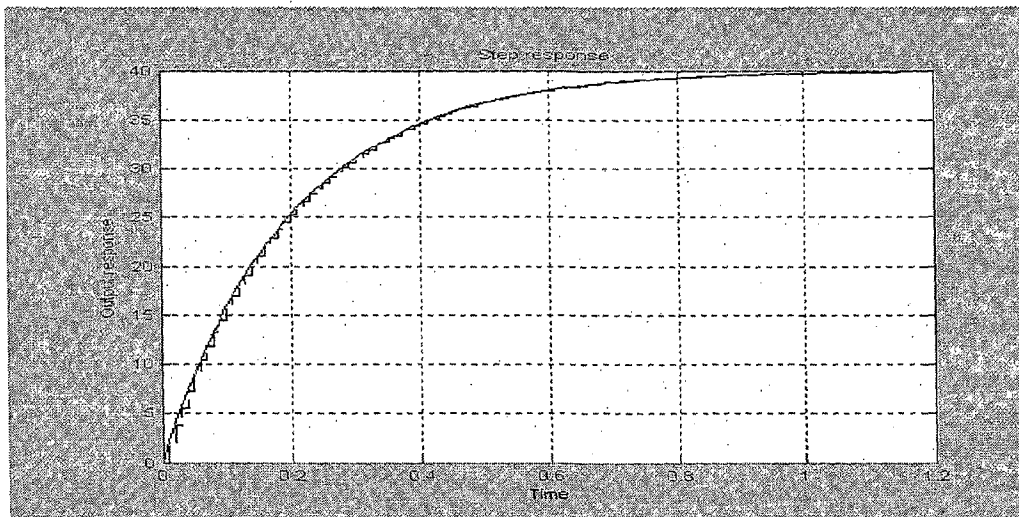
Fig. 6.34 Plot between continuous and discrete data(without controller)
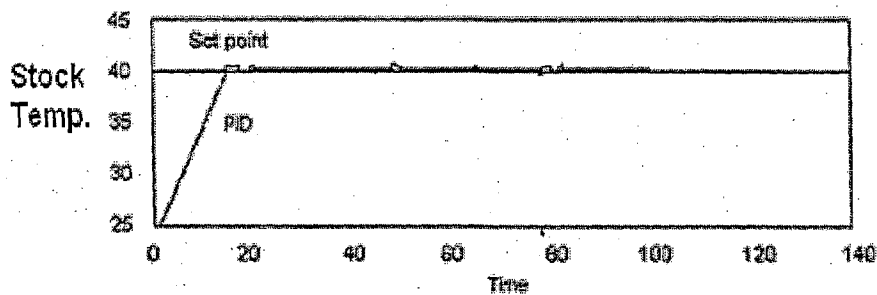
Fig.-6.35 PID controller response
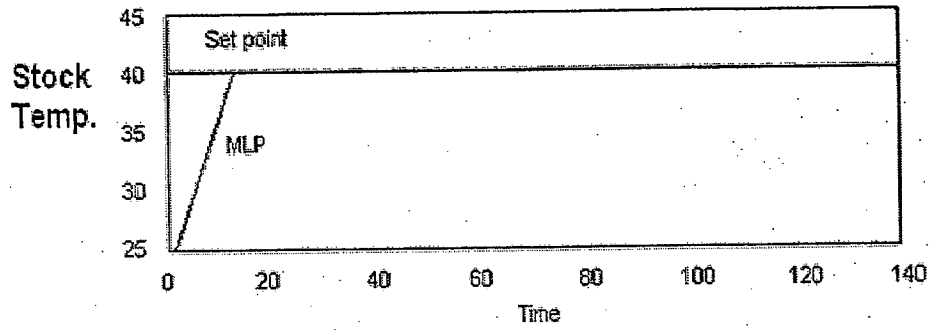
Fig.-6.36 MLP neural network controller response
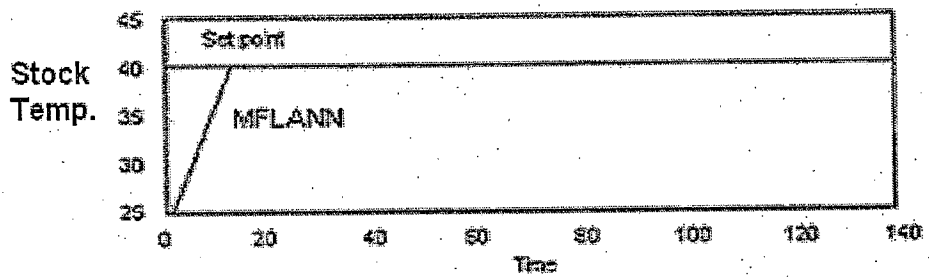
Fig.-6.37 MFLANN neural network controller response
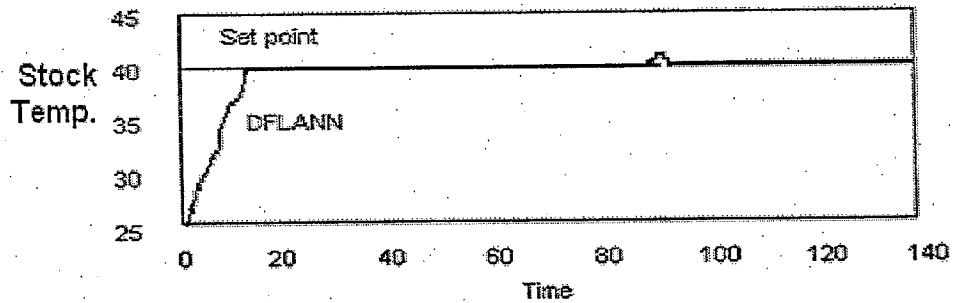
Fig.-6.38 DFLANN neural network controller response

Table:6.9 Comparison of PID ,MLP, DLFANN , and MFLANN controllers

	Performances Criteria		PID Controller	MLP	DLFANN	MFLANN
Set point	Steady state	Time(s)	560	380	380	270
		Value	40	39.88	39.86	40
	Overshoots	Max. (^{0}C)	Nil	Nil	Nil	Nil

193

		Min.	Nil	Nil	Nil	Nil
	Undershoot	Max.	Nil	0.16	0.11	Nil

Table 6.9 shows the values of settling time, and overshoots for PID, MLP, DLFANN, and MFLANN controllers. Based on the results it can concluded that the settling time of MLP and DLFANN controllers are less as compared to other ANN architecture. Therefore MLP and DLFANN controllers give comparable values. Therefore either design can be used.

Case-6.7: Basis weight control (Analog system):

As shown in Chapter-5, there are two dynamic models relating stock flow rate and basis weight are available , both in analog eqns[5.71a,5.72a] as well as in digital form eqns.[5.71b,5.72b], in addition to the model derived by order reduction process and its z transformed equation. The analog model along with conventional and ANN controllers are simulated. The results of analog simulation are interpreted as under:

6.7.1: Effect of discrete and continuous signals for basis weight:

The simulation results of the process dynamics for continuous and discrete signals without controller as shown in fig. 6.39 reveals that the continuous signal represents basis weight values with the std. deviation of the order of 0.1593, mean of the order of 0.477, while std. deviation of the order of 0.1642, mean of the order of 0.474 are obtained for discrete signal.

6.7.2: Comparison between conventional and ANN controller data:

The Simulink model between stock flow rate and basis weight as shown in fig.5.14, in chapter-5 is used. Industrial data are used for training the network (table-6.10). The analog simulation results of basis weight model with PI controller are given in fig.6.40 (set-point response for the closed loop system) and in fig.6.41 (closed loop response for a

unit step disturbance). The mean value of the normalized basis weight is obtained of the

order of 0.8233 in the former case (fig.6.40) whereas the value of normalized basis weight

is reduced to 0.06144 in the later case (fig.6.41). Also more oscillation is exhibited in the

case when unit step input for disturbance variable is used. Basis weight response using

ANN controller at the rated basis weight at 59% of the gate opening(normalized value

1.00) are given in fig-6.42 and fig.6.43 where PID , and ANN data are compared with mill

data. The maximum data of ANN tally with Mill data. The artificial neural network training

response is shown in fig.6.44. The data from ANN based control provide quite satisfactory

control as except the range of data between 5 to 7. PID control based data is found to be

inferior to the ANN controller data.
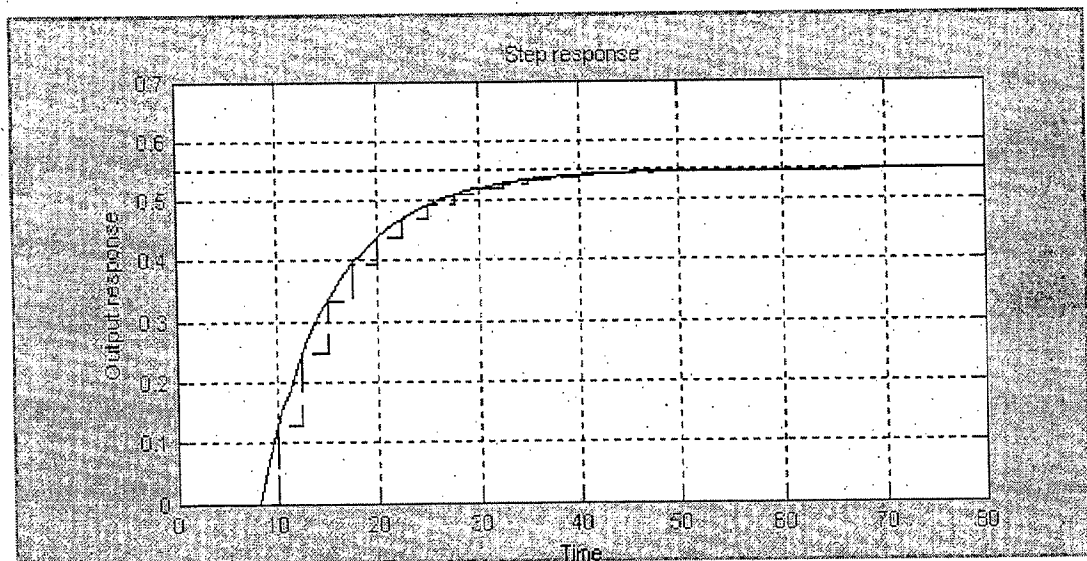
Fig. 6.39 Simulation results of continuous and discrete system (without controller) when sampling period=2.5s
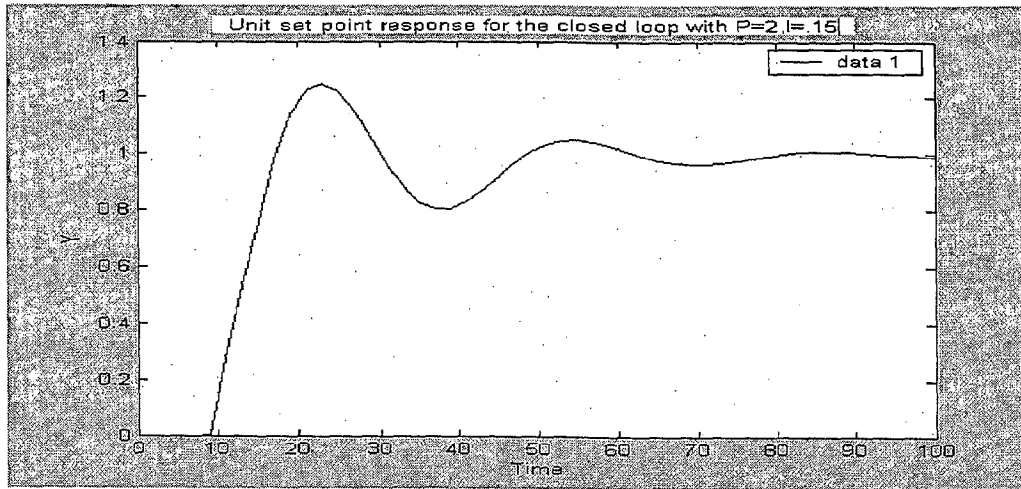
Fig. 6.40 Unit step point response for closed loop system
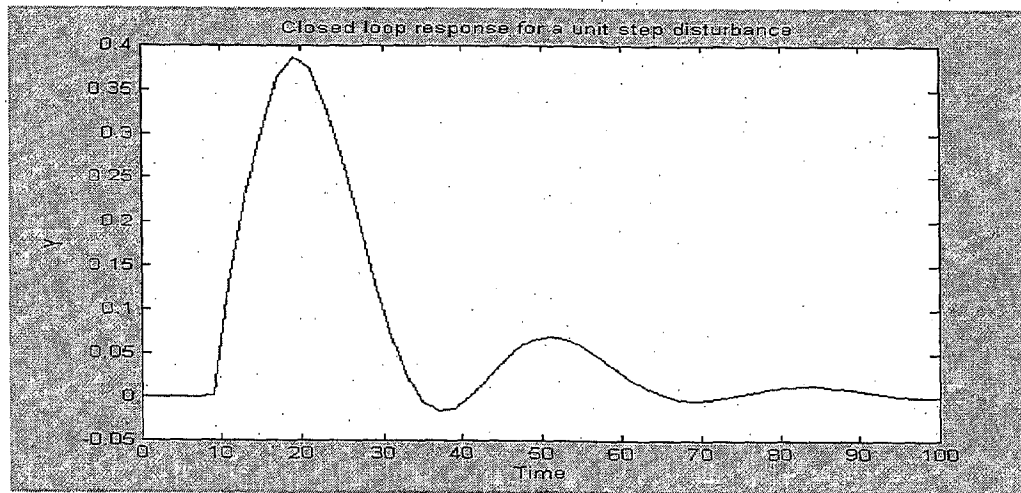
Fig. 6.41 Unit step point response for a unit step disturbances
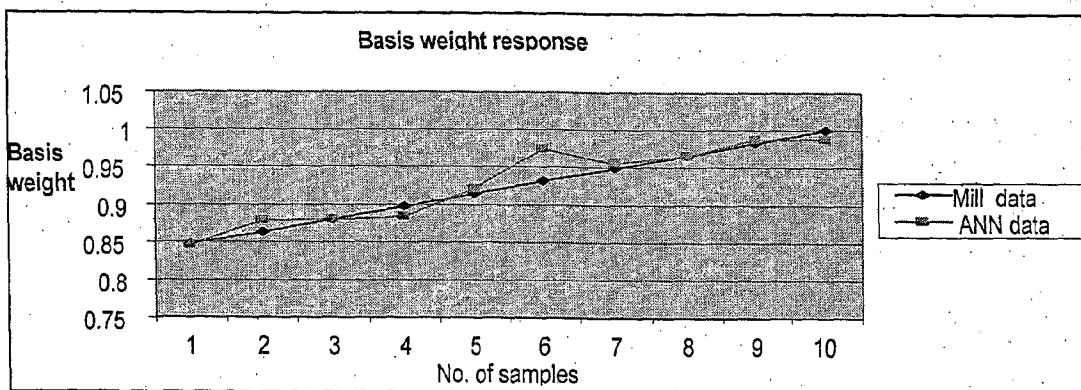
Fig-6.42 Basis weight test result
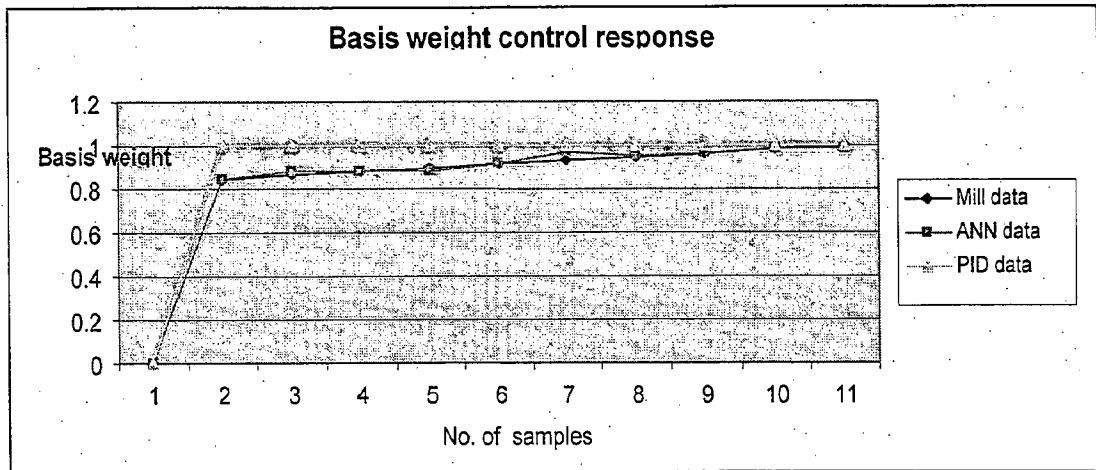
Fig. 6.43 Comparison between mill data, ANN, PID data
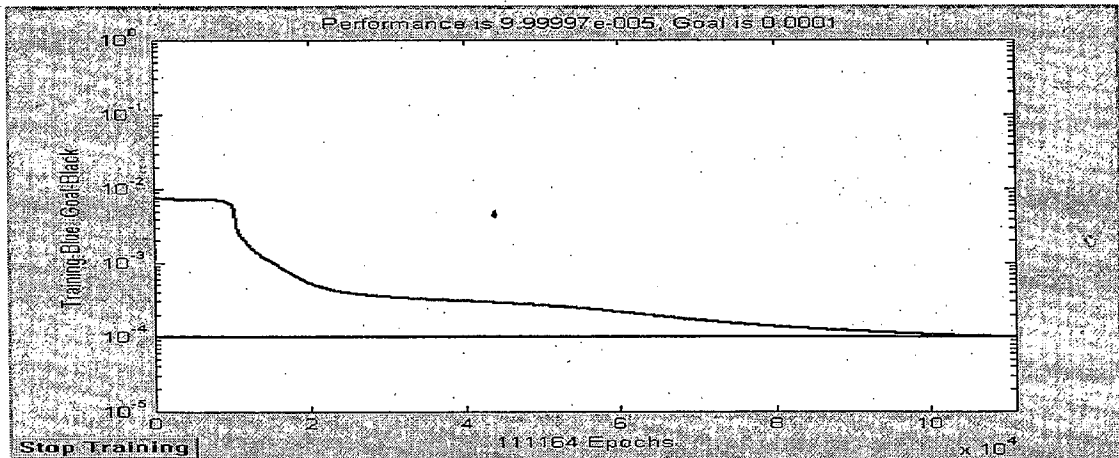
Fig. 6.44 ANN training response

Training data for basis weight ANN controller have been obtained as under.

Table: 6.10 Mill data and comparison between PID & ANN data

S..No	Normalized basis weight(Mill data) BW in %		Stock flow LPM & Normalised		Basis weight(PID data)	Basis weight(ANN data)
1	50%	0.847	3004	0.8159	1.0	0.846
2	51%	0.864	3079.65	0.8364	1.0	0.878
3	52%	0.881	3155.10	0.8569	1.0	0.881

6.8.2: Comparison between conventional and ANN controller data

For simulating the eqns.[5.84 and 5.85] in chapter-5 with MATLAB software, the artificial neural network is trained using different neural network algorithms like gradient descent technique, Levenberg-Marquardt(LM) algorithm and GDX.

The figs.6.45b to 6.48 show the performances of different networks, when the network is designed as 1:5:1, error goal is e^{-005} met at 18502 epochs in case of gradient descent algorithm. The training error goal is met at 5 epochs in case of Levenberg-Marquardt algorithm while the training error goal is met at 234 epochs in case of error gradient descent algorithm. The performance of dynamic model in digital form and artificial Neural Network model are found out with the help of MATLAB programming, shown in table-6.11. The minimum error is observed in case of gradient descent and LM techniques. Figs. 6.49 to 6.51 indicate the basis weight output response with respect to number of samples. The maximum number of samples of dynamic model closely tally with those obtained from gradient descent technique but the training time is large compared to Levenberg -Marquardt algorithm and error gradient descent technique. The results are more clearly compared in table 6.10.
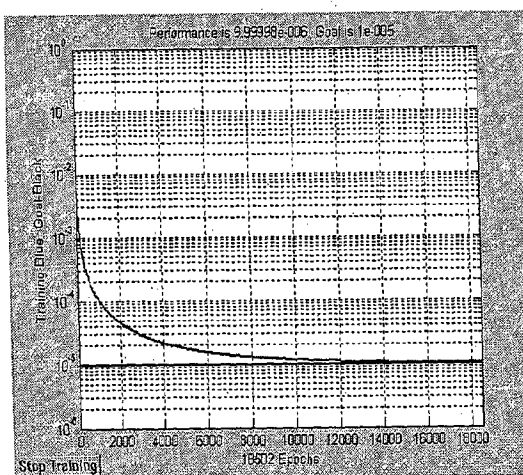
Fig.-6.45b ANN training response   Fig.- 6.46ANN training response(LM)
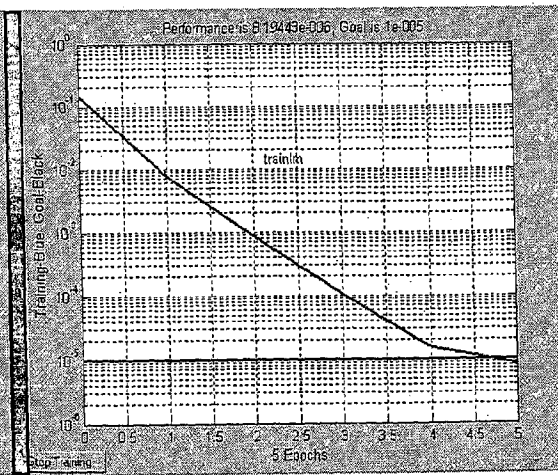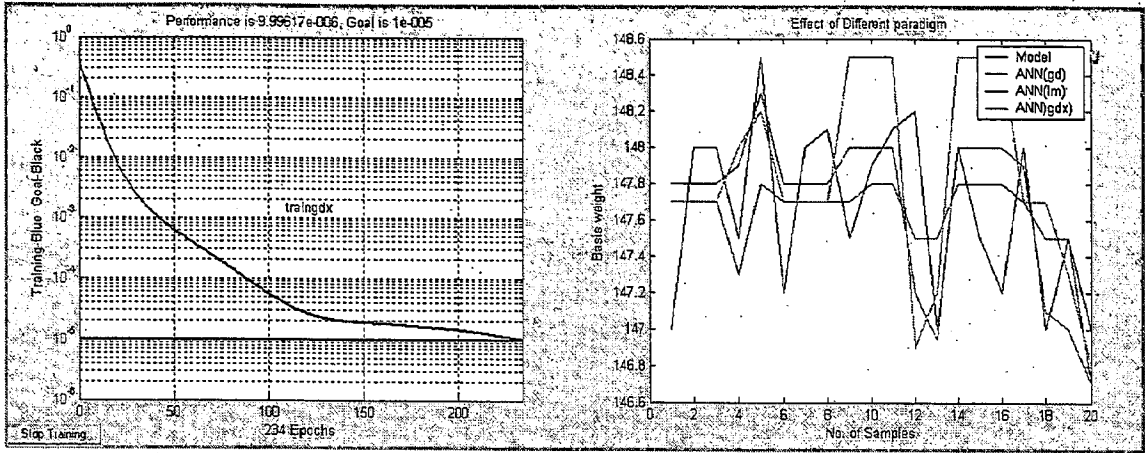
Fig.-6.47 ANN training response(gdx)   Fig.-6.48 Effect of different paradigm
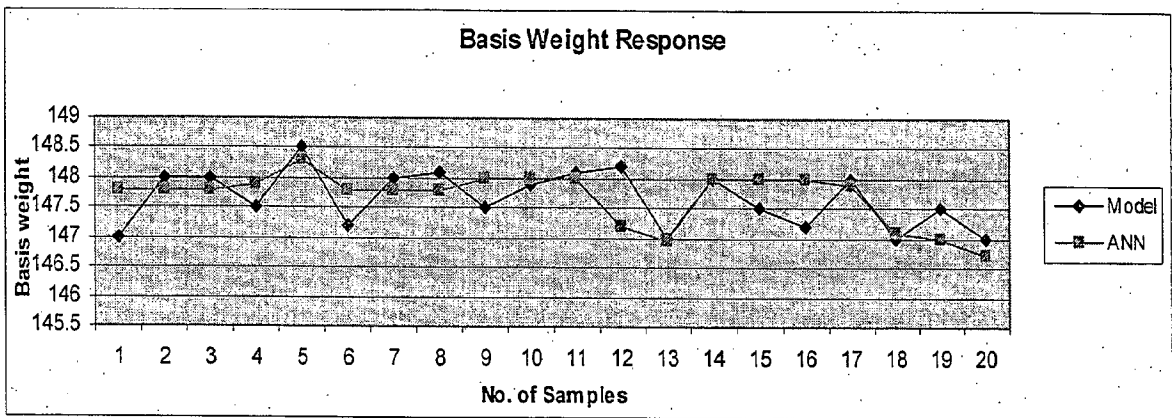
Fig.-6.49 Comparison between model based data and ANN data
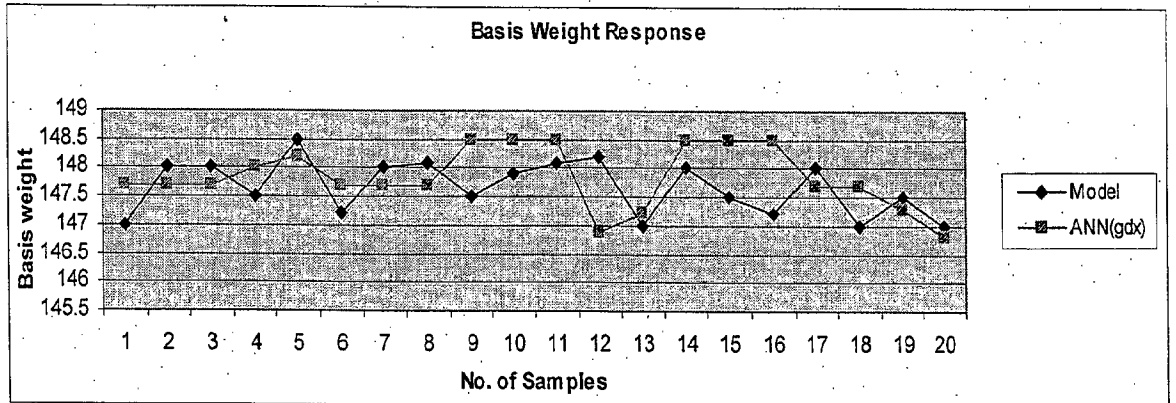
Fig.-6.50 Comparison between model based data and ANN data(gdx)

201

Basis Weight Response
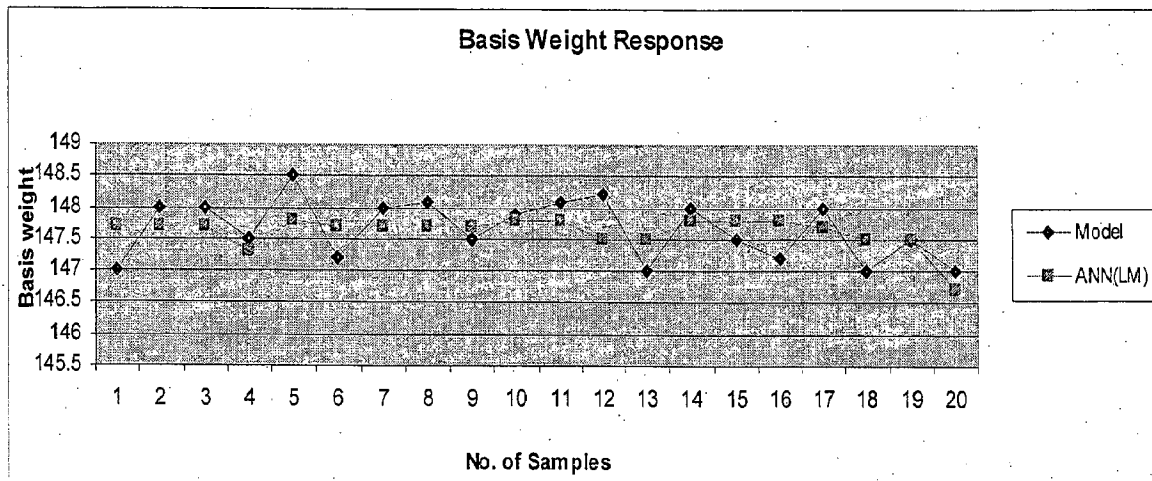
Fig.-6.51 Comparison between model based data and ANN data(LM)

Fig.- (6.49 to 6.51) Basis weight output response with respect to number of samples

Table:6.11 Comaprison of performances between ANN controllers

Performances criteria	Model based Data	ANN(Gradient. Descent)	ANN(Levenberg-Marquardt)	ANN(gdx)
Minimum	147.0	146.7	146.7	146.8
Maximum	148.5	148.3	147.8	148.5
Mean	147.7	147.7	147.6	147.8
Median	147.7	147.8	147.7	147.7
Standard deviation	0.4751	0.4414	0.2567	0.5424
Range	1.5	1.6	1.1	1.7

[B] ANALYSIS OF MIMO SYSTEM OF PAPER INDUSTRY:

Case-6.9: Total head and stock level control:

The simulation results of eqns. [5.86,5.87] for continuous and discrete system are shown in figs. 6.52 and 6.53(for Y_{11} & Y_{12}) without using controller. These are interpreted as under:

6.9.1: Effect of discrete and continuous signals for total head and stock level:

The fig. 6.52 shows the performance in terms of std. deviation of the order of 0.1778, mean value of data of the order of 0.444 for continuous signal but for digital signal, and the std. deviation of the order of 0.187, and mean value of data of the order of 0.436 are obtained. However, the other statistical data remain the same.

202

6.9.2: Comparison between performances conventional and different ANN methodologies:

The results have been computed using BPNN, perceptron and ART1 network for single neuron, for MIMO(two input single output ,TISO) and SISO system (as the case may be). It is well known that perceptron network is valid for single layer only and BP and ART are used for multi-layer NN problems. In this investigation various equations, for BP, eqns.[5.86 and 5.87], for perceptron, equations, eqns.[5.90 and 5.91] and for ART [5.86 eqns 5.87] are employed for computation. The tuning parameters like learning rate, momentum coefficient are used with all the above mentioned equations. The results are computed through MATLAB and simulations are carried out. The training data are obtained from air cushion headboxes from two paper mills in India. The training parameters for headbox problem are given in table-6.12.

Table: 6.12 Parameters values and ranges

Number of hidden layers	Number of hidden neurons	Learning rate	Momentum Factor
1.0	2-14	0.5-0.9	0.5-0.9

The eqns.[5.90, 5.91] given in Chapter 5 represent the output in terms of total head and stock level in head box control system. From figs 6.54 to 6.55, it is evident that the lowest error occurs at learning value of 0.6 for network training. Therefore 0.6 is considered as optimum. The values of momentum coefficient have been varied between 0.5 to 0.9. From figs 6.56-6.57, it is clear that there is continuous linear decrease of error with the increase of momentum coefficient up to value of 0.9, there is no substantial change occurred thereafter. Besides most of the previous investigators employed the value o momentum factor close to 0.9. Therefore 0.9 has been chosen as optimum value o momentum factor in this present investigation.

The effect of hidden nodes on error is shown in fig-6.58. The normalized data of total head as a function of the number of samples is shown in fig.-6.59. The figs.(6.59 to 6.60) further indicate the comparison of values for output 1(total head) and output 2(stock level) for MIMO system. The values are more clearly shown in table 6.13. For SISO (Single input single output) system as indicated earlier perceptron neural network is used. The simulated data are shown in figs 6.61 and 6.62. The figs indicate the comparison of values for output 1 and output 2 with actual values. It is evident that the values are closely tallying with each other. The effect of iterations on error for training is shown in fig.-6.63. The error is continuously decreased with the increase of number of iterations. For MIMO system the error has become minimum of the order of 0.0002.
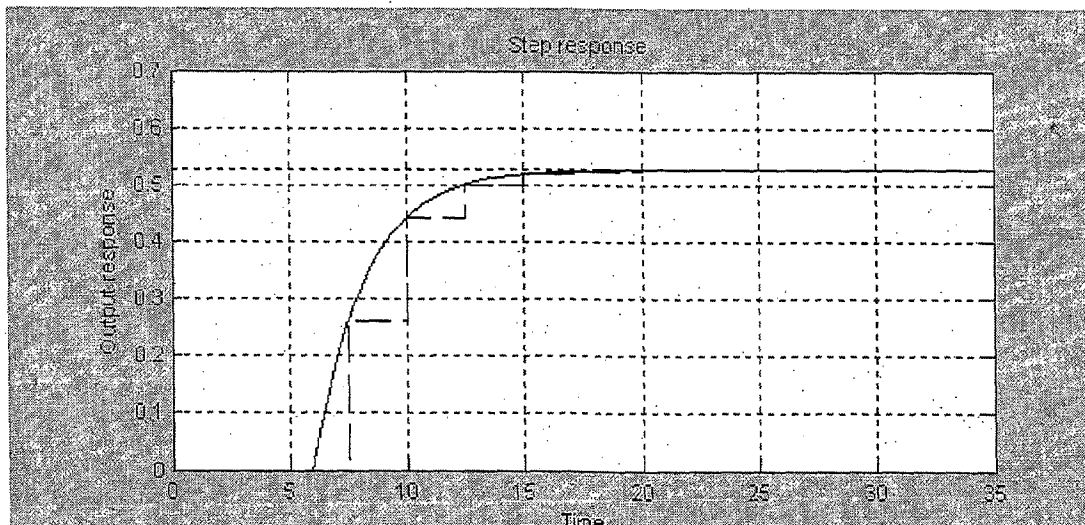
Fig.6.52 Simulation result of continuous and discrete data(Y_{11})
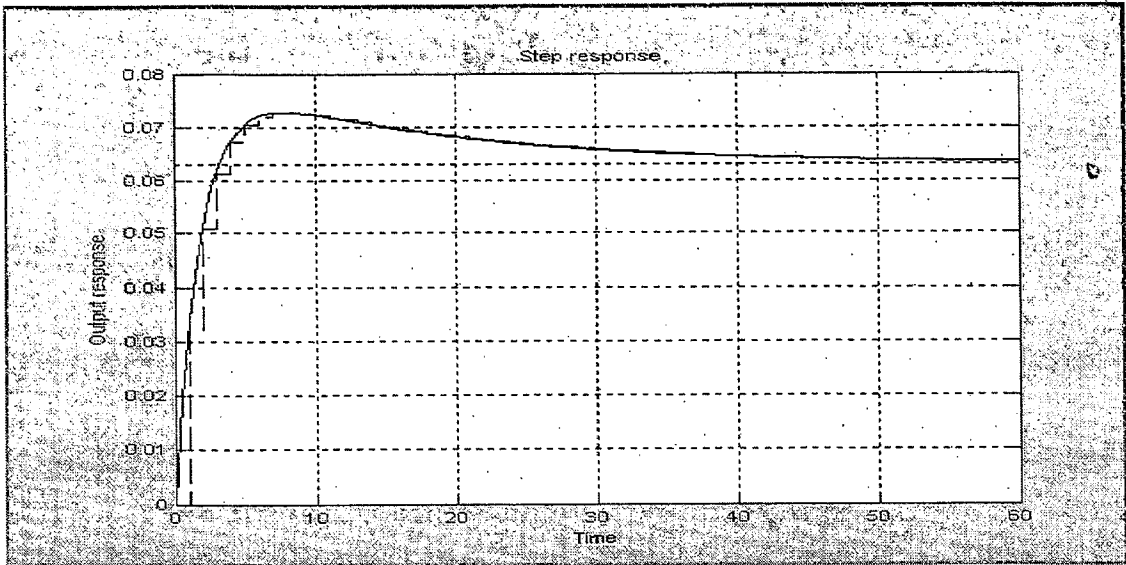
Fig.6.53 Simulation result of continuous and discrete data(Y_{12})
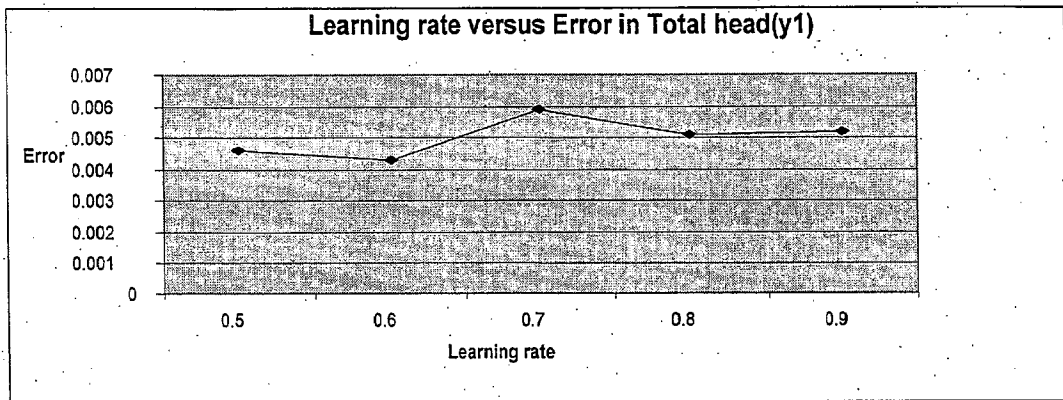
Fig.6.54 Effect of learning rate (total head)
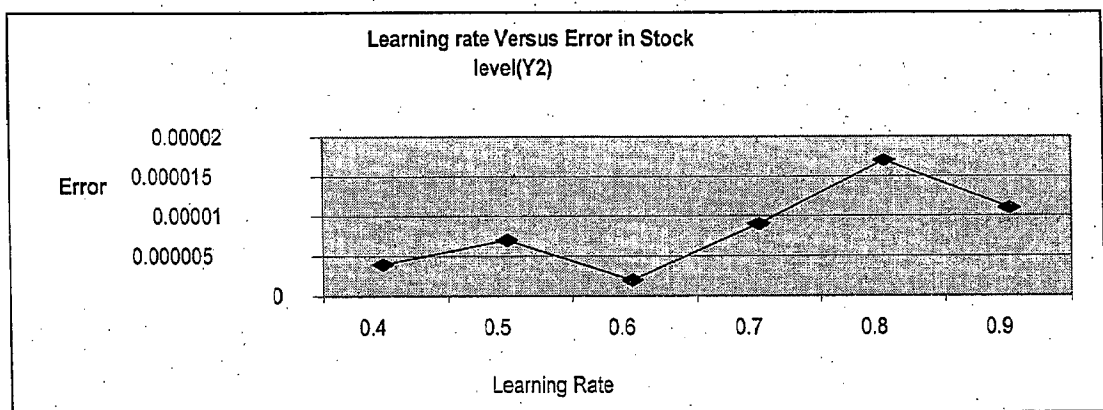
Fig.-6.55 Effect of learning rate (stock level)
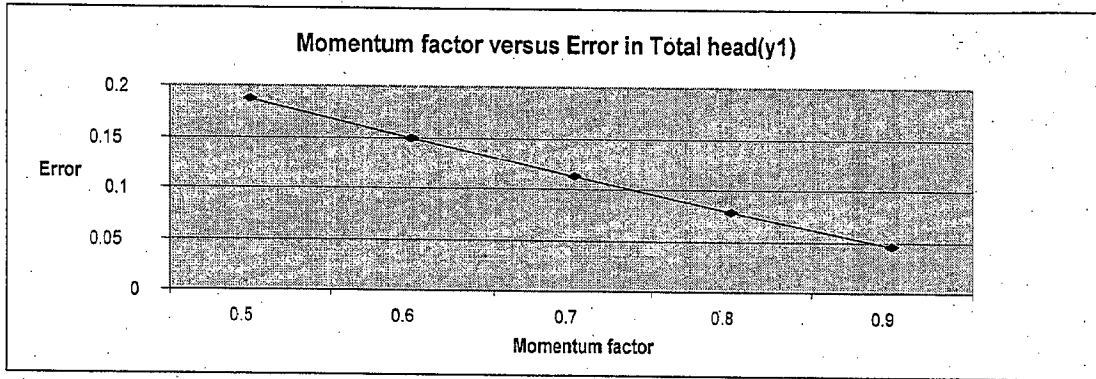
Fig.-6.56 Effect of momentum factor (total head)
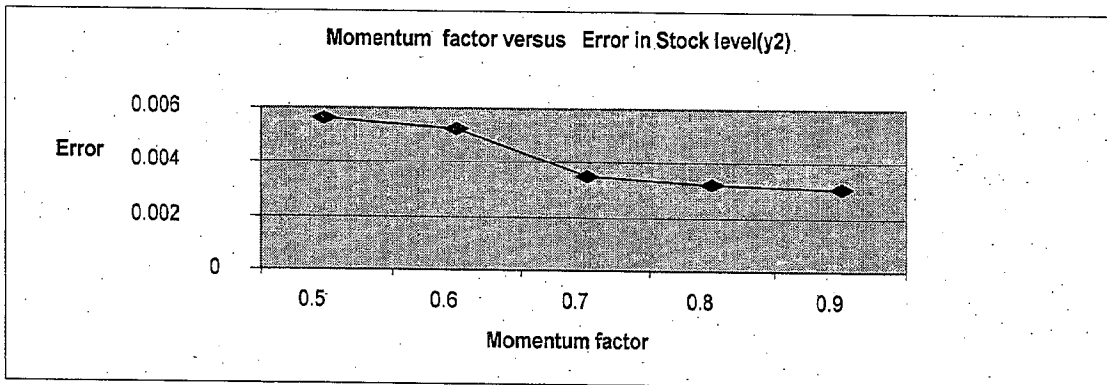
Fig.-6.57 Effect of momentum factor (stock level)
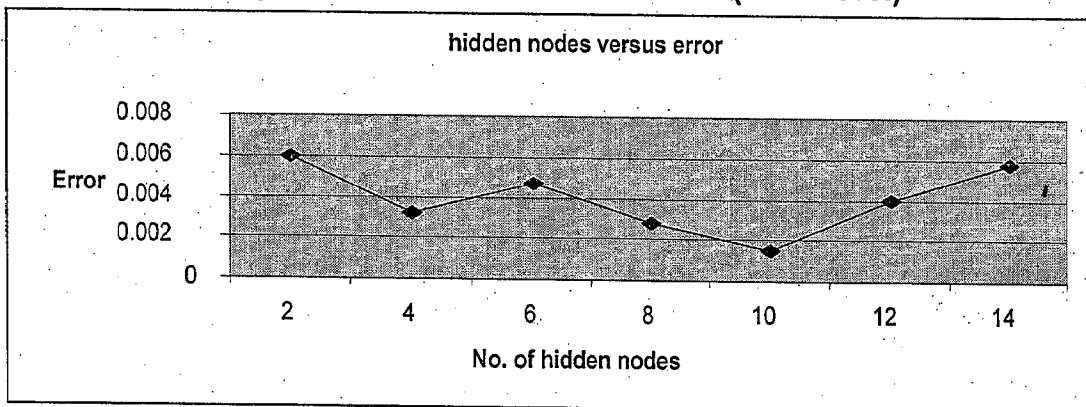
Fig.-6.58 Effect of hidden nodes

For MIMO system

Output 1 of testing data

No. of samples	1	2	3	4	5	6
ANN	0.8416	0.9386	0.9504	0.9493	0.9491	0.9477
Actual	0.8533	0.9066	0.953	1	0.9498	0.9431

Fig.-6.59 Comparison between actual and ANN data for total head

Output 2 of testing data

No. of samples	1	2	3	4	5	6	7	8	9
ANN	0.638	0.637	0.636	0.63	0.63	0.63	0.6	0.63	0.63
Actua	0.637	0.656	0.67	0.656	0.637	0.63	0.6	0.63	0.6
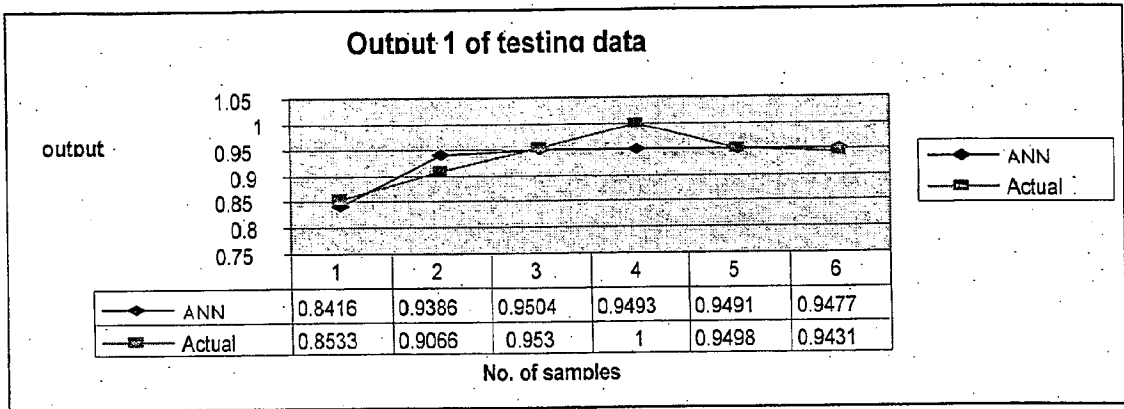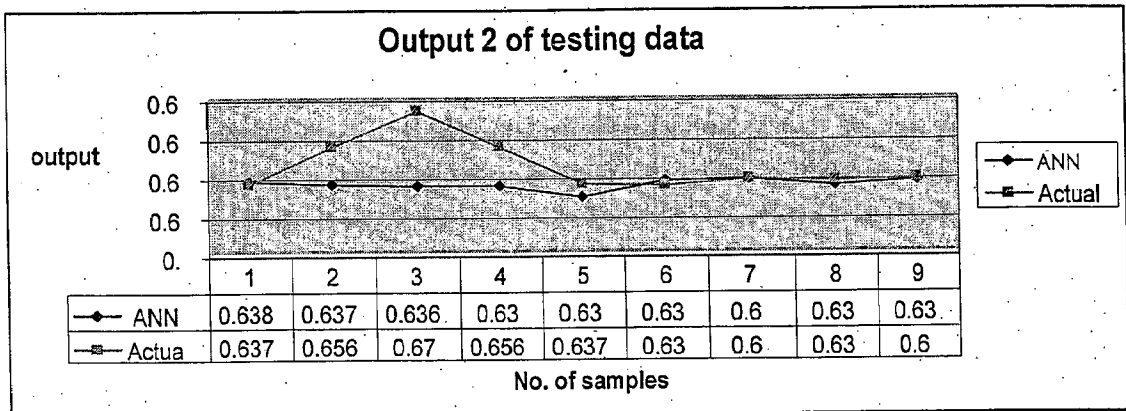
Fig.-6.60 Comparison between actual and ANN data for stock level

For SISO system:

Output 1 of testing data
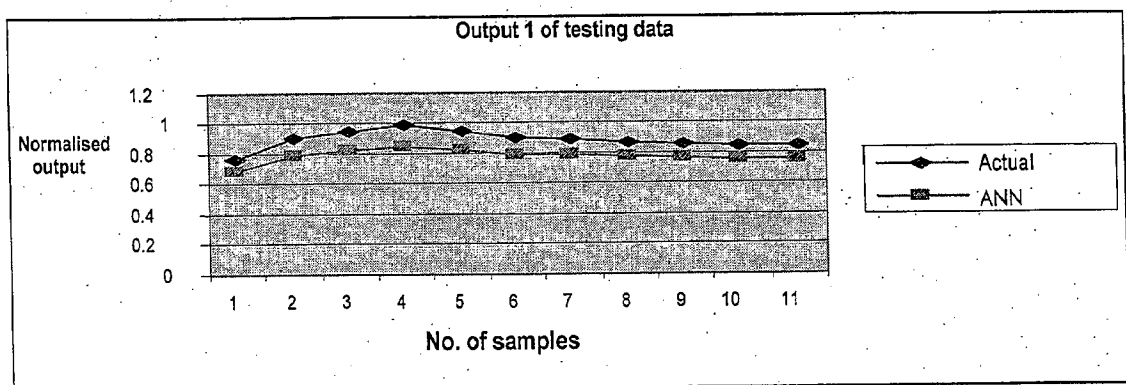
Fig.-6.61 Comparison between actual and ANN data for total head
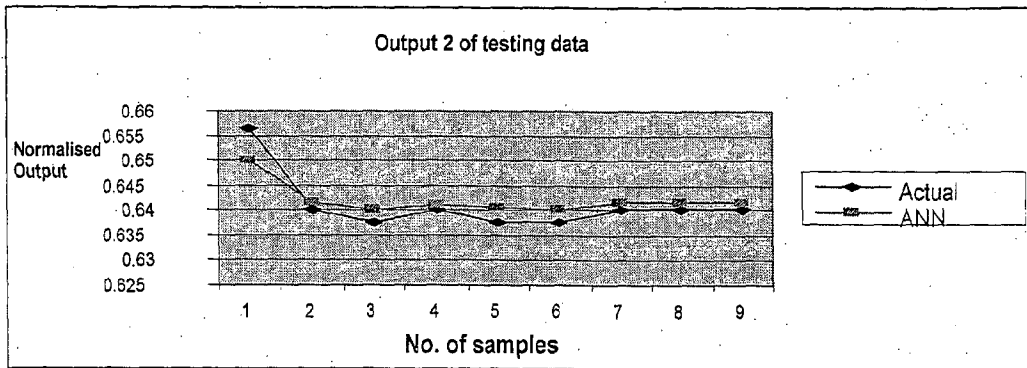
Fig.-6.62 Comparison between actual and ANN data for stock level
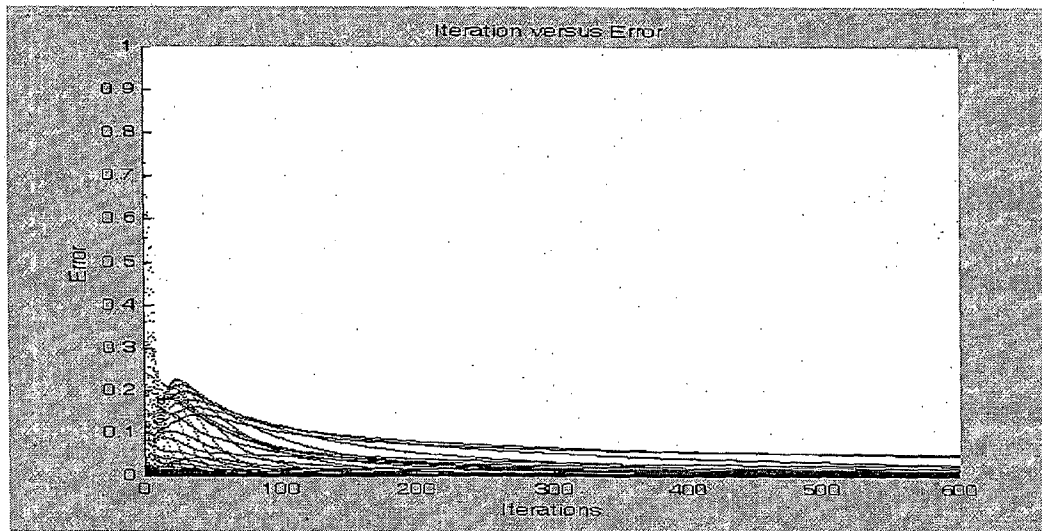
Fig.-6.63 Training response
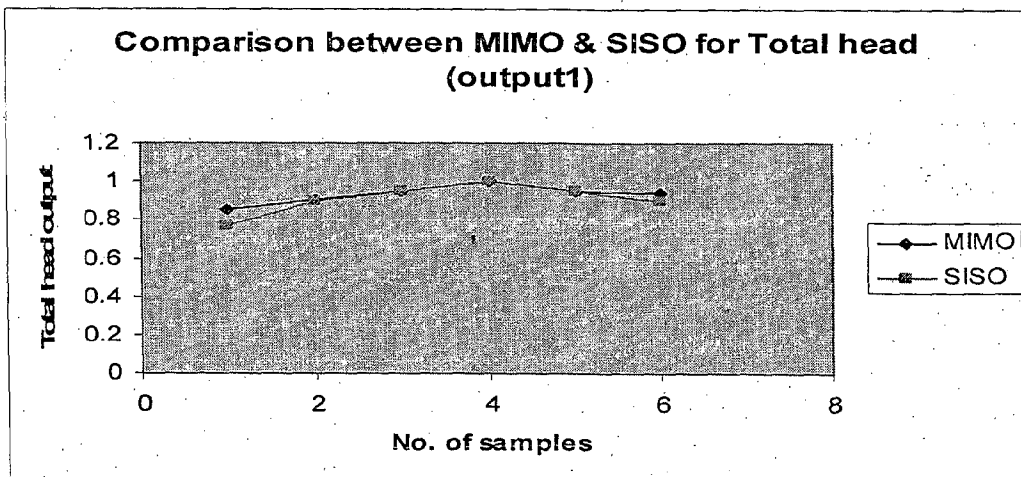
Fig.6.63a Comparison between MIMO and SISO for Total head
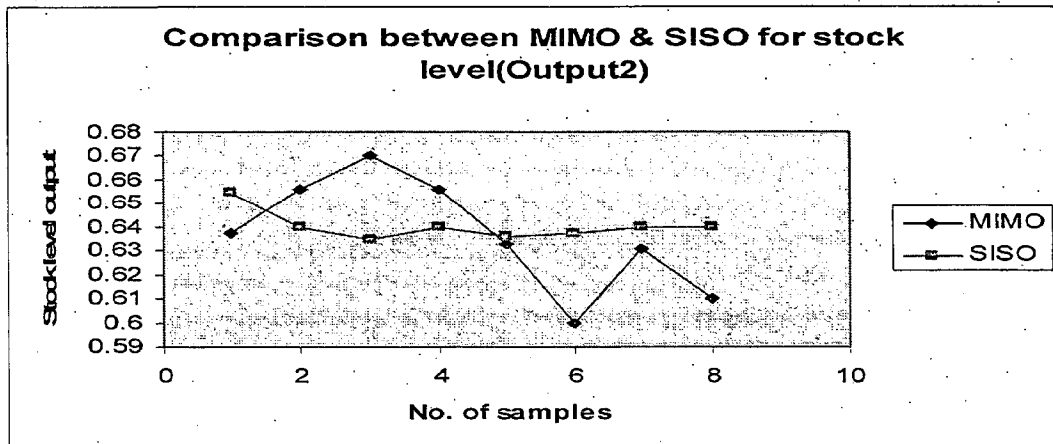
Fig. 6.63b Comparison between MIMO and SISO for stock level

The equations[5.90,5.91] for decouplers given in Chapter-5 are used for estimating data for total head and stock level. Figs.6.63a and fig.6.63b are drawn for comparing the ANN data for MIMO and decoupled SISO systems. The data when analyzed statistically, the following important conclusions are drawn.

Maximum error of the order of 0.0851, minimum error of the order of 0.0 and average error of the order of 0.0237 for total head have been obtained.

The data from fig 6.63b was analyzed statistically. Max error of the order of 0.035, min error of the order of 0.009 and average error of the order of 0.0205 for stock level were obtained.

Table:6.13 Comparison between ANN methodologies

Performances criteria	Perceptron		BPNN		ART1
MIMO	Y_1	Y_2	Y_1	Y_2	To overcome the problem of learning stability
Min error %	---	---	-3.5	-0.3	
Max. error%	---	----	5.05	5.6	
	----	-----			
Average error	-----	----	0.775	2.65	
SISO					
Min. error %	10.5	0.0	------	------	
Max. error %	15.5	0.9	-----	----	

| Average error | 13.0 | 0.45 | ----- | ----- | |

All the profiles indicate that the ANN controllers satisfy the requirement of adequate control for the MIMO system comprising of total head and stock level.

Case-6.10: Comparison of simulated data between PID and ANN controller for air pressure and level:

The modeling eqns.[5.92 to 5.135] for air pressure and level of the pressurized headbox have been described in chapter 5. The simulation results of eqns.[5.128,5.130,5.132 & 5.134] without controller are shown in figs. 6.64 to 6.67. The responses found out are found to be quite interesting. The pressure profile introduces overshoot but stock level exhibit first order characteristics. The nature of the responses became different based on the assumptions. When controllers are used, the responses display clearly second order system with overshoots of the order of 22.7% and 6.8%. The performances between PID controller and ANN controller for L_{head}(neu), P_{head}(rho) are shown in table 6.14a, and 6.14b. These profiles tally with those shown by Kikiewich et al.(75).
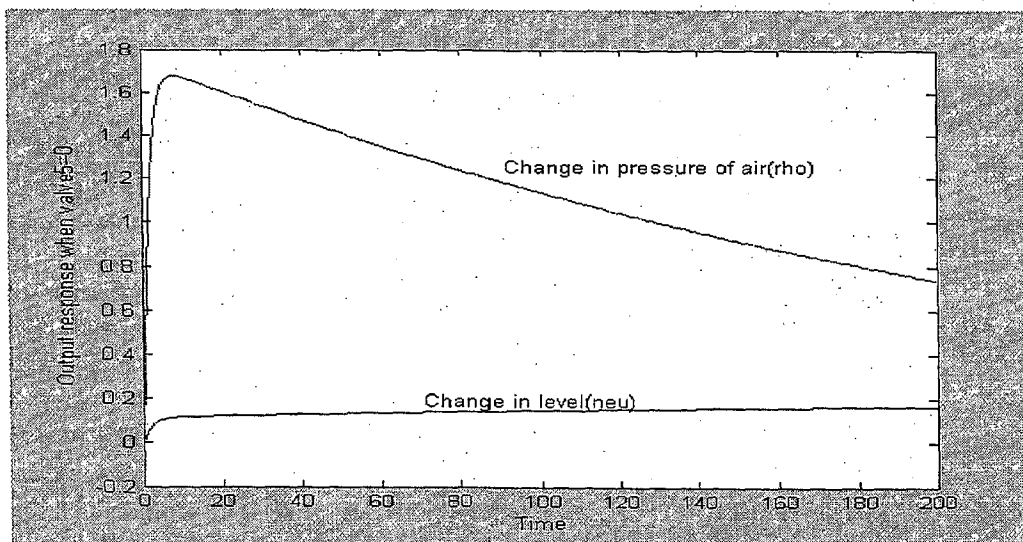
Fig.-6.64 Time characteristics of pressurized flow box when $\mu_5=0$
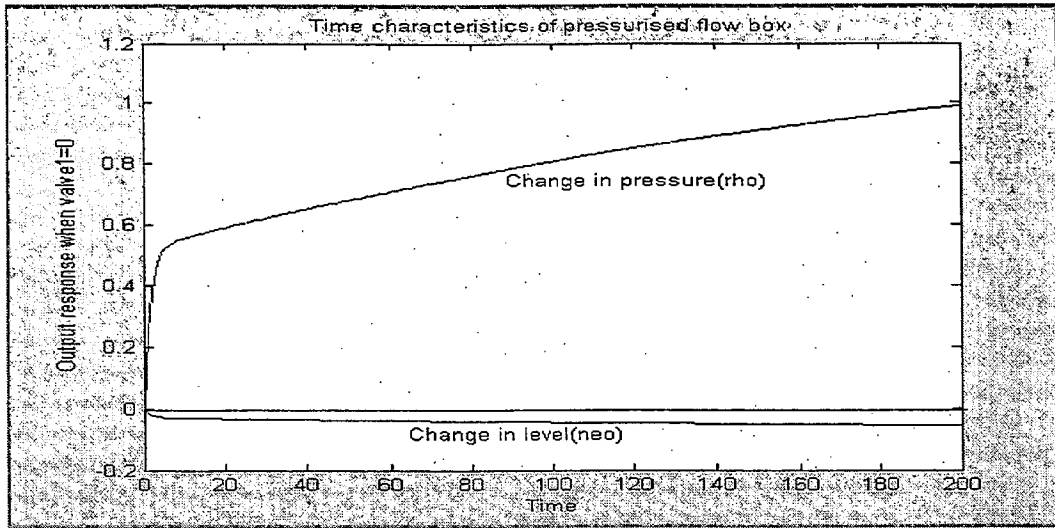
Fig.-6.65 Time characteristics of pressurized flow box when $\mu_1=0$
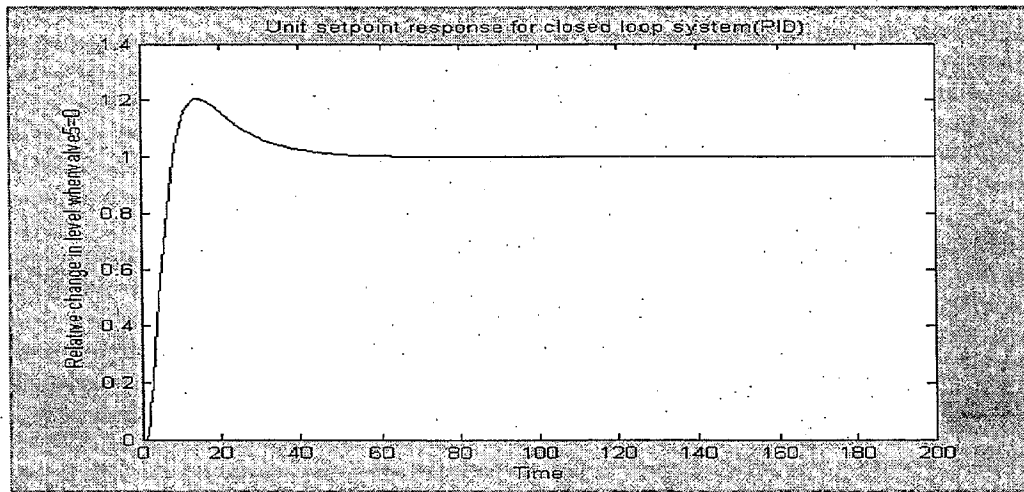
Fig.-6.66 Unit set point response for closed loop system for L_{head1}, when $\mu_5=0$
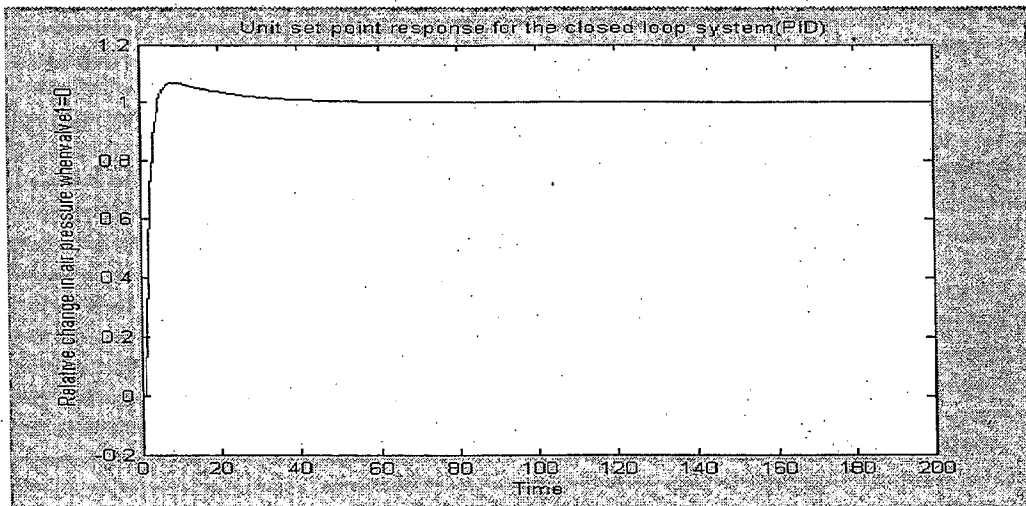
Fig.-6.67 Unit set point response for closed loop system for P_{head1}, when $\mu_5=0$

211

After simulating the process, data is used for training the network. The plots 6.68 to 6.70 show the errors between PID and ANN data with a given set point. Both the controllers show over damped system. Statistical data are also depicted in table 6.15. Which show that the ANN controller gives approximately the same value as the conventional controller provides. The comparison between PID and ANN is more clearly shown in figs.6.69 to 6.70 where it is found that except two values of ANN other tally very closely. Therefore it can be concluded that that the ANN controller can be used for MIMO system successfully.
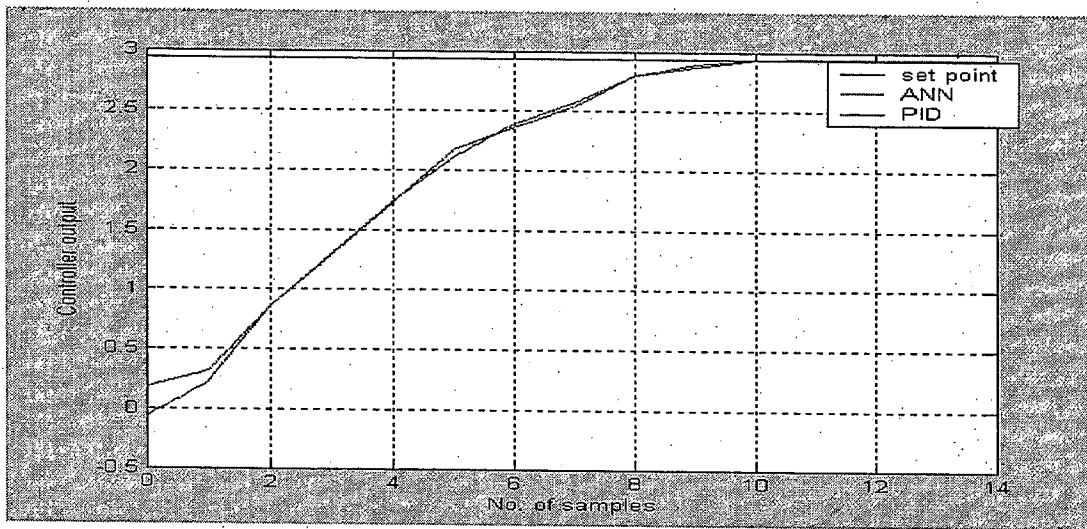
Fig.-6.68 Comparison between classical and ANN data for L_{head1}, when $\mu_5=0$
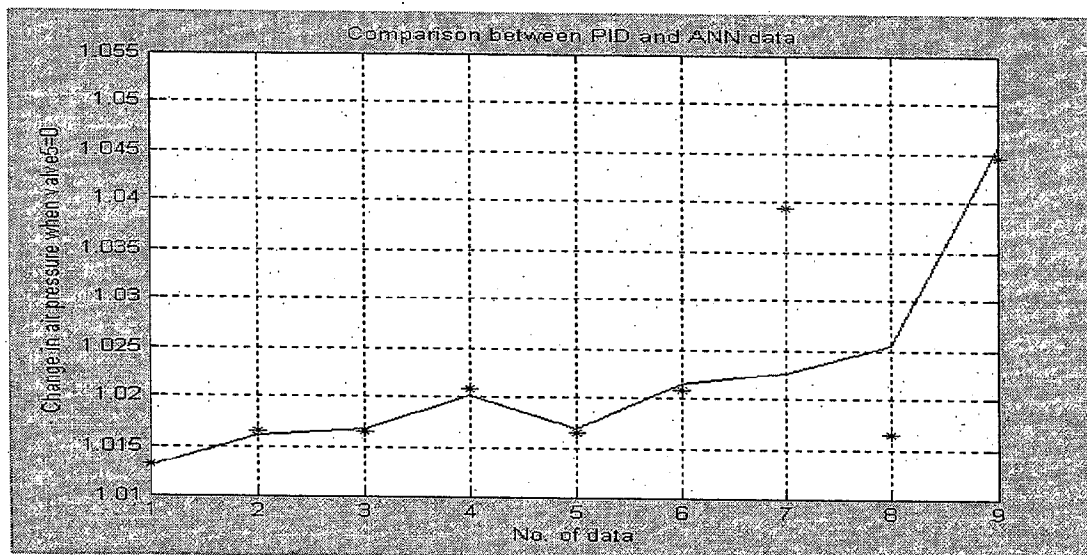
Fig.-6.69 Comparison between classical and ANN data for P_{head1}, when $\mu_5=0$
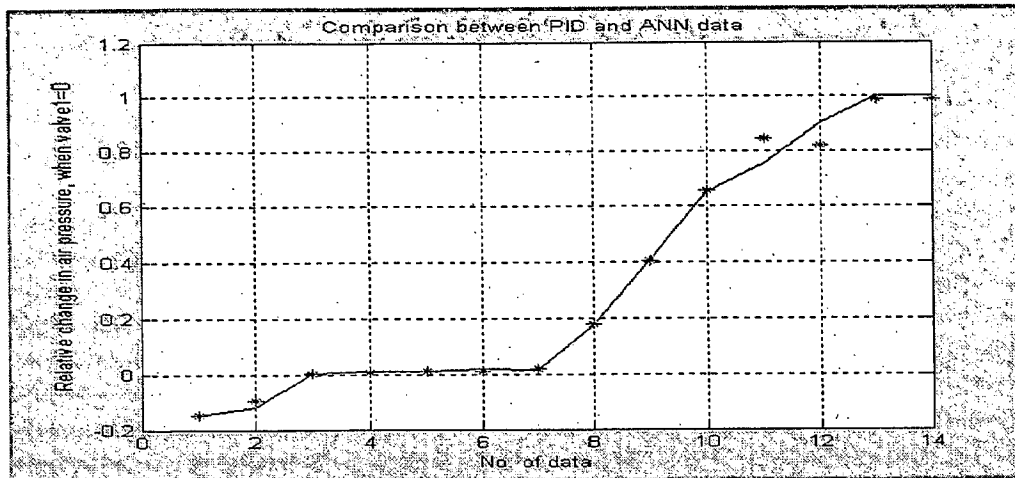
Fig.-6.70 Comparison between classical and ANN data for P_{head2}, when $\mu_1=0$

Table: 6.14a Comparison between PID controllers for L_{head}, P_{head}

Performances criteria	PID value for (L_{head})	PID value for(P_{head})
Max. overshoot	22.7%	6.8%
Delay time(s)	5.4	2.14
Min.	0.0000	0.0000
Max.	1.2270	1.0680
Mean	0.5174	0.8179
Median	0.4415	1.0000
Std.	0.5122	0.3852

Table: 6.14b Comparison between PID & ANN controller for L_{head}, P_{head}

Performances criteria	P_{head2}		L_{head1}	
	PID	ANN	PID	ANN
Min.	-0.1503	-0.1507	0.1280	-0.0621
Max.	1.0000	0.9900	2.9470	2.9380
Mean	0.2834	0.2841	2.1240	2.1000
Median	0.0209	0.0175	2.5800	2.5400
Std.	0.4088	0.4059	1.0050	1.0480
Range	1.1500	1.1410	2.7690	3.0000

Table:6.15 Performances of air pressure and level

L_{head1}	Min. error	-0.0551
	Max. error	0.0852
	Average error	0.0242
P_{head1}		
	Min. error	-0.0009
	Max. error	0.0165
	Average error	0.0038
P_{head2}		
	Min. error	-0.0912

213

	Max. error	0.082
	Average error	-0.0008

Case-6.11: Comparison of simulated data between PID and ANN controller for stock flow and stock level:

Using the eqns.[5.136 to 5.142], the closed loop system model of headbox having interactions between stock flow and stock level has been simulated with the help of MATLAB Simulink toolbox (fig.5.27, Chapter-5) . The simulation results for Y_1(stock flow) and Y_2(stock level) are shown in fig. 6.71. The responses of these two control variables are completely opposite. These profiles tally with those shown by Whalley et al.(166).These data have been used for training the neural network. During training the neural network, the network performance of the order of 9.998 e^{-005} and error goal 0.0001 is met at 115830 epochs (fig. 6.72).
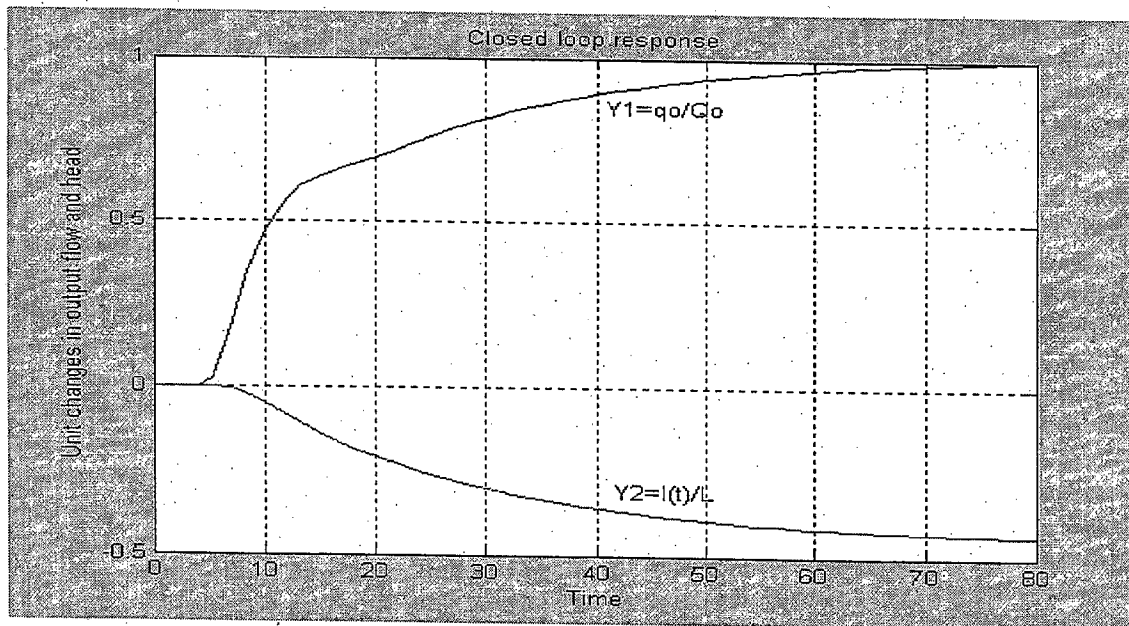
Fig. 6.71 Simulation results of headbox model
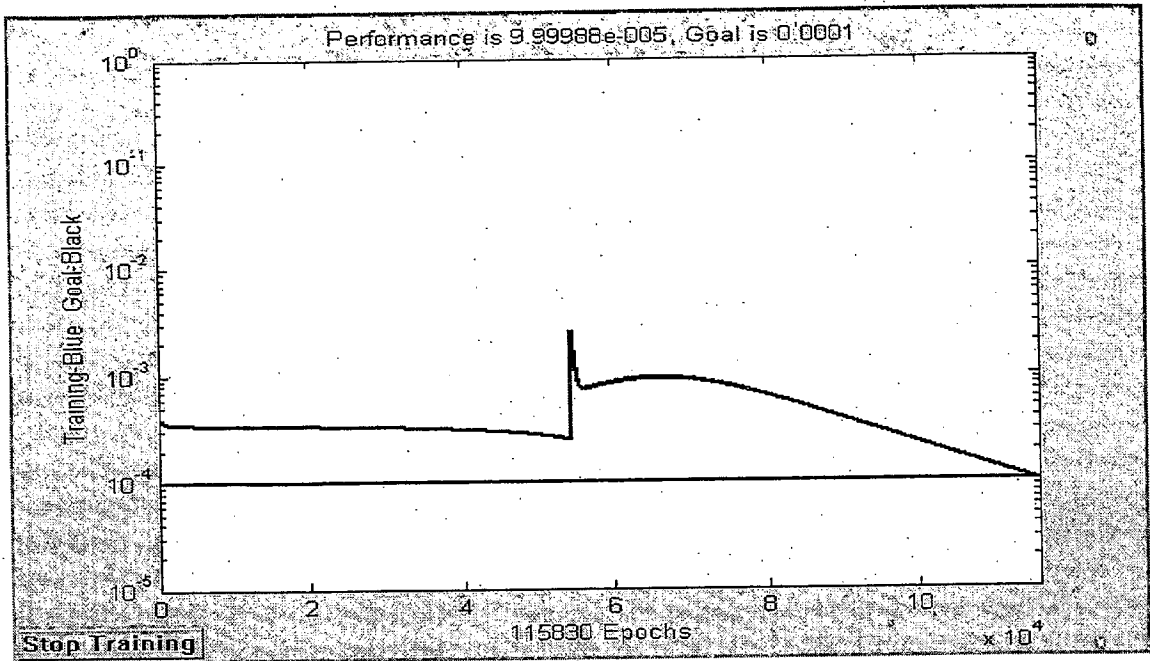
Fig 6.72 Artificial neural network training response

The ANN and model responses for stock flow and stock level are shown in figs.5.73 and 5.74 respectively. The responses for both the cases, namely for stock flow and stock level based on model and ANN closely resemble each other. However slight departure is noticed in the case of stock flow at the initial stages of data. Errors between models data and ANN data are shown in table 6.16.
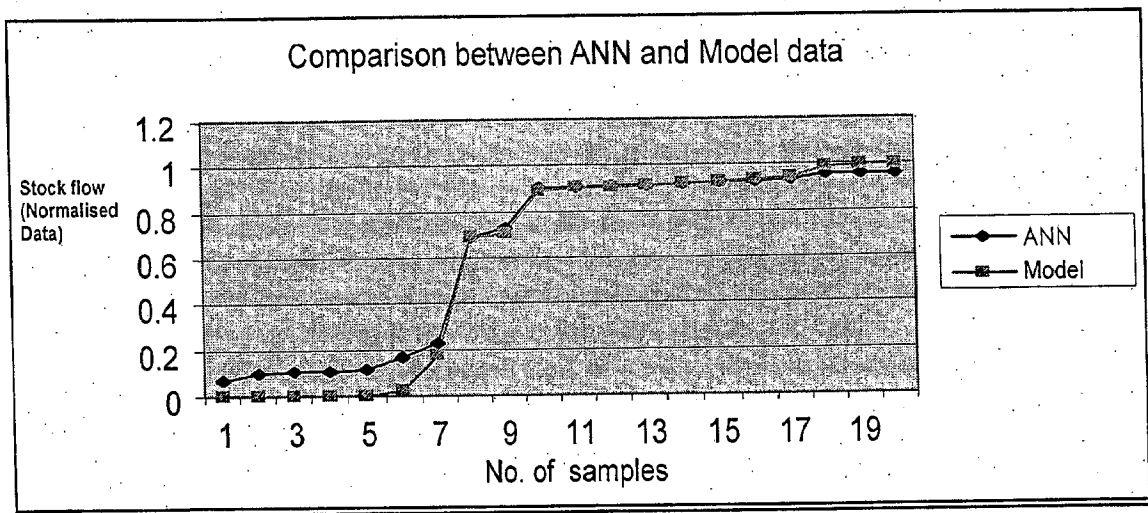
Fig. 6.73 Comparison between ANN and model data(stock flow)
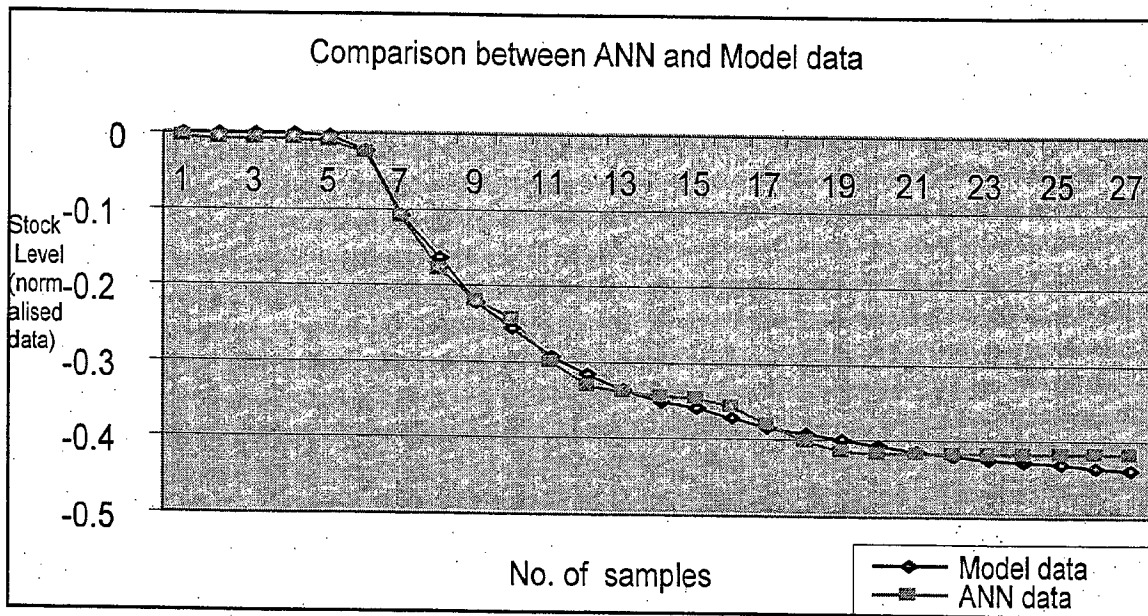
Fig. 6.74 Comparison between ANN and model data (stock level)

Table: 6.16 Errors between model data and ANN data

Stock flow	Min. error	-0.1477
	Max. error	0.038
	Average error	-0.020
Stock level	Min. error	-0.0168
	Max. error	0.020
	Average error	0.002

Case-6.12: Retention control:

The various models for retention control are explained in Chapter 5, Section.5.12.1. The eqn[5.146] represents the model of the paper machine containing the first pass retention as output , thick stock flow as input and two disturbances namely: consistency and fines content of the thick stock stream.

6.12.1: Effect of discrete and continuous signals for retention:

Using eqn.[5.146], and assuming retention and thick stock flow only, the simulation runs are carried out and response profile for both analog and digital system is drawn in fig 6.75b. This figure shows that the mean data of the order of 0.8897, median of the order of

0.8425, std deviation of 0.0975 for continuous signal and for discrete signal, the mean value of 0.8806, median of 0.8385, std deviation of 0.0997 are obtained.

6.12.2: Comparison between conventional and ANN controller data:

The closed loop control system for retention process is also simulated with MATLAB Simulink toolbox. The PID simulation response is shown in fig. 6.76. This simulated data obtained from PID has been used for designing the ANN controller. During training the neural network, the network performance in terms of parameter gradient descent term of the order of $9.82 \ e^{-005}$ and error goal 0.0001 are met at 101 epochs (fig. 6.77). The PID controller indicates delay time of the order of 1.25s, rise time of 25s and settling time of 26s. On the other hand, the ANN controller response removes overshoot of the order of 0.1, delay time of 0.5s, and settling time of 0.1s. The comparison between ANN and PID controller is made in fig.6.78 and data are shown in table 6.17.
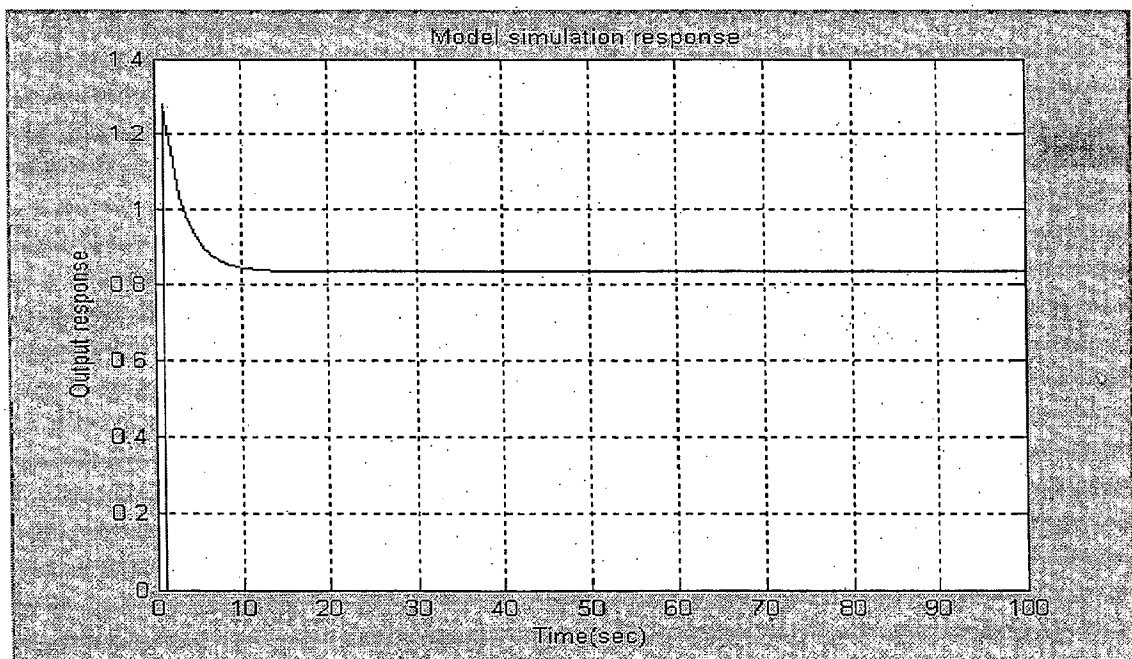
Fig. 6.75a Retention model simulation without controller
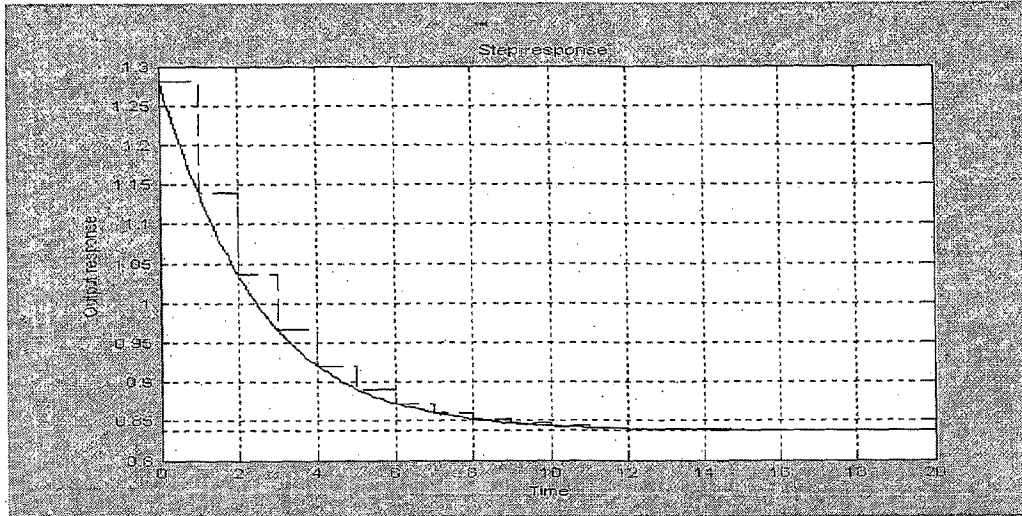
Fig. 6.75b Simulation results of continuous and discrete data
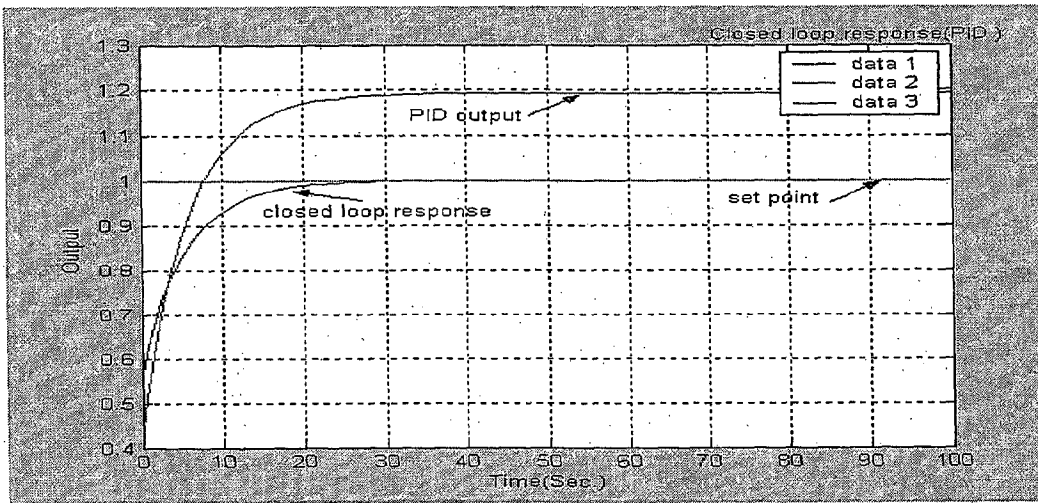
Fig. 6.76 Closed loop response (PID controller)
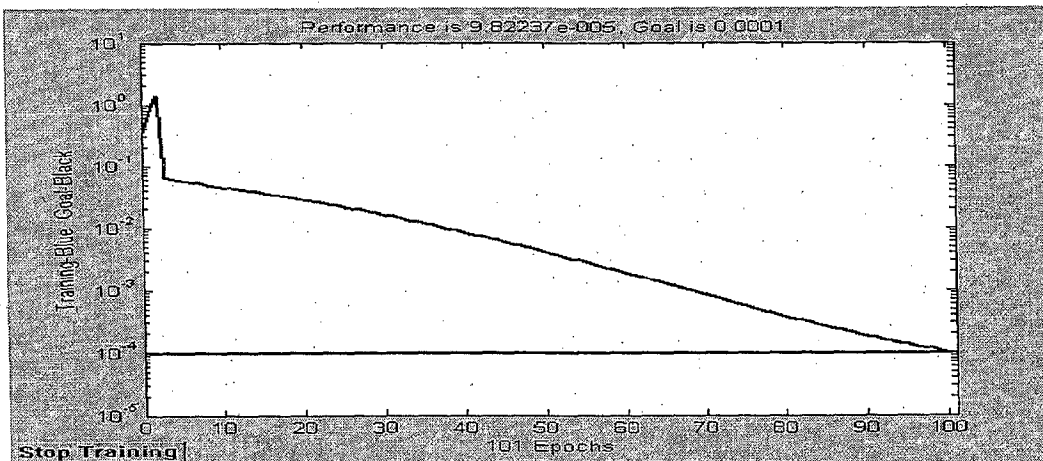
Fig. 6.77 Training response

218

Comparison between PID & ANN Controller
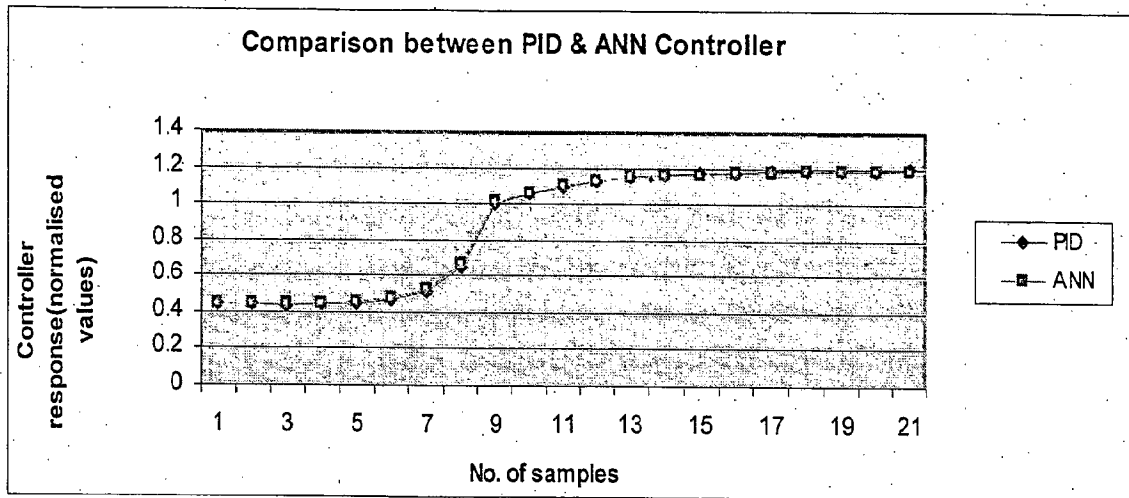
Fig. 6.78 Comparison between PID & ANN Controller

Table: 6.17 Errors between simulated data and ANN data

Performances criteria	PID controller	ANN controller
Min. value	0.438	0.439
Max. value	1.190	1.185
Mean	0.890	0.892
Median	1.096	1.099
Std.	0.335	0.332
Range	0.752	0.742
Min. error between PID and ANN	0.001	
Max. error between PID and ANN	0.005	

The ash content data from mill was analyzed statistically. These data have also been used for training the neural network. The comparison between mill data and ANN data are shown in fig. 6.80. Maximum error of the order of 7.32, min error of the order of 0.21 and average error of the order of 3.507 for Ash Content (ANN & Mill Data) were obtained. It reveals that the mill data values revolve around those of ANN data. The data tally very closely which further indicate that performances of PID and ANN are comparable.
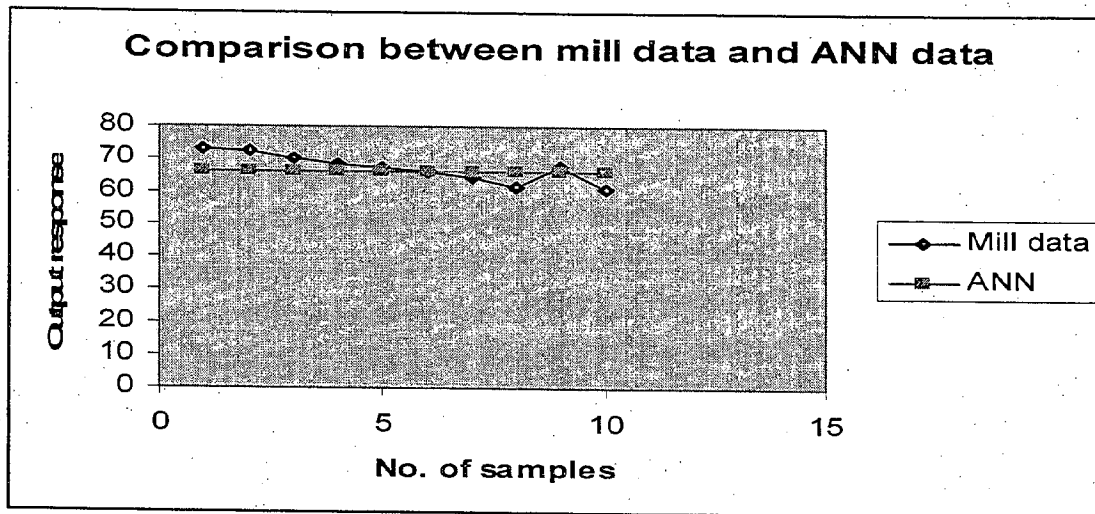
Fig. 6.80 comparison between Mill data(Ash content) and ANN data

The variation of retention and ash content as a function of time are shown in figs. 6.81a and 81b. Fig 6.81a indicates max., min. and average values for the fines content of the order of 52.1, 41.1 & 46.57 respectively. Max., min. and average values for the FPR were 73.2, 60.6 & 66.544 respectively. Max., min. and average values for the FPFR were 35.5, 24.16 & 29.623 respectively. The data is given in table 6.18
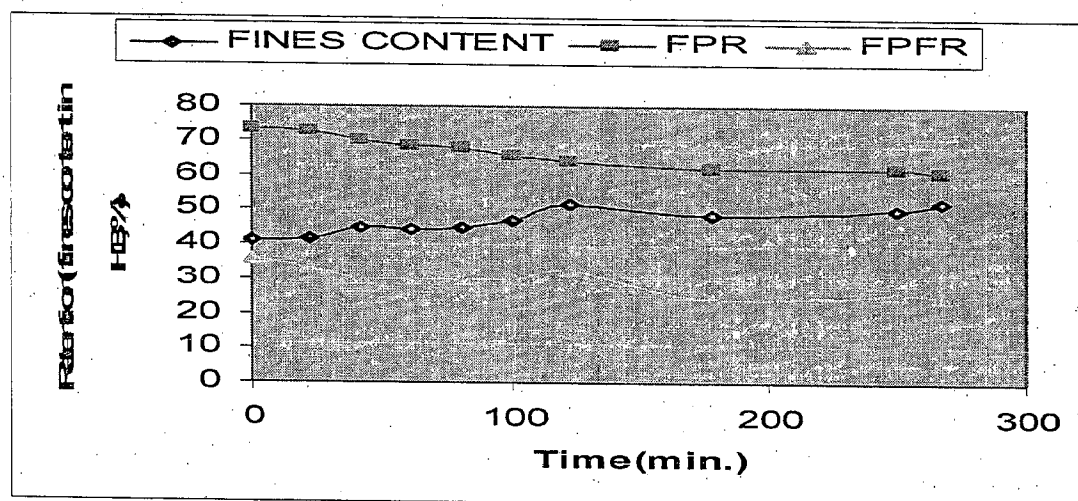
Fig. 6.81a Retention data

Table -6.18 Retention data(mill data)

FINES CONTENT	FPR	FPFR
41.10	73.20	35.50
41.67	72.50	33.30
45.00	70.00	30.00
44.16	68.33	29.67

220

45.00	67.50	30.00
46.67	65.80	30.00
51.67	64.17	32.50
48.33	61.67	24.16
50.00	61.67	25.80
52.10	60.60	25.30

Fig. 6.81b shows the comparison between mill data(retention) and neural network data. It indicates the minimum error, maximum error, and average error of the order of .007, 6.573, and 1.151 respectively. In this investigation, the neural network model works well. The data are given in table 6.19.
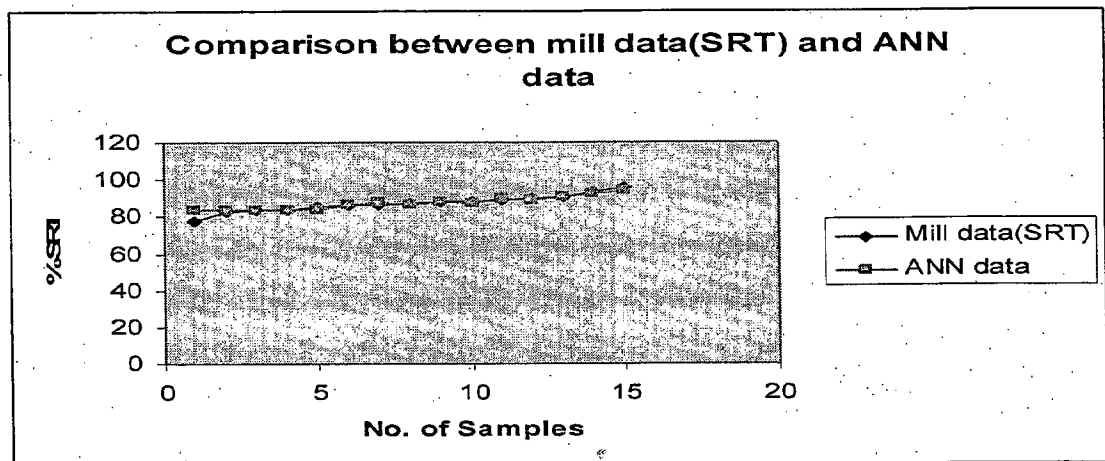
Fig.:6.81b Comparison between mill data and ANN(Solid retention)

Table:-6.19 SRT mill data and ANN data

No. of Samples	Mill data(SRT)	ANN Data
1	0.809	0.8787
2	0.872	0.88
3	0.877	0.878
4	0.88	0.876
5	0.89	0.876
6	0.90	0.90
7	0.91	0.92
8	0.91	0.90
9	0.92	0.92
10	0.92	0.914
11	0.93	0.937
12	0.94	0.935
13	0.95	0.948
14	0.98	0.964
15	1	0.98

The ANN simulsated data very closely tally with the actual data obtained from experiments in the mill. Thus it can be concluded that ANN based control can be used for retention and ash control in a paper mill.

6.13: Conclusions:

This chapter concludes that the ANN controller can be used for controlling SISO, TISO and MIMO systems. In simulating various SISO systems (such as consistency, total head, stock level, pH, stock temperature and basis weight) in paper mill approach flow and headbox, TISO system(thick stock consistency and white water consistency) and MIMO system(total head and stock flow, air pressure and stock level, stock flow and stock level, and retention) it is found that it takes less time to reach at steady state value,decreases the overshoot,improves delay time. When artificial neural network is trained successfully then ANN controller can give precise and immediate action to the final control element which corrects the plant variable. More detailed conclusions are given in Chapter 7, conclusions and recommendations.

CHAPTER-7
CONCLUSIONS AND RECOMMENDATIONS

In the present investigation design of artificial neural network based control system has been analyzed and designed for adaptation in Indian paper mill. To examine its feasibility, performances of conventional controllers (P/PI/PID) and ANN controllers are compared through simulations in MATLAB Simulink toolbox.The parameters studied were both SISO, and MIMO systems in the approach flow systems and headbox of paper machine wet end process. The SISO systems were thick stock consistency,stock flow,total lead,stock level,pH of stock,stock temperature and basis weight. The TISO(two input and single output) system was only consistency(consistency of thick stock and white water consistency). For MIMO system parameters involving interaction of parameters were:stock flow and stock level,air pressure and stock level for air cushion headbox, total head and stock flow, and retention of fibre fines for basis weight and consistency.

In order to achieve the above objective strategy of methodology of systematic investigation on the estimation and controlling of process parameters for both classical control(P/PIPID) and ANN with relevant algorithms has been developed in terms of both analog (continuous signal) and digital(discrete signal) techniques.

The detailed dynamic modeling of processes such as consistency(SISO and TISO), were made in analog systems whereas digital dynamics for basis weight with zero order hold is derived from first principles using unsteady state material and/or energy balance equations. However,modeling of process dynamics of pH(SISO),level(SISO) and temperature(SISO) were done iteratively through computer simulation using Simulink tool within a broad range of parameter available in literature. The simulation was, however, based on the analysis of closed loop control system including adjustment of selected

controllers. For air cushion headbox detailed derivation of the dynamics were derived especially as in most of the Indian paper mills(medium to large capacity) are using this type of headbox.

Other analog models for SISO systems like total head(SISO),basis weight(SISO), and all MIMO systems as indicated above were used from published information. All models either open loop or negative feedeback closed loop were developed in this study and transformed in to digital models including the process models.

For consistency control only for SISO system both Lambda and Ziegler Nichols (Z-N) tuning methodologies with Bode stability criterion have been used to just examine the effect of tuning on responses. For other cases, SISO, TISO, MIMO (both analog and digital) computer simulation (MATLAB Simulation techniques with SIMULINK tool) were employed for tuning.

For ANN solutions, adaptive linear neural network (ADALINE), perceptron neural network(PNN), back propagation neural network(BPNN), adaptive resonance theory(ART1) and augmented back propagation network(ABPN) were used.Two ANN control architectures used, for training of neural controllers were :supervised control, and direct inverse control.

All single loop control architectures(SISO and MIMO) have been converted to neural network based control system using different types of activation functions with sigmoid/ log sigmoid and linear equations.For the case of SISO systems an ANN control system (BPNN) along with the necessary algorithm has also been designed. All MIMO systems however all the above mentioned ANN methodology were used. The network was trained with PI/PID simulated data in all the cases except stock flow, basis weight and retention in which cases experimental/ industrial data were used for training.

For simulation of MIMO system considered in this present investigation both relative gain array(RGA) and decoupling techniques were used. RGA was employed for estimating the degrees of interaction and pairing of controlled and manipulated variables between different sets of control loops whereas decoupling technique was used for adjusting the interaction. The relative gain between 0 to 1 are only considered for analysis.

Data were computed from various models for both SISO and MIMO systems and for continuous and digital signals using the classical controller and neural network based control with the help of MATLAB SIMULINK toolbox and the algorithm developed for the purpose.

From the plethora of data from MATLAB Simulation of the process parameters, some dynamic characteristics have been drawn in various graphs with response as a function of time for all the above mentioned parameters when unit step input signal is applied as a forcing function and then performances are evaluated.While for consistency control, the dynamic responses using both PI & PID are studied and compared with the performances of ANN based controller, the cases of total head, stock level and pH only PI and ANN, for temperature and basis weight only PID and ANN were employed, analyzed and compared. From the detailed analysis the following noteworthy conclusions can be made:

- The comparison of dynamic responses of PI, PID and ANN based controller with unit step input signals for headbox consistency control indicates that ANN controller removes the overshoot and improves the settling time while the settling time of PI controller is found to be larger. The addition of derivative action attempts to reduce sluggishness of the PI control.

- Higher values of λ time of the order of 15s or 16s would be the best tuning parameter for consistency controller. Comparing the performances between

lambda and Z-N tuning method,the later is found to be slightly better. This should be unlikely. The dynamics also displays mostly overdamped characteristics.On analysis of responses the performance for continuous signal is found to be better compared to digital signal. These aspects need further investigation.

- In case of neural network controller design, the selection of optimum number of neurons in the hidden layer plays an important role. The neural network control reduces the error and gives satisfactory results between 18 to 20 neurons in the hidden layer. One can use the different number of neurons in the hidden layer (16 to 24 neurons) and different values of momentum factor. The learning rate 0.9 and momentum factor 0.8 can be chosen as the most acceptable values.

- For flow control, J/W ratio profile as a function of speed indicates that ANN controller gives good prediction when simulated with the data obtained from industry or from theoretical models. It is evident that above the speed of 450 m/min the values obtained from ANN simulated results and the data obtained from industry closely tally with each other. However there are noticeable deviations in the range of values between 300.3 m/min to 450 m/min. This also needs further study.

- For total head, SISO system ANN controller indicates the overshoot(less than 5.6%) while PI controller indicates the overshoot approximately 28.1% which is much greater than 5.6%. ANN controller also improves the delay time by 0.8 s.

- For headbox level control analysis, it is clear that ANN controller decreases the overshoot. The delay time and settling time for ANN controller are 2.1s and 10s respectively while PID controller presents the delay time and settling time of the

order of 3s and 12s respectively, which are greater than ANN controller time. Statistical data amply clarifies that the ANN controller can give quick response.

- In case of pH controller design and analysis, it is found that the performances of both the controllers, namely conventional as well as ANN are the same. Therefore any one can be used for pH control.

- In case of temperature control, the four controllers namely PID, MLP, DLFANN, and MFLANN have been tested using simulation tests for analyzing their ability to track varying set point, reject or recover from disturbances and perform under variable delay or dead times. MLP and DLFANN controllers give comparable values. Therefore either design can be used.

- Comparison between PID, ANN and Mill data of basis weight shows that the error is minimized with the help of ANN controller. The error goal (0.0001), mean square error MSE (9.99997e-005/0.0001), and gradient (3.24514e-005/1e-010) meet at 111164 iterations. Thus ANN controller removed overshoot and had better performance than conventional (PI) controller.

- From the analysis of responses of digital basis weight control and on comparison of three ANN methodologies such as BPNN, LM and the gradient descent technique, the latter is found to be best suitable.

- For MIMO (TISO) systems, on comparing it is found that three types of ANN taxonomy namely, perceptron, back propagation and adaptive resonance theory(ART). The minimum error is found of the order of 0.0002 during training in case of using back propagation methodology. For SISO system using perceptron neural network. The minimum error was found of the order of 0.10 whereas the same for back propagation was 0.05. In case of BPNN also, the data is closely

tallied with actual data. Therefore, BPNN is the best ANN for designing control system with sigmoid function for head box control of paper mill compared to other taxonomies.

- In case of air pressure (P_{head}) and level (L_{head}) data analysis, when relative change in opening of inlet valve c_1, $\mu_1=0$, the pressure has been increased but level of the headbox is decreased. When relative change in opening of inlet valve c_5, $\mu_5=0$, the pressure has been decreased but level of the headbox is increased. The maximum number of ANN controller data tallied with the simulated data with minimum delay time. ANN controller response reached immediately at steady state.

- ANN controller error goal performance is met at 115830 epochs. In case of ANN controller, the delay time for stock flow response is found to be less than PID controller response time. All model data and ANN data are closely tallied with each other. ANN controller error goal performance is met at 101 epochs. All model data and ANN data are closely tallied with each other.

- ANN controller can be used for both SISO and MIMO systems. It takes less time to reach at steady state value. When artificial neural network is trained successfully then ANN controller can give precise and immediate action to the final control element which corrects the plant variable.

- The neural network models work well for nonlinear systems where the network provides clues as to underlying physical phenomena, especially where data is the only method of defining the phenomena.

- The ANN controller is robust in the sense that the controller is independent of a prior knowledge of delay time, and process dynamics. Generally MIMO systems are complex which can be solved by ANN which are trained on data only. There is

minimum theory required and there are no software bottlenecks.

- More detailed investigation are required for MIMO system when there are interaction between more than two input and more than two output variables. In headbox these types of interaction exemplify total head, stock flow and wire speed.

- Robust design,resiliency and sensitivity analysis with suitable MIMO tuning methodology should be attempted.

- All the parameters for control in headbox should be analysed using z transforms for digital control system and suitable method for stability criterion for discrete data system must be used.

- Most of the problems in wet end paper machine are either feed forward type or involves multiloop control strategy. Multiloop systems like feed forward- feedback, cascade, ratio, split range etc. must be analyzed.

- Many ANN architectures such as RBF, ART2 should be used for comparison purposes.

- Other Neuro-Fuzzy, Neuro-GA, Neuro-Fuzzy-GA based control system may be attempted.

- Other control system based on simulated annealing can also be attempted.

- The ANN models can also be applied to examine the effect of couch roll vacuum, pressure applied in the press, steam temperature in the drier, and moisture content of paper.

NOMENCLATURES

Chapter-3

D_a=Diameter of pipe

D_b=Diameter of throat of meter

v_a=Average upstream velocity

v_b=Average down stream velocity

P_a, P_b=Upstream pressure, down stream pressure

α=Kinetic energy correction factor

Z_a= Elevation from datum line

η= Efficiency of pump

W_p=Work done by pump

h_f=Friction head(fluid)

g=Acceleration of gravity

v= Jet velocity(also called mean spouting velocity)

g =Acceleration of gravity

H=Head of stock behind the slice

K= Constant

C_V= The coefficient of discharge

A_v=The cross-sectional area at the vena contracta

A_S=The area of slice opening

C_c =The coefficient of contraction

Q= Total flow through the head-box(making allowance for any header bypass, bleed flows, etc.)

b=Slice opening

w=Slice width or opening

V= Actual speed of stock from the head-box

ω =Width of stock stream flowing on the wire

C_q= The coefficient of volume discharge

V_s=Average velocity under the slice lip

C_c=Contraction coefficient

K_1, K_2=Unit conversion constants

S_s= The loss of dry fiber on machine

C= The consistency of stock supplied on the wire(depends on the quality of paper produced)

ms= The mass of over dry fibre

S_k = The final dryness of paper

q=Grammage

V_n= The speed of paper at the pope reel

b_n=The width of paper web

S=Loss of stock on the wire

δ_s=Cross sectional shrinkage in the dryer

ξ= Drag coefficient of wire in relation to stock stream

β=Lag coefficient of wire in relation to couch roll

w_n= Width of paper web on the pope reel and width of stock stream flowing on the wire

w_o= Trimmed width of paper

Z= Trim at the cross cutter

r =Wet end trimming

d = The thickness of the jet
q = Head-box flow rate
C_o = Orifice coefficient

Chapter:4

T = The training samples.
ε = The normalized error between the network output and the actual output
I_1, I_i, I_l = Input to input layer
a_1, a_i, a_l = Output from input layer
b_1, b_j, b_m = Output from hidden layer
C_1, C_k, C_n = Outputs from output layer
η = Learning rate,
α = Momentum coefficient;
V = Weight between i/p and hidden layer.
W = Weight between hidden layer and o/p layer
T_a, T_b, T_c = Targets
p = Number of training patterns
E = Total mean square error,.
δ = Gradient descent term
A_i = The output of ith logarithmic neuron in the input layer.
B_i = The output of ith exponent neuron in the input layer
C_j = The output of jth exponent neuron in the output layer
D_j = The output of jth logarithmic neuron in the output layer
X = Input vector
μ_j = Center of a region called a receptive field
σ_j = Width of the receptive field
$G_j(x)$ = Output of the jth neuron

CHAPTER:5

m_i = Inlet mass flow rate of thick stock
m_d = Dilution water flow rate
m_o = Thin stock flow rate
c_{yi} = Consistency of thick stock
c_{yd} = Consistency of dilution water
c_{yo} = Consistency of thin stock
V = Volume of head-box tank
ρ = Density of thin stock
q_i = Thick stock volumetric flow rate, m_i/ρ
q_o = Thin stock volumetric flow rate, m_o/ρ
q_d = Dilution water volumetric floe rate m_d/ρ,
$G_c(s)$ = Transfer function for a PID controller,
$G_p(s)$ = Transfer function for consistency process
K_c = Controller
K_p = Process gain,
ζ_I = Integral time gain
ζ_d = Derivative time gain
θ_d = Time delay in the process.
ζ = Process time constant

232

V=Total volume of the solution in the flow box;

C_i= Total concentration of the ith component in the effluent stream;

F=Total flow rate of the feed(thick stock, chemicals and white water);

u= Flow rate of the titration stream (acid or base);

C_{fi}=Total concentration of titration stream(acid or base).

u= Flow rate(input)

x=Concentration(output)

W= Mass of stock in the system

w_{in}=Mass of inflowing stock

w_{out}=Mass of out flowing stock

V= The volume of the stock

h_c=Heat capacity

F_i, F = Liquid inflow and outflow rates respectively

u_1=fan pump control input

u_2 = air valve control input

Y_1=total head output

Y_2= stock level

m_{fb}=Amount of stock present in the flow box

m_{in}=Amount of incoming stock

m_{out}=Amount of outgoing stock

m_{ol}=Stock flow through the overflow line

t=Time

A_{fb}=Average cross-section area of flow box

h_1=hydrostatic pressure

ρ_s=Density of suspension

ρ_a=Density of air

u_1=Relative deviation of level

P=Air pressure

H=Height of stock to the axis of valve

μ_1=Relative change in the opening of inlet valve

A_c=Cross section of valve opening

C_{d1}=Discharge coefficient

C_1=Inlet valve

P_{11}=Pressure before entering valveC_1

P_{12}=Pressure after valve C_1

P'=Relative change in pressure of air

C_2=Slice opening

A_{lip}=Cross-sectional area of lip opening

C_{d2}=Discharge coefficient

C_{d3}=Discharge coefficient

b=Width of air flow

h_3=Height of overflow

T_{fbl}=Time constt. For flow box for level of stock in the box

w_1, w_2, w_3 =load factors

$K_{1v1}, K_{2v1}, K_{1p}, K_{2p}, K_{1v2}, K_{3p}$=Constant factors depending on the sped of the machine

m_{ch}= Amount of stock present in the channel

m_{ou}, m_{oo}= Corresponding flow of stock in channel

i of stock

A_{ch}= Average area of cross-sectional of the channel

h_{ch}= Height of stock level in channel

V_{ch}=Volume of channel

A_{op}=Cross-sectional area of outlet pipe

T_{fblo}=Time constt. For flow box stock level in the overflow pipe

W_{21}=Factor depending on u_1

m_{air}= Amount of air present above the stock level in the flow box

m_{sup},m_{rem}=Amount of air supplied and removed from the flow box

V_3=volume of air above stock level in the flow box

A_{c5},A_{c6}=Cross-sectional area of overflow valves C_5, C_6

K_5,K_6=loss factors

P_{51},P_{52}=Inlet & Outlet pressure of valve C_5

P_{61},P_{62}=Inlet & Outlet pressure of valve C_6

T_{air}=Time constt. Of flow box for air cushion

W_4=Load factor

T_{tv1},T_{tv2}=Time constt. For turbulence in the channel depending on u_1, u_2

$y(k)$ =The retention value at sample value at sample number k,

K_{ret} =Machine-dependent constant

C_{WW} = Consistency white water

C_{HB} = Consistency in head box

γ= Retention

F_{sf}=Thick stock flow

C_{ts}=Thick stock consistency

Y_F=Thick stock fines content

REFERENCES:

(1) Aidun Cyrus K. and Agnes E.K, Hydrodynamics of the forming section: the origin of non-uniform fiber orientation, TAPPI Journal, vol.78, no. 11, pp.97-106, Nov. 1995.

(2) Akesson Johan, Parameter optimization of a paper machine model, Deptt. of automatic control, Lund university, box118,22100,Lund.

(3) Andre M. Shaw, Francis J. Doyle III and Schwaber James S., A dynamic neural network approach to nonlinear process modeling, Journal of computer chem. Engg. , vol.21, no. 4, pp 371-385, 1997.

(4) Appel D.W. and Yu Y.S., Free-streamline analysis of flow from nozzles, flow through side inlets and flow past corners, Studies in engineering mechanics, no. 17, Centre for research in engineering science, University of Kansas, Lawrence, KS.

(5) Banerjee Sujit, and Grimes D.B., Improving centrifugal cleaner efficiency through temperature mismatching, Tappi Journal, 84(1), pp.97, 2001.

(6) Banerjee, Sujit, Etzler, F, An algorithm for estimating contact angle, Langmuir,11, 4141(1995).

(7) Banerjee, S., Pendyala K., Buchanan M., Yang R., Abu-Daabes M., and Otwell L.P.E, Process based control HAPs emissions from drying wood flakes, Environ., Sci. Technol,40,2438(2006).

(8) Barry Lennox, Montague Gary A., Andy M. Frith, Chris Gent, and Vic Bevan, Industrial application of neural networks-an investigation, Journal of process control,no. 11,pp.497-507, 2001.

(9) Baughman D.R., and Liu Y.A., Neural networks in bio-processing and chemical engineering, Academic press limited, oval road, London, pp 40-47, 1995.

(10) Beecher A.E., Dynamic Modeling technique in the paper industry, TAPPI Journal, 46, pp 117-120, 1963.

(11) Belderud Jonas et al, Parameters affecting disturbance propagation through the wet end of a paper machine, Appita Journal,vol.58,no.1, pp.40-44, Jan. 2005.

(12) Benard Widrow and Micheal A. Lehr, 30 years of Adaptive neural network: perceptron, madaline, and back propagation, Proceedings of the IEEE, vol.78, no.9, pp.1415-1442, Sept. 1990.

(13) Berrada Mouhsine, A state model for the drying paper in the paper product industry, IEEE transaction on industrial electronics, vol.44, no.4, Aug.1997.

(14) Bhartiya, S., Fundamental thermal hydraulic pulp digester model with grade transition, AICHE Journal, 49(2), pp.411-425, 2003.

(15) Bhat N. and McAvoy T. J, Modeling chemical process systems via neural computations, IEEE control system magazine,pp.24-90,1990.

(16) Bihani B.L., Jaspal N.S., and Bhargava R.L, Cooking of North Kanara hardwoods, IPPTA Souvnir, pp.313-318, April 1964.

(17) Bihani B.L., The bleaching of pine pulp, vol.-5,no.1,T27-T32, March 1968.

(18) Bihani B.L. et al., Towards higher chemical recovery efficiency, IPPTA Journal, vol. x, no.4,pp.227-230, Oct 1973.

(19) Blaesi John and bruce Jensen, Can Neural networks complete with process calculations? , INTECH Journal, vol.30, no.1-12,pp.34-37,1992.

(20) Bristol, E.H., On a new measure of interactions for multivariable process control, IEEE Trans. Auto. Control, AC-11, pp.133,1966.

(21) Britt, K.W, Hand book of pulp and paper technology, second ed., Van Nostrand Reinhold company, pp.464,1970.

(22) Chao,H.H et al., Headbox control, ibid ,pp.458.

(23) Charos G.N, Arkun Y., and Taylor, R.A., Model predictive control of an industrial lime kiln, TAPPI Journal, pp.203-211,Feb.,1991.

(24) Chen S., and Billings S.A, Nonlinear system identification using neural networks, International Journal of Control, 51 (6), pp.1191-1214, 1990.

(25) Coughanowr D.R, Process systems analysis and control, McGraw-Hill, Inc., IInd edition 1991.

(26) Daniel B. Smith, and Edward Louis L., Dynamic mathematical model of a rotary lime kiln, TAPPI proceedings, Engg. Conference, pp.447-455,1991.

(27) David wood, Head box control developments, Paper Technology, pp34-38, June 1995.

(28)   Dayal B.S., Macgregor J.F.,Taylor P.A., Kildaw R., and Marcikic S., Application of feed-forward neural networks and partial least squares regression for modeling kappa number in a continuous kamyr digester, Pulp & paper Canada,vol.95,no.6,pp.26-32, 1994.

(29)   De Vries, W.R and Wu S.M, Evaluation of process control effectiveness & diagnosis of variation in paper basis weight via multivariate time series analysis, IEEE AC 23, pp.702-708,1978.

(30)   Demuth H. and Beale M., Neural networks toolbox users guide, mathworks,1997.

(31)   Desmond Yan and Mehrdad Saif, Neural network based controllers for non-linear systems,CH3243-3,IEEE,pp.331-336, 1993.

(32)   Di Massimo. C.,Willis.M.J., Montague. G.A., Kambhampati C., Hofland ,A.G, and Tham M.T., On the applicability of neural networks in chemical process control presented at AIChE annual meeting,Chikago,1990.

(33)   Dion, J.L, Garceau J.J. and Richard Baribeault, Preliminary test results of a new acousto-optical process for on-line characterization of fibre size, TAPPI Journal vol. 70,no.4,April 1987.

(34)   Dion, J.L, Garceau, J.J, and Morisette,J.C., Acouto- Optical evaluation of fiber size in wood pulp,Proceedings of SPIE, 1986 Quebec Int .Symp. on optical and Optoelectronics Appl. Sciences and Eng., 6 June,1986.

(35)   Dion, J.L, Garceau, J.J, and Morisette,J.C., Nouveau procede acousto-optique de caracterisation des pates, Pulp and Paper Canada vol 88, no.3 ,T-64-T-67,1987.

(36)   Dion, J.L, Pierre, Brodeur, Garceau, J.J, and Chen R., Charaterisation Acouto Optique des fibres: nouveaux resultants, Proceedings of Congress ACPPP-CPP EXFOR 88, Montreal, Janvier, pp-4-8, 1988.

(37)   Dumdie, D.P, A systems approach to consistency control & dry stock blend, TAPP J, 71(7):135,1988.

(38)   Eaton H.A.C and Oliver T.L., Learning coefficient dependence on training set size Neural networks, Electrical engg. Update , vol.5, pp35-39., May-June 2006.

(39)   Edward Peter J., Murray Alan F., The application of neural networks to the papermaking industry, IEEE transactions on neural networks, vol 10, no.6 pp.1456-1464, Nov 1999.

(40) Francis J. Doule III, Computational issues in the application of model based control to the pulp and papers industry, Fundamental advances in the pulp and paper industry, AICHE symposium series no. 322, vol.95, pp.165-172,1999.

(41) Francis J. Doule III , Reaction profile control of the continuous pulp digester, Chemical engg. science, 54, pp.2679-2688, 1999.

(42) Gandhi Pimal, Design of artificial neural network controller for speed control of DC motor , Electrical engg. update magzine, pp 35, May –June 2006.

(43) Garceau, J.J, Goel, K.N and Ayroud, A.M, Optimization of high yield kraft pulping variables to obtain maximum ring crush, TAPPI Journal, 57(6)137, 1974.

(44) Garceau, J.J, Goel, K.N and Ayroud, A.M, TAPPI Journal, 57(8),121, 1974.

(45) Ghosh A.K, Drysim, A combine audit and simulation tool to improve overall dry end efficiency ,Appita Journal, vol. 51,No.4,274-280,1998.

(46) Ghosh A.K, Optimization of paper machine dryer section, Paperex international technical conference, New Delhi, Dec.3-5,2005.

(47) Ghosh A.K, Rae C. and Youdan.J., Off-line analysis of properties of the paper web: a diagnostic tool to reduce variability, Appita Journal,vol. 54,No.5,413-419,2001.

(48) Ghosh A.K, Use of pilot refiner and screening system to improve stock quality, Appita Journal, vol.55,no.2, pp.112-117,2002.

(49) Goel Rajiv, Instrumentation and control for paper machines, IPPTA Journal, vol.14,no.4, pp.61-65,Oct-Dec. 2002.

(50) Gornik M., G. Novak and Govekar, Modeling coated paper properties: application of neural networks, International journal of system science, vol. 28, no.9, pp.865-870, 1997.

(51) Graupe D., Drauss D.J and Moore,J.B, Identification of auto regression moving average parameters of times series, IEEE Trans. Automatic Control, vol. AC-20, pp104-106, 1975.

(52) Grosdidier P., and Morari M., A computer-aided methodology for the design of decentralized controllers, Computer chem. engg, 11, pp.423,1987.

(53) Harriott Peter, Process control, Tata Mc-Graw Hill publishing company Ltd, New Delhi,1974,

(54) Haykin S., Neural network: A comprehensive foundation, Prentice Hall,1999.

(55) Heaven E. M. et al. Application of systems identification to paper machine model development and simulation, Pulp and paper Canada, 97:4, pp.49-53,1996.

(56) Hernandez E. and Arkun Y., Study of the control-relevant properties of backpropagation neural network models of nonlinear dynamical systems, Journal of Computers Chem. Engg., vol. 16, no. 4, pp.227-240,1992.

(57) Hertz J., Krogh A., and Palmer R.G, Introduction to the theory of neural computational, Addison Wesley, reading, mass,1991.

(58) Hong Helena Mu, Kakad Y.P, and Sherlock B.G, Application of artificial neural networks in the design of control systems, Deptt. Of Electrical and Computer engg., University of North Carolina at Charlotte,9201 University city Blvd, Charlotte, NC 28223,USA.

(59) Hong Wang, Ai Ping Wang and Stephen R Duncan, Advanced process control in paper and board making, Pira international publishers, 1997 Surrey, 1997.

(60) Hovd, M., and Skogested S., Sequential design of decentralized controllers, Automatica, 30,pp.1601,1994.

(61) Huang, S. and Huang Y., Bounds on the number of hidden neurons in multilayer perceptrons, IEEE trans. on neural networks, 2(1),pp. 47-55, 1991.

(62) Hunt K.J,and Sbarbaro D., Neural network for control systems-A survey, Automatica,28 (6), pp.1083-1112, 1992.

(63) Hykin S., A comprehensive fundamental, MacMillan college publishing co. Newyork,1994.

(64) Irwin G., Brown M., Hogg B., and Swidenbank E., Neural network modeling of a 200 MW boiler system, IEE Proc. on control theory application, vol.142,no.6 pp.529-535,Nov. 1995.

(65) Jagadeesan S. and Krishnagopalan G.A, Liquor concentration measurement fo causticizing control, APPITA Journal, vol.48, no.3, pp. 207-212, 1994.

(66) Johnson Ralph K, Principle of control as applied to paper machine wet en operation, Wet end operations short course, TAPPI press, Atlanta,pp.345 356,May4-8,1992.

(67) Johnson Ralph K., Principles of measurement as applied to paper machine we end operations, Wet End Operations short course, Tappi Press, Atlanta, pp.32 1992.

239

(68) Johnstan R.E., Non-interactive control of pressurized flow boxes in papermaking system, in F.Bolam(ED), Trans. symposium Brit paper and Board manufacture, Assn.Oxford, vol.2, pp. 509-512, 1970.

(69) Kapoor S.K., Sood Y.V., Panda P.C., Pant R., and Panda A, Improving the printing quality of indigenous newsprints, Proceedings of IPPTA Silver Jubilee International Seminar & workshop, Appropriate Technologies For Pulp & Paper Manufacture in Developing Countries, 1-26,1989.

(70) Kauko Leiviska, Paper making science and technology, Process control, Book 14, Finnish Paper Engineers, Association and TAPPI,1999.

(71) Kerekes R.J and Koller E.B., TAPPI, 64(1):95-6(1981);64(4):104,1981.

(72) Keswani, S.L, Indigenous capability for electronic process control in pulp and paper industry, IPPTA annual general meeting & international seminar, Hotel Hyatt regency, New Delhi, March 8th 1984.

(73) Khalid M, Omato S. and Yusof R., Temperature regulation with neural network and alternative control scheme, IEEE transactions on neural network, vol.6, no.3, pp.572-582, 1995.

(74) Khalid M, Omato S., A neural network controller for a temperature control, IEEE control system mag., vol.8, no. 1 pp2-13, 1992.

(75) Kikiewich Z., and Panday, R.S.D., Theory and design of paper machine, vol.-I, Tara book agency Varanasi,1983.

(76) Kooi Steven B.L.and Khashayer Khorasani, Control of the woodchip refiner using neural networks, TAPPI Journal, pp-156-162, June 1992.

(77) Kumar Prasanna V.S and Sudha Rani M., Paper machine process control optimization, IPPTA Journal, vol.-9,no.2, pp.1-8, June 1997.

(78) Laurie R.Ben and Lou Heavner, Neural networks in the process industries, INTECH Journal, vol.43, pp.50-53,Dec.1996.

(79) Lavigne J.R, Instrumentation applications for the pulp and paper industry, Miller freeman publication,1979.

(80) Lippmann R.P., An introduction to computing with neural nets, IEEE ASSP Magazine, vol.4, no.2, pp. 4-22,1987.

(81) Luyben W.L, Process modeling simulation, and control for chemical engineers, McGraw-Hill Publishing company, IInd edition 1990.

(82)   Luyben W.L., Simple method for tuning SISO controllers in multivariable systems, IEC Process Des. Dev., 25, pp.654,1986.

(83)   Mardon, J., A theoretical and experimental investigation into the stability & control of paper machine headboxes, Papier och tra 48(1):3; 48(5) 301,49(4a):189(1966/7).

(84)   McAvoy,T.J., Interaction Analysis, ISA, Research Triangle Park, NC, 1983.

(85)   Miller,W.T., Sutton R.S. and Werbos P.J. , Neural networks for Control, MIT press, Cambridge, MA., 1990.

(86)   Mirchandani, G. and Cao W., On hidden nodes for neural networks, IEEE Transactions on circuits and system, 36(5), pp.661-664, 1989.

(87)   Misra, N.D, Process control in an integrated pulp and paper mill, Kothari desk book series, The paper industry, H.C Kothari publications, Madras.

(88)   Moody, J.E, Hanson S.J., and Lippmann R.P (Eds.), Advances in neural information processing systems 4,SanMateo,CA Morgan Kaufmann publishers pp.555-562,1992.

(89)   Mukherjee S., Modeling of the Paper making machine, National system conference, pp.342-344,2003.

(90)   Nagrath I.J. and Gopal, Control systems engineering, New AGE International publishers, Fifth Edition,2007.

(91)   Nancy J. Sell P.E, Process control fundamentals for the pulp and paper industry, TAPPI process control textbook, Tappi Press, Atlanta,pp.428, 187,GA,1995.

(92)   Narendra K.S and Parthasarathy K., Identification and control of dynamical systems using neural networks, IEEE Transactions on neural networks, vol.1,pp 4-27,1990.

(93)   Nelson, D. , Optimizing paper machine dryer control-A case study, pulp & paper Canada,97:11,pp.43-49,1996.

(94)   Nenad Milosavljevic and Pertti Heikkila , Modeling a scrubber using feed-forward neural networks, Tappi Journal, vol.82,no.3, pp197-201, March 1999.

(95)   Nissinen A.I., Koivo H.N., and Huhtelin T.J., Headbox control using a multivariable PI controller in a distributed automation system, Pulp & paper Canada,pp.38-41 98:5(1997).

(96) Onabe,F., Measurement and control in paper chemistry in Paper chemistry, ed. Roberts,J.C., Chapman and Hall Press, London, 1991.

(97) Orccotoma Jose Antonio, Jean Paris, and Michel Perrier, Paper machine controllability: effect of disturbances on basis weight and first-pass retention, Journal of process control, 11,pp 401-408,2001.

(98) Ozgur Kisi and Erdal Uncuoglu, Comparison of three back-propagation training algorithm for two case studies, Indian Journal of Engineering and material sciences, vol. 12, pp 434-442, Oct 2005.

(99) Panda Abinash, Prabhu S.G. and Garg O.P., Energy conservation in Paper Industry- IPPTA, vol.23(4), pp 101,Dec. 1986.

(100) Panda Abinash, Theoretical approaches to improvement of pulp yield by sulphate pulping, IPPTA Journal, vol.6 , no.2 , pp.41-47, April 1969.

(101) Paulapuro H.,P et al., Identification of the pilot paper machine for adaptive retention control, Proc. control system,92, pp279-281, Whistler,1992.

(102) Paulonis, A.M, Krishnagopalan, A., A TAPPI Journal, 71(11):87,1983.

(103) Paulonis, A.M, Krishnagopalan, A., A TAPPI Journal, 73(6):205,1990.

(104) Paulonis, A.M, Krishnagopalan, A., Application of cooking liquor analysis to on-line estimation of pulp yield and Kappa no. in a kraft batch digester, Pulping conference, pp.555-560, 1988.

(105) Pearson. John. H., Automatic headbox operation, vol.46,no.10, pp192,1963.

(106) Pfeifer, R.J. and Wilhelm R.G., Comparing on-line gauging statistics from different paper machine, Proc. TAPPI Process and product quality conf., pp51-60,1992.

(107) Pollard J.F., Broussard M.R, Garrison D.B. and San K.Y, Process identification using neural networks, Computers chem. engg., vol.16,no.4, pp.253-270,1992.

(108) Potusek F, Washing of Pulp Collect. Czech. Chem. Commun., vol.62,1997,626-644.

(109) Potusek F. and Milichovsky M., Displacement washing of kraft pulp, Zbornic 21,conference slovenskey spolocnosti chemickeho inzinieerstva, vyhne(slovakia),23.

(110) Potusek F, Papir a celuloza 49,9,1994.

(111) Psaltis D., Sideris A. and Yamamura A., A multilayered neural network controller, IEEE control system mag., pp.17-21,April 1988.

242

(112) Puri Yogesh, and Keswani S. L, Indigenous capability for electronic process control in pulp and Paper industry. IPPTA, Annual general meeting & international seminar, Hotel Hyatt regency, New Delhi-110017, March 8-9, 1984.

(113) Qian Yu, Patrick Tessier, and Dumont G.A., Modeling a wood-chip refiner using artificial neural networks, Tappi Journal, vol.78,no.6 ,pp167-174, June 1995.

(114) Ramani Vengimalla, Ramarao,B.V, and Chase,G.G, Modeling of filler retention in compressible fibrous media, Journal of separation and purification technology,ELSEVIER,pp.153-161,1999.

(115) Ramani Vengimalla, and Ramarao,B.V, Filler retention in preformed fibrous media, TAPPI engg. conference,1995.

(116) Rao A.R.K. et al., Economic utilization of alum in sizing, IPPTA Journal, vol.xiii, no.-1,pp.72,1976.

(117) Rao A.R.K. et al., Improved pulping of mixed hardwoods from central India,xvi,(4),pp.153,1979.

(118) Rao A.R.K. et al., Higher yield with polysulphide pulping, IPPTA Souvenir,pp.35,1977.

(119) Rao, N.J.,.Ray A.K, and Bansal M.C., Role of Instrumentation in efficient operation of paper plants part-1 for small paper mills, IPPTA, vol.21, No.1, ,pp 56-62, March 1984.

(120) Ray Harmon W and Ogunnaike B.A., Process dynamics modeling and control, Oxford University Press, New York, 1994 pp-982.

(121) Rigopoulos A., Y. Arkun and Kayihan F., Control relevant disturbance modeling of paper machine full profile properties using adaptive PCA, Pulp and Paper Canada Journal, vol-III, 98:11,pp.42-45, 1997.

(122) Rooke Paul E. and Hong Wang, Applying combined neural network and physical modeling to the retention process in papermaking, Appita Journal., vol.55,no.4, pp281-186, July 2002.

(123) Rosenbrock H.H, Computer Aided control system design, Academic press, London, 1974.

(124) Rudd John B. P.E, Using a neural network controller for advanced control applications, TAPPI Proc., Engineering conference, pp 101-113, 1991.

(125) Rudd John B. P.E, Using a neural network system for advanced control, TAPPI Journal, pp-153-159, Oct. 1991.

(126) Rumelhart,D.E, Hilton,G.E., and Williams, R.J, Learning internal representations by error propagation, Parallel distributed processing. vol.1. Cambridge: MIT press, pp.318-62, 1986.

(127) Sankaranyranan P.E., Microprocessor based basis weight scanning instrumentation, Journal of instrumentation society India, vol.17(4), pp.319-331,1987.

(128) Sankaranyranan P.E., Modeling a paper machine for basis weight and moisture control, Proceedings of IPPTA Silver Jubilee International Seminar & workshop, Appropriate Technologies For Pulp & Paper Manufacture in Developing Countries, 1-19,1989.

(129) Sankaranyranan P.E. and Prasad G., Model of a paper making machine for profile control, Kothari desk book series, H.C. Kothari Group Publication, Madras,pp. 219-223.

(130) Saucedo, V.M and Krishnagopalan G.A, Kinetics and state space modeling of modified kraft pulping, fundamental advances in the pulp & paper industry, AICHE symposium series no. 322, vol.95, pp.7-13,1999.

(131) Savkovic-Stevanovic J., Neural networks for process analysis and optimization: modeling an applications, Computer chem. engg., vol. 18, no. 11/12, pp 1149-1155, 1994.

(132) Scharcanski Jacob and Dodson C.T.J, Neural network model for paper formin process, IEEE transaction on industry application,vol.33,no.3,pp.826-40,May/Jun 1997.

(133) Scott ,Gary M.,and Ray, W. Harmon, Neural network process models based o linear model structures, Neural computation, 6(4), pp.718-738,1994.

(134) Scott ,Gary M.,and Ray, W.Harmon, Creating efficient non-linear neural networ process models that allow model interpretation, Journal of process control,3(3),pp 163-178,1993.

(135) Scott ,Gary M.,and Ray, W.Harmon, Experiences with model-based controllers based on neural network process models, Journal of process control, 3(3), pp. 179-196,1993.

(136) Scott Gary M., Ph.D. Thesis on Knowledge based artificial neural networks for process modeling & control-University of Wisconsin, Medison,1993.

(137) Scott Gary M.,Shavlik Jude W. and Ray, W. Harmon, Refining PID Controllers using neural networks, neural computation, 4(5),pp.746-757, 1992.

(138) Scott. B. Pantaleo, A new headbox design featuring consistency profiling decoupled from fiber orientation response, TAPPI Journal, vol.78,no.11,pp.89-95,Nov.1995.

(139) Seborg Dale E., Edgar T. F., and Mellichamp D.A., Process dynamics and control, John Wiley & Sons Publication, IInd edition 2004.

(140) Sharad Bhartiya, Feedback grade transition in a continuous pulp digester using model based management of kappa profile, Deptt. of chemical engg., IIT Bombay, Powai, Mumbai 400076.

(141) Shen, S. H., and Yu C.C., Use or relay-feedback test for automatic tuning of multivariable systems, AICHEJ., 40,pp.627,1994.

(142) Shinskey, F.G., Process Control Systems, 4th edition, McGraw-Hill, New York, 1996.

(143) Shukla S.R. and Asimananda Khandual, Artificial neural network for textile application: A review, Journal of color Technology and Management, vol.1,no.-1, pp 27-30, Jan 2004.

(144) Singhal D.K, Basis weight control for small paper mills, IPPTA, vol.8,no.3, pp.75-78.Sept. 1996.

(145) Singhal D.K, Modeling and simulation of approach flow for GSM control, IPPTA Journal, vol.17, no.1, pp.75-80, Jan.2005.

(146) Sinha, N.K. and Kustra, B., Modeling and identification of dynamic systems,-Van Nostrand Reinhold Co. 1988.

(147) Sivanandam S.N, Introduction to neural networks using MATLB-6.0, Tata MAGRAWHILL.

(148) Sivanandam S.N., Introduction to artificial neural networks, Vikas publishing house pvt. Ltd.2003.

(149) Skogestad, S., and Postlethwaite,I., Multivariable feedback control: Analysis and design, John Wiley & sons ltd., New York,1996.

(150) Smith B.W., Designing for control in papermaking systems, in F.Bolam(ed), Trans. Symposium brit paper & Board manufacture. Assn. Oxford, vol.1, pp 44-95, 1970.

(151) Srinivasan Vanchinathan and Krishnagopalan Gopal,A., Kraft delignification kinetics based on liquor analysis, TAPPI, vol.78, no.3,pp.127-132, March 1995.

(152) Stephanopoulos G., Chemical process control An introduction to theory and practice, Prentice Hall of India Pvt. Ltd., New Delhi, 1997.

(153) Surya p. Chitra, Use neural networks for problem solving, Chemical engineering progress p-44-52, April1993.

(154) Talvio P.A, A study of paper machine headbox control system with linear transfer function, IFAC 1966,session 22, paper 22A, London.

(155) Tee, L.H. and Wu, S.M., An application of stochastic and dynamic models for the control of a paper making process, Techometries, vol. 14, No.2, pp481-96, 1972.

(156) Temesgen, M., Simulation of evaporator system in pulp and paper plant, ME dissertation, University of Roorkee, Roorkee,1999.

(157) Tuladhar A, Devies M.S., Vim C., and Woods G.R., Headbox modeling and wet end pressure pulsation analysis, Journal of pulp and paper Canada, 98:9,III, pp.91-94,1997.

(158) Turnbull Paul F. , One-dimensional dynamic model of a paper forming process, Tappi Journal,vol.80, no.1,pp.245-252, Jan 1997.

(159) Ull mann, R. and Garceau, J.J., Pulp Paper Canada, 6(1):TR14(1980).

(160) Vanhala Jukka, Pekka Pakarinen,and Kimmo Kaski, Paper web quality profile analysis tool based on artificial neural networks, International conference on tools with AI, Boston, Massachusetts, pp.343-346,Nov. 1993.

(161) Viharos Zs. J., Monostori L., and Vincze T., Training and application of artificial neural networks with incomplete data, Project work (project no. 2/040/2001),National research foundation, Hungary, Grant no. T034632.

(162) Vijayalakshmi Pai G.A and Rajsasekran S., Neural networks, Fuzzy logic and genetic algorithms, Prentice-Hall of India private Ltd, 2nd edition 2003.

(163) Waller H. Michael, Design and development of headboxes, Paper science & engg. deptt. Miami University Oxford., TAPPI short notes wet end operations, pp.61-70,1991.

(164) Weber R., and Gaitonde N.Y., Non-interactive distillation tower analyzer control, Proc. Ame. Control conference., Arlington, VA, p.87, 1982.

(165) Webros,P.J., Backpropagation through time: What it is and how to do it, Proceedings of the IEEE,vol.78, no.10 ,October 1990.

(166) Whalley R., Ebrahimi M., Optimal control of a paper making machine headbox, Journal of applied mathematical modeling ,26,pp.665-679,2002.

(167) Wilhelmsson B. et al., Modeling multicylinder paper drying-Validation of a new simulation program, TAPPI Journal,vol.79, no.4, pp.157-167,April 1996.

(168) Willis M.J., Massimo C.Di, Montague G.A, Tham M.T, and Morris A.J., Artificial neural networks in process engineering, IEE proceedings-D, vol.138, no.3, pp.256-264,May 1991.

(169) Willis M.J., and Montague G.A, Artificial neural networks in process estimation and control," Automatica, 28(6),pp. 1181-1187, 1992.

(170) Wilson J.A and Zorzetto L.F.M, A generalized approach to process state estimation using hybrid artificial neural network/mechanistic models, Computers chem. Engg., vol.21, no.9,pp.951-963,1997.

(171) Wright, R.A, and Kravaris C., Nonlinear control of pH process using the strong acid equivalent, Ind. Eng. Chem.Res., vol.30,pp.1561-1572,1991.

(172) Xia,Q, et al. Modeling and control for drying section of paper machine, Pulp and paper Canada, 95:9,pp.54-59,1995.

(173) Zhu,Q, Xia J., Rao M. and Zurcher J., A neural network for modeling pulp process Journal of pulp and paper Canada, 98:9, pp- 35-38, 1997.

(174) Zurada J. M., Introduction to artificial neural systems, Jaico publishing house Delhi, sixth edition 2003.

APPENDICES:

Appendix :-1

Table: 1.1 Transfer Functions
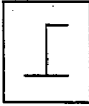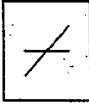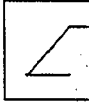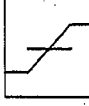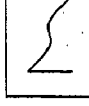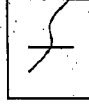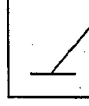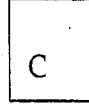
Name	Input/Output Relations	Icon	MATLAB Function
Hard Limit	$y = 0 \quad x<0$ $y = 1 \quad x≥0$		Hardlim
Symmetrical Hard Limit	$y = -1 \quad x<0$ $y = +1 \quad x≥0$		Hardlims
Linear	$Y = x$		Purelin
Saturating Linear	$y = 0 \quad x< 0$ $y = x \quad 0≤x≤1$ $y= 0 \quad x>1$		Satlin
Symmetric Saturating Linear	$y = -1 \quad x<-1$ $y = n \quad -1≤x≤1$ $y = 1 \quad x>1$		Satlins
Log-Sigmoid	$y = \dfrac{1}{1+e^{-mx}}$		Logsig
Hyperbolic Tangent Sigmoid	$y = \dfrac{e^{x}-e^{-x}}{e^{x}-e^{-x}}$		Tansig
Positive Linear	$y = 0 \quad x<0$ $y = x \quad 0≤x$		Poslin
Competitive	$y = 1$ neuron with max n $y = 0$ all other neurons	C	Compet

Table: 3.1 Typical Control Loop Dynamics (Nancy)

Typical sensors/Typical Parameters	Time constant
Fast beta gauge	20ms
Slow beta gauge	100ms
Pressure, flow	1sec.
Fast Consistency	3sec.
Slow Consistency	10sec.
Slow temperature	20sec.
Fast temperature	8 sec.
Total head	1.0sec.(process), 3.0sec.(closed loop)
Fan pump speed	0.1sec.(process), 0.3(closed loop)
Basis weight	1.0min.(process), 3.0min.(closed loop)
Level	1.0min.(standpipe); 1hour(chest)

Table: 3.2 Measuring devices and their characteristics

Parameters and Measuring devices	Static/Dynamic models/ Dynamic characteristics	Comments
Temperature RTD	$R=R_o(1+\alpha t)$; Sensitivity (Pt):$\approx$0.00385Ω/ Ω/°C(Germany Practice) to 0.00392 Ω/ Ω/°C (US practice) (Ni): 0.005/°C at room temperature Range :- 100 to + 600 °C(or 900 °C with ceramic materials), time constt.=0.2 to 0.5s in flowing water, 2 to 5s in air	Bridge measurement, multiplexing essential
Thermistor	$R=R_o\,e^{[\beta(1/T-1/T0)]}$ Sensitivity of 0.1 Ω/ Ω/°C (or 30 mV /°C) are possible. Time constant for uncoated thermistor): 10	Widely used in industry where shock and vibration occur, for dynamic temp. measurement

Thermocouple	s(air) and 1.0 s in water. Coating with Teflon will increase the values by 2.5 times and above. Range:-50 °C to +150°C, time constt.=1s(water),10s(in air)for uncoated thermistor; time constt.=25s in air, 10s in water for coated with teflon $E=aT+bT^2$ For J type with reference temperature of 0°C, sensitivity: 0.0515 mV/°C(50μV/°C) For range of 0°C to 760°C, accuracy of 0.1 °C The response time can be less than 0.1 s(0.2 to 0.5 s) Second order transfer function; For J type thermocouple, time contt.=0.05s to 1s in air; sensitivity=0.0515mv/°c, response time=51.5μv/°c(iron-constantan) (T)response time=40μv/°c(Cu-constantan) (K)response time=40μv/°c(chromel-alumel) (E)responsetime=62μv/°c(chromel-constantan)	Remote indication, For special purpose where high sensitivity is needed
Flow Variable head meter Variable area meter Electromagnetic flow meter	Output value= $b(t)=bi+(bf-bi)(1-e^{-t/\tau})$; Response time≈ ms Time constant of the order of 0.05 s(0.025mm wire) and 1 s(0.125mm wire) in still air	No moving part Direct visual indication No obstruction in the flow line of meter fluid
pH pH meter	Tranfer Function(G)=	Glass electrode is quite adequate for pH

Pressure Manometer Strain gauge	T.F= $1/(\zeta s+1)$ or second order: $1/(\zeta^2 s^2 +2\zeta \zeta s+1)$ $e^{-2.6s}/(21.6s+1)(2.9s+1)(2.1s+1)$ $Q_{act}=c_d k(\Delta h)^{.5}$ Fast dynamics $Q_{act}=c_d(A_t-A_f)(2g)^{.5}/[(1-(A_t-A_f)^2/A_t^2]$ $[V_f(\rho_f-\rho_{ff})/A_f \rho_{ff}]$ flow=$\alpha(\Delta P)^{0.5}$ $E_o=[4BQ/d]* 10^{-8}$ pH =log(1/hydrogen ion conc.) $H=(P_1-P_2)/\rho g$ Second order $1/(\zeta^2 S^2+2\zeta \zeta s+1)$ Useful resistance=120 Ω(range 60-1000Ω) Gauge factor=2 for metals and -50 to -200(semi conductor) Sensitivity of metallic strain gauge=10^{-6} strain $P=Ay^2/V_r-Ay$	measurement upto 9.0. Static pressure
Mc-leod Gauge Bourdon tube gauge		Low pressure
	$I=I_0 e^{-\mu\rho x}$ $l = Ioe^{-\lambda/c}$ Response time 1.0 sec. Dead time 6 to 10s and total stabilizing time 15s	Covers very high pressure ranges
Level beta and gamma ray Differential pressure devices		For solid and liquid level measurement For remote indication, only for liquid level
Consistency Mechanical Rod sensor Rotor sensor Optical sensor Microwave sensor NIR consistency analyzer		Least affected by the flow variation
		Suited for single fiber slurry application, not sensitive to normal flow. Obtained by bump test for consistency of steady state value 3.1 to 2.9%
Basis weight Beta gauge		For fast basis weight control

ANN parameters	$V_1(L_{head})$	$\rho_1(P_{head})$	$\rho_2(P_{head})$
Input nodes	2.0	2.0	2.0
Hidden nodes	5.0	5.0	5.0
Output nodes	1.0	1.0	1.0
Activation function	Tansig	Tansig	Tansig
Algorithm	Gradient descent	Gradient descent	Gradient descent

Table:5.2 Process dynamics

Parameters	Time constt.	Process gain	Process transfer functions
Consistency	$T_d=6.84s$ $T_p=3.84s$	$K_p=-2.035$ $K_p=-0.0407$ For λ tuning=15s $K_p=0.03$ $K_p=-0.0625$ $K_p=0.042$ $K_p=0.0625$	$G_p=-0.2.035e^{-6.84s}/(3.84s+1)$ $G_p=-0.0407e^{-6.84s}/(3.84s+1)$ $G_p=0.03e^{-\theta ds}/(1+10s)$ $G_p=-0.0625e^{-5s}/(1+5s)$ For fine consistency For hardwood consistency
	$T_p=10s$ $T_d=5,10,20s$ $T_p=5s$ $T_p=3s,$ $T_d=3s$ $T_p=5s,$ $T_d=5s$		
Flow	$T_{pipe}=0.50$ $T_v=0.8s$ $T_m=2s$ $T_p=2.4s$ $T_p=8.0s$ $T_p=10.0s$ $T_p=5.0s$	$K_p=1.5$ $K_p=4.0$ $K_p=24.0$ $K_p=23.4$	$G_p(s)=1.5/(0.5s+1)(0.8+1)(2s+1)$ $G_p(s)=1.5/(2.4s+1)$ $G_p(s)=K_pe^{-\theta s}/(\tau s+1)$ $G_p(s)=4.0/(1+8.0s)$ $G_p(s)=24.0/(0.5s+1)(8s+1)(2s+1)$ for hard wood $G_p(s)=23.4/(0.04s+1)(1.0s+1)(4.0s+1)$ for pine flow
Total head	$K_p=1,$ $T_d=0.2s$ $T_i=0.2,$ $\lambda=0.4s$		Current regulator & motor speed are assumed first order

	$\tau=1.0s$; closed loop $\tau=2\text{-}3s$ $k_p=1.05$, $\tau=3s$		
Level	$\tau_d=10s$ $\tau_{pcl}=10s$; $\tau_p=5s$ $\tau_i=60s$; $\tau_p=20s$	$K_p=0.00449$ $K_p=0.00167$ $K_c=1.0$ $K_p=0.005$ $K_p=0.1$ $K_p=0.0025$	$G_p(s)=K_p e^{-\theta s}/s$ $G_p(s)=0.00449e^{-10s}/s$ $G_p(s)=0.00167/s\,(10s+1)(5s+1)$ $G_c(s)=0.0167/s\,(60s+1)$ $G_p(s)=-1.6(1-0.5s)/s(3s+1)$ $G_p(s)=0.005/s$ $G_p(s)=0.1e^{-3s}/s$ $G_p(s)=0.0025/s\,(20.0s+1)$
pH Harriott(52)	$K_p=5.67$ $\tau_p=1.8s$ $\tau_d=19.9s$ $K_P=0.8$ $\tau_d=0.2min$ $\tau_p=1.5min$ $\tau_m=0.05min$ $K_P=6.4$ $\tau_d=0.2min$ $\tau_p=1.5min$ $\tau_m=0.05min$		$G_p(s)=5.67e^{-19.9s}/(1.8s+1)$ $G_p(s)=0.8e^{-0.2s}/(1.5s+1)$ $G_m(s)=1/(0.05s+1)$ $G_p(s)=6.4e^{-0.2s}/(1.5s+1)$ $G_m(s)=1/(0.05s+1)$
Temp	$\tau_1=20s$, $\tau_2=8s$ $\tau_d=4s$; $\tau_1=6s$, $\tau_2=30s$ $\tau_d=10s$; $\tau_1=20s$, $\tau_2=5s$ $\tau_d=5s$;	$Kp=5$ $Kp=1.25$ $Kp=0.6$	$G_P(s)=K_P\,e^{-\zeta_d s}/(1+\zeta_1 s)(1+\zeta_2 s)$ $G_p(s)=5e^{-4s}/(1+8s)(1+20s)$ $G_p(s)=1.25e^{-10s}/(1+6s)(1+30s)$ $G_p(s)=0.6e^{-5s}/(1+20s)(1+5s)$ $G_p(s)=0.131(2.57s+1)/s(0.23s+1)$ $G_p(s)=15.3(0.23s+1)/(2.57s+1)$ First order system without dead time $G_P(s)=20/(40.2s+1)$ Or first order $=k/(\tau s+1)$
Basis weight	$\tau=10s$ $K=0.0056$ $\tau_i=0.021min.$		$Y(s)=[0.55e^{-8s}/(7.5s+1)]u(s)$ $Y(s)=[0.40e^{-10s}/(8.0s+1)]u(s)$

Table: 5.3 Z-N tuning equations

Controller type	Proportional gain	Integral gain	Derivative gain
Proportional	$1/k[\tau/T]^{-1}$	------------	----------------
PI	$0.9/k[\tau/T]^{-1}$	$K_p/3.33\,\tau$	------------
PID	$0.9/k[\tau/T]^{-1}$	$1/2.0\,\tau$	$\tau/2.0$

Table: 5.4 λ-tuning equations for interactive algorithms

Process model	K_c , K	K_i	T_d
$K_p/(1+\tau s)$	$\tau/K_p\lambda$	$60/\tau$	--
$K_p e^{-\theta_d s}/(1+\tau s)$	$T/K_p(\lambda+\theta_d)$	$60/\tau$	--
$K_p e^{-\theta_d s}/(1+\tau s)$	$T/K_p(\lambda+\theta_d/2)$	$60/\tau$	$\theta_d/120$
$K_p e^{-\theta_d s}/(1+\tau_1 s)(1+\tau_1 s)$	$\tau_i/K_p(\lambda+\theta_d)$	$60/\tau_1$	$T_2/60$
K_p/s	$2/K_p\lambda$	$30/\lambda$	--
$K_p e^{-\theta_d s}/s$	$(2\lambda+\theta_d)/K_p(\lambda+\theta_d)^2$	$60/(2\lambda+\theta_d)$	--

Table: 5.5 Dynamic parameters for temperature

Process	K_P	ζ_{P1} (s)	ζ_{P2} (s)	ζ_d (s)	Ξ
First order	20.0	40.2*	-------	----	--------
First order with delay	1.0	12.12*		2.376*	
Two first order are joined in series	1.0	10.0	5.0	-------	1.06
Two first order are joined in series With delay	5.0	8.0	20.0	4.0	1.1
Second order with delay	5.0	8.0	5.0	4.0	1.02
	1.25	6.0	30.0	10.0	1.3
	0.6	20.0	5.0	5.0	1.25
Second order	1.0	192*			0.48

* The values in the equation of transfer functions are in minutes.

Table: 6.1a Lambda tuning controller response (when λ=15sec)

Time(sec.)	Output response
1.0667	0.3251
5.0428	0.4370
10.086	0.5344
15.031	0.6343
20.074	0.7242
25.020	0.7958
30.063	0.8522
35.009	0.8937
40.051	0.9248
45.094	0.9472
49.940	0.9626

Table: 6.1b Lambda tuning controller response (when λ=16sec)

Time(sec.)	Output response
5.05	0.41995
10.11	0.5218
15.04	0.6264
20.10	0.7208
25.033	0.7953
30.090	0.8540
35.020	0.8965
40.077	0.9282
45.134	0.9501
50.065	0.9660
60.053	0.9843
69.914	0.9928

Table: 6.3 Relationship between wire speed and pressure or vacuum applied to head box eqns. [3.1 - 3.3]

No. of Data	Speed (m/min) C_v=0.98	C_v	Total head (m)	Pump operation V=Vacuum P=Pressure	V=$\sqrt{2gh}$ (m/min)	C_v	Calculated/Actual or J/W
1.	300.3	0.983	1.3208	P	303.24	0.99	1.0098
2.	315.31	0.986	1.4478	P	317.49	0.993	1.0069
3.	330.33	0.983	1.6002	P	333.78	0.993	1.0104

256

4.	345.345	0.982	1.7526	P	349.31	0.993	1.01148
5.	360.36	0.982	1.9050	P	364.18	0.993	1.01060
6.	375.375	0.985	2.0574	P	378.47	0.993	1.0082
7.	390.39	0.988	2.2098	P	392.24	0.993	1.0047
8.	405.405	0.987	2.3876	P	407.71	0.993	1.0056
9.	420.420	1.05	2.5654	P	422.62	0.993	1.0052
10.	435.435	0.985	2.7686	P	439.04	0.993	1.0082
11.	450.450	0.983	2.9718	P	454.86	0.993	1.0097
12.	465.465	0.988	3.1446	P	467.90	0.993	1.0052
13.	480.48	0.984	3.3782	P	484.97	0.993	1.0093
14.	495.495	0.985	3.5814	P	499.34	0.993	1.0078
15.	510.510	0.984	3.81	P	515.03	0.993	1.0088

Appendix:-2

MATLAB PROGRAMS:
[1.1] Consistency simulation program:

```
%Author: Rajesh Kumar
%To train backpropagation artificial neural network
clear
fid=fopen('rajesh.txt','w');
maxerr=1.0;
saveerr=1.0;
b=1;
in=input('Enter number of Input Nodes: ');
ih=input('Enter number of hidden Nodes: ');
io=input('Enter number of output Nodes: ');
sqerr=0;
v=rand(ih,in);
w=rand(io,ih);
alpha=input('Enter alpha: ');
learn=input('Enter Learning rate: ');
tri=input('Enter Number of Training Sets: ');
disp('Enter Inputs: ');
for t=1:tri
   for i=1:in
      imat(t,i,1)=input('');
```

```
        end
        disp('Enter Outputs: ');
        for i=1:io
            omat(t,i,1)=input('');
        end
    end
    imaxx=max(imat);
    omaxx=max(omat);
    imax=max(imaxx);
    omax=max(omaxx);
    inii=imat/imax;
    toi=omat/omax;
    j=1;
    fprintf(fid,'Initial Weights randomly generated: ');
    fprintf(fid,'\n');
    fprintf(fid,'Weights(in->hid): ');
    fprintf(fid,'%f ',v);
    fprintf(fid,'\n');
    fprintf(fid,'Weights(hid->out): ');
    fprintf(fid,'%f ',w);
    hold on;
    Back propagation algorithm ..
    ...........
    ..................( program as  described in 2.1, appendix-2)
    disp('See the Weights in out.txt!!');
    if(b==1)
        disp('Enter Inputs to the trained Neural Network: ');
        for i=1:in
            ti(i,1)=input('');
            tini(i,1)=ti(i,1)/imax;
        end
        tinh=v*tini;
        for i=1:ih
            touth(i,1)=1/(1+(exp(-tinh(i,1)*alpha)));
        end
        tino=w*touth;
        disp('The Outputs from the trained Neural Network: ');
        for i=1:io
            touto(i,1)=1/(1+(exp(-tino(i,1)*alpha)));
            plot(j,touto);
            fprintf('%f ',touto(i,1)*omax);
        end
        fprintf('\n');
    end
    save w2 w;
    save v2 v;
    hold off;
    fclose(fid);


% Consistency plot
t=0:.01:10;
y=(1-.3915*exp(-.6856*t)+.3337*exp(-.1037*t)-.9423*exp(.0484*t));
plot(t,y);grid
%t=55;
% conversion for continuous to discrete(PI)
a=tf([0 -39.45 10.46 .809],[209.67 76.46 26.28 .809]);
>> b=c2d(a,2.5)
```

```
>> step(a,'-',b,'--');grid
% conversion for continuous to discrete(PID)
a=tf([-7.86 -.97 .616 .1],[5.27 6.28 1.616 1]);
b=c2d(a,2.5);
step(a,'-',b,'--');grid
```

[1.2]Training program for consistency
```
net=newff([.5967 1;.6 .6],[10 1],{'logsig','logsig'},'traingd');
net.trainparam.show=100;
net.trainparam.lr=.6;
net.trainparam.epochs=80000;
net.trainparam.goal=1e-5;
p=[.6019 .6 .6 .6 .5976 .6043 .6066 .606 .6043 .6024 .6007 .5995 .5984 .5978 .5973 .5971
.5969 .5968 .5967 .5967;.6 .6 .6 .6 .6 .6 .6 .6 .6 .6 .6 .6 .6 .6 .6 .6 .6 .6 .6 .6];
t=[.6 .6 .6 .6 .6 .6 .6 .6 .6 .6 .6 .6 .6 .6 .6 .6 .6 .6 .6 .6];
net=train(net,p,t);
a=sim(net,p);
gensim(net,.001);
```

[2.1] %Training for flow control
```
%To train Artificial Neural Network
clear
fid=fopen('dpt.text','w');
% C=[B1 B2 B3]; where B1=B(:,1)./max;
% B2=B(:,2)./max; B3=B(:,3)./max;
load Siso2;
load F; % column of set points for different wire speed
net=newff([.58824 1; .34667 1],[6 1],{'tansig','tansig'},'traingdx');
in=2;
ih=6;
io=1;
v=rand(ih,in);
w=rand(io,ih);
alpha=.6;
learn=.4;
tri=14;
iniii=Siso2(12:25,1:2);  % inputs from matrix B(training sets,input+output)
toii=Siso2(12:25,3);      % output from matrix B,coulon depends on no of outputs
inii1=iniii(:,1);
inii2=iniii(:,2);
inii=[inii1 inii2];
toi=toii(:,1);
epoch=1;
fprintf(fid,'Initial Weights randomly generated: ');
fprintf(fid,'\n');
fprintf(fid,'Weights(in->ih):  ');
fprintf(fid,'%f ',v);
fprintf(fid,'\n');
fprintf(fid,'Weights(ih->io): ');
fprintf(fid,'%f ',w);
 as algorithm.....
```
[2.2]% for testing
```
clear
  in=2;
  ih=6;
  io=1;
  load v1;
  'ad w1;
```

```
alpha=.9;
tini=[70/77.5;20/20];
tinh=v*tini;
 for i=1:ih
     touth(i,1)=1/(1+(exp(-tinh(i,1)*alpha)));
 end
 tino=w*touth;
  for i=1:io
     touto(i,1)=1/(1+(exp(-tino(i,1)*alpha)));
     tact=touto*18.875;
     fprintf('%f ',tact);
 end
 fprintf('\n');
```

[3]% Total head program

```
load nancyt;
load nancyhead;
load nancyspeed;
net=newff([.0000 1.0000],[8 1],{'tansig','tansig'},'traingd');
net.trainparam.show=100;
net.trainparam.lr=0.6;
net.trainparam.epochs=1500;
net.trainparam.goal=1e-3;
p=b';
t=a';
net=train(net,p,t);
gensim(net,.001)
% conversion of continuous to discrete
a=tf([0 0 0 70.09 6307.88 56070],[.425 41.8 1538.5 14520.09 26307.88 56070]);
b=c2d(a,2.5);
step(a,'-',b,'--');grid
```

[4] % Stock level program

```
load levelin;
load lavelout;
load levelref;
net=newff([1.0000 1.0000;0.0000 1.0000],[3 1],{'tansig','tansig'},'traingd');
net.trainparam.show=100;
net.trainparam.lr=0.1;
net.trainparam.epochs=15000;
net.trainparam.goal=1.5e-3;
a=r';
in=lo';
p=[a;in];
t=li';
net=train(net,p,t);
gensim(net,.001);
% conversion of continuous to discrete
a=tf([0 1],[.2 1]);
b=c2d(a,.01);
>> step(a,'-',b,'--')
```

[5] %Training for pH

```
load phtar;
net=newff([7 7;0 7],[12 1],{'logsig','logsig'},'traingd');
net.trainparam.show=100;
net.trainparam.lr=.6;
```

260

```
net.trainparam.epochs=80000;
net.trainparam.goal=3e-4;
p=[7 7 7 7 7 7 7 7 7 7 7 7 7 7 7 7 7 7 7 7 7 7 7 7 7 7 7 7 7 7 7 7 7 7 7 7 7 7 7 7 7 7 7 7 7 7 7
7 7 7 7 7 7 7 7 7 7 7 7 7 7; 0 0 0 0 .0002 .0010 .0052 .0262 .1306 .6482 2.0510 3.2934
4.3425 5.1927 5.8555 6.3522 6.7085 6.9510 7.1048 7.1921 7.2315 7.2384 7.2246 7.1991
7.1683 7.1365 7.1065 7.0798 7.0573 7.0391 7.0248 7.0141 7.0064 7.0012 6.9978 6.9959
6.9951 6.9949 6.9952 6.9957 6.9964 6.9971 6.9977 6.9983 6.9988 6.9992 6.9995 6.9997
6.9999 7 7 7 7 7 7 7 7 7 7 7];
t1=target;
t=t1';
net=train(net,p,t);
a=sim(net,p);
gensim(net,.001);
% conversion of continuous to discrete
a=tf([0 7],[15 1]);
b=c2d(a,1);
step(a,'-',b,'--');grid

% conversion of continuous to discrete for temperature
a=tf([0 40],[.2 1]);
b=c2d(a,.01);
>> step(a,'-',b,'--');grid
```

[6] Basis weight general program
```
% conversion of continuous to discrete
a=tf([0 .55],[7.5 1],'inputdelay',8);
>> b=c2d(a,2.5)
```
(i) Transfer function:
$$z^{-800} * \frac{0.0007328}{z - 0.9987}$$
Sampling time: 2.5

(ii)Transfer function:
$$z^{-4} * \frac{0.1074}{z - 0.7316}$$

Sampling time: 2.5
```
>> step(a,'-',b,'--')
```

[7.1]   % Total head and stock level(BPNN) Training
```
load Siso2; % n=[n1 n2 n3 n4]; n1 n2(fan pump input and air valve input)
% are the inputs and n3 n4 (total head and stock level)are outputs.
fid=fopen('rajesh.txt','w');
maxerr=.001;
saveerr=.001;
b=1;
in=1;
ih=2;
io=1;
sqerr=0;
v=rand(ih,in);
w=rand(io,ih);
alpha=.9;
lrn=.6;
tri=14;
imat=Siso2(12:25,1)/77.5;
```

```
omat=Siso2(12:25,3)/18.875;
imaxx=max(imat);
omaxx=max(omat);
imax=max(imaxx);
omax=max(omaxx);
inii=imat/imax;
toi=omat/omax;
j=1;
Back-propagation algorithm(as 2.1 program)
....

....
```

[7.2] % For testing

```
in=1;
ih=2;
io=1;
v=[1.7301;-2.3953];
w=[4.0942 -14.3059];
alpha=.9;
tin= .8;
    thidden=v*tin;
    for i=1:ih
        ttt(i,1)=1/(1+(exp(-thidden(i,1)*alpha)));
    end
    tinn=w*ttt;
    disp('The Outputs from the trained Neural Network: ');
    for i=1:io
        output(i,1)=1/(1+(exp(-tinn(i,1)*alpha)));
        actual=output;
        fprintf('%f',actual);
    end
% conversion of continuous to discrete (y11)
a=tf([0 .528],[2.2 1],'inputdelay',6);
>> b=c2d(a,2.5);
```

Transfer function:
$$z^{(-600)} * \frac{0.002395}{z - 0.9955}$$

```
Sampling time: 2.5
>> step(a,'-',b,'--');grid
% conversion of continuous to discrete (y12)
a=tf([1.28 2.2016 .5161],[1 1.84 .616]);
b=c2d(a,1);
```
Transfer function:
$$\frac{1.28 z^2 - 2.538 z + 1.258}{z^2 - 1.982 z + 0.9818}$$
```
Sampling time: 1
step(a,'-',b,'--');grid
```

[7.3] % Cluster discovery (ART1 Program)

```
m=input('enter maxm number of clusters:');
rho=0.7;
L=[2];  % initialize parameter
%bottom up weights(from F1 to F2)
b=[.67 0.0 .2;0.0 0.0 .2;0.0 0.0 .2;0.0 .67 .2];
% top down weights( from F2 to F1)
```

262

```
t=[1 0 0 0;0 0 0 1;1 1 1 1];
s=[0 0 1 1];
q=sum(s);
c=[0 0 1 1];
x=c';
a=b';
%net input to each node in F2
y=a*x;
%if reset is true then we take largest term of y say y1 or y2 or y3
% 2 for y2 has highest value
t1=t(2,:);
t2=t1';
h=s*t2;
u=h/q;
if u>=rho
 delb=b
delt=t
 return


% the value of u is greater than rho, so weights are remain same
% if u is less than rho, so y2 is set to -1.0,and other y1 y3 are as same as calculated reset
is true
% s0 y3 is greater then t3=1111
else
t2=t(3,:);
t3=t2';
h=s*t3;
u=h/q ; % u is greater than rho so update weights are
db=[(L*x)/(L-1+h)]; % this is the third column of b
delb=b(:,1:2);
ddelb=[delb db]
end
```

[8] % Air pressure and level(Rho, Neu) training
```
[8.1]load neuinnorm1;
load neuoutnorm1;
load neure1;
net=newff([1.0000 1.0000;.0001 .8291],[5 1],{'tansig','purelin'},'traingd');
net.trainparam.show=100;
net.trainparam.lr=0.01;
net.trainparam.epochs=350000;
net.trainparam.goal=1.5e-4;
r=t';
in=a3';
p=[r;in];
t=a4';
net=train(net,p,t);
gensim(net,.001);
[8.2]
load rhoout1;
load rhoin1;
load rhot1;
net=newff([1.0000 1.0000;.0003 .0011],[5 1],{'tansig','purelin'},'traingd');
net.trainparam.show=100;
net.trainparam.lr=0.05;
net.trainparam.epochs=35000;
net.trainparam.goal=1.0e-4;
```

263

```
p=[1 1 1 1 1.1 1 1 1 1; .0003 .001 .0002 .0011 .0002 .0011 .0003 .0004 .0008 .0006];
t=[.9604 .9589 .9578 .9564 .9555 .9543 .9517 .9435 .9616 .9644];
net=train(net,p,t);
gensim(net,.001);
```
[8.3]
```
load rhoout2;
load rhoin2;
load rhot2;
net=newff([1.0000 1.0000;-1.0000 .1435],[5 1],{'tansig','purelin'},'traingd');
net.trainparam.show=100;
net.trainparam.lr=0.01;
net.trainparam.epochs=150000;
net.trainparam.goal=5.0e-4;
m=I';
in=j';
p=[m;in];
t=k';
net=train(net,p,t);
gensim(net,.001);
```

[9] % Stock flow and stock level control Training
```
%To train Artificial Neural Network
clear
fid=fopen('m.txt','w');
load ref; % tcon.mat means input consistency
load stocklevel;
in=1;
ih=3;
io=1;
v=rand(ih,in);
w=rand(io,ih);
alpha=.9;
learn=.6;
tri=61;
imat=tnorm;   % inputs from matrix B(training sets,input+output)
omat=y2;      % output from matrix B,coulon depends on no of outputs
imaxx=max(imat);
omaxx=max(omat);
imax=max(imaxx);
omax=max(omaxx);
inii=imat/imax;
toi=omat/omax;
epoch=1;
.....
...... Backpropagation algorithm(as program 2.1).....
```

[10] % Retention training
As described in program 2.1, appendix-2. but values of data has been changed according to retention process.
```
% conversion of continuous to discrete
a=tf([1.28 2.2016 .5161],[1 1.84 .616]);
>> b=c2d(a,1);
```

Transfer function:

$$\frac{1.28\ z^2 - 2.538\ z + 1.258}{z^2 - 1.982\ z + 0.9818}$$

Appendix:-3

1. Static model for total pressure and stock level (hydrostatic head) in all kind of headboxes:

Let P, ρ, V, f, l, D, v, m, g and h refer to pressure, density, specific volume, friction factor, length, diameter, velocity, mass, stock height and acceleration due to gravity respectively, then the following static models can be written as

Potential energy due to stock head=mgh

Potential energy due to pressure $=P/\rho= PV$

Kinetic energy$=mv^2/2$

Loss due to friction$= 2flv^2/gD$

(a)In order to get required jet speed and stock from the slice, static energy is converted into kinetic energy,

$$mgh=mv^2/2 \qquad\qquad or \qquad\qquad v=\sqrt{2gh}$$

(b)If pressure energy is converted in to kinetic energy(K.E),then

$PV= mv^2/2$

(c)If both combined static energy & pressure energy are converted to K.E one can write

$mgh+PV= mv^2/2$

The above equations are applied to three types of headboxes as under:

[A] Open headbox:

Actual flow speed of stock, $V_m<V$, due to friction in the slice lip and flow resistance through the baffles & perforated rolls.

If Vs, V_n , refer to wire speed and nominal speed of machine(dryer part) respectively

$V_s<V_n$

Φ=discharge coefficient depending on actual speed of stock on the wire in relation to the theoretical speed

$\Phi=V_m/V$ [1]

Lag factor of stock, $\xi=V_m/V_s=0.90\text{-}0.95$ [2]

Ψ, lag factor of wire speed in relation to nominal speed of the machine,

$\Psi=V_s/V_n$ [3]

Putting the value of Vs in eqn.[3], one can get

$\xi\ \Psi V_n= \Phi V$

Or $V_n= \Phi V/\xi\ \Psi = \Phi\sqrt{2gh}/\xi\ \Psi$

Or $V_n{}^2= (\Phi/\xi\ \Psi)^2\ 2gh$

Hydrostatic head, $h= (V_n{}^2/2g)\ (\xi\ \Psi/\ \Phi)^2$

[B] Closed headbox(hydraulic headbox):

$PV=mv^2/2$ or $v=\sqrt{(2PV/m)}$

$P=mv^2/2V \qquad (v^2/2)\ m/V \quad$ or $\quad (v^2/2)\ \rho v/V$

$P=(v^2/2)\rho \quad$ or $\quad v=\sqrt{2P/}\ \rho_{liq}$.

If $\xi\ \Psi V_n= \Phi V$

Or $V_n= \Phi V/\xi\ \Psi \quad$ or $\quad (\Phi/\xi\ \Psi)\ (\sqrt{2p/}\ \rho_{liq})$

Or $P= (\xi\ \Psi/\Phi)^2\ (V_n{}^2/2)\ \rho_{liq}$ [4]

[C] Pressurized flow box with air cushion:

$mgh+PV= mv^2/2$ [5]

if $V=m/\ \rho_{liq}$

Putting the value of V, the eqn. becomes

or mgh + Pm/ ρ_{liq}= mv^2/2

v^2=(2mgh/m)+ (2Pm/ ρ_{liq}m) = 2gh+2P/ ρ_{liq} [6]

or v= √(2gh+2P/ ρ_{liq}) = √ 2(gh+P/ ρ_{liq})

Normal speed of stock flow

ξ ΨV_n= ΦV

or V_n =(Φ/ξ Ψ) [√ 2(gh+p/ ρ_{liq})]

From eqn.,   2P/ ρ_{liq}= V^2- 2gh

Or P=[(V^2- 2gh) ρ_{liq} /2]

Putting the value of P in eqn.[6], one can get

(ξ Ψ/Φ)^2 (V_n^2/2) ρ_{liq}= [(V^2- 2gh) ρ_{liq} /2]   [7]

2. Geometrical design of headbox slice:

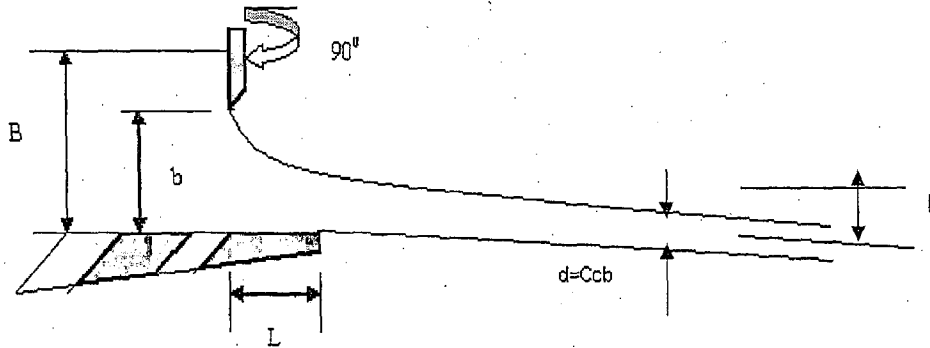### Flow from a vertical slice:

Fig.A-1 Dimensions for flow from a vertical slice

The primary variables which govern the angle of outflow and contraction coefficient for a vertical slice are shown in fig.A-1. The variables are as given below.

where B=Depth of stock at the slice

      b= Slice opening

      L=Bottom lip extension

      C_c= Geometric ratio

      d=Thickness of the jet

      β= Jet angle

The angle of outflow and the contraction coefficient have been calculated for a vertical slice from the parametric equations

L/B=(1+c^2/ π) ln(1-c/1+c)+(c cos β/ π)ln(1+cos β/1-cos β)-c sin β   [8]

b/B=(1-c^2/ π)tan^{-1}(2c/1-c^2)-(c sin β/ π)ln(1+ sin β/1- sin β)+c cos β   [9]

in which c=d/B=C_cb/B is a geometric ratio related to the contraction coefficient C_c. These equations were derived by conformal transformation applicable to ir-rotational flows and are presented in a report by Appel D.W et al(4).

266

Equations to calculate C_c and β:

The following equations have been derived empirically by fitting curves to data calculated from the parametric equations(71). The various values of the constants (contraction coefficient) are used, shown in table A-1.

$$C_c=(a_0-a_1y/1-a_2y)\exp[-(a_3-a_4y/1-a_5y)X^f]+(a_6-a_7y/1-a_8y) \qquad [10]$$

Angle of outflow

$$\beta= [(b_0+b_1x-b_2y+b_3y^2-b_4xy+b_5xy^2)/(1-b_6y)^2]\exp[(-b_7-b_8x+b_9y+b_{10}xy)/(1-b_6y)] \qquad [11]$$

where

$x = L/b$ and $y = b/B$; and $0\leq x \leq 5.0$; $0\leq y \leq .95$

3. Flow from a 45°slice:

The primary variables which govern the angle of outflow and contraction coefficient for a 45^0 slice are shown in fig.A-2
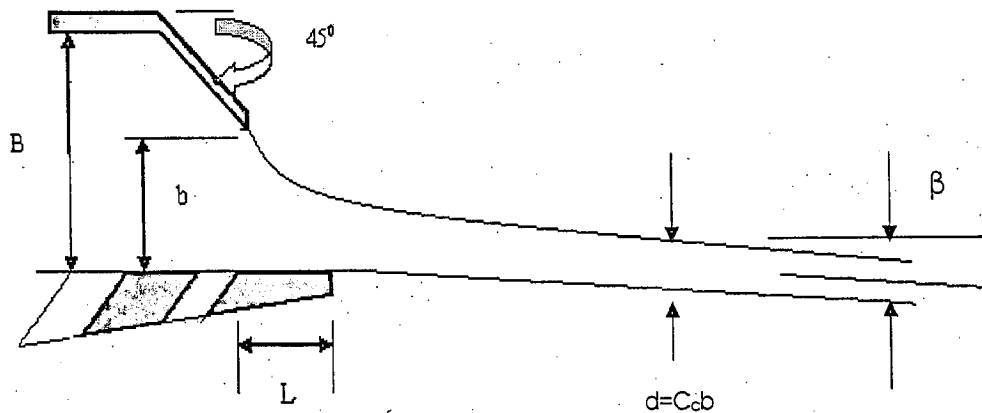

Fig. A-2 Dimensions for flow from a slice

The angle of outflow and contraction coefficient was calculated from the parametric equations.

$$L/b = 1-2 \left[\frac{\cos\beta\ln[\tan(\beta/2)]+\sin\beta\ln[\tan(\pi/4-\beta/2)]+\pi/2(\cos\beta+\sin\beta)+(1+c^2/c)(\tanh^{-1}c)+(1-c^2/c)(\tan^{-1}c)}{(\cos\beta-\sin\beta)\ln[\tan(\pi/8+\beta/2)]+(\cos\beta+\sin\beta)\ln[\tan(\pi/8-\beta/2)]+\pi\cos\beta+(1+c^2/c)(\tanh^{-1}\sqrt{2}c/1+c^2)+(1-c^2/c)(\tanh^{-1}\sqrt{2}c/1-c^2)} \right]$$

[12]

$$C_c = d/b = \left[\frac{\pi}{(\cos\beta-\sin\beta)\ln[\tan(\pi/8+\beta/2)]+(\cos\beta+\sin\beta)\ln[\tan(\pi/8-\beta/2)]+\pi\cos\beta+(1+c^2/c)(\tanh^{-1}\sqrt{2}c/1+c^2)+(1-c^2/c)(\tanh^{-1}\sqrt{2}c/1-c^2)} \right]$$

[13]

In which $c=d/B=C_c b/B$ is a geometric ratio related to the contraction coefficient C_c. For the case that b/B=0, the equations can be reduced to

$$L/b = 1-2 \left[\frac{\cos\beta\ln[\tan(\beta/2)]+\sin\beta\ln[\tan(\pi/4-\beta/2)]+\pi/2(\cos\beta+\sin\beta)+2}{(\cos\beta-\sin\beta)\ln[\tan(\pi/8+\beta/2)]+(\cos\beta+\sin\beta)\ln[\tan(\pi/8-\beta/2)]+\pi\cos\beta+2\sqrt{2}} \right]$$

and   [14]

$$C_c = d/b = \left[\frac{\pi}{(\cos\beta-\sin\beta)\ln[\tan(\pi/8+\beta/2)]+(\cos\beta+\sin\beta)\ln[\tan(\pi/8-\beta/2)]+\pi\cos\beta+2\sqrt{2}} \right]$$

[15]

These equations were derived by applying conformal transformations to ir-rotational flows and are presented in the report by Appel and Yu. Additional information flows from nozzles having angles from 10 to 30⁰ presented by Attwood W, et al. The various values of the constants are used, shown in (tableA-2).

Equations to calculate C_c and β:

$C_c = [(a_0 - a_1 y/1 - a_2 y)\exp[-(a_3 - a_4 y/1 - a_5 y)x^f] + (a_6 - a_7 y/1 - a_8 y)]$ [16]

$\beta = [(b_0 + b_1 x - b_2 y + b_3 y^2 - b_4 xy + b_5 xy^2)/(1 - b_6 y)^2] \exp[(-b_7 - b_8 x + b_9 y + b_{10} xy)/(1 - b_6 y)]$ [17]

where x=L/b and y=b/B and $0 \le x \le 5.0$; $0 \le y \le .95$

4. Flow from a nozzle(slice) with inclined upper lip:

The primary variables which govern the angle of outflow and contraction coefficient for a nozzle with inclined upper lip are shown in fig.A-3. The angle of outflow and contraction coefficient were calculated for a nozzle with an inclined upper lip from the parametric equations. The various values of the constants are used, shown in table 3.
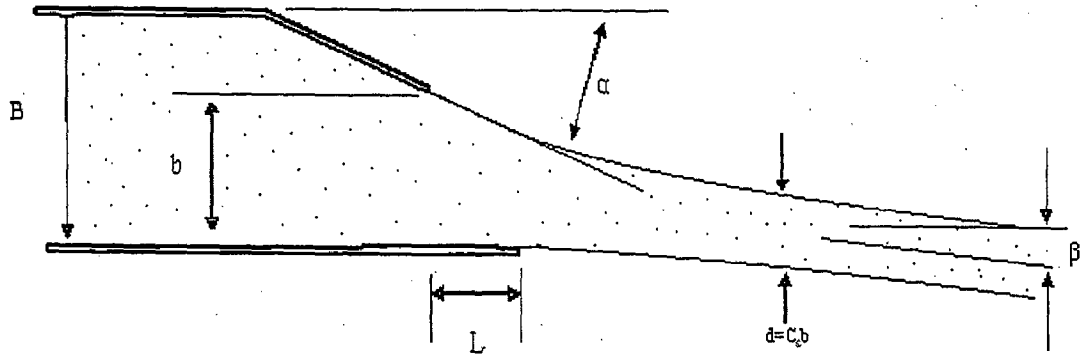
Fig.A-3 Dimensions for flow from a slice

$$L/B = c/\pi \ \ln\left[\frac{(1-c^{\pi/\alpha})}{(1+c^{\pi/\alpha})} \ \frac{(1+\cos\pi\beta/\alpha)}{(1-\cos\pi\beta/\alpha)}\right] \ -c\,\beta \qquad [18]$$

$$b/B = (c\alpha/\pi)\ln\left[\frac{2(1+\cos\pi\beta/\alpha)}{(1+c^{\pi/\alpha})^2}\right] \ +c \qquad [19]$$

in which $c=d/B=C_c b/B$ is a geometric ratio related to the contraction coefficient C_c applicable for small angles of lips(α less than 10^0).

Equations to calculate C_c and β:

$$C_c=[(a_0-a_1y)/(1-a_2y)]\ \exp[-x^f(a_3-a_4y/1-a_5y)]+(a_6-a_7y/1-a_8y) \qquad [20]$$

$$\beta=[(b_0+b_1x-b_2y+b_3y^2-b_4xy+b_5xy^2)/(1-b_6y)^2]\ \exp[(-b_7-b_8x+b_9y+b_{10}xy)/(1-b_6y)] \qquad [21]$$

where $x=L/b$ and $y=b/B$ and $0\le x \le 5.0$; $0\le y \le .90$
Values of coefficient to be used(when $\alpha=10^0$) are given in tableA- 3.

Table:A-1 Values of the coefficient to be used(vertical slice)

	C_c		B	
A_0	0.06461	b_0		158.3
A_1	0.06575	b_1		278.6
A_2	1.00162	b_2		235.9
A_3	3.91592	b_3		80.84
A_4	3.15442	b_4		439.9
A_5	0.73227	b_5		166.1

A_6	0.60597	b_6	0.7481
A_7	0.46721	b_7	2.008
A_8	0.84737	b_8	2.981
F	1.11253	b_9	1.389
		b_{10}	2.416

Table: A-2 Values of coefficient to be used(45° slice)

C_c		B	
a_0	0.07021	b_0	141.1
a_1	0.07085	b_1	200.9
a_2	0.97351	b_2	195.8
a_3	3.31994	b_3	57.71
a_4	3.22893	b_4	293.0
a_5	0.95911	b_5	97.58
a_6	0.74306	b_6	0.7566
a_7	0.68406	b_7	2.222
a_8	0.93916	b_8	2.527
F	1.10383	b_9	1.571
		b_{10}	1.971

Table:A- 3 Values of coefficient to be used(inclined upper lip)

C_c		B	
a_0	0.02870	b_0	38.14
a_1	0.03062	b_1	39.56
a_2	1.06208	b_2	75.27
a_3	2.90190	b_3	37.14
a_4	3.07832	b_4	77.78
a_5	1.06000	b_5	38.23
a_6	0.92788	b_6	91.86
a_7	0.98750	b_7	2.124
a_8	1.06449	b_8	2.121
F	1.09008	b_9	2.104
		b_{10}	1.947

Table:A-4 Estimation of theoretical velocity at the slice for eqn.[3.4]

V	m/min	m/min	m/min
H	mmHg	mmH_2O	Kpa
K	265.7	30.98	84.85